Understanding Bone Cell Interactions with Silicate Species Released from Bioactive Glasses

Joel Turner

A dissertation submitted in partial fulfilment

of the requirements for the degree of

Doctor of Philosophy (PhD)

Division of Surgery and Interventional Science

University College London

2023

i. Declaration

I, Joel Turner, confirm that the work presented in this thesis is my own. Where information has been derived from other sources, I confirm that this has been indicated in the thesis.

Signature: Joel Turner

Date: 30/10/23

ii. Acknowledgements

I would first like to give thanks to my primary supervisor Professor Gavin Jell, for without him, none of this work would be possible. Thank you for all your kindness, patience and support to get me to where I am today. To my secondary supervisor Professor Julian Jones, thank you giving me access to your lab and providing me with research support. I look forward to working with both of you in the future. To Professor Marilena Loizidou, thank your encouragement and for creating a safe, kind and supportive working environment.

Thank you to the Advanced Characterisation of Materials – Centre for Doctoral Training (ACM-CDT) for providing training, support and the means to present my work internationally. Specifically, I would like to thank Chris Howard from the ACM for being a good mentor and friend. I would like to make special mention to Ms Heike Lee-Muller for not only providing me with a job but being such a good friend in the final months of my PhD. One final massive thank you to Mrs Nicola Mordan for her friendship and providing me the skills that allowed me to finish the PhD.

I would also like to thank members of my research group and department: Carolina, Amy, Azi, Medina, Adriana, Maria, Elena, Alex C/G, Komal, Akshay, Sam, Kelly, Fawaz, Patricia, Christina and many more. I am deeply grateful for all the help in the labs, all the fun times and all the times you picked me up when things didn't go to plan. I want to extend a similar thanks to my best friends Adam and Michael for always being there when I needed you.

This thesis is dedicated to my mum and dad for without whom these last few years would not have been possible. I will be forever grateful for your love and support.

And finally… To future Joel

If you are reading this, I want you to look back at this thesis and remind yourself that if you work hard enough, anything is possible. Wherever you are now, I hope you're happy. Best of luck.

Yours sincerely,

Joel (2023)

UCL Research Paper Declaration Form

referencing the doctoral candidate's own published work(s)

1. **For a research manuscript that has already been published** (if not yet published, please skip to section 2)

   a) **What is the title of the manuscript?**

   The effect of Si species released from bioactive glasses on cell behaviour: A quantitative review

   b) **Please include a link to or doi for the work**

   https://www.sciencedirect.com/science/article/pii/S1742706123005469

   c) **Where was the work published?**

   Acta biomaterialia

   d) **Who published the work?** (e.g., OUP)

Science direct

   e) **When was the work published?**

   15/10/23

   f) **List the manuscript's authors in the order they appear on the publication.**

   Joel Turner, Arkhash Nandakumar, Nikhit Anilbhai, Aldo R. Boccaccini, Julian R. Jones, Gavin Jell

   g) **Was the work peer reviewed?**

   Yes

   h) **Have you retained the copyright?**

   Yes

   i) **Was an earlier form of the manuscript uploaded to a preprint server?** (e.g., medRxiv). If 'Yes', please give a link or doi)

   No

   If 'No', please seek permission from the relevant publisher and check the box next to the below statement:

   ☒

*I acknowledge permission of the publisher named under **1d** to include in this thesis portions of the publication named as included in **1c**.*

2. **For multi-authored work, please give a statement of contribution covering all authors** (if single author, please skip to section 4)

   Joel Turner: Lead author - designed article search. Responsible for data collection, meta-analysis and writing

   Arkash Nandakumar – Assisted in data collection.

   Nikhit Anilbhai – Assisted in data collection.

   Aldo Boccaccini: Provided guidance for search design, data retrieval and writing.

   Julian R. Jones: Provided guidance for search design, data retrieval and writing.

   Gavin Jell: Supervising author – article idea conception, oversaw meta-analysis, writing and submission

3. **In which chapter(s) of your thesis can this material be found?**

   Chapter 1

4. **e-Signatures confirming that the information above is accurate** (this form should be co-signed by the supervisor/ senior author unless this is not appropriate, e.g., if the paper was a single-author work)

   Candidate

   Joel Turner

   Date:

   29/10/23

   Supervisor/ Senior Author (where appropriate)

   Professor Gavin Jell

   Date

   30/10/23

iii. Abstract

Despite 50 years of silicate bioactive glass (SBG) research and commercial success, the effect of soluble silicate (Si) species on cellular responses remains poorly understood. This includes how Si is internalised, excreted, and localised within bone cells. With an aim to optimise SBG ion release rates for more precise control of cell behaviour, this thesis attempts to investigate silicate ion uptake dynamics in osteoblasts whilst examining some of the roles these ions may play in bone regeneration.

By using a systematic analysis of previous *in vitro* literature, this thesis demonstrated, for the first time, a relationship between [Si] and cellular response. An [Si] range where an increased reporting of desirable cellular interaction was found (~30-40 ppm, $P \leq 0.001$), whilst the frequency of negative outcomes increased by ~3x above 50 ppm (1.8 mM) Si. This systematic approach also provided quantitative evidence of the variance in methodological practices to assess responses to bioactive glasses and the need for greater standardisation.

Liquid state ^{29}Si-NMR revealed that BGs release orthosilicate species up to 2 mM Si, whilst above this concentration both ortho and disilicate were identified. Sodium silicates (SS) were found to produce more and larger precipitates in water and cell culture media than BGs dissolution products (up to 3mM Si) up to 3 mM, suggesting that other ion may influence Si species and particle formation. Intracellular [Si] was observed to be lower in cells cultured in 45S5 BG dissolution products compared to SS, suggesting that Si species may be important in cellular uptake. An increase in intracellular [Si] was observed up to a maximum of 250 μM/cell after 4 days. Following the replacement of Si-conditioned media with media alone, intracellular [Si] decreased ($P \leq 0.001$), along with an increase in [Si] found in the supernatant suggesting the excretion of Si from cells.

Si particles released from both BGs and SS were found to be localised within lysosomal vesicles (STEM-EDX and fluorescence imaging) in both osteoblast and osteoclast cells suggesting an endosomal uptake route. A clatherin-mediated endosomal inhibitor (Dynasore hydrate), however, did not reduce Si uptake suggesting aggregation post-uptake or a non-clatherin (e.g., caveolae) mediated uptake mechanism.

This thesis suggests an [Si] range that may be more likely to produce, positive, negative and non-significant cell responses, whilst demonstrating how Si species, (in addition to other ions released from BGs) are important in influencing intracellular [Si] and Si localisation. These results are important in informing the composition of new BGs that release quantities of Si that produce desirable cell responses.

iv. Impact statement

This thesis attempts to improve our understanding (experimentally and by systematic reviews) of bone cell interactions with silicate species alone and those released from SBG dissolution products. The following study will therefore have the following impact:

1. Scientific impact

Despite a vast number of studies highlighting the effects that BG dissolution products have on cells, little is known about what effect Si has on cells and whether this could be affected by the presence of other therapeutic ions (namely calcium, sodium and phosphorus). This thesis improves our understanding of how the concentration of Si and other ions released from bioactive glass affect the formation of different Si species and complexes. For the first time, disilicates, in addition to orthosilicates were identified at above 2 mM Si in BG dissolution products suggests initiation of Si polymerisation and possible formation potentially cytotoxic nanoparticles. This may help to explain the high variance in cell responses to different glass compositions and their respective dissolution products reported *in vitro*. Quantification of Si uptake and secretion, along with intracellular localisation over time, provides a method of tailoring Si release toward specific cell types and diseases.

2. Translational impact

This study provides a better understanding of Si uptake, intracellular localisation and how cell behaviour is affected by different Si species released from BGs. Novel BG formulations may therefore tailor their respective Si release to obtain more desirable cell outcomes *in vitro*, thereby accelerating the translation to in vivo and clinical trials. A review of previous studies (chapter 1) also highlights the variance in methods used to quantify cell behaviour. This may help to standardise these practices leading to better comparison between studies and therefore faster translation.

v. Contents

vi. List of Figures

vii. List of Tables

viii. List of Abbreviations

Chapter 1. Introduction and Literature review

1.1 Clinical need for bone substitute materials

Given stabilisation and adequate blood supply after minor injuries, damages to bone eventually heal giving complete functional restoration. Diseases causing impaired wound healing, however, such as diabetes, osteoporosis and 'non-union' fractures resulting from major traumas do not completely heal and hence require surgical intervention. Graft procedures that involve taking tissue from the same human (an autograft), another human (an allograft) or from an animal (a xenograft) and implanting it into damaged bone is the most common method of bone repair[1]. From a clinical perspective, the autograft procedure is still the 'gold-standard' for effectively repairing damaged bone[2]. In this case, healthy bone (commonly pelvic[3]) is removed from the patient and surgically attached to fill and integrate with regions of damaged bone. Although like most graft treatments, their limitations are largely due to the shortage of donors, pain caused by donor site morbidity[4, 5], rejection following surgery and diseases causing impaired bone healing. Approximately, 2.2 million bone grafting procedures take place annually to repair bone defects with close to 500,000 of those occurring in the United States alone[6]. The need for methods of regenerating bone after trauma without requiring donor tissue has prompted additional research into implantable biomaterial alternatives that can artificially stimulate bone cells to begin the healing process.

1.2 Current approaches to bone regeneration

Prior to 1980, metals and rigid (non-biodegradable) polymer implants were the most common method of repairing weight bearing bones following damage or

disease. Whilst these were designed to be 'bioinert' (does not elicit a response from the host), most implants triggered a fibrous encapsulation or did not form a stable interface with bone or surrounding tissues, making them prone to failure[7]. An ideal solution to this problem would be to not only form a strong bone with existing bone but biodegrade at a similar rate to the formation of new tissues (resulting in little to no implant remaining in the body long term). The mechanical properties of new implants are also important as they should mimic those of natural bone but be soft enough to be cut to shape or injected to fit patient specific bone defects during surgery. Current material replacements used for this objective can be grouped into three major categories, biopolymers, bioceramics and hybrids (a composite mixture of the two). A vast number of *in vitro/vivo* studies are now researching how these materials can be tailored to encompass most (if not all) of the ideal properties to optimise effective bone restoration. Further research is also conducted into how these materials could be made or 3D printed into scaffolds (or 'monoliths') that mimic the natural architecture and porosity of bone (e.g., trabecular vs cortical) whilst promoting attachment of healthy cells and subsequent bone growth. The following sections will outline the progress made in ceramic and polymer-based materials whilst highlighting the potential flaws in each design.

1.2.1 Biopolymers

Naturally occurring biopolymers including chitosan[8, 9], collagen[10, 11] and alginate[12, 13], have been widely adopted in scaffolds due to their recognisable surface protein signature, allowing for enhanced cell attachment and proliferation. A major benefit of polymers compared to ceramic based materials is that their mechanical, physical and degradable properties are more predictable following adjustment of chemical structures. Polyglycolic acid (PGA) and polylactic acid (PLA) for example, are commonly used due to their tuneable degradation and mechanical properties. A further advantage of these polyester-type materials is the ease of enzymatic biodegradation inside the body and

filtration of non-toxic monomeric waste products after implantation[14]. A major disadvantage, however, of biopolymers used to regenerate bone is that are unable to bond or form stable interfaces with mineral components of bone owing to the chemical mismatch at bone-material interfaces.

1.2.2 Bioceramics

A ceramic can be defined as a non-metallic or organic material that often present hard and brittle mechanical properties. Whilst ceramics can be found naturally (e.g., hydroxyapatite in bone), ceramics can be made artificially by heating inorganic materials (e.g., silica) to temperatures often in excess of 1000°C and allowing to cool slowly. This methodology allows time for a repeated arrangement of atoms (or crystal lattices) to form, greatly increasing its strength. 'Bioceramics' (a name used for ceramics purposed for use with the human body) have been widely adopted in regenerating bone due to their unique ability to form strong bonds with existing healthy bone. A frequently used clinical bioceramic is synthetic hydroxyapatite (SHA - $Ca_{10}(PO_4)_6(OH)_2$), a material designed to mimic the mineral component of native bone. Due to the absence of trace ions, however, found in natural bone (e.g., lithium, magnesium, strontium or silicon) and its thermodynamic stability at physiological pH, resorption of SHA is often slow, resulting in implants remaining in the body for years after implantation[15]. Biphasic calcium phosphates such as β- or α-tricalcium phosphate (TCP) present an increased solubility at a range of pHs and thus exhibit a potentially more appropriate resorption rate[16]. Despite this, previous studies have suggested that the dissolution rate of TCP alone may be too high to be used as bone fillers and has hence prompted synthesis and biological evaluation of composite TCP-HA ceramics[17]. Bioactive glasses (BGs), a ceramic with amorphous networks, have come to light as an alternative to crystalline calcium-phosphate based ceramics that provide lower sintering temperatures, tuneable dissolution rates and ease in incorporating trace ions.

1.3 Silicate-based bioactive glasses (SBGs)

Invented by Professor Larry Hench, bioactive glasses were designed to retain the ability to bond strongly to existing bone, but also dissolve at a rate appropriate to match the growth of new bone. The first bioactive glass (later referred to as '45S5' or 'Bioglass®') was based on a quaternary Si-P-Na-Ca system. This ceramic comprised an amorphous ('glass') silicate network which was modified by compounds containing phosphorus, sodium, and calcium (Mol% - 46.1: SiO_2, 24.4: NaO_2, 26.9: CaO, 2.6:P_2O_5). Melt-derived Bioglass® requires heating its precursor compounds to over 1300°C, before rapid quenching in distilled water. This method prevents/reduces the formation of atomic crystals forming, thereby achieving a majority 'amorphous' (as opposed to crystalline) silicate network. As a glass, the ceramic can then dissolve when immersed in solution, allowing it to release therapeutic ions (e.g., Si, Na, Ca and P).

The formation of hydroxyl groups (Si-OH) at the surface of the glass enables the formation of a crystallised HA surface layer via the nucleation of calcium phosphates found in blood, cell culture medium or released from the glass itself[18]. The newly formed HA layer then allows bioactive glasses to form strong bonds with existing healthy bone mineral. Effective bonding in this case (although not well understood), can also be attributed to interactions with the protein components of bone. A range of studies have shown that the addition of SBGs could enhance immobilisation of fibronectin[19, 20] and fibrinogen[21, 22], leading to increased cell attachment[19]. Comparatively little is known, however, about the interactions of SBGs and collagen (the most common protein found in bone) other than its it conformational change once adsorbed to BG surfaces[23]. By varying the molar ratio of elements in the BG structure (e.g., 58S[24] or S53P4[25] BGs) or substituting for other network modifiers (e.g., magnesium[26], strontium[27] or lithium[28]), the mechanical properties, rate of ion dissolution and thus biological interactions can be tailored. An increase to surface area and glass porosity can be

achieved by manufacturing BGs via a sol-gel[29, 30] or electrospinning[31, 32] process instead of melt-derivation, thereby allowing for tailoring of ion release rates in solution.

Since their creation, BGs have been used commercially in a variety of applications including ocular (middle ear bone), dental and orthopaedic (load bearing bones e.g., spine) restoration. Commercial products in dental and orthopaedic repair based on 45S5 Bioglass® have been the most successful amongst these applications with 'NovaBone' (formally Perioglas®) implanted into over 1.5 million patients worldwide[33]. Initial success of Perioglas® was observed in periodontal (jawbone) defects during clinical trials[34, 35] and *in vivo* studies[36, 37]. Bioglass® was also later modified contain fluoride and sold as a toothpaste (NovaMin), which was shown to reduce hypersensitivity by filling dentin microtubules with newly formed BG-induced HA[38]. Other products including Biogran® used for jaw defect repair contains the same composition as Bioglass® but have a smaller particle size distribution (300-360 μm). Perioglas was later used in orthopaedic restoration (under the name NovaBone) by mixing glass particles with the patient's own blood before working it into the defect site as a putty during surgery. NovaBone has been shown to perform equally well as iliac crest autografts in posterior spinal fusion for approximately 40 patients with scoliosis[39]. BonAlive, a product based on S53P4, has also been evaluated in clinical trials for both dental and orthopaedic applications[40–42].

Compared to human clinical trials, a larger number of studies exist evaluating BGs in animal models, also yielding mixed results. BGs have been shown to outperform HAs in repairing 6 mm critical sized defects in femoral condyle of rabbits[43]. A similar result was observed in the mandible of beagles, 4 weeks after implantation[44]. Novabone was also shown, however, to perform poorly in the spinal repair of sheep, displaying only 20% bone infill compared to 42% with injectable putty[45]. Discrepancy in reported *in vivo* outcomes may be explained by considerable variance in experimental design including species, BG granule sizes

and the choice of glass compositions. Another explanation for variance may be due to a lack of understanding and evidence of the role that ions released from BGs (referred to as 'dissolution products') play in altering the behaviour and communication of bone cells.

1.3.1 SBG dissolution products and rates of release

The dissolution and subsequent uptake of ions from bioactive glasses by cells may explain why some bioactive glasses outperform commercial bioceramics and other BGs *in vivo*. Whilst calcium[46, 47], phosphate[48–50] and sodium[51, 52] ions have all been shown to play roles in bone cell metabolism, angiogenesis, growth, and mineralisation of bone, comparatively little is known as to the role of silicate ions in bone formation. Xynos *et al*., observed that osteoblasts cultured in BG dissolution products (DPs) alone produced favourable osteogenic gene expression *in vitro*[53]. They suggested that the presence of silicate ions could be a possible explanation for SBGs outperforming HAs *in vivo*. The rationale for the addition of silicate to HA-based materials[54, 55] and novel bioceramics[56], is now mostly attributed to dietary studies suggesting that silicate ions played a critical role in both human and animal bone formation and remodelling.

Although the role of silicate ions in this process are not fully understood, *in vitro* studies involving bone cells and silicate releasing materials have attempted to explore its impact on bone formation. Silicate ions are thought to be involved in the synthesis of collagen, mineral deposits, and the communication between osteoblasts (bone forming cells) and osteoclasts (bone resorbing cells) in the mediation of bone remodelling and repair[57–59]. Further evidence of silicate ion uptake is seen *in vitro* by demonstrating increased proliferation and gene expression in osteoblasts when in the presence of silicate-conditioned culture mediums[60]. The absence of silicate ions has also been shown to produce ineffective bone formation in humans and animals[61, 62]. Although to date, no study has demonstrated what intracellular concentration of silicate ions is

required to produce these responses or what effect silicate ions may have on cell behaviour to influence bone formation. To do this, it is important to investigate how these ions are up-taken overtime, what mechanisms enable their transport into the cytoplasm and the quantity needed to elicit bone regeneration. Experiments in this thesis will attempt to determine the specific species of silicate ions released from bioactive glasses and how they may influence Si uptake and intracellular localisation.

1.4 Physiological roles of silicate species (Si) in humans and animals

Silicon is the most abundant element on Earth, comprising 26% of the crust by weight[63]. In nature, silicon is stabilised by oxygen atoms and is most commonly found in the form of silica (SiO_2). Silica is present in a variety of forms dependent on whether it is in a soluble or a relatively insoluble state (e.g., tridymite, cristobalite and quartz). Soluble silicate in solution is frequently referred to as 'silicic acid', an umbrella term that describes different Si species, ortho, di or trisilicates (containing 1, 2, or 3 silicon atoms per molecule respectively). Orthosilicate becomes a disilicate molecule by forming an 'oxygen bridge' (Si-O-Si). The structure of orthosilicate can found in Figure 1.1. The form that Si takes or whether it is stable as monomer or polymer species, may be important in determining cellular interactions.

1.4.1 Silicate speciation

The Si ion species in cell culture media is likely to be dependent on pH, temperature, Si concentration and other ions present in solution. G. B. Alexander first demonstrated (1953) that Si species was dependent on Si concentration ([Si]) using a silicate-molybdic acid reaction. In this reaction, silica is added to molybdic acid producing silicomolybdate, thereby turning the solution yellow. This reaction was observed to occur more rapidly at lower [Si] compared to

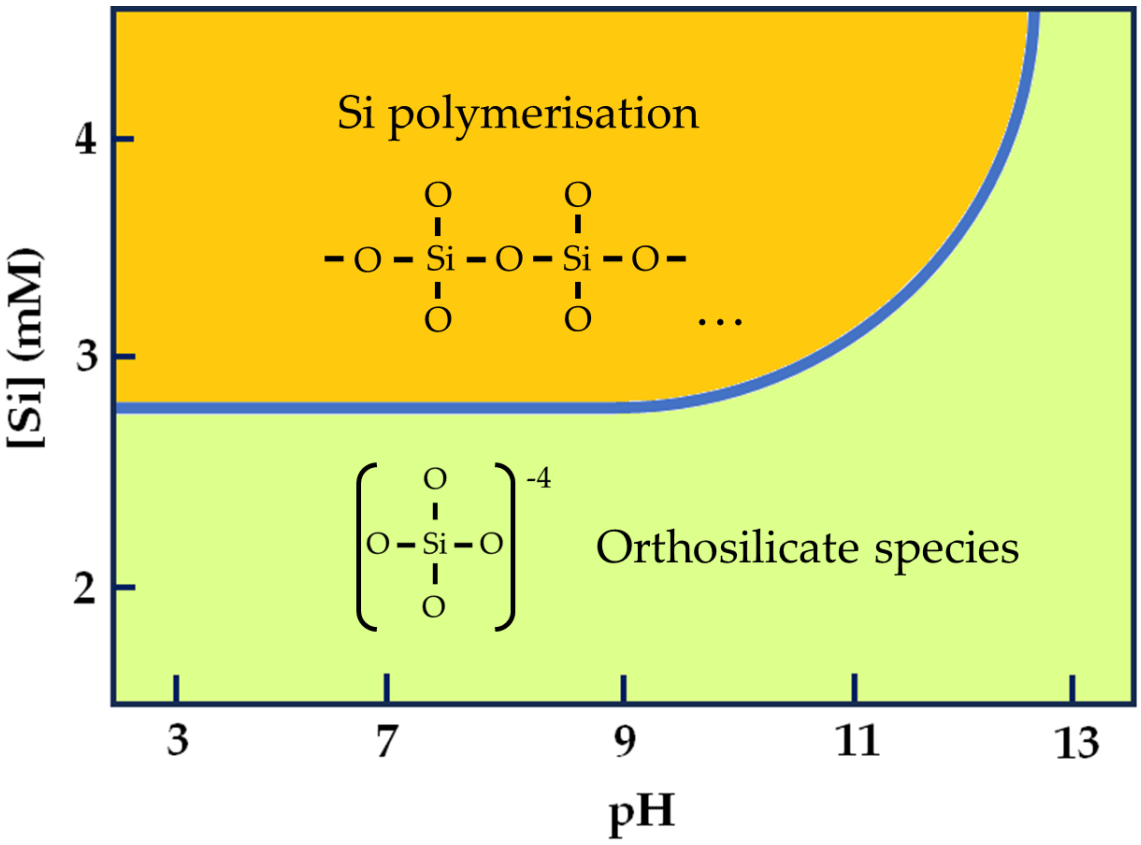

Figure 1.1 - **The relationship between pH, [Si] and the formation of different Si species**.

Polymerisation is shown to occur between 2- and 3-mM Si, pH 9 in water as demonstrated by R. Iler using a silico-molybdate reaction. Adapted from R. Iler[65].

higher, suggesting that polymerisation of Si may play a role in this reaction[64]. By adjusting the silica concentration and pH of solutions and observing the time for each solution of silicomolybdate to change colour, R. Iler (1975) was able to determine experimentally that increasing the [Si] caused increased Si chain length. They showed that at pH <9 and [Si] above 2 - 3 mM (56 - 84 ppm) caused an increase in the time to produce a colour shift, inferring that polymerisation may occur at this concentration[65]. The relationship between [Si], pH and the abundance of monosilicate species (reported graphically by R. Iler[65] and modified in later studies[66]) is shown in (Figure 1.1).

If polymerisation does occur (pH ≤ 9), the pH of the solution has been shown to dictate the size and formation rate of silica particles. Kley *et al.*, observed that smaller particles were formed at pH 8 with increasing sodium silicate concentration when comparing solutions at pH 7[67]. Despite this, the

silicomolydate reaction can only determine the proportion of monosilicates to polysilicates in a solution and can't accurately quantify them (especially when the solution may have a mixture of different species). It is also unclear how a solution containing a mixture of other salts, ions and biological molecules (as present in cell culture media for example) may influence the silicomolydate reaction.

The use of ^{29}Si nuclear magnetic resonance (^{29}Si-NMR) emerged in later studies as an accurate method to determine the proportion of Si species in solids and solutions. Solid state ^{29}Si-NMR has been used to determine the proportion of Si species in bioceramic silicate network (e.g., bioactive glasses[68, 69]). Due to the insensitivity of liquid state ^{29}Si-NMR and the low abundance of naturally occurring ^{29}silicon isotope in silica (~4%[70]), however, determining Si species present at biologically relevant concentrations (≤10 mM) in solution is difficult. Previous studies have shown that by using ^{29}Si enriched silicates, Si species could be determined at lower concentrations. Harris *et al* reported that at 500 mM that ortho (Q^0), di (Q^1) and trisilicate (Q^2) species exist, where Q^n equals the number of silicate bridges per molecule, (-O-Si-O-)[70]. Their study demonstrated the effect of [Si] on the presence of Si species, showing that 9.6 mM produced only orthosilicate species. It is unclear, however, if Si produces only orthosilicates or whether ^{29}Si-NMR was too insensitive to detect disilicates at this concentration. Although polymerisation has been shown to occur above 2 mM Si, it remains unclear which species (ortho, di or trisilicates) exist below this concentration and under what conditions dimer or trimerisation occurs. It is equally unclear if released at the same [Si], BGs and silicates produce the same Si species and how the dissolution media (e.g., water or culture media) or pH affect this. This thesis will attempt to provide evidence of Si species at biologically relevant concentrations (and its effect on Si uptake into cells – Si uptake and secretion dynamics in osteoblasts).

1.4.2 Dietary silicate

Several major sources of Si have been identified in the diets of humans and animals. Whilst the majority of dietary Si has been shown to come from beverages including mineral water, beer, and coffee (approximately 55%[63]). The concentration of Si in municipal water can vary anywhere between 4 – 20 ppm (0.14 - 0.71 mM) depending on the size of the city[63], whilst bottled water has been observed to vary between 8-85 ppm (0.28-3.1 mM) in some major brands[71]. Foods including grain and vegetable (14 and 8% respectively[72]) matter has been found to contribute a considerable proportion of this, which may go some way to explaining the relatively high concentrations in beer and coffee. Absorption of silicon in the body has been verified via its quantification in urine following ingestion of ^{32}Si isotopes[73]. The absorption (or 'bioavailability') of silicon in the body via the gastrointestinal tract is largely thought to be influenced by its species. Jugdaohsingh *et al* showed that whilst solutions assumed to contain only monomeric species of Si were absorbed and excreted in the urine of healthy patients ([Si] determined by ICP-OES), those containing polymeric species were not detected in either[74]. In addition to this study using a small patient cohort (n = 5), however, the species of Si in solutions given to patients was not determined by Si-NMR and thus it is unclear what proportions of species (ortho, di and trisilicates) were present in 2 mM monomeric or polymeric Si solutions before ingestion. It is equally unclear what effect further dilution or interaction with serum proteins in the blood had on distribution of Si species and eventual excretion in urine.

In drinking water, orthosilicate is believed to be the major species present, whilst relatively insoluble polysilicates are believed to form the majority of silicon found in plants[75]. This suggests that, since ~41% of Si content in humans comes from solid foods[76], breakdown of polysilicates to more absorbable orthosilicates may occur during digestion. In addition to the species of silicate, other factors including fibre[77] and other minerals may affect silicon absorption. Low calcium

content in the diets of rats and humans have been shown to increase the absorption of silicon[78], suggesting that these two ions may compete for cellular uptake pathways or form insoluble precipitates that are less bioavailable. Unlike insoluble silicate-based materials, most soluble silicate species are generally presumed to be safe to intake with a no-observed-adverse-effect level (NOAEL) being reported[79].

In the body, Si is present at its highest concentration inside of major connective tissues including the aorta, trachea, tendon, bone, and skin[80]. It has been suggested that high concentrations in these regions is due to the binding of orthosilicates and glycosaminoglycans[81], a carbohydrate responsible for supporting protein fibres and maintaining turgidity in extracellular matrices. Others have stipulated that Si also plays a role in crosslinks between proteoglycans and collagen[82]. Silicon supplements have been shown to increase collagen content in calves[83], whilst conversely, low silicon diets have shown to decrease collagen content in the lower tibia of rats[84]. These studies both observed a positive correlation between serum silicon content and hydroxyproline, a major

Table 1 - **A summary of the dietary studies (non-bone related) investigating the effect of Si on a) absorption of Al and b) hair, skin and nails.** [291–297]

a)

Authors	Species	Time	Administered [Si]	Findings
Foglio *et al.* (2012)	Mouse (n=40)	12-15 months	<43 mg/L Non-specific dosage	Al^{3+} without Si = ↓ Nitrergic/NAPDH-d+ neurons, ↓ nNOS activity, ↓ Neuron body size
Exley *et al.* (2006)	Human (n=5)	5 days	Non-specific conc' 1x 1.5 L Volvic water	Alzheimer's patients' + Si: Urinary excretion = ↑ [Si], ↑ [Al]
Reffitt *et al.* (1999)	Human (n=8)	32 hours	27-55 mg/L 2-2.5L Daily	Healthy males + Si: Urinary excretion = ↑ [Si], no change in [Al]
Edwardson *et al.* (1993)	Human (n=5)	6 hours	2.8 mg/L 1x 100 ml orange juice	Healthy males/females + Si: Blood plasma, ↓ [Al]

b)

Authors	Species	Time	Administered [Si]	Findings
Wickett et al. (2007)	Human (n=48)	9 months	Tablet 10 mg / day	Female hair + Si: ↑ Tensile strength, elasticity and thickness
A. Lassus (1997)	Human (n=15)	90 days	Si gel 3 times daily to skin	Psoriasis males/females + Si: ↓scaling, induration, erythema and acanthosis
A. Lassus (1993)	Human (n=47)	90 days	10 ml oral + gel twice daily	Healthy females + Si: ↑skin thickness/turgor. ↓mottles/wrinkles

component of human and animal collagen. Little is known, however, as to whether Si directly combines with collagen in its formation or upregulates protein synthesis inside cells (or both). Other literature has highlighted silicon's importance in maintaining healthy hair, nails, and skin by stimulating fibroblast cells to produce collagen, a major component of their respective extracellular matrices[85, 86]. Further experiments have also linked regular silicon intake to the prevention of Alzheimer's disease by inhibiting the accumulation of aluminium in the brain[87, 88]. The effect of Si in these studies is summarised in Table 1.

1.4.3 Silicate and bone

The majority of studies have emphasised the impact of dietary silicon in bone formation[63, 76, 89], showing that inadequate intake of silicon can lead to osteoarthritis and osteoporosis[90]. *In vivo* experiments in animal models have reported the effect that deficiencies in dietary silicon can have on bone structure and remodelling. The most dramatic impact of Si-deficient diets can be observed in early *in vivo* studies by Schwarz and Carlisle *et al.* Schwarz *et al*., demonstrated that rats resulted in shorter and distorted skull formation following an Si-deficient diet[91]. Carlisle *et al*., on the other hand observed a reduction in overall weight[61], whilst X-ray, histological and biochemical data demonstrated reduced collagen content and overall malformation of chick skull bones (Figure 1.2)[92]. Despite this, several studies have since failed to observe any significant differences in both chicks[93] and rats[94]. The abundance of Si in the environment, combined with insensitivity of instruments at the time may have contributed to inaccuracies in measuring Si content in 'Si-deficient' diets, thus inflating or producing no differences in observed data[95].

Si supplemented (or 'Si-surplus') diets has been used to investigate whether silicon could restore healthy Bone Mineral Density (BMD) in patients suffering from osteoporosis. Ovariectomised (OVX) rats have frequently been used to model osteoporosis due to their low oestrogen levels and thus similarity to

postmenopausal women (a demographic with increased frequency of osteoporosis incidence[96]). Silicon supplementation has been shown to increase BMD, bone volume and mineral content in OVX rats[97–99]. The beneficial impact of silicon supplementation has been suggested to be related to varying levels of calcium in animal diets. Kim *et al* observed that Si could increase the BMD of non-OVX rats with increasing calcium in their diets. BMD, however, decreased with Si supplementation in rats with high calcium diets[100]. Similar results were achieved in OVX rats, demonstrating increased BMD in femur and tibia bone in calcium deficient groups, whilst showing no significant change in high calcium diet groups[101]. Reasons for the relationship are mentioned in the previous section, including competition for uptake pathways into cells or the potential for formation of calcium silicate complexes. Relatively few studies, however, have investigated the hypothesis that Si-supplemented diets could reduce overall bone resorption[102], whilst decreasing the surface area of osteoclasts *in vivo*[97].

Whilst most studies have presented the positive effects of increased Si intake on mineral content, studies have shown the quantities of Si in bone to be the same in both mineral and collagen components[103]. Unlike mineral, however, no one method can quantify the levels of collagen in whole tissues. Where studies have observed no significant differences in mineral content with an increase in Si, differences may have been found in the production of collagen.

Compared to animal studies, relatively fewer published studies of the effect of dietary silicon exist using human subjects (~23 in animal models vs 6 in humans[80]). The majority of these studies are short term Si diet supplementation studies (4 out of 6) with long term epidemiological making up the rest. Likely due to the strongly negative outcomes to bone health observed in animal studies, however, the effects of Si-deficiency have never been studied in humans. The first epidemiological study by Jugdaohsingh *et al*., attempted to determine if a relationship existed between dietary silicon and BMD in 1251 men and 1596 pre-menopausal women over a ten-year period[104]. BMD measurements by X-ray

absorptiometry revealed that increases in dietary silicon positively correlated with increases in mineral density in both groups (adjusting for compounding factors). The other epidemiological study by Macdonald *et al* observed that Si intake was positively correlated with spinal and femoral BMD in over 3000 pre- and post-menopausal women[105].

The first supplementation study by Schiano *et al* showed that increasing Si intake led to increased trabecular bone volume in osteoporotic patients (n = 16)[106]. Studies of Si and osteoporotic subjects (n = 8) have since shown it to be more effective than sodium fluoride and etidronate at increasing femoral BMD[107]. Patients that were healthy but had low bone mass (n = 114) were also observed to produce a significant increase in femoral BMD with Si supplements[108]. Although in contrast, recent results by Choi *et al.*, found that there was no correlation between daily total silicon intake and BMD of calcaneus bone in a cohort of 400 Korean males aged between 19 to 25[109]. Despite this, their results did report a positive correlation between dietary silicon intake from vegetables

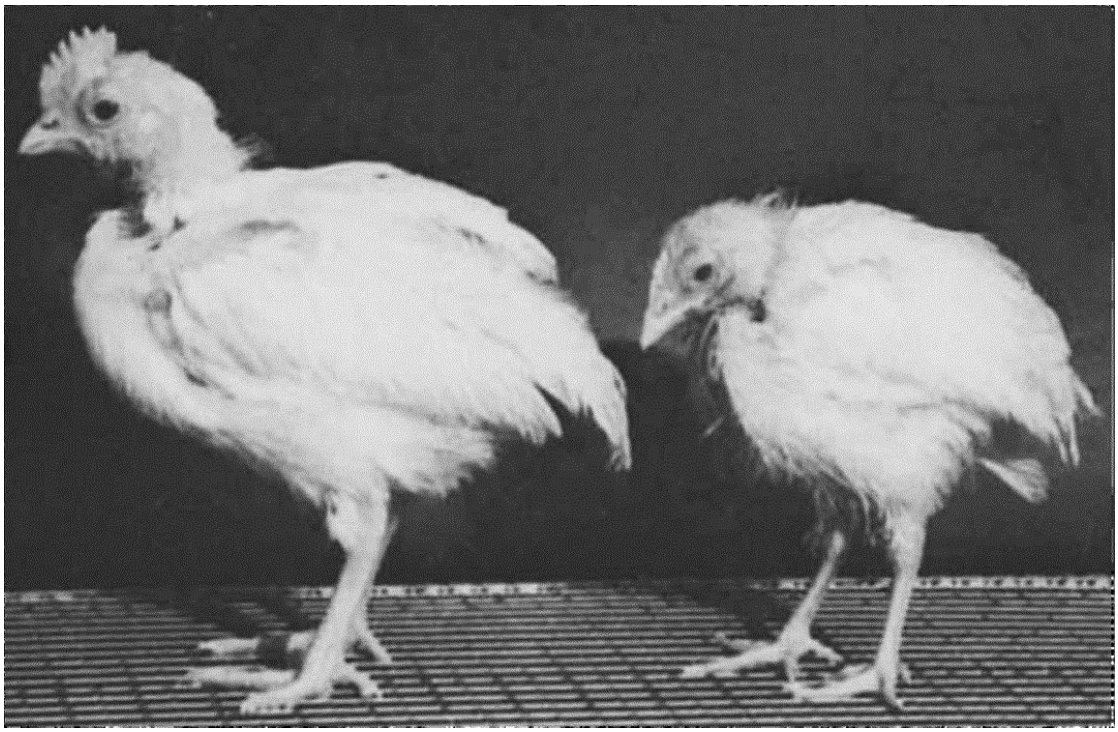

Figure 1.2 - **The effect of dietary silicon deficiency on the skeletal health of chicks (1976)**

Chicks fed a silicon sufficient (left) and deficient (right) diet[61]. Later studies have debated whether this effect is due to Si removal alone or the combined unintentional removal of other ions essential to healthy bone formation (e.g., calcium).

and serum total alkaline phosphatase (ALP) activity, an enzyme produced by cells involved in bone formation. This study and others suggest that the greatest benefits of Si supplementation and dietary may be in patients with pre-existing conditions affecting overall bone formation, whilst producing little to no effect in healthy subjects.

1.5 Evidence of the role of Si in SBGs *in vivo*

Successful regeneration of bone using BGs has been reported in both human and animal *in vivo* models. Although clinical trials provide a more accurate representation of BG efficacy in humans, successful outcomes are often difficult to repeat or compare due to large variance in glass properties (ion release rates and composition) along with patient characteristics (diet, lifestyle, and genetics). Evidence of the quality of bone formation in these studies is often limited to non-invasive imaging techniques such as X-ray or radiography making them difficult to evaluate the extent of success. Whilst less representative, SBGs in animal models offer better repeatability and the ability to perform more precise examination of subsequent bone formation (or lack thereof).

Even when desirable differences in bone restoration are observed, attributing their success to any one ion (e.g., Si) is difficult due to poor understanding of the combinatory effects of releasing a multitude of ions (Ca, P, Na etc.) all at once, instead of individually. Both study designs, however, still fail to make consistent conclusions as to the best BG composition due to high variance in measuring success (E.g., bone volume, weight, area). These study limitations make determining whether Si and increasing Si mol % in BGs is beneficial to cell responses.

1.5.1 Human studies

Despite over wide variety of SBG compositions tested *in vitro* or *in vivo*, only products based on 45S5 and S53P4 (45 and 53 mol% Si respectively) have been

tested frequently in clinical trials. Both glasses have been reported to integrate well with existing bone after dental root extraction[110, 111], defect repair in cases of periodontitis[112, 113], osteomyelitis[114, 115] and spinal restoration [116–118]. These glasses have, however, never been directly compared in a human clinical trial making it difficult to determine whether there exists a relationship between Si mol% in BG networks and outcomes reported in clinical trials. Sol-gel derivation of S53P4 also allows them to have a greater surface area compared to melt-derived 45S5, producing a potentially faster dissolution rate *in vivo*. In addition, the application of these two glasses in clinical trials is significantly different making direct comparison of beneficial Si mol% difficult. Of the 93 clinical studies since 1980 involving 45S5 BG products, only 8 (~9% of articles) focused on applications other than dental or periodontal (e.g., orthopaedic, sinus or orbital reconstruction)*. Comparatively, 19 of the 71 clinical studies (~27% of articles) involving S53P4 BG related products focused on non-dental applications.

Mixed clinical trial results were observed, however, in products containing S53P4 BGs such as BonAlive®. Whilst this product produced cortical bone twice as thick as autografts in defects left by bone tumour removal[119], autografts procedures performed better in spinal fusion following vertebral column displacement (88 vs 100% fusion rate after 11 years)[120]. This BG also did not fare well for restoration spinal burst fractures producing fusion in only 5 out of 10 implants compared to 100% fusion in the autograft group[121]. BGs have since been used as coatings for metallic implants, but ultimately perform poorly due the high dissolution rate of BGs and thus weakening of implant-bone bonding over time.

Despite these successful observations, to date, no single study has compared the two glasses directly *in vitro* and therefore no conclusions can currently be made as to whether an increase in Si mol% (in S53P4) significantly benefits bone formation. If a direct comparison had been made in human studies, differences in the composition of the two glasses would make attributing any positive effects in bone regeneration to Si difficult. Whilst S53P4 has a higher mol % Si compared

Web of science: Topic: Bioglass OR Perioglas OR NovaBone OR NovaMin AND NOT period% OR Dent* OR Oral

to 45S5, this percentage is produced by reducing the mol % of Ca, P and Na, therefore altering cell responses or the ability to form complexes with Si. Direct comparisons of the different glass compositions have only been achieved in animal models.

1.5.2 Animal studies

The first *in vivo* studies of SBGs (1977) in rat femurs by Hench *et al.*, showed that whilst 45S5 scaffolds (1x2x2 mm) produced bonds to existing bone that reflected the shear strength of native cortical bone, silica only controls did not bond at all. This study demonstrated that lower Si weight% in 45S5 could achieve faster degradation and better bonding than silica alone but also shows the necessity of network modifying ions (P, Ca, and Na) to produce successful surface HA formation. Since then, the introduction of the 'Oonishi' model, which involves drilling uniform ~6-15 mm critical-sized defects in bone, has helped in both standardisation and comparison of *in vivo* outcomes.

Melt-derived 45S5 bioactive glasses have been compared to sol-gel derived 58S and 77S bioactive glasses (58 and 77 mol% Si respectively). Wheeler et al, observed in a rabbit model that by 8 weeks 45S5 BGs had produced the highest percentage bone infill compared to the sol-gel glasses[122]. Although by 12 weeks, all glasses had filled the defect site equally (~5x more than unfilled controls $p \leq 0.05$). The study also observed that 45S5 grafts produce little to no degradation compared to 58S and 77S, whose nano porosity gives them a greater surface area and thus dissolution rate. 58S was found to degrade more then 77S given its lower Si mol%. Very similar results were obtained by Hamadouche *et al.*, who reported higher numbers of osteoclasts in the sol-gel grafts compared to 45S5, is also unclear what effect the absence of sodium in sol-gel glasses has on bonding and overall cellular behaviour. The impact of increasing Si mol% has also been shown in phosphate free glasses (SiO_2–CaO–Na_2O). Fujibayashi *et al* showed that bone growth in White rabbits by BGs (50-70 mol% Si) decreased with increasing

Si mol% [123]. Whilst only 50 mol% Si was able to produce bone after 1 week, those containing 60% and above did not bond or form new bone over the whole 12-week period. More recently Biosilicate® was compared to Bioglass (49 and 45 weight% Si respectively) *in vivo*[124]. Both glasses were shown to produce increased bone formation compared to a control in Wistar rats. Histological observation of intra-bone structures, however revealed Biosilicate to produce more osteoblasts and a higher bone cortical volume[125]. Conclusions from these studies seem to suggest that increasing Si mol% in glasses may be beneficial up to a point (~50-60% Si), at which a further increase often hinders over bone formation. It is unclear whether this is due to undesirably slow degradation rates or negative effects at the cellular level (or both). Subsequently, the effect of Si species alone and in the context of BG dissolution products has been explored *in vitro*.

1.6 Evidence of the role of Si alone and in SBGs *in vitro*

By using a systematic approach, the following section presents quantitative evidence of roles that Si plays when released from bioactive glasses and alone (non-dissolution products). This review also quantitatively compares and discusses the variance observed in methodology used to evaluate cell responses to BG dissolution products, therefore highlighting the need for methodological standardisation. The following results presented in section 1.6 are adapted from Turner *et al*[126].

1.6.1 The role of Si alone

A number of publications have demonstrated that Si species (not derived from SBG dissolution) can promote (*in vitro)*, cell proliferation[60, 127–129], osteogenic differentiation[127, 129–131], and promote desirable gene expression for bone

regeneration[57, 60, 129–131]. Other studies observed that Si species can increase the

a)

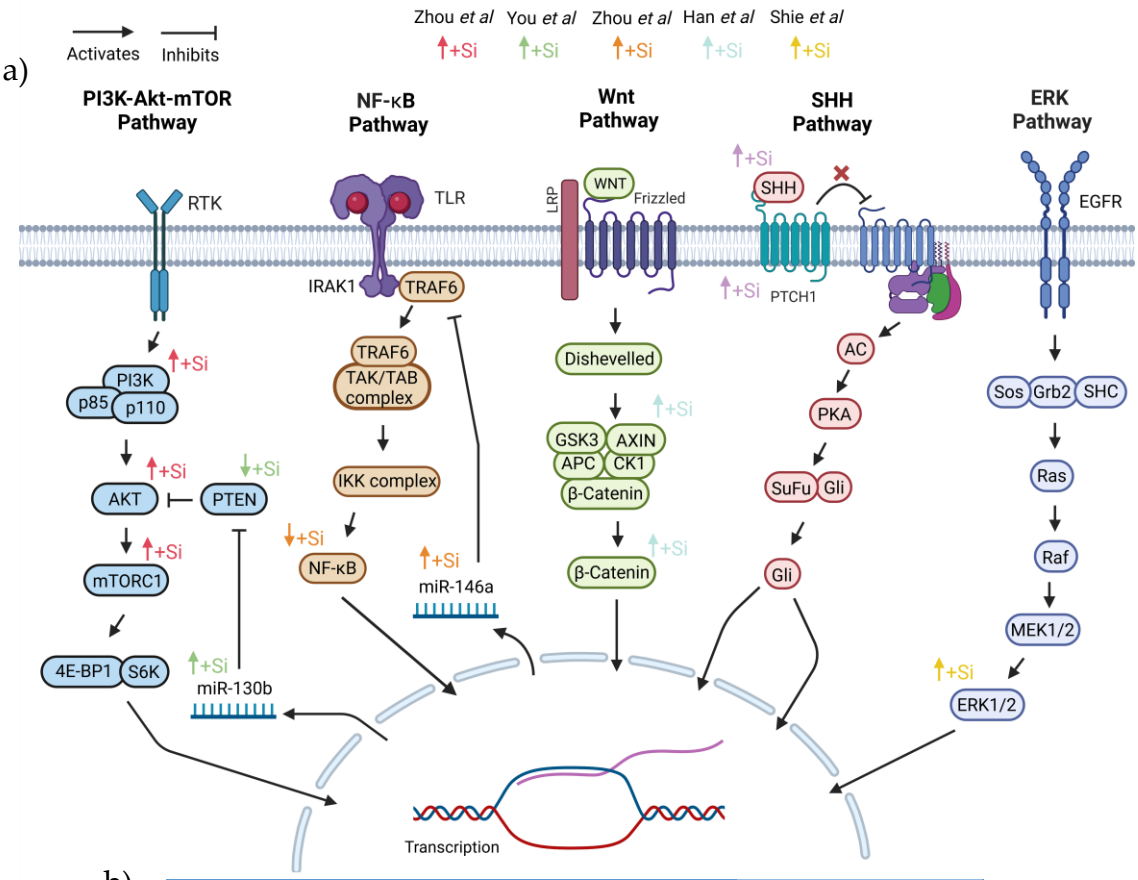

b)

Author	Cell type	[Si]	Pathway	Effect
You et al [133]	MC3T3-E1	10,20,50 μM	multiple	↑miR-130b ↓ PTEN (miR-130b inhibits PTEN)
Zhou et al [122]	MG-63 U2-OS	10 μM	PI3K-Akt-mTOR	↑ PI3K ↑Akt, ↑P-Akt ↑mTOR, ↑P-mTOR
Zhou et al [119]	BMSC (human)	10 and 50 ppm (357μM, 1.8 mM)	NF-kB	↑ miR-146a, ↓ NF-kB
Han et al [118]	BMSC (human)	0.63 mM	WNT/SHH	WNT pathway: ↑ B-Catenin, ↑ AXIN2 SHH pathway: ↑ SHH, ↑ PTCH1
Shie et al [134]	MG-63	4mM	ERK	↑ ERK, ↑ pERK

Figure 1.3 - **A summary of the studies investigating the effect of Si on specific cellular pathways.**

Only 5 papers have studied the effect of Si on cellular pathways, each suggesting a different mechanism (a). More information about these studies can be found in (b) [129, 186, 240, 271, 272]

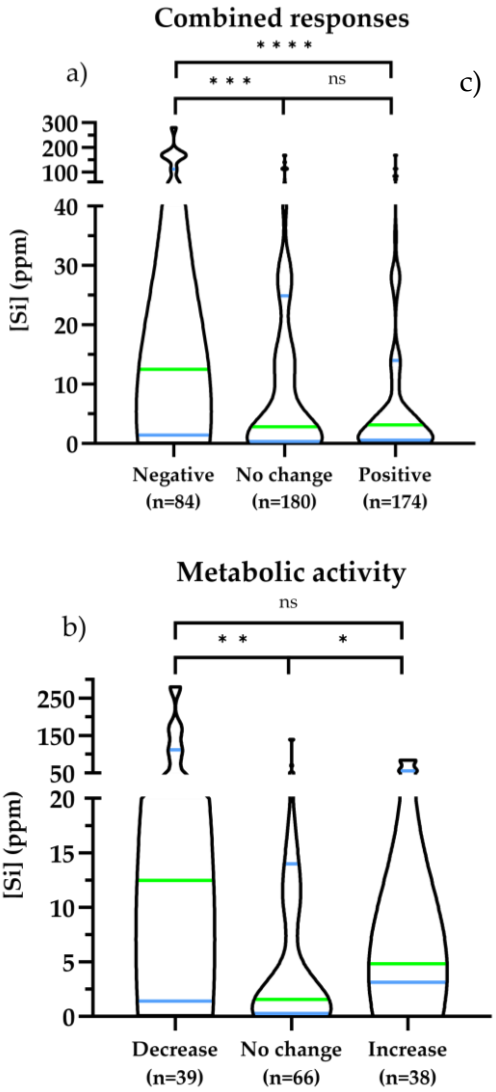

c)

N.a = 22		*N.a*	*n*	*n%*
Cell types	Osteoblast	15	274	62
	Stem cell	5	96	22
	Fibroblast	3	22	5
	Myocyte	2	22	5
	Osteoclast	3	18	4
	Endothelial	2	17	3
	Hepatocyte	1	3	<1
Cell species	Human	17	334	78
	Mouse	6	93	21
	Rat	1	1	<1
Cell behaviour characterisation	Metabolic activity	12	131	31
	ALP activity	9	92	22
	Cell number	8	95	23
	Biomineralisation	6	34	8
	Cell death	3	32	8
	Collagen production	5	28	7
	OCN production	2	11	3
	VEGF production	1	4	<1
Silicate source	Sodium silicate	17	292	65
	Silicon chloride	2	59	13
	Calcium silicate	1	36	8
	Dimethylsilanediol	1	36	8
	Beer	1	14	3
	(3-Aminopropyl)-triethoxysilane	1	12	3

Figure 1.4 - **The effect of Si derived from non-dissolution products on cell behaviour.**

*The median [Si] that is reported to cause a negative, no change or positive responses in all observed cell (a) and metabolic activity (b) responses in-vitro following exposure to silicate species derived from non-dissolution product. Quantification of number of articles (N.a), number of data points (n), percentage of total data points (n%) is presented in (c). [Si] above ~12ppm was observed to produce negative responses when compared to no change and positive outcomes in overall cell responses. In contrast, [Si] below ~2ppm was associated with no change responses in metabolic activity. *=p≤0.05, **=p≤0.01, ***=p≤0.005, ****=p≤0.001, n=number of data points.*

differentiation of osteoblast-like cells[128, 132], cause a significant decrease in osteoclast-like cell differentiation (100 μM Si) and regulate osteoblast and osteoclast crosstalk by modifying OPG-RANKL expression[57]. Several different intracellular mechanisms have been suggested for Si-induced cell behaviour. For example, Zhou *et al.* observed that sodium silicate (10-50 ppm/0.36-1.8 mM)

increased ALP activity in human osteoblasts whilst inhibiting NF-κB activity (a factor shown to inhibit osteoblastogenesis[133] and upregulate osteoclast formation[134]) by increasing the expression of microRNA-146a[130]. Si (0.6 mM/18 ppm) has also been shown to upregulate the Sonic Hedgehog (SHH) pathway (a regulator of genes associated with cell proliferation) in BMSCs by increasing expression of β-Catenin[129]. A summary of these and other suggested Si-induced pathways can be found in Figure 1.3*. Whilst these studies demonstrate that Si species affect bone cell behaviour, there is considerable variation within the literature in terms of both [Si] concentrations used, the cell type and species and whether different [Si] concentrations cause desirable or undesirable cellular outcomes.

1.6.2 The role of Si in BGs

A broad range of [Si] released from BG dissolution products have been used to investigate cellular interactions *in vitro* (from ~1 ppm[135, 136] to over 200 ppm[137]) with concentration dependant effects reported. For example, a concentration dependant increase in ALP activity in MC3T3-E1 cells was reported with SBG-conditioned medium containing [Si] ~10[138], 30[139] and 50[140] ppm. Similarly, Tsigkou Studies have observed that [Si] between 15-50 ppm could increase the metabolic activity[141] and cell proliferation[142] in foetal osteoblasts. Bielby *et al.*, reported [Si] as high as 160 ppm could increase bone formation and cell proliferation of murine and human osteoblasts[137]. Other studies have, however, shown adverse cellular outcomes with increasing [Si], in SBG conditioned media[135, 143] or found increased [Si] to have no significant effect[27]. It is unclear if the cellular interactions reported from SBG dissolution products are due to the Si ions acting independently or in combination with the other ions released from SBGs (e.g., Ca, P, Na). Different types or compositions of SBGs have different types of ions released and different ion release profiles. For example, 58S sol-gel derived glasses (60 mol% SiO_2, 36 mol% CaO and 4 mol% P_2O_5) do not contain sodium, whist most melt derived bioactive glasses do. Obata *et al.*,[144] directly compared the effect of varying the Si-

*Web of science search: Topic: ("silicate ions" OR "Soluble silicate" OR "silicic acid") AND Abstract: Pathway OR mechanism

concentration without altering the concentration of other ions and showed that increasing the concentration of Si species from 10 to 50 ppm in media conditioned with 45S5 Bioglass® increased metabolic activity, ALP activity and calcium deposition in osteoblast-like (SaOS-2) cells[145]. The same study, however, reported a significant reduction in metabolic activity when using MC3T3-E1 cells, suggesting cell-type specific responses to [Si]. Beilby *et al.*, also observed that whilst 58S (sol-gel) BG dissolution products (163 and 203 ppm Si) caused increased cell numbers in mouse-derived but not in human-derived osteoblast cultures[137]. The systematic approach used within this study will help determine if there is commonality in cellular response to [Si] released from SBGs, if there are differences between cellular responses to different types of glasses (e.g., sol gel or melt-derived) and the *in vitro* model parameters used (e.g., cell type/species/outcome measurements).

In vitro testing of BGs is important for ensuring safe translation and for understanding SBG-biological interactions, leading to the development of new BGs for specific applications. Compared to *in vivo* studies, *in vitro* SBG analysis allows for greater control over the experimental parameters, has lower variability, costs less, and often allows for greater resolution/characterisation and flexibility in analysis parameters. There is, however, considerable variation in the approaches used to evaluate SBGs *in vitro*, making comparative analysis from the literature difficult. While some of this experimental variation is undoubtably due to differing applications of the SBG (e.g., bone or wound) and experimental goals, there remains considerable variation in the experimental approach for SBG used for the same application and for similar investigational aims. Jablonska *et al.* provide an excellent overview of the approaches and assays used to evaluate SBGs *in vitro* and discusses the need for standardisation[146]. The focus of this review is to quantitatively compare *in vitro* outcomes of SBG dissolutions products and cellular interactions reported within the literature, and thereby facilitating the discussion on strategies for standardisation.

In addition to differing biological assays, there are also variations in the methodology used to obtain SBG conditioned media, the approach used to measure [Si] within the media, the reporting of methodological outcomes, and the respective assessment of successful cellular outcomes. This is perhaps best highlighted by the 22% of publications studying cellular response to SBG but not reporting the concentration of ions in the dissolution products used in their *in vitro* study (Figure 1.5). Or the variable terminology used within the literature (viability, proliferation, and toxicity) to describe metabolic assays outcomes when studying SBG-cell interactions.

Using a systematic analysis of the literature, this study aims to determine if there is relationship between [Si] released from SBGs and cell behaviour *in vitro*. The systematic approach also allows a reflective discussion on the methodological practices within the bioactive glass field to investigate biological response *in vitro*.

1.6.3 Review methodology

Web of science and Pubmed search engines were used to search for articles involving the use of both Si-containing BGs and their respective dissolution products on cells in vitro using the following search terms: ("bioactive glass*") OR bioglass AND (osteo* OR Macrophage* OR fibroblast* OR endothelial* OR chondro* OR monocyte* OR ("stem cell*")) AND ((Extract* OR ("conditioned Medi*") OR ("dissolution product*") OR ("Ionic product*") OR ("degradation product*")). A total of 665 articles were collected. Reviews, conference abstracts, book chapters and duplicates were removed. Articles were also excluded if results did not quantitatively assess cellular responses to dissolution products or measure [Si] in the cell culture media used for their in vitro experiments. To reduce the number of possible confounding factors (e.g., topography, porosity, surface area, surface chemistry and mechanical properties), only cell responses to dissolution products on tissue culture plastic were considered and not those of cells in direct contact with BG surfaces.

Following the exclusion of these and others that did not meet the exclusion criteria (Figure 1.5), a total of 76 articles were analysed. The [Si], glass composition, cell types, species, and changes to cellular behaviour (as determined by the percentage difference relative to the control without SBG DPs) were then collected from each article. To avoid bias during data extraction from studies, all collected values from studies had to be agreed by a second author. In the event of disagreement, a third author would be consulted and a decision for inclusion reached.

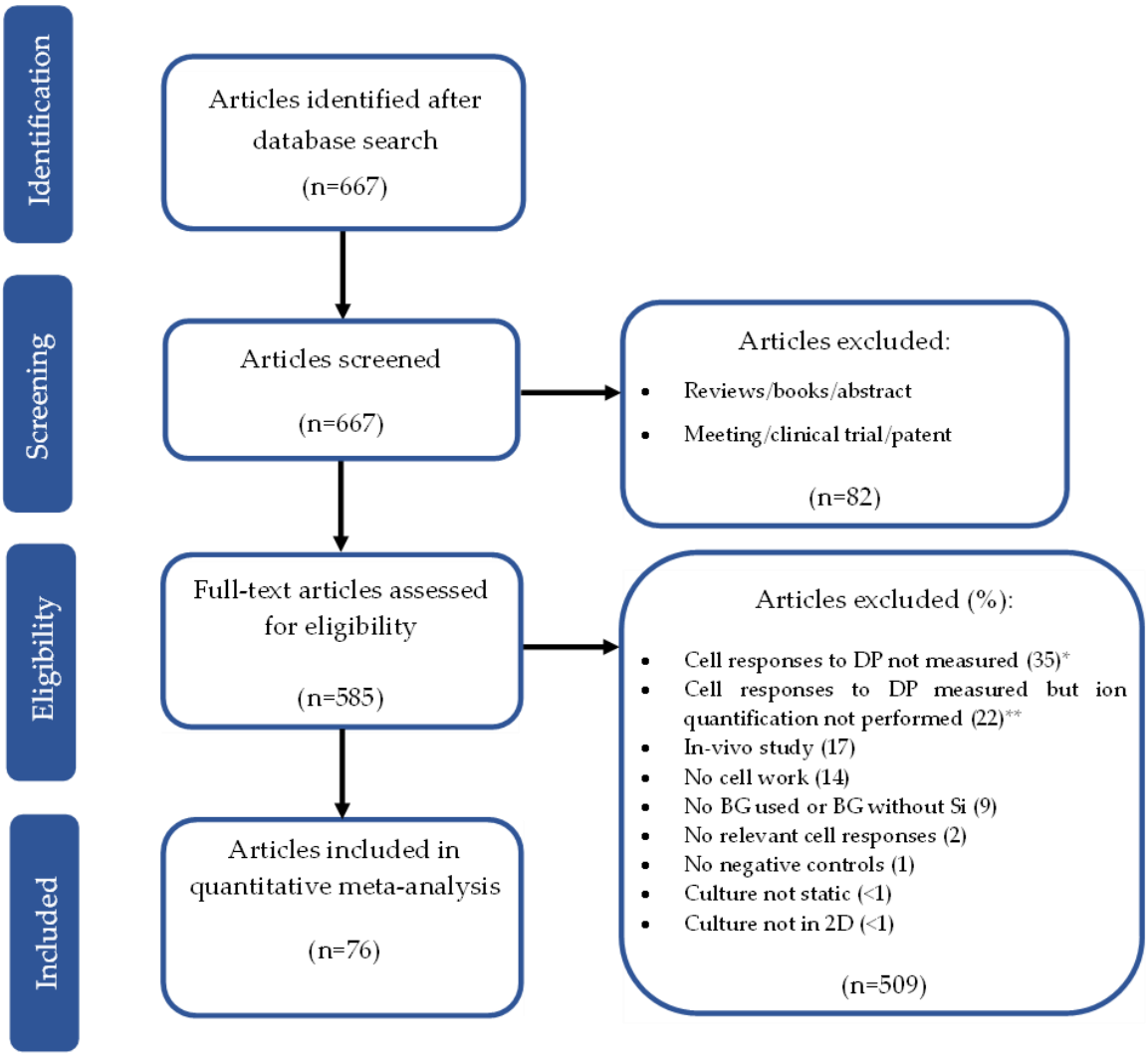

Figure 1.5 - **Prisma chart describing the process of article selection and the article exclusion criteria.**

**Includes cell cultures on scaffolds, ion quantification not performed in culture mediums and cells directly exposed to BG particles. **includes studies that quantified ion concentrations in DPs but did not report [Si].*

To determine the relationship between cellular response and [Si], at each [Si] data point, it was recorded if there was a significant increase ($P \leq 0.05$), a significant decrease, or no significant difference ($P > 0.05$) in cell behaviour compared to a non-treated control (without Si species or SBG dissolution products) as reported by the article. Quantitative cell responses to SBGs were recorded and grouped according to the type of behaviour (Figure 2c). For comparison of the effects of [Si] on cell behaviour, a minimum of 5 articles and 3 data points (e.g., 3 different [Si] or time points compared to control) were required for a response to be included for analysis. Cell behavioural outcomes in response to [Si] were then grouped according to different cell responses, along with their respective cell type, cell species and type of SBG. In addition to extracting cell responses to individual cell behaviours (e.g., biomineralisation or metabolic activity), we also investigated if there were overarching commonalities in cellular response to [Si]. This allowed the inclusion of cell behavioural assays where there was limited data and a larger data pool to minimise the impact of variations in paper specific experimental approaches (time points, cell type, media, cell seeding density etc.). Cell responses were combined as nominally desirable for regenerative medicine/material-interactions (e.g., increased proliferation, metabolic activity, expression of angiogenic factors, extracellular matrix production and decreased cell death), or undesirable (increased cell death, decreased proliferation, decreased biomineralisation etc.). For gene expression, due to the desirability of up- or down-regulation being dependent on the specific gene/inflammatory factor expressed/experimental aims, this data was analysed separately to other cellular responses but using the same methodological approach. The cell behavioural assays included in the combined figures are detailed in the result tables.

Protein production and enzyme activity (e.g., ALP activity and osteocalcin) data included a mixture of non-normalised data and data normalised to cell number (e.g., to DNA) or protein content. Normalised, non-normalised and combined

data were analysed separately and together. For this review, stem cells were categorised as: a) undifferentiated primary cells, b) capable of self-renewal without differentiation and c) could differentiate into more specialised cell types. Stem cell types included were derived from, adipose, mesenchyme, urine, dental pulp, and deciduous teeth.

The effect of calcium, phosphorus and sodium ion concentration ([Ca], [P] and [Na] respectively) released from glass dissolution products on cell responses was also evaluated. When comparing individual experimental parameters (e.g., type of SBG or cell type) the [Si] range was also determined as a possible confounder. For example, if the range of [Si] for articles investigating human cells was significantly different to the [Si] range used in articles investigating non-human cells. Unless stated in the results, the range of [Si] were not significantly different between the parameters studied.

To investigate whether Si species (not derived from SBG dissolution products) could influence cell behaviour directly, additional articles were collected (22 articles total). Articles were collected from WOS and Pubmed according to the following search terms: "orthosilicic acid" OR orthosilicate OR "soluble silica" OR "silicate ions" OR "soluble silicon" OR "ionic silicon" OR "biological silicon" (Topic) AND osteoblast* OR Macrophage* OR Fibroblast* OR endothelial* OR chondrocyte* OR monocyte* OR "stem cell*" OR osteoclast* OR myocyte* (Topic). Full dissolution of Si in these studies was assumed and therefore quantitative analysis of [Si] in Si-conditioned media was not recorded. All other exclusion criteria were used as in Figure 1.5 for SBGs.

1.6.4 Data analysis methodology

More than 1375 data points (excluding gene expression) were extracted from 76 SBG and Si articles. Once groups containing different cell responses, cell type and species group were formulated, each were then individually assessed for normal distribution using a Shapiro-Wilks test. Normally distributed significant differences between the [Si] that caused increased, decreased or no changes in cell behaviour was determined by a One-way Analysis of Variance (ANOVA) and post-hoc Tukey's test for multiple comparisons. Differences in non-normally distributed datasets were determined by a Kruskal-Wallis test, followed by a Dunn's test for multiple comparisons. Bin widths for plots assessing the frequency of cells responses compared to [Si] were chosen based on quartiles of [Si] distribution to ensure a near equal number of data points in each. The correlation of [Si] and percentage differences in cellular response (compared to the control) was also evaluated using a Spearman's correlation test. All results were statistically significant if they exceeded 95% confidence. Average [Si] is presented as median (M_d) 'X' ppm or mean (M_n) as 'X' ppm ± 'X' standard deviation.

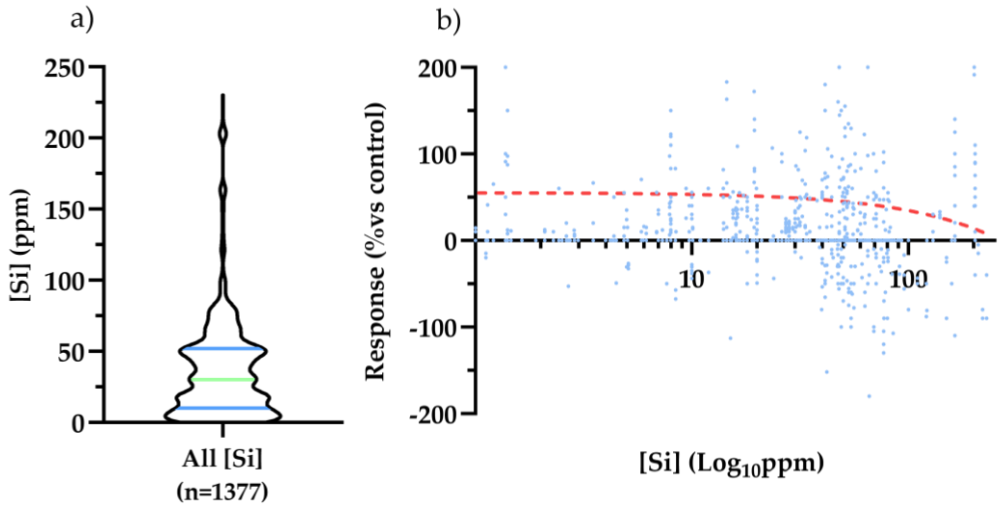

Figure 1.6 - **[Si] and cellular response percentage change.**

Linear regression analysis of the relationship between [Si] and 'response'### percentage change compared to a control (a). Frequency distribution of all [Si] values used in SBG dissolution products (b). 'Response' refers to any beneficial (+ve), negative (-ve) or non- significantly different cellular outcome (e.g., ECM mineralisation, proliferation, cell death etc.) as define in review methodology.

1.6.5 Descriptive comparison of SBGs compared with the wider field

The search criteria initially identified 665 *in vitro* research, articles involving *in vivo* data only (20%), no quantitative assessment of cellular responses to dissolution products (39%, e.g., cell morphology comparisons, or lacking an untreated control) or did not report [Si] in the media (22%) were excluded (Fig. 1). Research articles used for analysis were found to be dominated by those investigating bone (63%) followed by wound healing (17%), dental applications (12%), immunological responses (5%) and cartilage (3%) (Fig. S1a). A similar distribution of BG applications was found in both the articles collected during initial searches (n=665), and the articles selected for analysis, indicating that the analysed articles were representative of the wider SBG field (Fig. S1b).

1.6.6 Methodology used to analyse *in vitro* responses to SBG dissolution products

Human cells (59% of articles), stem cells (39%) and osteoblasts (34%) were the most commonly used cells (respective to species and cell type) to investigate SBG DPs and their cellular interactions. Metabolic activity assays were the most frequently reported cellular outcome (68% of articles), which could be due to 10993 ISO standard, which suggests the reporting of cellular metabolic activity in response to medical devices. There was high variance in the type of metabolic assays used (Figure 1.11g), with both MTT and WST-8 assays the most frequently observed (51% and 29% of articles respectively). Metabolic assays that produce soluble products e.g., WST-1, WST-8, Presto and Alamar blue, as opposed to MTT which requires a solvent to dissolve insoluble formazan crystals, were more frequently used in the last five years. The use of MTT in the last 5 years (33% of articles investigating metabolic activity) was lower than that of the previous 5 years (2016-2011, 67% of articles). Whilst most articles used metabolic activity

assays, normalisation of this data (metabolic activity per cell number) was observed in only ~2% of collected articles. Only 24% of articles used a direct measure of cell number (as opposed to metabolic activity) and of these, 85% quantified DNA from lysed cells (Figure 1.11g). The most common cell-culture time points used to study SBG DP interactions were for 3 time points (when evaluating metabolic activity) (1, 3, 7 days accounted for 24% of articles). Approximately 25% of articles used 2 time points or less (1 and 2 days accounted for 15% of papers). For studies that investigated in vitro bone nodule formation or biomineralisation (12% of articles), quantification of calcium deposition was the most common outcome measurement (90% of articles), compared with nodule area (7%) and nodule count (3%).

The most common bioactive glass composition (within the search criteria) was 45S5 Bioglass® (30% of articles), whilst the commercial composition S53P4 (Bonalive®) accounted for 3% of articles. Sol-gel glass of the composition 58S and 70S30C were investigated in vitro (12% and 1% of articles respectively), in addition to the melt-derived 13-93 composition (1% of articles). Approximately 54% of articles, reported on SBGs compositions that were unique to the individual article within our search criteria, often these articles were investigating the effect of additional therapeutic ions (e.g., Co, Sr, Li) added to the base SBG composition. Magnesium and strontium (both 10% of articles) were the most common additional ion investigated.

The mean [Si] within the cell culture media used to investigate SBG dissolution products with cells (*in vitro*) was 37.8 ppm ± 36.6 (Figure 1.6a). Interestingly, for some cell and species types, researchers used (on average) different [Si] concentrations (Figure 1.12). A higher [Si] was used in human cells (M_n = 41.5 ppm ± 37.3) compared to non-human cells (M_n = 32.5 ppm ± 34.8) and studies using stem cells (M_n = 41.1 ppm ± 34.3) used a higher [Si] range compared to non-stem cells (M_n = 35.6 ppm ± 37.8).

1.6.7 Does Si concentration influence cell responses?

When all cellular responses were combined, there was a [Si] concentration dependent effect on cell behaviour, where the [Si] that caused increased (positive) effects (M_n = 40.3 ppm ± 41.2), was higher than the [Si] that caused no significant difference (M_n = 32.2 ppm ± 28.3), but lower than the [Si] that caused decreased (negative) outcomes (M_n = 59.8 ppm ± 48.2) (Figure 1.7, $P \leq 0.001$). The most frequently reported outcome, on the effect of [Si] on cellular responses, were not significantly different (no change) to untreated controls without SBGs (788 data points). This compared with 437 [Si] reported data points that caused significantly increased outcomes and 157 data points reporting significantly decreased outcomes. The frequency of negative outcomes was also observed to increase with increasing [Si] (Figure 1.7b). Negative outcomes were found to occur ~3 times more frequently above 50 ppm [Si] than compared to below. The frequency of reported significantly positive outcomes were found to be most common in the [Si] range 30-60 ppm (33%). There was, however, only a very weak negative correlation between [Si] and the magnitude of cell response (percentage difference to the untreated control without SBG dissolution products), (R=-0.08) (Figure 1.5b).

a)

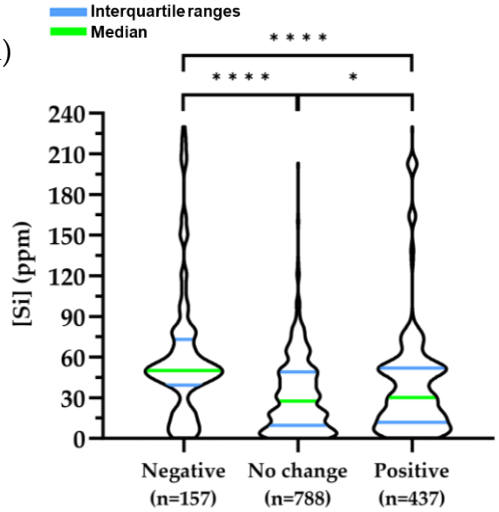

b)

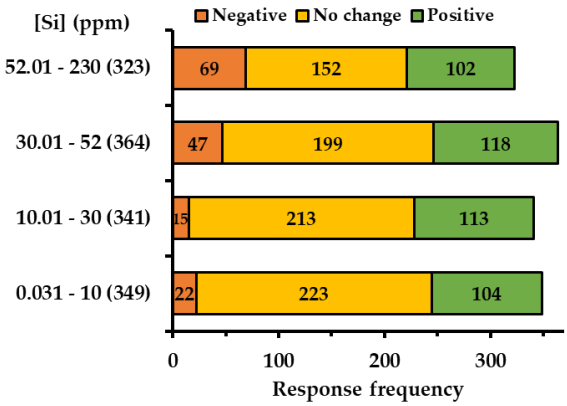

c)

N.a = 76		*N.a*	*n*	*n%*
Cell types	Stem cell	32	549	40
	Osteoblast	26	529	38
	Endothelial	10	144	10
	Fibroblast	4	43	3
	Chondrocyte	2	54	4
	Macrophage	4	35	3
	Osteoclast	1	12	1
	Osteocyte	1	9	1
	Keratinocyte	1	9	1
	Cementoblast	1	2	<1
Cell species	Human	42	815	59
	Mouse	15	264	19
	Rat	11	221	16
	Rabbit	4	56	4
	Cow	1	14	<1
	Dog	1	12	<1
Cell behaviour characterisation	Metabolic activity	52	718	52
	ALP activity	22	216	16
	Cell number	12	127	10
	Biomineralisation	15	121	9
	Cell death	10	59	4
	Collagen production	7	48	3
	OCN production	5	45	3
	VEGF production	10	48	3
Glass types Si,Na,Ca,P only)	45S5	23	278	38
	58S	9	148	20
	60S	5	59	8
	80S	2	38	5
	S53P4	2	15	2
	Other	41	188	26
Glasses containing	Strontium	5	90	18
	Copper	4	69	14
	Cobalt	4	60	12
	Fluorine	3	64	13
	Boron	2	42	8
	Lithium	4	39	8
	Zinc	3	30	6

Figure 1.7 - **The effect of [Si] released from bioactive glasses on cell behaviour.**

*The median [Si] (a) and frequency (b) that is reported to cause a significant negative (decrease), no significant difference (no change) or a positive significant (increase) in all observed cell responses in vitro, following exposure to Si released from bioactive glasses. [Si] above 50 ppm was found to cause significantly more negative outcomes, whilst positive cellular responses occurred at higher [Si] than outcomes that were not significantly different to non-Si controls (Median=30 and 25 ppm respectively – a). Quantification of number of articles (N.a), number of data points (n), percentage of total data points (n%) is presented in (c). *=P≤0.05, ****=P≤0.0001.*

1.6.8 Does cell type and species influence overall responses to dissolution products?

The [Si] reported to cause decreased (negative) outcomes in human cells (M_d = 54.3 ppm) was, on average, higher than non-human cells (M_d = 31.4 ppm), suggesting that human cells can tolerate higher [Si] levels (Figure 1.8a). There was no difference between human and non-human cells in the [Si] that was reported to cause positive outcomes. The median [Si] in studies using human cells (M_n = 41.5 ppm ± 37.3) were found, however, to be significantly higher than those using non-human cells (M_n = 32.5 ppm ± 29.6). This higher [Si] range in human cell studies, may therefore, account for the difference between human and non-human cells, rather than cell specific responses. Cell type (primary vs non-primary, or stem cells vs non-stem cells) did not significantly influence the [Si] reported to cause negative or positive cellular responses (Figure 1. a/c). Whilst the range of [Si] used to investigate primary and non-primary cells was not significantly different, there was a difference between the average [Si] used to investigate stem cells (M_n = 41.3 ppm ± 34.2) and those using non-stem cells (M_n = 35.6 ppm ± 37.8) ($P \leq 0.001$). Considering that higher [Si] is associated with increased negative effects (Figure 1.6), the lack of significant differences between stem cells and non-stem cells, may suggest increased tolerance to a higher [Si] range in stem cells (compared to non-stem cells).

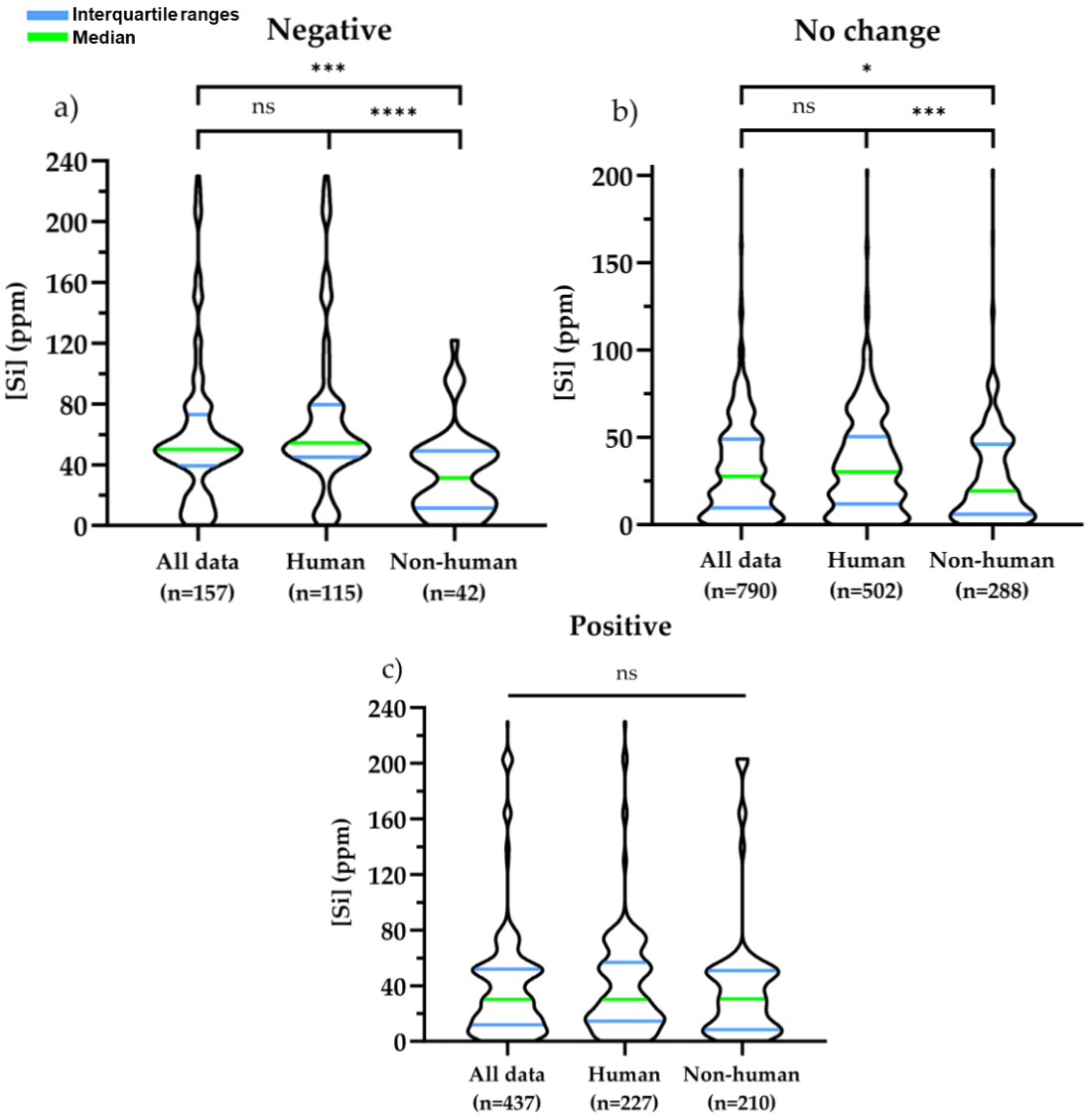

Figure 1.8 - **Species cell responses to [Si] released from bioactive glasses and ceramics.**

*Comparisons between cell species in response to [Si], negative or undesirable cellular responses (a) or no significant change (b) were reported at lower [Si] in no-human cells compared to human cells (a) *=P≤0.05, **=P≤0.01, ***P=≤0.001, ****=P≤0.0001.*

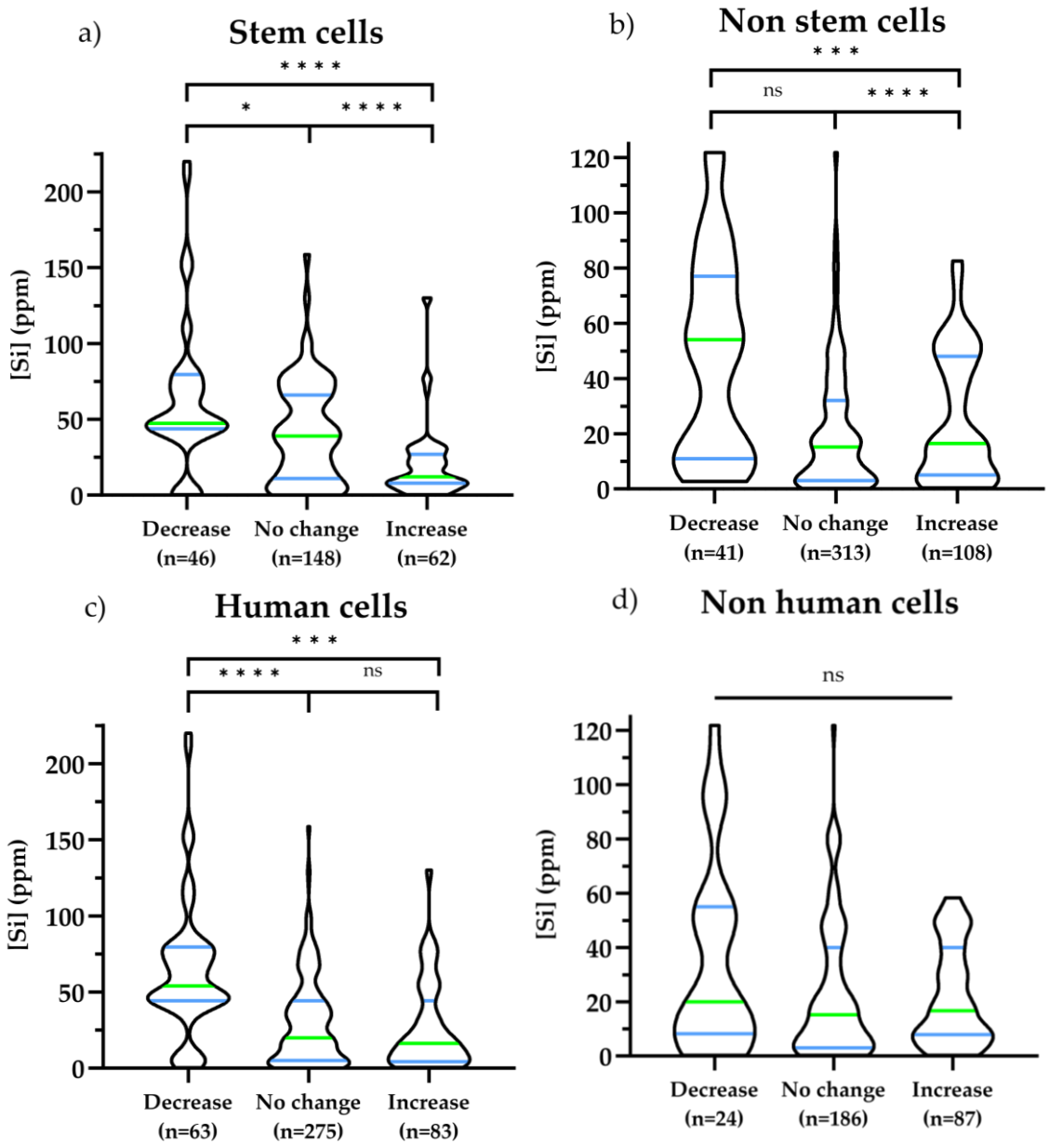

Figure 1.9 - **[Si] and metabolic activity of cell type and species.**

*[Si] above 50 ppm was found to cause negative cell responses in stem cells (a) and human cells (c) when compared to non-stem and human cells (b and d). *=P≤0.05, **=P≤0.01, ***=P≤0.001, ****=P≤0.0001, n=number of data points.*

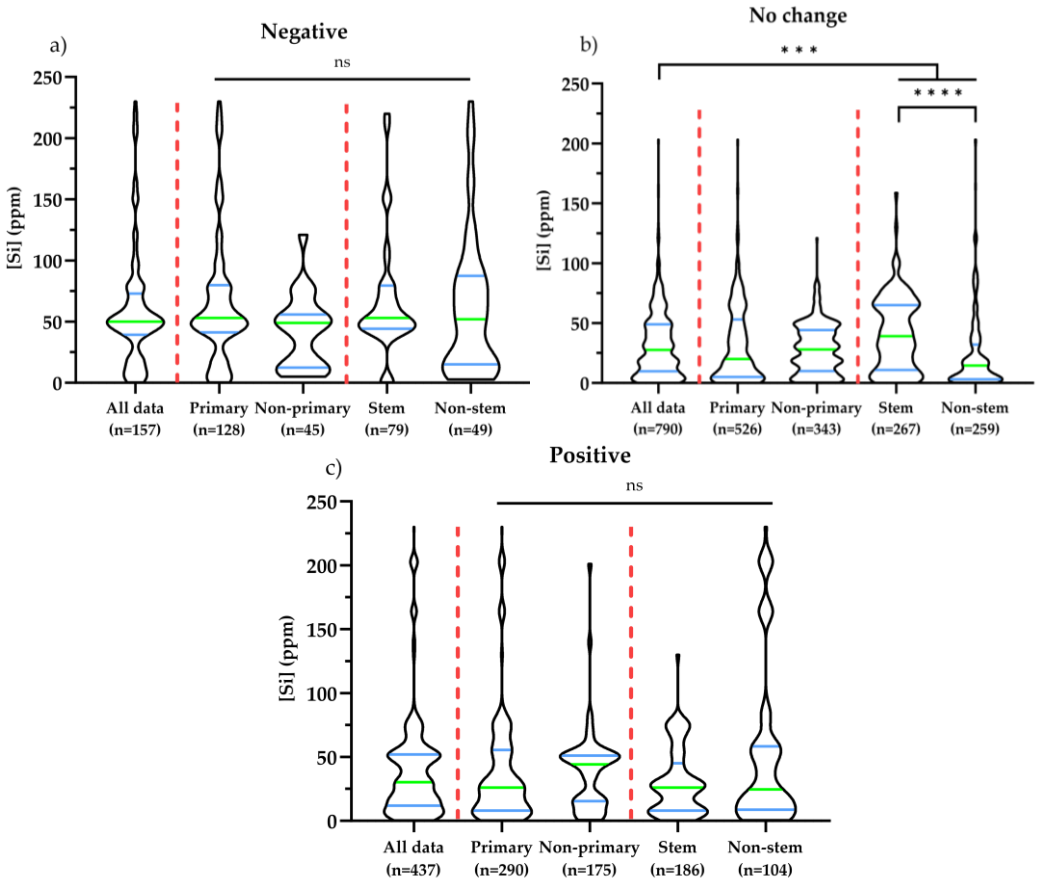

Figure 1.10 - **Cell type responses to [Si] released from bioactive glasses and ceramics.**

*A higher median [Si] was reported to cause a positive or desirable cellular response in non-stem cells compared to stem cells (p≤0.005). 'Primary' contains all in-vitro studies and responses from non-cancerous or immortalised cell lines. 'Stem' contains cells that adhere to characteristic definitions 'a', 'b', and 'c', as described in methods and materials. *=p≤0.05, **=p≤0.01, ***=p≤0.005 when compared with 'all data'. Red dotted lines highlight that primary cells were compared to non-primary, and stem to non-stem cells.*

1.6.9 Metabolic activity, cell number and death

Metabolic activity (Figure 1.7c) was the most common cellular assay used to analyse cell responses to SBG dissolution products (52% of articles) and produced similar trends to those in overall cellular response (Figure 1.7a) where an increase in the frequency of negative responses was observed in metabolic activity responses with increasing [Si] Figure 1.7b). Studies that used [Si] at or above 90 ppm, did not report increased metabolic activity (Figure 1.11a). It is interesting to note that the [Si] that was reported to cause decreased metabolic activity in human cells was higher than the [Si] that caused positive outcomes,

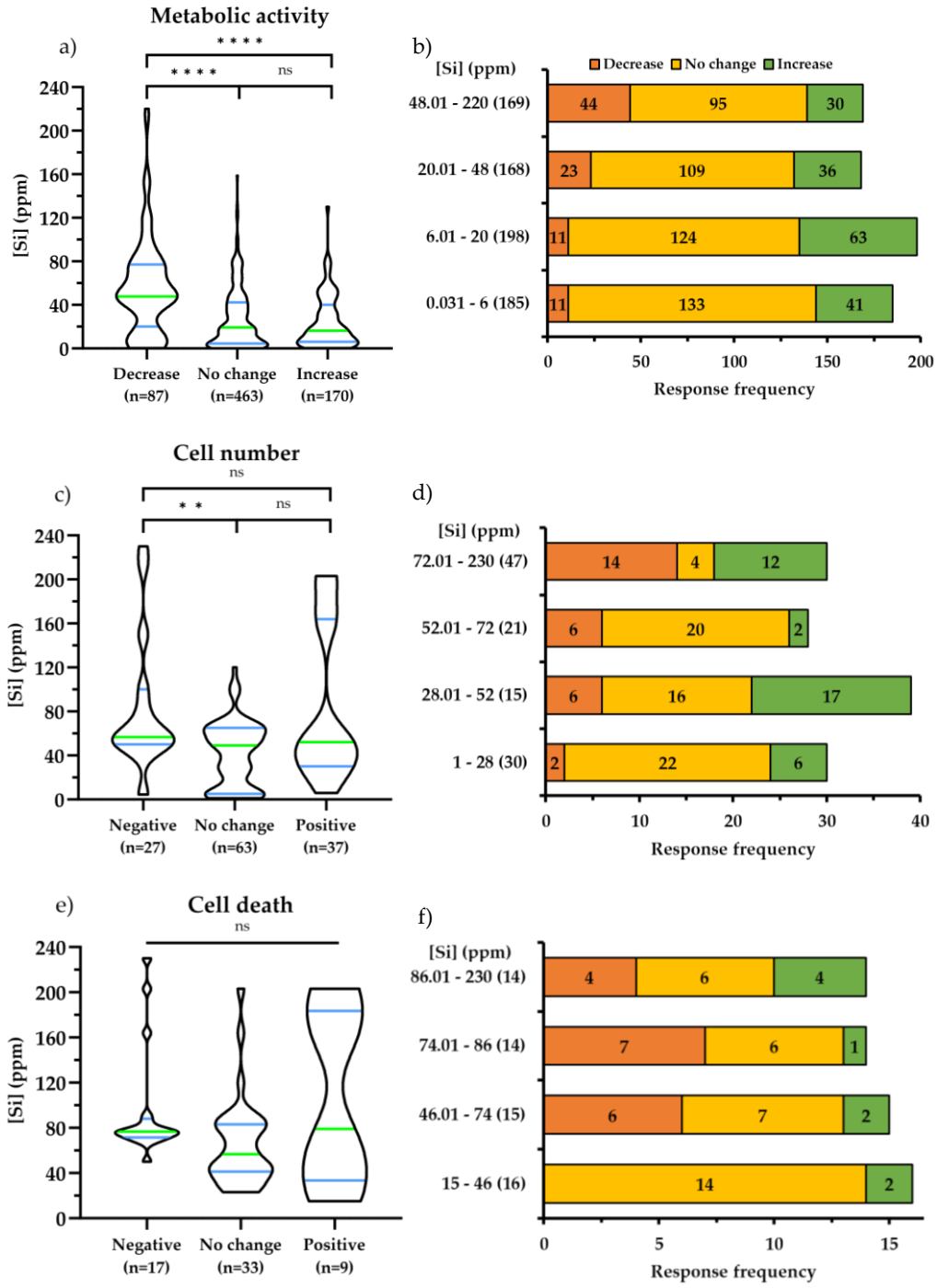

Cell behaviour characterisation	*Assay type*	*n*	*%*
Metabolic activity (N.a=52)	CCK-8	35	49
	MTT	42	36
	Alamar/Presto blue	65	8
	MTS	61	4
	XTT	30	2
		17	
Cell number (N.a=19)	DNA quantification	96	83
	Cell counting (Manual or software)	21	18
Cell death (N.a=10)	Membrane integrity	51	82
	DNA fragmentation	8	13
	Apoptotic morphology	3	5

Figure 1.11 - **The influence of [Si] released from bioactive glasses on cell metabolic activity, proliferation, and cell death.**

*Median [Si] and frequency of negative, no change and positive proliferative cell responses of metabolic activity (a/b), cell number (c/d) and cell death (e/f) following culture with bioactive glasses and ceramics. Quantification of frequency and percentage of assay types used in studies are presented in (g). Significant differences were observed in negative metabolic cell responses above ~50 ppm compared to no change and positive data. No significant trends were found in proliferation or cell death responses. *=p≤0.05, **=p≤0.01, ***=p≤0.005, ****=p≤0.001, N.a=number of articles, n=number of data points, n%=percentage of total data points.*

but this was not observed in non-human cells (Figure 1.9c). There were no other species or cell type specific differences in the metabolic activity, cell number or cell death responses to [Si] observed.

Cell number data was similar to metabolic activity, demonstrating that concentrations of Si above 40 ppm were associated with an increase in the frequency of negative cell responses (Figure 1.8c/d). There was, however, no difference between the [Si] reported to increase or decrease cell number, with the most reported outcome that [Si] did not significantly change cell number. There was also no significant difference observed in the mean [Si] reported to increase cell death (Figure 1.11e/f), but this may reflect the limited data points (4% of articles - Figure 1.7). The frequency of reported significant cell death outcomes did, however, increase with increasing [Si], with 44% of data points above 60 ppm reported to cause a cell death compared to 2% below this concentration.

1.6.10 Osteogenic and angiogenic responses to [Si].

No significant differences were observed between [Si] and osteoblast differentiation markers (osteocalcin and ALP activity), biomineralisation, or VEGF (Figure 1.12a-d). When considering the differentiation of stem cells alone (9 articles), the same was true i.e., there was no difference in the [Si] that caused increased or decreased osteogenesis/angiogenesis. Given the difference in ALP

expression at different stages of osteogenic differentiation, the effect of time was also considered. No difference in ALP activity were observed at any time point up to (and including) one, two or three weeks. The frequency of articles reporting an increase in ALP activity in response to [Si], is, however, 3 times more common than decreased ALP activity. Most studies (70% of articles, 75% of data points) normalised ALP enzyme activity to either cell number (total DNA) or total protein, but only 33% of articles (30% of data points) normalised osteocalcin or VEGF production (30% of articles) to cell number. Without normalisation it is difficult to determine whether the influence of [Si] on ALP activity is due to cell number differences or individual cell response. No differences, however, were found in the effects of [Si] on either the ALP normalised or non-normalised data. Several different methods were used to determine biomineralisation, with Alizarin red staining being used most common, followed by elemental analysis and nodule (number and area) quantification. For articles that quantified calcium levels by cetylpyridinium chloride extraction (the most common quantification approach) there was no relationship between [Si] and calcium deposition. When all gene expression responses to [Si] were combined, in a similar manner to other cellular responses, increasing [Si] was associated with negative outcomes. The median [Si] that caused decreased gene expression (negative responses) Mn = 38.28 ppm ± 30.25 was higher than [Si] reported to cause increased gene expression (Figure 1.12a). Most genes studied were associated with osteogenic differentiation (e.g., RUNX-1, OSX, BSP, ALP, BMP), extracellular matrix (ECM) production (collagen type I) or angiogenesis (VEGF), where an increase gene

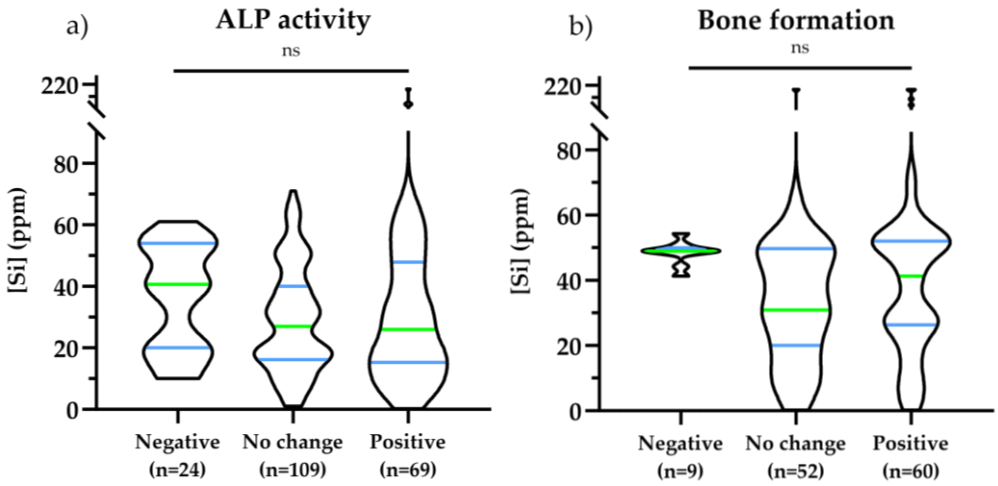

Cell responses	*Cell type*	*n*	*%*	*Assay type frequency (%)*
ALP activity	Stem cell	79	35	PNPP substrate reaction (100)
(N.a=27)	Osteoblast	129	58	Data normalised (79)
	Dental cells	15	7	
Biomineralisation	Stem cell	55	45	Calcium quantification (90)
(N.a=19)	Osteoblast	66	55	Nodule area (7)
				Nodule count (3)
VEGF production	Stem cell	13	34	ELISA (100)
(N.a=10)	Osteoblast	17	45	Data normalised (30)
	endothelial	6	16	
	Fibroblast	2	5	
Osteocalcin production	Stem cell	24	55	ELISA (100)
(N.a=6)	Osteoblast	20	45	Data normalised (31)

Figure 1.12 - **The influence of [Si] in cell type specific responses.**

Median [Si] and frequency of negative, no change and positive ALP activity (a), biomineralisation (b) and osteocalcin (c) and VEGF protein production (d) cell responses following culture in mediums containing Si released from bioactive glasses and ceramics. Quantification of frequency (n) and percentage of cell, species and material types used in studies are presented in (e). No differences were found in any response type. N.a=number of articles, n=number of data points, n%=percentage of total data points, 'data normalised' refers to data that has normalised to cell numbers.

expression would be desirable. Decreased gene expression for VEGF, ALP, OCN, OSN, RUNX-2, collagen T1, were observed at higher [Si], but the reverse was observed for OSX and BSP (Figure 1.12b).

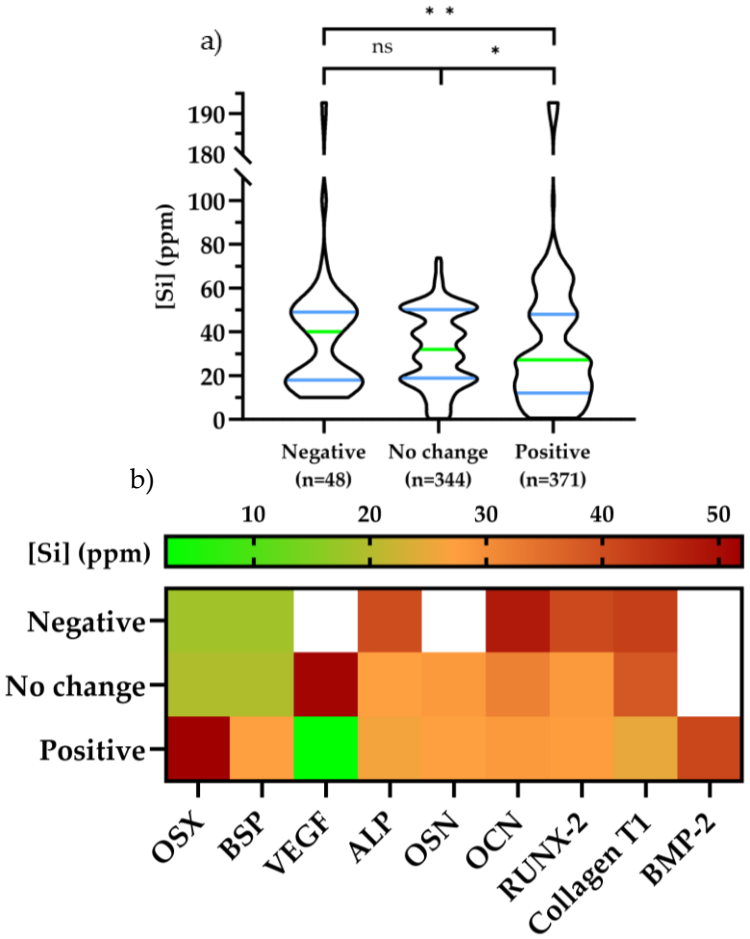

Figure 1.13 - **[Si] and gene expression.**

*Positive outcomes when all observed genes were combined (a) occurred at significantly lower [Si] than both negative and no change responses. No significant differences were found between the responses of individual genes and [Si] (b). *=P≤0.05, **=P≤0.01, n=number of data points, blank (white) squares show where no data was collected.*

1.6.11 Glass types

Different SBG compositions have been produced for various medical applications, but it is unclear if there is commonality between the type of BG and *in vitro* cellular outcomes. The most common SBG composition used within our data set was melt-derived 45S5 Bioglass® (23 articles), followed by sol-gel derived 58S (9 articles). We compared cellular outcomes between all melt-derived BGs (containing just Si, Ca, P, Na), with 45S5 Bioglass®, 58S glasses and glasses containing additional therapeutic ions (e.g., Sr, Co, Mg). Interestingly, negative,

and positive cellular responses to 58S dissolution products, were observed to occur at a higher [Si] than for the other glass types. (Figure 1.14b). The range of [Si] in 58S studies is, however, higher (M_n = 69.0 ppm ± 65.0) than the other SBGs (P≤0.01). Additional therapeutic ions were found to alter the cellular response to [Si] concentrations, where positive outcomes occurred at lower [Si] compared to 45S5, and negative outcomes occurred at higher [Si] compared to 45S5. Considering Si and the therapeutic ions are released proportionally, this may indicate the influence of the therapeutic ions on cellular response.

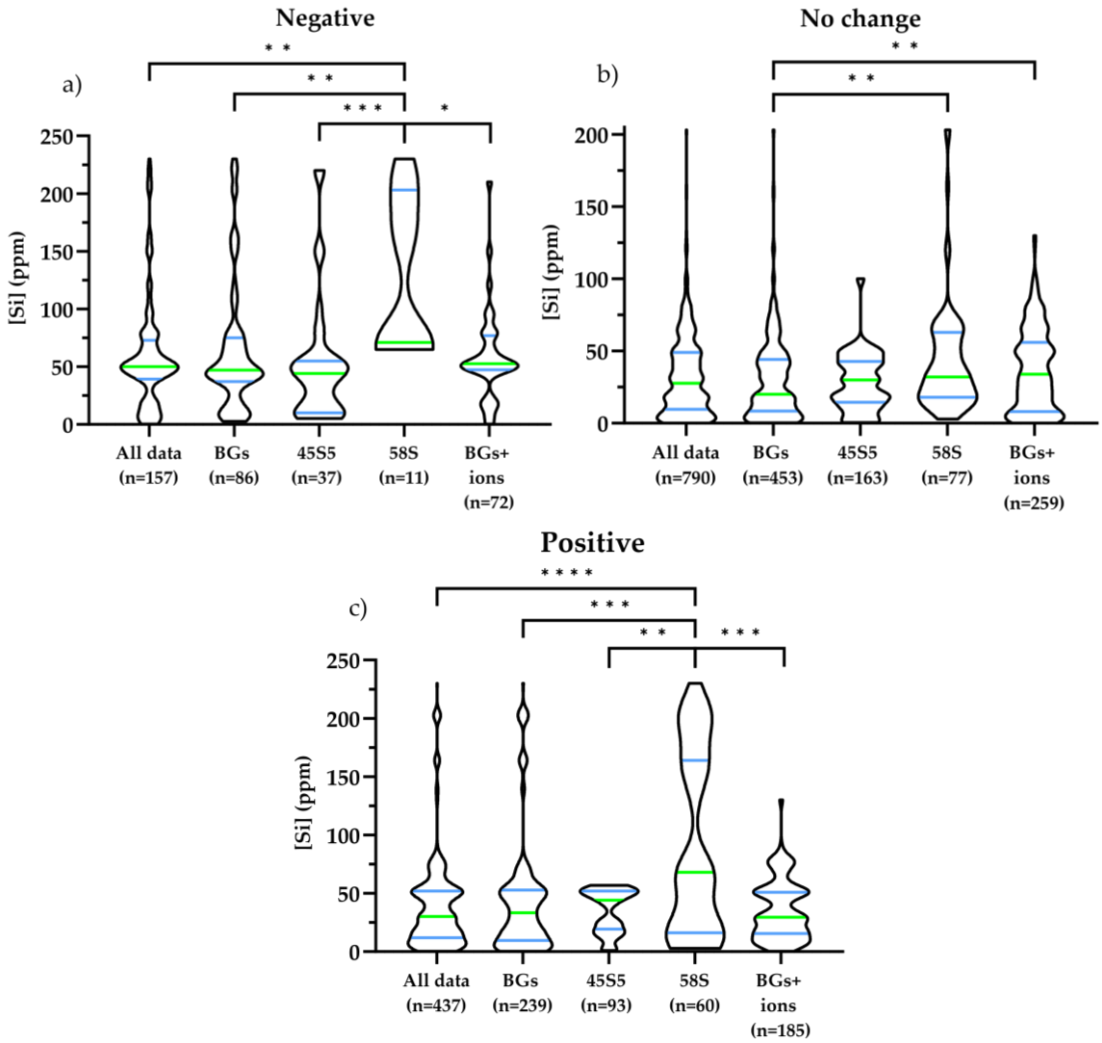

Figure 1.14 - **Glass types and [Si].**

*Median Si of negative (a), no change (b) and positive (c) cell responses to all observed in-vitro studies when cultured with Si released from 45S5 bioactive glass ('45S5'), BGs containing only silica, calcium, phosphorus and sodium ('BGs') and the addition of other metal ions ('BG+metal ions'). An increase in [Si] was observed to cause both negative and positive outcomes when released from 58S. Different material categories are compared with combined cell responses ('all data'). *=p≤0.05, **=p≤0.01, n=number of data points.*

1.6.12 The effect of calcium, sodium, and phosphorus ions in dissolution products

The concentration of other ions released from SBGs, apart from [Si], may also influence cellular interactions. The concentration dependent effects of calcium,

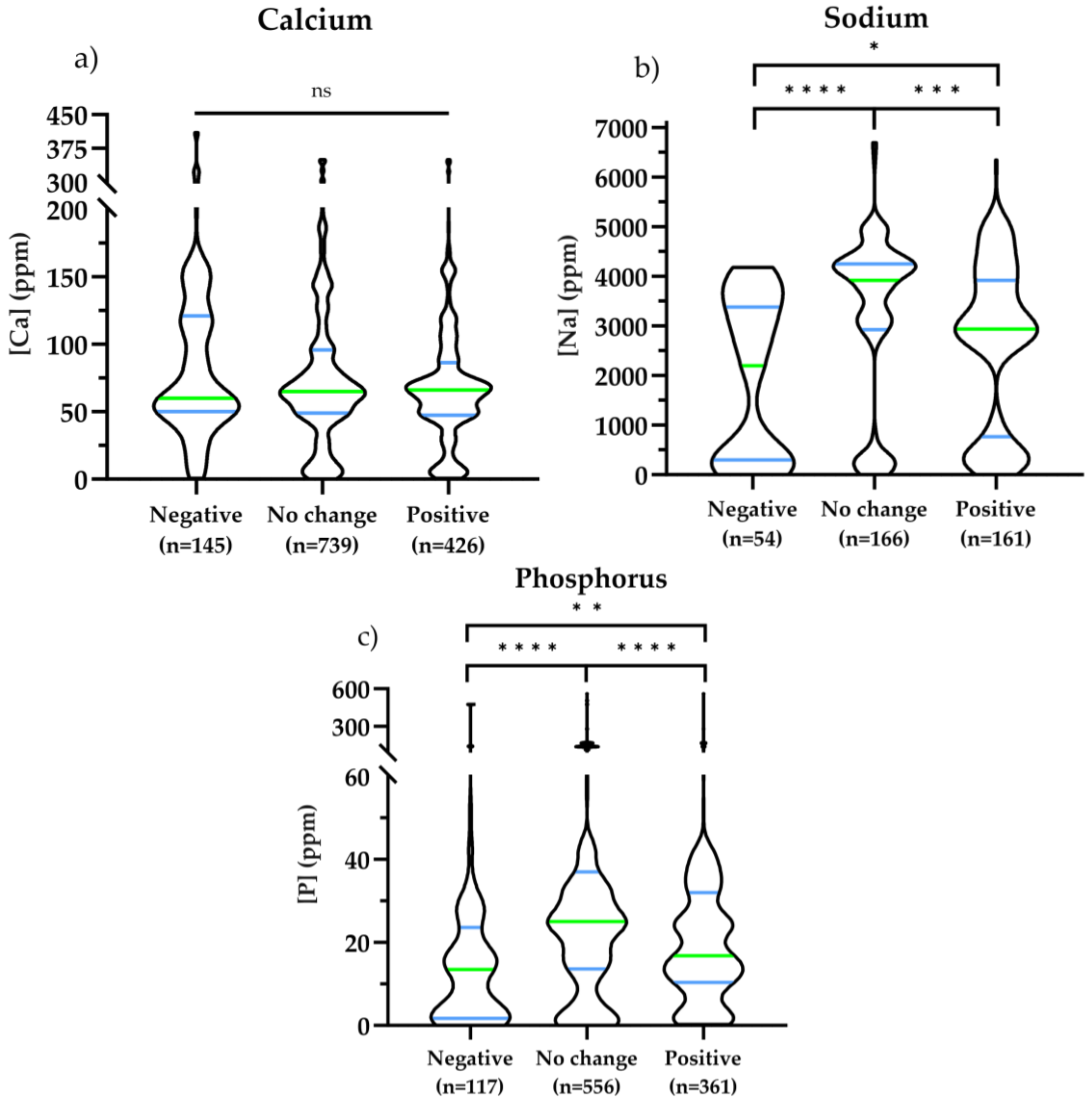

Figure 1.15 - **The influence of [Ca], [Na] and [P] on overall cell responses.**

*Cell responses in all observed in-vitro studies when cultured with dissolution products containing calcium (a), sodium (b) and phosphorous (c). Overall responses to Sodium at between 3500 and 4500 produced significant no change data compared to negative and positive data. Concentration between 18 and 25ppm in phosphorus were found to cause positive responses whilst no significant trends were observed in either calcium. *=p≤0.05, **=p≤0.01, ***=p≤0.005, ****=p≤0.001, n=number of data points.*

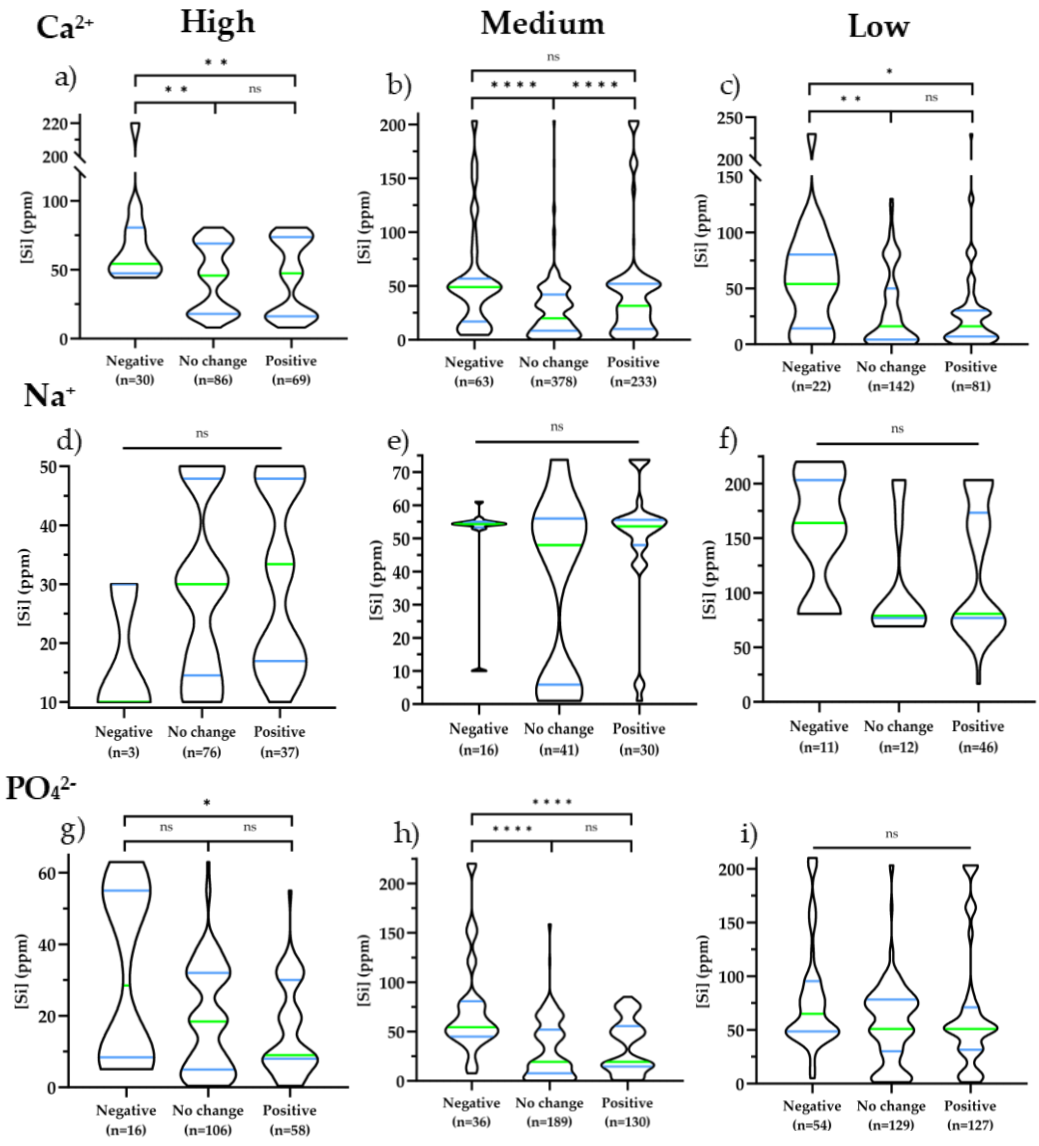

j)

Ions	*High (ppm)*	*Medium (ppm)*	*Low (ppm)*
Calcium	125-83.31	83.3-41.61	41.6-0
Sodium	5000-4001	4000-3001	3000-2000
Phosphorus	40-26.661	26.66-13.31	13.3-0

Figure 1.16 - **Determining the influence of Ca, P, Na on cellular responses to Si released from bioactive glasses.**

*Each ion is divided into ranges determined by where the majority of data exists in Fig. 8a, b, c. Ranges are divided into equally into three groups 'highest, 'medium', and 'lowest' concentrations of Ca, P and Na reported in the culture medium. [Ca] at high and medium concentration were observed to cause negative and no change cell response at concentrations above ~50ppm Si. [P] at medium concentration was observed to cause no change cell responses when [Si] ~50ppm. No visible trends were observed with any Na concentration grouping. *=P≤0.05, **=P≤0.01, ****=P≤0.001, n=number of data points.*

phosphorus and sodium ([Ca], [P], [Na] respectively) on cell behaviour were, therefore, also compared (Figure). Contrary to the effects of [Si] concentrations on cell behaviour, the concentration of [P] that is reported to have negative cellular outcomes (M_d = 13.5 ppm) were lower ($P \leq 0.001$) than the [P] reported to have positive outcomes (M_d = 16.8 ppm). A similar effect of [Na] on cell was reported, with negative outcomes occurring at a lower median [Na] (M_n = 1963 ppm ± 1599) compared to those producing positive effects (M_n = 2673 ppm ± 1630). No significant differences were identified in the effect of [Ca] on cellular behaviour (Figure 1.15a). it was also investigated whether these ions influence the concentration at which Si affects cell behaviour. Concentration ranges of each ion ([Ca], [P], [Na]) were split into equally sized 'high', 'medium' and 'low' groups. A similar cellular response to [Si], as observed in all data (Figure 1.16), was found in SBG medium regardless of [Ca] level, with higher [Si] concentrations associated with negative outcomes. The difference between the mean [Si] causing negative and positive outcomes, was however, greater in the 'low' [Ca] group (41.6-0 ppm), compared with higher [Ca] (125-83 ppm), indicating that calcium may influence the effect of [Si] (Figure 1.16) on cell behaviour. Interestingly, [P] appeared to have the opposite effect, where a greater difference between cellular responses to [Si] (the difference in the reported negative or positive effects) was present in the groups containing more phosphorus within the SBG media, and there was no difference in responses to [Si] in the group with the 'low' [P] concentration (13.3-0 ppm) (Figure 1.16) No significant trends were observed between [Si] and [Na] in any group.

1.6.13 Differences between Si species and BG dissolution products on cell behaviour.

To investigate whether Si species could influence cell behaviour independently of other ions released from BG (Na, Ca and P), additional articles focusing on the individual effect of Si species (not resulting from BG dissolution products) were

collected (22 articles). In a similar manner to BG conditioned medium, Si ions alone also caused increasingly negative outcomes with increasing [Si]. The median [Si] reported to cause a negative outcome (Mn = 56.6 ± 77.6 ppm) was significantly different (P≤0.001) to that reported to cause no change (Mn = 18.7 ± 33.9 ppm) and positive outcomes (Mn = 15.4 ± 30.5 ppm). These Si concentrations were significantly lower when compared to responses to [Si] in SBG dissolution products (P≤0.001). There was, however, a difference in the [Si] range used in Si ions used alone (Mn = 24.5 ppm ± 47.0) compared to those in dissolution products (Mn = 37.8 ppm ± 36.5) (P≤0.0001), which may be a confounding factor in interpreting the difference between SBGs dissolution products and Si alone. Whilst sodium silicate was the most common Si precursor for conditioning cell culture medium (65% of articles), silicon chloride (13%) and calcium silicate (8%) have also been studied. No differences were found between Si source and cell outcomes.

1.6.14 Discussion

By using a systematic quantitative approach, this review compared cellular responses to [Si] released from SBGs within the literature. Despite different experimental models (cell types, seeding densities, media, outcome measurements etc.) and different compositions of SBGs, commonalities were still observed on the effect of [Si] on cell behaviour. This is important for developing our understanding of how soluble Si effects cell behaviour (which remains poorly understood), and for the optimisation of Si releasing materials with tailored ion release profiles for specific applications. By collating the *in vitro* methodology used in SBG research, this review also provides a comprehensive overview of practices used to investigate SBGs interactions with cells and reflects on the methodological approaches that provide comparable results.

1.6.14.1 The concentration dependent effect of Si on cell behaviour

A concentration-dependent effect of Si (both within SBG dissolution media and Si alone) was observed when all cell responses were combined. In SBG dissolution media the frequency of negative outcomes reported in the literature was approximately 3 times higher above 52 ppm Si. This result identifies commonalities in the cellular response to Si, despite the variance in methodological approaches. Limited quantities of data or a lack of standardisation in experimental approaches for specific cell outcomes (e.g., VEGF expression or cell death), necessitated the grouping together cellular responses into "desirable" or "undesirable" cell responses. Whilst increased proliferation/metabolic activity/VEGF expression is usually described as a positive/desirable outcome in *in vitro* biomaterials research, this is clearly not always the case *in vivo* e.g., increased myo-fibroblast proliferation could be associated with contractile fibrotic membrane formation [147] or undifferentiated cells (e.g., osteoblasts) often having a period of proliferation followed by differentiation where there is a decrease in proliferation [148]. Combining the experimental data (as in Figure 1.7) loses this nuance but provides a larger data pool to observe commonalities, that would not be present in smaller data sets, where the variances in experimental approaches between studies can mask overarching trends.

How Si influences cell behaviour remains unclear and is likely to depend upon both the concentration, form (soluble or insoluble) and possibly the Si species (e.g., ortho- di- or polysilicates). Studies by Iler *et al*., suggested that below pH 9, [Si] at approximately 2 - 3 mM (56 - 84 ppm) in water begins to polymerise, where below this concentration Si is thought to be predominately the monomer orthosilicate ($Si(OH)_4$)[65]. The [Si] that initiates polymerisation in body fluids or cell culture media, however, remains unclear. The formation of silica

nanoparticles from the polymerisation of orthosilicate units, is likely to alter Si uptake and cellular interactions. Silica nanoparticles have been associated with cellular toxicity[149, 150], for example Gong *et al*., found that silica nanoparticles (15, 30 and 100 nm in diameter) caused apoptosis and that this was likely caused by increased Reactive Oxygen Species (ROS) damage[151]. Si has, however, also been reported to protect cells from oxidative stress[152, 153].

If ROS is important in cellular response to [Si], part of cellular variance observed in negative outcomes to [Si] (above 50 ppm, Figure 1.7 and Figure 1.10) may be due to variance in each different cell type's ability to resist oxidative stress, in addition to differences in the amount of free radical scavengers present in cell culture media. For example, in osteoblast mineralisation studies, additional free radical scavengers such as ascorbic acid (~50 μg/ml) are commonly added to osteogenic media [154], and this may explain osteoblast viability in the presence of high levels of [Si] (112 ppm[60]) where Si particles are more likely. Other cell types like endothelial cells have been reported to show increased cell death in response to [Si] as low as 14 ppm[153]. Stem cells have been shown to resist oxidative damage via increased intracellular antioxidant concentrations compared to terminally differentiated cells[155]. This may explain why there is no difference in the medium [Si] that causes negative outcomes in stem cells compared to non-stem cells (Fig. 3b) despite a higher [Si] range used (on average) to treat stem cells.

Undesirable cellular outcomes, with increasing Si (non-dissolution products) were also found when Si ions alone were used (not from SBGs) although at lower [Si] compared to those from dissolution products (Fig. 9a). The release of other BG ions (e.g., phosphorus, calcium, and sodium) may account for this difference. Both calcium and phosphate ions have been reported to increase cell metabolic activity, proliferation[156, 157] and mineralisation[158, 159], possibly by increasing the rate of oxidative phosphorylation and thus ATP production [160, 161]. Alternatively, higher [Ca] and [P] may also increase apatite formation, silicate-calcium or possibly Si-HA complexes, thereby lowering the availability of soluble ions

within the media. Other ions may also have an effect on pH in culture media, a factor that has been shown to affect the [Si] that polymerisation occurs at and cell behaviour [65, 162].

The number of different glass types is likely to also contribute towards the variance in cellular responses observed. Positive and negative outcomes were observed in sol-gel 58S at higher [Si] than in other BGs. This is likely to be due to higher ion ranges used in studies in sol-gel studies (due to the increased surface area, higher mol% Si and the absence of sodium in 58S networks increasing the rate of Si release)[163]. Despite evidence suggesting that Si could increase mineralised ECM in osteoblast cells[57, 58, 60, 129, 131], no correlations were found in either ALP activity or biomineralisation. A lack of differences in the effect of [Si] on ALP activity, may be due to variance in the respective cell seeding density which will likely influence the stage of osteoblast differentiation in each study[164, 165]. The influence of time on the effect of [Si] on ALP activity was therefore investigated (<1, 2 and 3 weeks) but did produce any significant differences.

1.6.14.2 Methodological approaches and the need for standardisation

There is considerable variance in methodology used to evaluate cell viability and functionality in response to SBG *in vitro*. Previous reviews have compared the methodological approaches used to assess cellular outcomes with BGs[146] and thus the difficulties in comparing outcomes from different studies. Generating data that allows for greater comparison between studies, would enable greater progress in the field, more impactful research and preserve resources (increasing sustainability). For these reasons we recommend a minimum reporting standard for *in vitro* studies with SBG dissolution products (Table 2). Although this review focuses solely on quantitative methods to investigate cell behaviour, qualitative responses (e.g., morphological changes) are still valuable but as they are rarely

quantified it is difficult to quantitatively compare outcomes from different studies.

Our results identified metabolic activity assays to be by far the most common assessment of cell viability. This is perhaps unsurprising given ISO standard 10993-5 suggest these assays (and MTT/XTT in particular) to be the primary method of evaluating cell behaviour in response to medical devices. ISO 10993-5 was, however, developed for assessing whether leachates from a device could cause toxicity rather than assessing an intentionally biodegradable device.

Table 2 - **Suggested minimum reporting standard for studies investigating the effect of SBG *in vitro*.**

**Some commercial kits (e.g., CCK-8) suggest that that they quantify cell number or proliferation, which is true if metabolic activity isn't affected by conditions/treatments.*

1. **Quantification of BG dissolution products in cell culture media:**

   Ion concentrations of SBG dissolution products should quantified in the cell culture media used for *in vitro* studies (approximately 40% of articles in our search did not report/quantify ion concentrations in media). Different media contains different ion concentrations (e.g., [Ca], [Na], [P]) and thus the total ion availability will vary in different media[152].

2. **Untreated controls**:

   Cells cultured in normal media on standard cell culture plastic should be compared to treated cells and included in the results for comparison purposes.

3. **Normalisation of protein production/activity**:

   To determine if the BG dissociation products are influencing cell phenotype or influencing cell number, the protein of interest should be normalised (e.g., to total DNA, or to a protein that is not affected by the treatment). The total amount of protein should also be reported.

4. **Cell number vs metabolic activity:**

   SBG dissolution has been demonstrated to alter cellular metabolic activity (Fig. 5a). Metabolic activity may, therefore, not equate to cell number. Cell number should be reported separately to metabolic activity. For clarity all metabolic assays should be referred to as metabolic assays as opposed to proliferation or cytotoxicity assays*.

5. **Stem cell source:**

   Isolation method, passage number and source should be included. Authors should state whether the stem cells were a single population (e.g., immunochemically isolated using FACs) or a mixed population of cells (using adhesion and centrifugation approaches).

6. **Availability of data.**

   Data should be made available online, for scrutiny, further analysis and extraction and comparison purposes.

Considerable variation in metabolic responses to [Si] was also observed (Figure 1.11a/b) which may in part be due to variance in metabolic assay used (e.g., MTT, WST-8 and Alamar blue). MTT was the most used metabolic assay to measure cell responses to SBG DPs, which may be due to ISO10993-5 recommending this assay. The MTT assay requires solvents (such as DMSO) to dissolve the formazan product, which therefore necessitates the termination of the cell culture[166]. Similar assays that produce soluble products (and thus don't require additional solvents) such as MTS and Alamar blue were more commonly used within in the last 5 years (2016-2021) compared to the previous 5 years (2016-2011) possibly for sensitivity[167] and resource preservation reasons, despite ISO10993-5 recommending an MTT assay. Media composition (e.g., pH buffers, serum type or percentage) and type (e.g., DMEM, RPMI or MEM-α) have also been shown to influence the outcome of metabolic assays [168, 169], further contributing to variance observed in metabolic activity responses.

The majority of articles that observed this cell response to dissolution products did so over 3 time points (1, 3 and 7 days – 24% of articles), approximately 25% of these studies reported only 1 or 2 time points (commonly up to 3 days). Although ISO10993-5 recommends cells be in contact with conditioned media for only 1 day, a culture of 1 week or longer may be necessary to observe other important cell behavioural changes (e.g., differentiation or ECM production). Less variance, however, was found in direct measures of cell number with most articles selecting total DNA quantification (95% or articles) over manual or imaging software analysis of cell number[164].

Although low variance in methodology was observed in methods to quantify protein production (largely ELISAs - enzyme-linked immunosorbent assay), no clear trends with [Si] were found (Figure 1.12). However, only 30% of observed studies using ELISA kits were found to be normalised to cell numbers or total protein concentrations. Gene expression (where expression is relative to a house-keeper gene) did, however, demonstrate a [Si] dependent response, where the

[Si] that caused a decrease in target gene expression was significantly higher than the [Si] that increased target gene expression (Figure 1.13a). Despite this, there is also not always a direct correlation between gene transcription and functional protein expression[170].

Variance was also observed in methodologies to evaluate biomineralisation, with quantification of calcium deposits by cells producing over 90% of data in this response. Calcium deposition assays, however, can be influenced by the dissolution of calcium ions from BG extracts, or spontaneous formation of apatite. Experiments involving more than one type of bone nodule quantification including area or volume were observed in less than 10% of studies. Other methods necessary to characterise similarities between *in vitro* and natural bone including elemental and mechanical analysis (not quantified) were rarely studied in observed articles. Previous studies have also shown that different cell types and species alter the amount mineral deposited during bone formation *in vitro*[171–173].

1.6.15 Conclusion and impact

This review has, for the first time, attempted to quantify the effect of Si species released from bioactive glasses on cellular responses. Negative cellular outcomes were more commonly reported in [Si] in excess of 50 ppm, whilst positive/increased responses to Si were more frequent in the range of 30-40 ppm. Whilst increasingly negative outcomes with higher [Si] is not by itself unexpected, identification of precise Si concentrations at which specific cell responses occur is useful in tailoring the Si release from novel SBGs. The systematic approach used in this study also presents an informative method to compare a large number of complex studies with high methodological variance (e.g., different cell types, experimental conditions and methods used to evaluate cellular responses). Differences in the methods used to assess cell behaviour may have contributed to the lack of statistically relevant changes in [Si] and bone cell

differentiation or angiogenesis. Standardisation of *in vitro* characterisation approaches to BGs, may provide more insight into the concentration dependent effects of [Si] and understanding of its various roles in cell behaviour.

Chapter 2. Identifying Si species released from bioactive glasses.

2.1 Introduction

It remains unclear what effect the type of Si species has on cell behaviour, or how other ions in the solution have on the Si species, especially those commonly released from bioactive glasses (Ca, P and Na). Previous studies have reported that the species of Si present in solution is affected by different factors including pH[64, 65] and [Si][65, 174]. For example, Jansson et al., demonstrated that an increase in [Si] in sodium silicates caused a decrease in orthosilicates (Q^0) and an increase in di, tri and longer chained species (Q^{1-3})[174]. Polymerised Si may lead to the formation of nanoparticles, which is likely to have different interactions with cells (including uptake mechanism) than Si ions alone. Si nanoparticles have been shown to promote osteogenesis[175] or produce apoptosis[150, 151]. [149]A decrease in the availability of orthosilicate ions may also reduce the beneficial effects of Si. This increase in polymerisation at higher [Si] may also partly explain why higher [Si] are associated with a larger frequency of negative responses as observed in the systematic reviews of previous studies (Figure 1.7).

It is unclear if other ions other components of blood or cell culture media (e.g., serum or pH buffers) may change the [Si] at which polymerisation or precipitation occurs. The presence of trace ions (e.g., molybdenum[64, 176] and aluminium[177, 178]) in solution has been shown to affect the [Si] at which different Si species (Q^{1-3}) form. Despite previous studies demonstrating that Si may polymerise between 2 and 3 mM in distilled water [65]using a silico-molybdate reaction[65], no mechanism of Si-Mo or Si-Al interactions has been suggested. Whilst Ca, P and Na have all been shown to play individual roles in bone remodelling, it is unclear if the effect of [Si] on cell behaviour could be modified

by these ions. Previous studies have suggested that calcium silicate complexes could inhibit the formation of Si bridges[78], thereby increasing the [Si] necessary for polymerisation. [Ca] at 'high' and 'low' concentrations (as determined in Figure 1.16j) was found to increase the [Si] necessary for positive and negative responses (Figure 1.16/c). No trends were observed in effect of P and Na on the effect of Si on cell responses in systematic reviews (Figure 1.15d-f and g-I respectively) or on the formation of different Si species.[150]Differences in cell culture medium (e.g., where DMEM contains 3 times less [P] than RPMI (Table 5) may explain differences observed in cell responses to BGs in vitro. Different cell culture media (containing equal antibiotic and serum %) has been found to alter levels of osteogenic differentiation and mineral formation in MC3T3-E1[179] and human MSCs[180]. If particulate Si is present in media, these may provide a

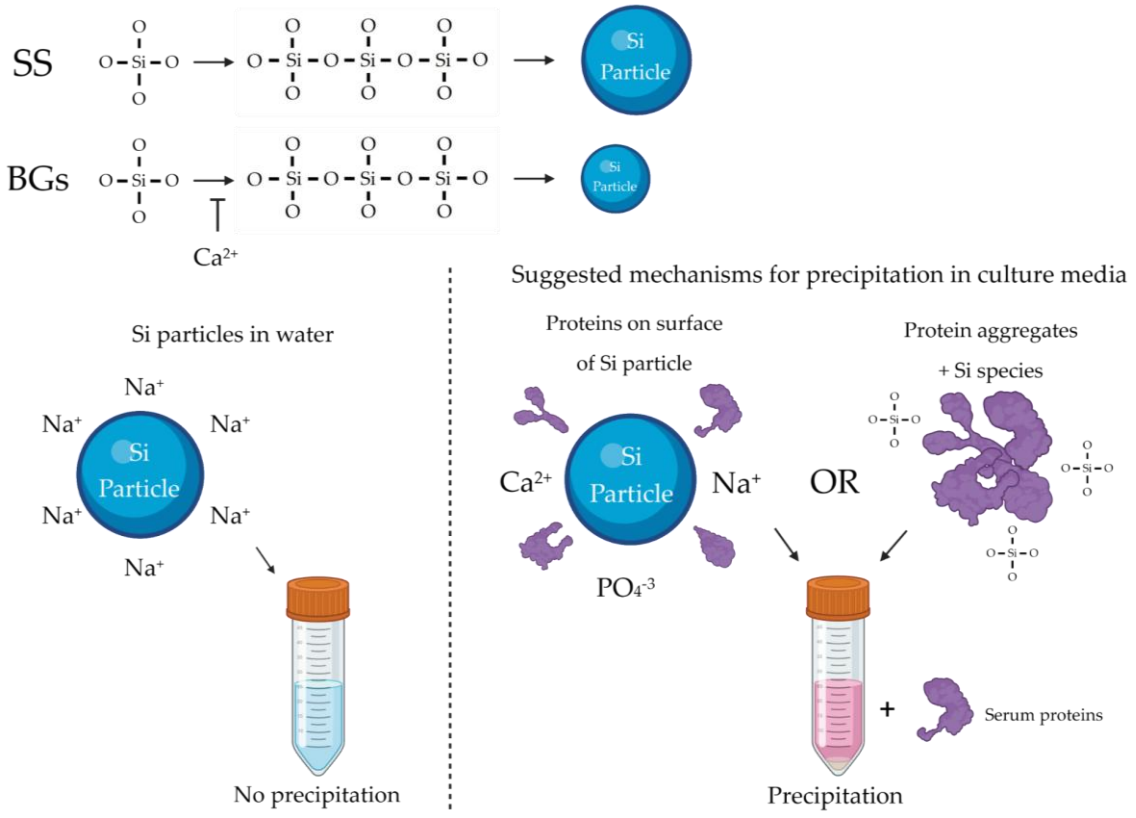

Figure 2.1 – **Comparison of the suggested Si particle formation, surface characteristics and their effect on precipitation in water and cell culture media following incubation at 37°C/5% CO_2.**

Precipitation was only observed in cell culture media and not in distilled water alone, suggesting that Si particle formation could provide a surface for serum protein attachment (e.g., BSA), increasing their size/visibility. Calcium released from BGs may inhibit Si polymerisation through the formation of Si-Ca complexes.

surface for protein adsorption, increasing overall size and uptake mechanism. Si ions could also produce complexes with serum proteins which may allow them to be uptaken via endocytosis instead of ion channels. A summary of both mechanism and the influence of ions is presented in Figure 2.1.

It is therefore important to improve our understanding of the factors that affect Si species in biological environments and polymerisation with the aim of releasing Si from BGs that elicits beneficial responses. This chapter will aim to investigate the relationship between [Si] in water and different mediums and how this affects the formation of Si different species and particulates.

2.1.1 Determination of silicate species from silicates and BGs

Orthosilicates are generally thought to be the only Si species released from BGs. This hypothesis has, however, never been proven experimentally. It is unclear whether the silicate network structure of BGs as a solid, reflects those released into solution as dissolution products. Solid state ^{29}Si-Nuclear Magnetic Resonance (^{29}Si-NMR) has been used show that Bioglass® as a solid contains a 21%Q^1, 40%Q^2, 26%Q^3 and 6%Q^4 silicate networks[181], suggesting that longer chained species may also be released when dissolved in solution. Manufacture of BGs through a sol-gel process, however, has been shown to produce BGs with a majority Q^4 species (36% in 70S30C BGs[182]) network. If Si species in solution are related to their species in solid state, then this may in-part explain variance in studies using melt-derived and sol-gel bioactive glasses. Studies that used Sol-gel glasses (58S specifically) were observed to produce negative, positive and no change cell responses at a higher median [Si] ($P \leq 0.001$) then compared to melt-derived 45S5 glasses (Figure 1.14), suggesting that they either they produce different Si species or that a lack of sodium affects cellular outcomes.

Due to the low Si concentrations found in the body (~1.7 – 3.5 μM) or in BG dissolution products (*in vitro*), verification of the Si species that cells interact with is difficult due to the sensitivity of Si NMR. Enrichment of sodium silicates with ^{29}Si was used by Harris et al., previously to quantify the effect of [Si] on the quantity of different Si species in solution[183, 184]. The same methodology has, to date, not been used to quantify the Si species released from BGs. If ^{28}Si in melt-derived or sol-gel bioactive glasses is substitute by ^{29}Si, the Si species released may be detectable. The use of more sensitive ^{29}Si-NMR instruments (700 MHz and above) to detect Si species, compared to those used by Harris et al.,[183] (<100 MHz) may also allow for Si species at lower concentrations to be detected.

2.1.2 Si particle interactions with bone cells

Although several intracellular pathways in bone cells have been shown to be altered by media containing silicate ions[130, 185, 186], it is likely that these Si-conditioned mediums are mixtures of small particles and ions rather than pure ionic solutions. Studies investigating the effects of silicate particles and nanoparticles (≤100 nm) on bone cells have reported both desirable and undesirable (size dependent) cellular outcomes. Silicate nanoparticles (~50 nm) have been shown to increase BMD and bone volume in mice in-vivo[187, 188]. *In vitro*, 30-60 nm particles have been observed to increase bone nodule formation, bone specific proteins and differentiation whilst inhibiting osteoclastogenesis via down regulation of RANK transcriptional regulator NFATC1[187, 189, 190]. The same studies, however, demonstrated that particles (100-450 nm), decreased cell viability, bone nodule formation and differentiation through an observed reduction in ALP and OCN gene expression[189]. It is unclear, however, if particles in these studies remain at a constant size throughout the culture or whether an increase occurs due to aggregation. It is equally unclear what effect the presence of serum proteins has on particle size and thus their effect on cellular responses. Compared to silicate particles alone, few studies of BGs have directly compared

the cellular outcomes between BGs intended as particles and those as 'ions' (dissolution products).

2.1.3 BG ion and particles interactions with bone cells

Several different methods to model the effect of BGs on cells exist in the literature. The use of dissolution products, compared to the direct addition of cells to BG solid materials or BG particles, allows an experimental focus on the ion release, without the confounding effects of other material properties known to effect cellular behaviour (e.g., topography, surface chemistry and mechanical properties). It is common within in-vitro bioactive glass literature to filter dissolution products before adding them to cell cultures. Whilst filtration through 0.2 μm syringe filters is intended to prevent infection and stop further glass dissolution, it is possible that nanoparticles ≤200 nm (not just ions) may still be present. It remains unclear, however, what fraction of BG dissolution products are in the form of particles and that of ions. It is also unclear whether particles only contain longer chain Si species or are formed from the precipitation of Si salts (e.g., Si-Ca, Si-P or Si-Na) or aggregation of proteins in serum. Lippens et al, observed that particles of 45S5 and 13-93 BGs decreased both metabolic activity and cell proliferation compared to no BG controls[191]. In contrast, their respective dissolution products produced no significant differences up to 0.5 w/v% in 45S5 and 2.5 w/v% for 13-93 at all-time points. It is unclear from this study what proportion of these dissolution products are in the form of ions and in the form of particles.

The following experimental chapter will investigate how [Si] effects the quantity of different Si species released from silicates and those from BGs. Further experiments will attempt to quantify particle sizes of silicates and BGs in water and cell culture media over time.

2.2 Chapter aims and hypothesis.

Systematic reviews in chapter 1 suggested an [Si] dependent effect on cell behaviour when cultured in BG dissolution products and Si alone. Little evidence exists, however, as to how different Si species may influence this dependence and what effect other ions play in this relationship. Polymerisation at specific [Si] and thus the formation of Si particles could provide an explanation for increasingly negative outcomes with increasing [Si] observed in previous studies. Ions such as calcium have, however, been predicted to form complexes with Si which may inhibit Si polymerisation. This chapter therefore attempts to determine which Si species exist at concentrations commonly utilised in *in vitro* studies (1 – 6 mM/28-168 ppm Si) and how particle formation is affected by the presence of components common to cell culture mediums (namely, foetal bovine serum (FBS)).

This chapter investigated the following hypothesis:

1. The effect of [Si] on the species of Si (ortho, di, tri and polysilicates) released from SS and BG dissolution products
   - Hypothesis: Increasing [Si] will produce longer chained species (di and trisilicates) within SS and BG conditioned culture media and water
2. The effect of [Si] on the quantity of ions and precipitates in SS and BG dissolution products in water and different cell culture media
   - Hypothesis: Increased calcium in BG dissolution products will produce less precipitates in culture media than Si alone
3. The physicochemical properties of particles/precipitates arising from SS and BG dissolution products in water and cell culture media
   - Hypothesis: The presence of FBS increases the size of precipitates in both BG dissolution products and Si alone in culture media

2.3 Materials and methods

2.3.1 Si species identification from sodium silicates by ^{29}Si NMR

To identify which Si species are produced in solutions containing only Si ions (non-dissolution products), sodium silicate hydrate (Fluorochem, UK) was dissolved in de-ionised water and species determined by liquid state ^{29}Si NMR. Investigation of the effect of [Si] on the presence and quantity of each species was performed by a serial dilution of stock solutions, whose concentrations were confirmed by inductively coupled plasma-optical emission spectroscopy (ICP-OES). The highest concentration was chosen at the point where Si solutions did not flow (became solid) and the lowest concentration at the point where Q^3 species were not visible (or detectable) in NMR spectra. The presence of species (Q^{1-4}) in each solution was confirmed using a Bruker Avance 500 MHz III HD NMR instrument and their quantity determined by the greatest relative intensity of each species peak in NMR spectra. Quantification of Si species distribution at each [Si] was performed by plotting the mean of the highest intensity peak within each Q species 1-3. To identify Si species at concentration similar to those used in *in vitro* studies, non-linear regression was used to identify the relationship between [Si] and each Q species. Curve fitting for each species was performed by comparing different exponentials using an extra sum-of-squares F test. The curve in each test that produced a $P<0.05$ continued onto the next comparison until one exponential was identified. A least squares regression method was used to fit each exponential with no specific handling of outliers or weightings. Curve fitting was then used to extrapolate down to [Si] used commonly in BG dissolution studies ([Si]=1-4 mM).

2.3.2 Preparation and species identification of ^{29}Si-bioactive glasses

To identify the species of Si released by BGs, melt-derived 45S5 bioactive glasses (46.1 mol% SiO_2, 24.4 mol% Na_2O, 26.9 mol% CaO, and 2.6 mol% P_2O_5) were synthesised and species quantified using the same protocols as those in studies involving sodium silicate hydrate (section 2.3.1). Based on enrichment of sodium silicates with ^{29}Si in previous studies[183, 184], quantification of Si species released from BGs was achieved by creation of a new 45S5 BG with ^{28}Si silicate networks replaced with silica containing ^{29}Si. Briefly, 35 mg of ^{29}Si enriched silica isotope (Isoflex, USA) was purchased and used in replacement for ^{28}Si silica. To retain the molar ratio of elements in the glass, compounds containing Na, Ca, and P were subsequently reduced in weight, producing a powder mixture of 250 mg total weight. The powder mixture containing silica isotope was heated to 1400 °C for 2 hours in a platinum crucible before melt-quenching. To prevent loss of yield during melt-quenching (owing to low glass weight), the melt was allowed to cool in air (instead of water). Crystallinity of the resulting glass was then verified by X-ray diffraction (XRD) using a modular powder diffractometer (Xpert Pro, PANalytical®). Briefly, 0.1g of glass was distributed evenly on a single crystal silicon stub for analysis. Cu Kα radiation at 40 kV and 40 mA was used. A 2θ angle was set between 10 and 60° and the number of steps and scanning time set at 3000 and 0.16s respectively. ^{29}Si BGs were then diluted in 5 ml of deuterium oxide solution and allowed to dissolve for 7 days. Glass supernatant was then removed by centrifugation filtered using a 0.2 μm syringe filter. The concentration of Si in the supernatants was then quantified by ICP-OES followed by dilution to 0.5, 1, 2, 3, 4 mM Si. Si species were then identified using a Bruker Avance Neo 700 MHz NMR instrument. Briefly, a single pulse experiment with a 30 degree pulse, a recycle delay of 5 seconds and 1H decoupling was used to record ^{29}Si NMR spectra.

2.3.3 Isolation, characterisation, and quantification of particles from sodium silicates and BGs by centrifugation

To investigate the influence of Si concentration on the formation of precipitates (or particles), dissolution products from SS and 45S5 BGs containing increasing [Si] were centrifuged, and pellets separated from supernatants. Briefly, sodium silicate hydrate (20 mg/ml) and BGs (50 mg/ml) were added to McCoy's 5A Glutamax (containing 10% v/v FBS and 1% v/v penicillin/streptomycin) and incubated a 37°C on a roller shaker (120 rpm) to produce stock solutions. Solutions of SS and BG were determined to reach full dissolution after 10 minutes and 3 days respectively by identifying a plateau in [Si] release over time using ICP-OES. Si in stock solutions were determined by ICP-OES and diluted in culture media to concentration: 0.5, 1, 1.5, 2, 2.5, 3 mM Si. Diluted solutions were then incubated in a 5% CO_2 incubator at 37°C for 24 hours to regulate pH and temperature. The pH of Si at each concentration was measured following incubation. Solutions (SS and BG precipitates) were then centrifuged at 10,000g for 10 minutes. The resulting pellets were then separated from supernatants and resuspended in distilled water. Solutions containing pellets were then recentrifuged at 10,000g for a further 10 minutes to remove any remaining medium containing Si. The concentration of Si in pellets and supernatants were then quantified by ICP-OES. The presence and quantity of serum proteins was estimated by measuring total BSA concentration ([BSA]) using a NanoDrop One^c microvolume spectrophotometer (Thermofisher scientific). The NanoDrop instrument was set to measure absorbance at 280 nm (peak absorption of amino acids found in BSA) and relate this to concentration using the Beer-Lamber law where [BSA] is equal to absorbance/(molar absorption coefficient x the path length). The same protocol of pellet isolation was then performed in both non-supplemented culture medium and distilled water. To verify the contents of isolated pellets, samples were freeze-dried following submersion in liquid

nitrogen and functional groups identified by Fourier transform infra-red (FTIR) spectroscopy using a Jasco-4000 spectrometer between a wavenumbers range of 4000 and 600 nm at a step size of 2 cm^{-1} with 20 scans used to provide each final spectra. Identification of the size of the isolated particles over time was assessed by nanoparticle tracking analysis (NTA) using a ZetaView particle tracking analyzer (ParticleMetrix). Differences in SS and BG size and distribution in different culture mediums (McCoy's 5A Glutamax, DMEM Glutamax, MEM-α and RPMI) were compared against controls, media alone (no Si) and silicate in water.

2.3.4 Statistics

A Robust Regression and Outlier Removal Test (ROUT) was used to determine if data contained anomalous or outlier values with a outlier sensitivity parameter ('Q') of 1% (Q=0.01). Significant outliers were then removed from overall data if $P \leq 0.05$. All data was then assessed for normality (Gaussian distribution) using a Shapiro-Wilk test. The statistical test used to determine significance between conditions was dependent on; the study design, whether data was normally or non-normally distributed and if multiple comparisons were required (Table 1). Differences between conditions were then determined to be statistically significant if $P \leq 0.05$. Asterisks (*) or hashes (#) are used to indicate significance between conditions where *=$P \leq 0.05$, **=$P \leq 0.01$, ***=$P \leq 0.001$, ****=$P \leq 0.0001$ etc. Non-linear regression was used to fit models to data used to predict Si species released from SS and BGs. Models were fit to data using a Least squares regression and iteratively compared using an Akaike's Information Criterion until the highest R squared value was achieved.

Table 3 - **Summary of the appropriate statistical test based on the specific experimental design.**

Comparison type	Normal distribution	Multiple comparisons	Non–normal distribution	Multiple comparisons
Two groups	Unpaired t test (+Welch's correction for non-equal SDs)	N/A	Mann-Whitney test	N/A
Two or more groups (one independent variable)	Brown-Forsythe and Welch ANOVA test	Dunnett's T3 test	Kruskal-Wallis test	Dunn's test
Two or more groups (two independent variables)	Two way ANOVA test	Dunnett's test	Freidman's test	Dunnett's test

2.4 Results

2.4.1 Effect of [Si] concentration on Si species

Liquid ^{29}Si NMR revealed an increase in [Si] resulted a decrease in Q^0 and an increase in Si bridging ($Q^{1\text{-}3}$). At the lowest observed concentration of Si (11,250 ppm Si), the intensity of Q^0 species was highest compared to all other species ($p \leq 0.005$ - Figure 2.2a). The concentration of Q^0 was found to decrease (with a one phase decay) with increasing [Si] up to 180,000 ppm Si (Figure 2.2b-e). At this concentration, intensity Q^0 was found to be lowest compared to all other observed species ($p \leq 0.005$ – Figure 2.2f). With increasing [Si], the relative intensity of Q^1 species increased linearly up to 180,000 ppm Si, whilst Q^2 and Q^3 were observed to increase and then plateau (a one phase association) at 90,000 and 45,000 ppm Si respectively (Figure 2.2e). At the highest [Si], the intensity of Q^2 species was found to be the greatest compared to all other.

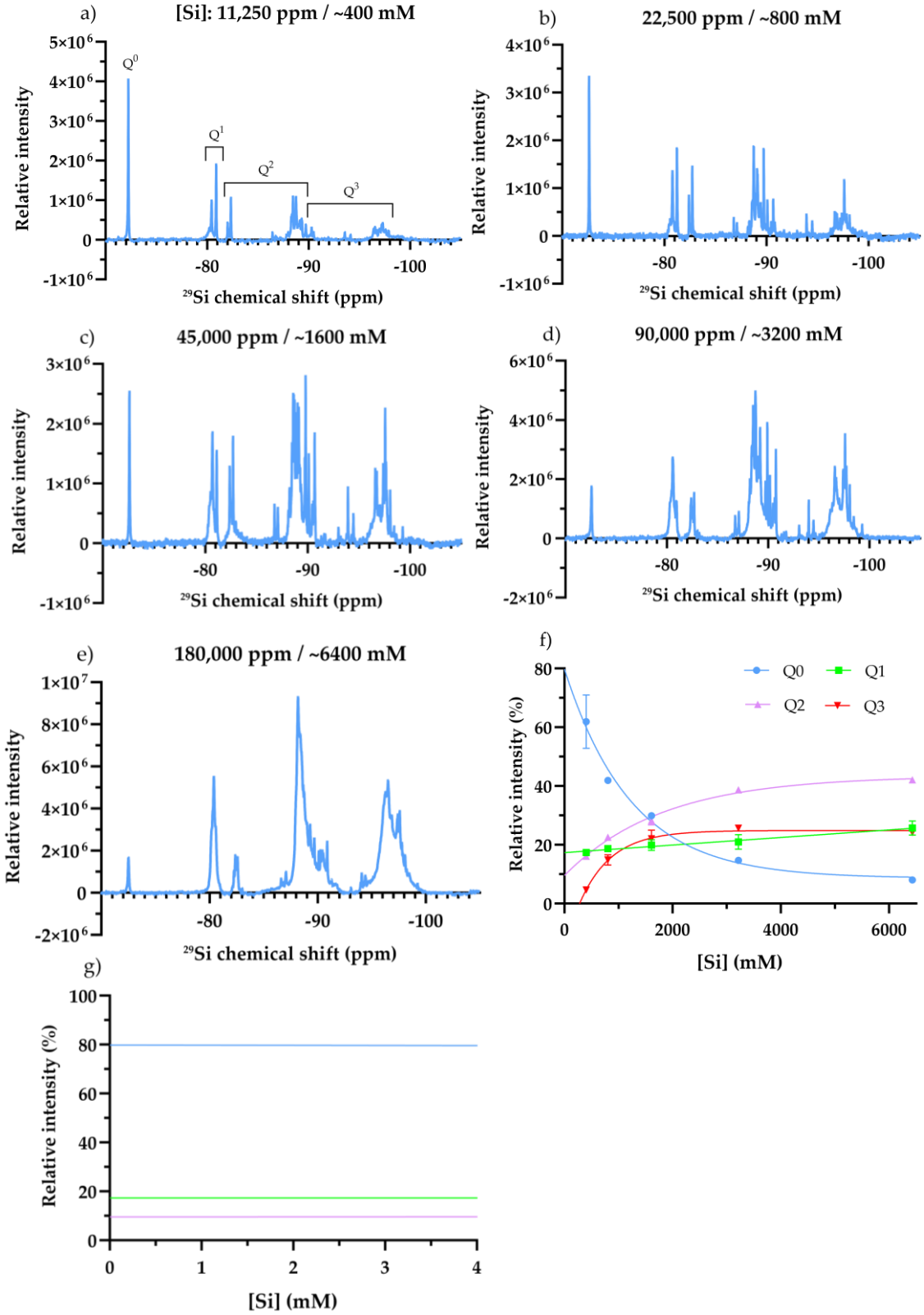

Figure 2.2 - **Determination of Si species in water with increasing [Si] using liquid state ^{29}Si-NMR**.

With increasing [Si] the concentration of orthosilicate (Q^0) species decreased, whilst all other species (Q^{1-3}) increased (a-e). A summary of the relation of different species with [Si] is shown in (f). Prediction of Si species at biologically relevant concentrations (0-4 mM Si) are shown in (g). Difference species are denoted by Q^n, where 'n' equals the number of silica bridges (Si-O-Si). N=3, (f) shows SD of these experiments. (a-e) is an example of spectra from a single experiment.

species ($p \leq 0.005$). Extrapolation of the changes in Q species with increasing [Si] was performed using non-linear regression and predicted that below 4 mM Si, only ortho, di (Q^1) and trisilicates (Q^2) exist (Figure 2.2g). Orthosilicates were found to have the highest intensity (79%) compared to di (18%) and trisilicates (9%).

2.4.2 Si species released from 45S5 bioactive glasses

The concentration of orthosilicate (Q^0) species was observed to increase with increasing [Si] in ^{29}Si-BG dissolution products up to 3 mM Si (Figure 2.3a-c) where

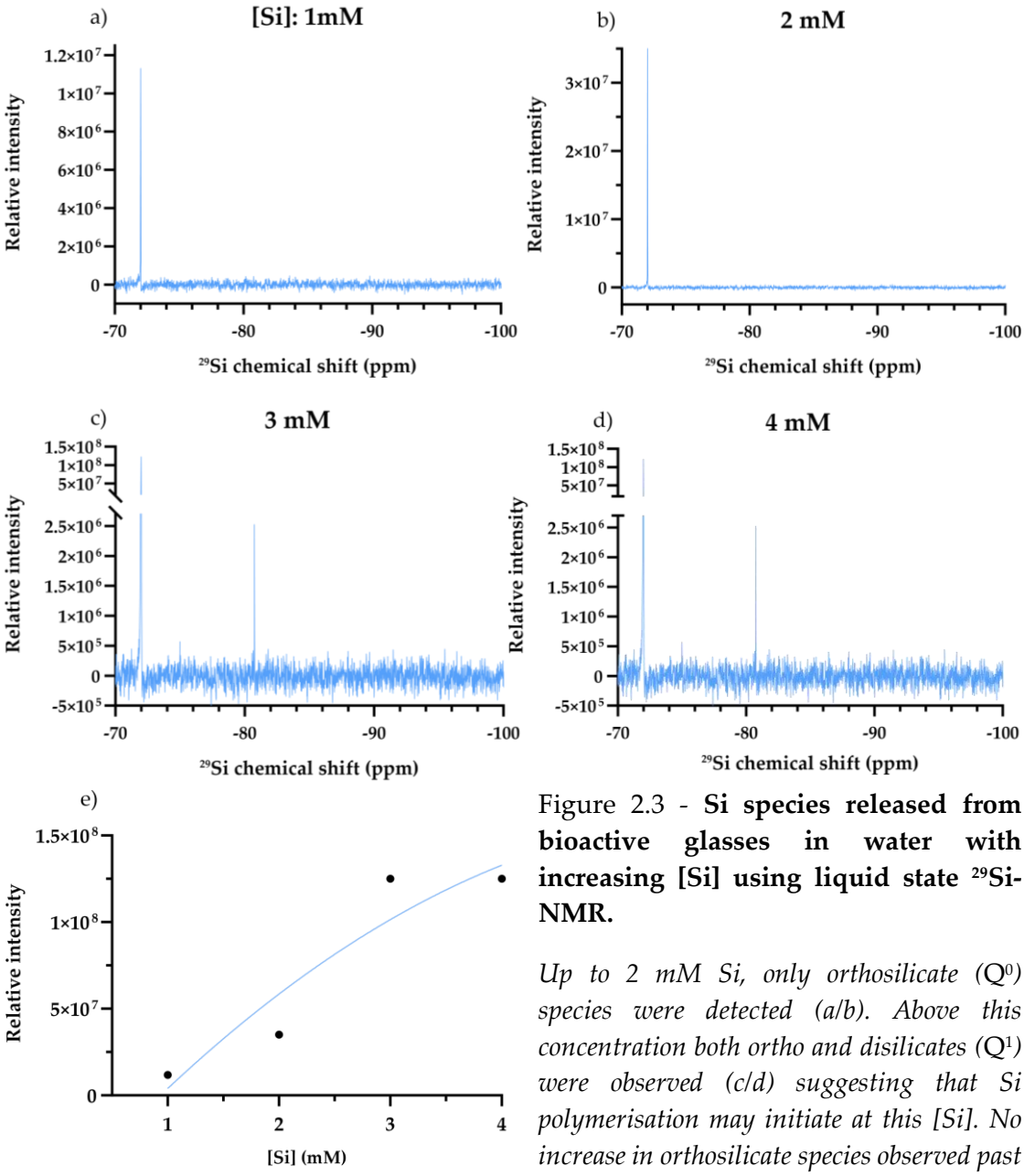

Figure 2.3 - **Si species released from bioactive glasses in water with increasing [Si] using liquid state ^{29}Si-NMR.**

Up to 2 mM Si, only orthosilicate (Q^0) species were detected (a/b). Above this concentration both ortho and disilicates (Q^1) were observed (c/d) suggesting that Si polymerisation may initiate at this [Si]. No increase in orthosilicate species observed past 3 mM Si (e).

a plateau was found (Figure 2.3e). Disilicate (Q^1) species were only observed, however, at concentrations of 2 mM Si and above, suggesting this concentration may be necessary for Si polymerisation (Figure 2.3c/d). The concentration of disilicate species increased from 3 to 4 mM Si. No visible peaks were observed in XRD spectra of ^{29}Si-BGs, suggesting isotope glasses were near completely amorphous (Figure 5.2).

2.4.3 The effect of [Si] on the properties of isolated precipitates from silicates and BGs media.

2.4.3.1 Elemental composition

Mean [Si] in isolated precipitates was observed to be significantly higher in SS compared to 45S5 at all starting/initial [Si] ($P \leq 0.01$ - Figure 2.4a). Whilst [Si] in the media of silicate samples was found to decrease with increasing (theoretical) [Si], no such differences were observed in BG supernatant media. Whilst [P] (Figure 2.4c) and [Ca] (Figure 2.4d) in BG particles were both found to increase with increasing [Si], a decrease was observed in their respective supernatants, suggesting the formation of precipitates (possibly hydroxyapatite). No significant differences were observed, however, in [Na] in particles or supernatants at any [Si]. To determine if serum proteins in media were involved in observed precipitates, the amount of BSA within the precipitates was quantified. [BSA] was observed to increase within the precipitates with increasing [Si] in both media types, suggesting the formation of a particle protein corona or protein aggregates (Figure 2.4f). [BSA] was found, however, to be higher in silicate samples compared to 45S5 at all [Si] ($P \leq 0.001$) except for 1 mM Si. pH of solutions before centrifugation and isolation of precipitates was found to be between 6.9 and 7.1 at all [Si].

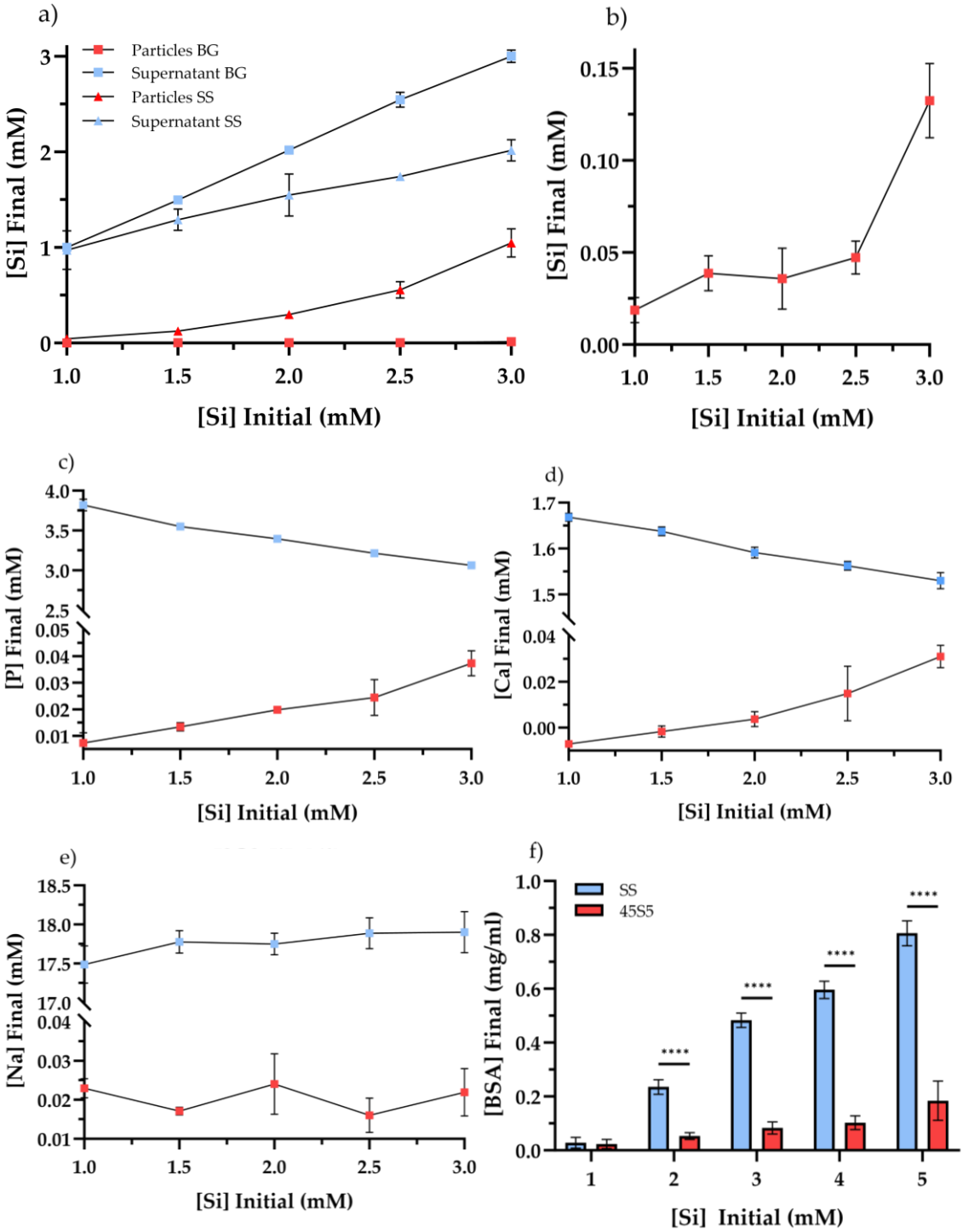

Figure 2.4 - **Comparison of isolated precipitation formed by SS and BG conditioned media after 1 day**

*Differences in [Ca], [P] and [Na] are shown in (c-e) whilst concentration of BSA in SS and BG precipitates is shown in (f). A lower [Si] was observed in precipitates isolated from BG dissolution products compared to Si alone. Decreased [Ca] and [P] but not [Na] were found in precipitates with increasing [Si]. Significantly greater concentrations of BSA were observed with Si alone compared to BG, suggesting BGs produce smaller particles in media. [X] 'Initial' and 'final' refers to the concentration of X before and after precipitate (referred to as 'particles') isolation by centrifugation. Values are presented as mean ± SD, N=3, ****(p≤0.0001).*

2.4.3.2 Functional groups

Siloxane (Si-O) bonds were observed in addition to carboxyl (C=O ~ 1700 cm^{-1}) and amine (N-H ~ 1400 cm^{-1}) functional groups from both silicates and BG precipitates (after 1 day) (Figure 2.5c/d), inferring an interaction between the particles and proteins in serum. Compared to SS from the manufacturer and 45S5 powders, Si-O bonds in their respective media particulates, were found to shift from between 800-1000 cm^{-1} to between 1000-1200 cm^{-1}. This implies a change in the environment of each Si-O bond, suggesting the formation of Si complexes or protein-particulate interactions. The transmission percentage of C=O and N-H bonds was found to be higher, however, in the silicate samples (~70-80%)

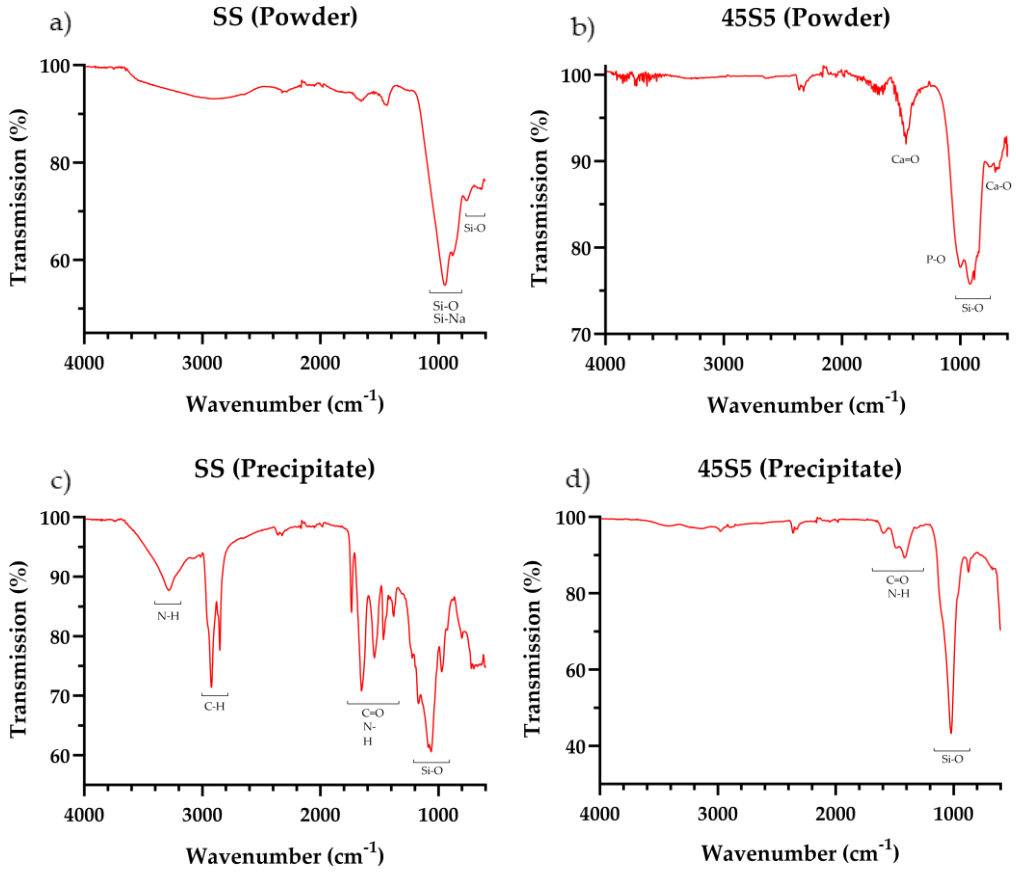

Figure 2.5 - **FTIR spectra of SS and 45S5 BG powders (a/b) and their corresponding precipitates isolated from media (c/d).**

Precipitates isolated from media over 1 day containing SS were found to contain a greater number of proteins associated functional groups compared to those isolated from BG dissolution products. Little to no phosphorus and calcium functional groups were identified in precipitates from BG dissolution products.

compared to those in BG spectra (~10%) (Figure 2.5d). Peaks representing Si-O bonds was found to be sharper in BG media samples then in silicate samples, suggesting (in contrast to elemental data - Figure 2.4c/d) that phosphate and calcium bonds (present in the original glass - b) did not contribute to the isolated particles.

2.4.3.3 Particle size

Particles in media containing SS were observed to be of greater average diameter in all media types, when compared to BGs ($P \leq 0.05$). Silicate particles were found to produce the greatest differences in size compared to BG particles when cultured in McCoy's 5A media (Figure e) after 8 days (220 vs 160 nm – $P \leq 0.01$). No significant differences, however, were observed between particles in McCoy's and DMEM and those media alone over the same time period, suggesting serum protein aggregation (without added particles) may occur during incubation at 37°C. Significant differences were found in those of silicate particles and MEM-α and RPMI media alone ($P \leq 0.05$), implying media composition may slow the rate of protein aggregation or particle growth. When compared in water, both SS and BG increased in average particle size over time. Similar to those incubated in culture media, SS particles were observed to have a greater average diameter than those of BG at all time points ($P \leq 0.05$), suggesting Si polymerisation may occur in SS samples but not in BGs.

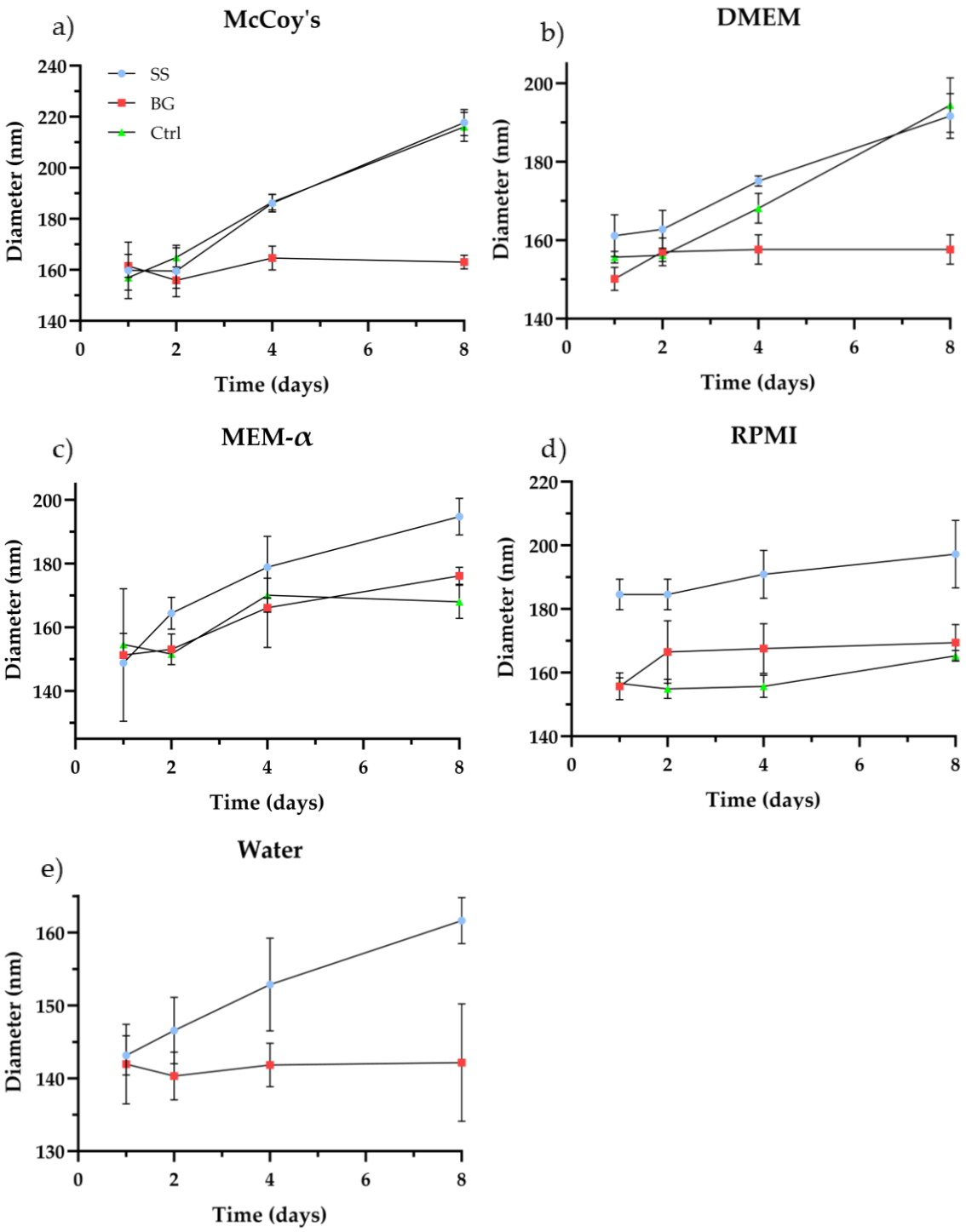

Figure 2.6 - **Particle size quantification in different media types (McCoy's, DMEM, MEM-α, RPMI) and water conditioned with 2mM Si SS and BG dissolution products determined by NTA.**

Conditioning with SS was found to produce larger particles over 1-8 days than those in BG dissolution products in all media types and water.

2.5 Discussion

Principle conclusions:

1. Si species are [Si] dependent
2. Polymerisation of Si in BG dissolution products occurs above 2 mM Si
3. The quantity of precipitates formed in culture media increases with increasing [Si]
4. BG dissolution production produce less precipitates in culture media compared to Si alone

This study has, for the first time, determined what species of Si is released from silicates and BGs at concentrations relevant to previous *in vitro* studies, in addition to the characterisation of precipitates in cell culture media and distilled water. With increasing [Si], the quantity of orthosilicate species (Q^0) decreased as longer chained species (Q^{1-3}) increased (Figure 2.1a). The width of the peaks, also implies each species (Q^{1-3}) may have more than one atomic geometry in solution, including branches and cyclical molecules[192]. This conclusion might also be drawn from the broadening of each peak (other than Q^0) with increasing [Si]. The small shift in each peak toward higher chemical shifts with increasing [Si] also indicates the presence of different molecular conformation due to the deprotonation of silicon hydroxyl groups (Si-OH) caused by increasing pH[193]. This trend is consistent with spectra obtained by Jansson et al, who showed that increasing the ratio of silica to sodium (in sodium silicates) produced longer chained species with increasing silica concentration[174]. Despite this, the concentration of Si species in this experiment is far higher than is present in the body (3.5 – 11.7 μM[194, 195]) or that used to investigate the role of silicate ions alone or released from bioactive glasses *in vitro* (range = 0.1 – 240 ppm / 0.003 – 8.5 mM - Figure 1.7).

The low abundance of naturally occurring Si^{29} isotopes in commercially available silica and Si^{29} NMR's inability to measure Si^{28} species means investigating Si species at low concentrations (≤5 mM) is difficult. Extrapolation of trends observed in our NMR data using non-linear regression allows us to estimate the

abundance of different species at low concentrations. Below 4 mM, our data predicts that orthosilicate species make up greater than 79% of all species, with di (18%) and trisilicates (9%) making up the rest (Figure 2.2g). This prediction is limited, however, to only showing the quantity of Si species in water and does not show how Si species may be affected by serum proteins, cell culture media or other ions released from BGs.

2.5.1 How does [Si] affect the concentration of Si species released from BGs?

Studies using solid state ^{29}Si NMR have shown that the silica network phase of 45S5 BG powders contained, 67.2% Q^2, 22.3% Q^3 and 10.1% Q^1 species[196]. Yamada *et al* suggested that BGs would release ionic Si species that follow their distribution in solids[197]. When ^{29}Si was used a network former (instead of ^{28}Si) in 45S5 BGs, only orthosilicate were observed up to 2 mM Si and above (Figure 2.3a/b) this concentration disilicates were found and increased with increasing [Si] (Figure 2.3c/d). It is unclear, however, if disilicates do not exist below 3 mM Si or whether ^{29}Si NMR is too insensitive to detect them and other species at low concentrations. Meinhold *et al*., (1985) suggested that both ortho and disilicates exist at all concentrations up to 12.5 mM (350 ppm) Si[198]. Although, others report that polymerisation, beginning with Si dimerisation occurs at a 2 - 3 mM Si[65, 199]. Si species released from ^{29}Si BGs therefore appears to be independent of its solid network structure with Q^0 making up the majority species in solution. Alternatively, rather than the species in solution being determined by the Q structure within the BG the solute and environment (e.g., pH, other ions, biological molecules and proteins) may play an important role in determining Si species.

Prediction of Si species from SS using non-linear regression at low concentrations (1-4 mM Si), however, demonstrated that ortho, di and trisilicates exist at all concentrations up to 4 mM Si (Figure 2.3g). Differences may be explained by the

presence of other ions (Ca, Na, P) released from BGs preventing Si polymerisation by forming Si complexes (E.g., Si-Ca). In addition, equations for non-linear regression may also not perfectly reflect trends between different species and [Si] at high concentrations, causing inaccurate predictions at low [Si]. Our results suggest therefore that ionic Si species may not follow those identified in the solid state and hence their stability in solution is likely to be more strongly influenced by their environment (e.g., temperature, pH and other ions or biological molecules).

Previous studies have shown polymerisation of Si species is mediated by pH[177], a factor that could be significantly influenced by highly charged ions like phosphorus (3^-) or calcium (2^+). Incubation in a 5% CO_2 atmosphere for 24 hours in addition to buffers in culture media, however, reduced the pH to between 6.9 and 7.1. This agrees with silico-molybdate experiments[65], suggesting that this reaction is pH dependent and that below pH 9, polymerisation is more likely. This may also explain why precipitation did not occur in stock solutions before incubation, despite an [Si] well over 3 mM during storage. Si NMR studies have shown, however, that sodium in particular can increase the concentration of orthosilicates species whilst decreasing the quantity of di and trisilicate species[177, 200]. Their authors hypothesise that Si-OH bonds are thermodynamically favourable in monomeric species whilst, Si-O-Na bonds are more likely in dimer and trimer species.

Orthosilicate ions have been shown to be more easily absorbed by the digestive track compared to polymeric species[201, 202]. Although, sodium ions could help stabilise monomeric Si species making them more effectively taken up by cells, no significant difference responses were found when comparing different [Na] on the effect of [Si] from BGs (Figure1.16d-f). No specific studies, however, have investigated how these calcium and phosphorus ions affect the concentration of different Si species in solution. It is likely, however, that (similar to sodium ions) Si-OH bonds may be replaced by Si-O-Ca or Si-O-P, effectively blocking siloxane

bridges (Si-O-Si) from forming. The formation of these complexes would therefore reduce the availability of orthosilicate species in solution. This may explain why a higher [Si] is required to produce negative and positive responses in SBGs (Figure 1.4a) compared to silicates alone (Figure 1.7a).

2.5.2 Properties of particles released from bioactive glasses and silicates

Whilst BG dissolution products in cell culture media are generally believed to only contain ions[203, 204] due to pre-culture filtration (≤200 nm), it is possible for particulates smaller than this to be present, or for precipitation (and particle formation) to occur after filtration. Precipitations were observed with both silicates and BGs in fully supplemented media after a 1-day incubation at 37°C (in the absence of cells). By centrifugation, these precipitates were able to be isolated and their properties characterised. With increasing [Si], the visually observed fraction of solid precipitation was found to increase up to 3 mM Si. Discrepancies between the amount of Si in particles obtained by silicate and BGs (Figure 2.4a), demonstrated that silicates produced larger and/or more precipitates compared to BG samples. A possible explanation is that cations also released by BGs, such as sodium and calcium, hinder precipitation. The solubility of BSA (negatively charged at pH 7[205]) has also been demonstrated to be influenced by Ca and P ions[206, 207], with decreasing concentration making them more easily pulled out of solution by centrifugation. Madeira *et al*., showed that [Na] up to 125 mM (no Si) caused precipitation of BSA, whilst concentrations above this inhibited it. This study also showed that [Ca] up to 13 mM also caused significant precipitation[207]. Interestingly, despite having a higher [Na] (50.2 mM) in media, BGs were found to precipitate less than SS (19.0 mM Na). This may suggest that protein precipitation is more strongly influenced by the number of surface binding sites which might be offered by silica particle formation (occurring more easily in SS).

Proteins were present in the precipitates as determined by FTIR (Figure 2.5c/d), suggesting interactions between silicate ions or particles and serum proteins may occur. Differences in transmission of carbonyl and amine peaks between spectra of silicate and BG demonstrated the differences in the amount of precipitation occurring in media. An increase [Si] correlated with an increase in protein interactions (as determined by [BSA]), which may be explained by an increase in number of Si particles. Whilst silane groups (Si-O) were identified in BG spectra, phosphate and calcium groups were not, suggesting that either they do not contribute to particle formation or that FTIR is not sensitive enough to detect them at low concentrations. A limitation of particle isolation by centrifugation, however, is the inability to determine whether proteins are directly bonding to silicate and BG particles or are simply pulled into pellets by centrifugal force. To confirm this, a specific Si-O-N bond may need to be identified in FTIR spectra. Although a solution to this problem may be to perform FTIR on these samples whilst suspended in water (liquid-FTIR), a very high concentration of these particles is necessary and thus may change the specific Si – protein interactions and thus relevance to previous *in vitro* studies.

NTA data showed, however, that the diameter of particles in silicates alone increase in distilled water (without serum proteins) over 8 days in comparison to no increase in BGs (Figure 2.6e). This suggests that Si polymerisation or protein aggregation may in fact be time dependent. The formation of Si complexes with calcium and phosphorus may again explain this, as silicate bridges (Si-O-Si) may be unable to form in BGs due to unavailability/blocking of free Si hydroxyl groups (Si-OH). Further NTA data showed that silicates alone formed larger diameter particles in McCoy's media (220 nm) compared to BGs (160 nm) over 8 days. Silicate particles of approximately this size have been shown to decrease bone nodule formation and cell viability[208]. Despite this, it is unclear what proportion of these particles are silicate and which are protein aggregates or complexes of the two (silica particles with a protein corona).

Although the same trend was found in all observed media types, differences in average particle diameter were observed between Si-conditioned media types. In addition, fully supplemented media alone, produced an increase or an equal average particle diameter to silicate or BGs. This suggests that serum proteins may aggregate over time whilst incubated at 37°C, thus making estimation of Si particle sizes in media difficult or inaccurate. The baseline concentration of salts[209, 210] and pH buffers in different media may prevent protein aggregation and thus may explain diameter and size distribution in media alone and with silicates (Figure 2.6 and Figure 5.1). Differences observed in the size of silicate and BG particles when cultured in different media types, might explain some of the considerable variance in outcomes reported in previous studies (see Figure 1.4). The cell type (e.g., primary vs cancerous) or media types used *in vitro*, may determine their uptake quantity and thus viability when cultured with different size particles[211]. A larger number of SS particles in culture compared to BG particles, may also explain why negative outcomes from cells were reported at a lower concentration (~10-20 ppm/~357-714 μM – Figure 1.4) than that of overall responses to BGs (~50 ppm/1.79 mM – Figure 1.7a)

Differences in characteristics (chemical and size) of these particles may raise the question whether SS particles serve as an appropriate model for studying the effects of silicates released from BGs. Alternatively, it may provide evidence for increasing the release of other ions including phosphorus and calcium to stabilise Si particles released from BGs. Although di and tri-sodium silicates powders have a 2:1 and 3:1 ratio of silica to sodium when manufactured, without identification of the species (via NMR) that each produce, it's unclear whether each produces the species its name implies. Quantification of the species at 2 mM Si from each of these sources via NMR (other than SS) would require ^{29}Si isotopes of di and trisilicates, which doesn't yet commercially exist.

2.6 Conclusion

This study, for the first time, has identified the species of Si released by 45S5 BGs, and has demonstrated differences in abundance, chemistry and physical properties of silicate and BG particles that arise in culture media and water. An increase in Si chain length was found to be [Si] dependent with an increase resulting in a rise in Q^{1-4} species. At [Si] relevant to previous *in vitro* studies (1-4 mM), only orthosilicate species were observed up to 2 mM Si in 45S5 BG dissolution products with both ortho and disilicate species found above this concentration, suggesting that Si polymerisation.

SS conditioned media was found to produce larger precipitates/particles than those in BG media, suggesting that Na, Ca and P may inhibit Si particle formation and thus Si-cell interactions. An increase in [BSA] was observed with increasing [Si] from both Si sources (significantly more in SS), suggesting a reduction in the bioavailability of serum proteins. Protein binding was also confirmed by FTIR spectra showing carbonyl and amine groups in both silicate and BGs samples.

In comparison to BGs, the average diameter of particles in silicate samples in water were observed to increase over time, suggesting that polymerisation may also time dependent. Particle size of precipitates was found to be different in different media types, which may explain the high variance in cellular outcomes reported in previous *in vitro* studies. This may be explained by differences in ion contents in different cell culture media contributing to Si particle formation.

Chapter 3. Si uptake and secretion dynamics in osteoblasts

3.1 Introduction

A systematic review of the literature, demonstrated a [Si] dependent effect on cell behaviour (Figure 1.7). It is not clear, however, how much Si is taken up by each cell, if Si is excreted from cells and what effect intracellular [Si] has on cell behaviour. A better understanding of the uptake and excretion dynamics may be important in determining the role of Si on cells and in designing bioactive glasses with specific release profiles tailored to individual cell types. Intracellular [Si] will likely depend on the species present, whether it is in ionic or particle form and the other components of the blood/cell culture media (e.g., serum and other ions)

3.1.1 Uptake and secretion of Si

To date, there are few articles that have investigated intracellular Si concentration. Obata *et al* demonstrated that after five days of osteoblast culture with 45S5 dissolution products, the Si concentration in cell supernatants decreased by ~5% suggested Si uptake or precipitation[145]. They also showed that 45S5 dissolution products produced higher intracellular [Si] compared to silicate-doped vaterite, suggesting that either the specific Si species released differs between source bioceramics or other ions alter uptake pathways/mechanisms. A

limitation of ICP-OES is, however, its inability to distinguish between ions and particles, both of which are vaporised inside of the instrument's plasma. Therefore, it is unclear what proportion of these Si conditioned mediums are ions or particles and what effect this has on intracellular [Si].

Other methods to quantify ions within cells, includes ion-selective microelectrodes which have been used to measure Ca, P and Na concentrations inside of cells[212]. Despite being able to quantify ion concentration at very low concentrations, there is no commercially available microelectrodes capable of quantifying silicon. In addition, this technique requires impaling cells with a needle tips electrodes, which is likely to influence cell behaviour[211].

To date no study has attempted to quantify Si species excretion from osteoblasts (or any other cell type) *in vitro*. Confirmation of this process occurring could provide evidence as to whether secretion and uptake happen simultaneously or only when a specific intracellular concentration of Si has been reached. Assessment of whether Si is secreted is more difficult to quantify, however, considering the low concentration of ions excreted diluted into a much larger volume of supernatant in-vitro. Isolation of exosomes from cell supernatants may provide evidence of Si secretion whilst shedding light on whether Si is involved in cell-cell communication in bone formation. If Si were to be found inside of exosomes, this may suggest that exocytosis may be (in addition to ion channels), one of the active mechanisms of Si transportation out of cells.

3.1.2 Si uptake mechanisms

Whilst most studies generally agree that Si is moved into cells in the form of ions, the major mechanism/pathway of Si translocation into cells remains poorly understood. Several previous studies have suggested different uptake pathways that focus on the role of transmembrane co-transporter proteins. Ratcliff *et al* observed that when dietarily Si-deprived, the protein expression of a sodium-

phosphate co-transporter (Slc34a2) was found to be upregulated in rat kidney tissues[213]. The same study showed that by upregulating this co-transporter in oocytes (frog derived cells), an efflux in germanium tetrahydroxide (an orthosilicate substitute) was observed. Despite this, no human cells were used in the study and thus it is unclear if the same mechanisms are present in humans, or bone cells in particular. Schroder *et al*, found that the sodium-bicarbonate co-transporter was the primary protein involved in uptake of silicon in diatoms[214]. Protein profiling on this co-transporter found it bared 46% amino acid similar to the same co-transporter found in humans, suggesting it may be responsible for Si transport in the body. Although like the phosphate co-transporter, this has yet to be studied in humans.

To date the only study conducted on human cells, showed that aquaporins (cell membrane water channels) conduct Si transport across the membrane. Garneau *et al* showed that by silencing the expression of specific aquaporins in HEK-293 (embryonic hepatocytes) cell line, an influx of Si compared to a non-silenced control was reported[215]. It is still unclear however, if silencing aquaporins negatively effects cell viability and thus its uptake rate. This observation is contradictory to our previous knowledge of charged ions, demonstrating that similarly charged ions required active (protein based) ion pumps to move ions across the membrane. More evidence is needed to understand how silicate ions could move across polarised membranes via passive processes.

The formation of (nano)particles via the polymerisation of orthosilicate ions could suggest, however, that endocytosis may (in-part) be responsible for the movement of Si into cells. The extracellular binding of Si to serum proteins (protein corona) may also increase particle size and therefore make particles more likely to follow an endocytic pathway. Nanoparticles of silica in range of 10 nm to 650 nm have been shown to be uptaken via endocytosis in osteoblast-like cells[216]. If this is the case, exocytosis may be a possible mechanism used by cells

to secrete Si[217]. Identification of Si uptake mechanisms may help to tailor Si release from BGs to target specific forms of uptake for optimal cellular responses.

3.2 Chapter aims and hypotheses

Whilst Si has been shown to be beneficial to cell responses, the specific intracellular concentration that elicit these response remain unclear. As presented in chapter 2, Si alone produced more precipitation than BG dissolutions products at the same [Si] in culture media and water. It is uncertain how this particle formation affects intracellular [Si] and therefore its influence cell behaviour. As such, this chapter aimed to assess impact this has on quantity and mechanism of Si species uptake in cells.

This chapter investigated:

1. The effect of [Si] and Si species on cell viability over time.
   - Hypothesis: Increasing [Si] and longer chained Si species (Di and trisilicates) will negatively impact upon cell viability
2. How intracellular [Si] varies over time between culture with Si alone and BG dissolution products
   - Hypothesis: Si alone will produce a higher intracellular [Si] than cells cultured in BG dissolution products due to greater formation of precipitates. A maximum intracellular [Si] exists in cells
3. How [Si] and Si species and in culture medium affect Si uptake mechanisms (endocytosis and active transport).
   - Hypothesis: Inhibition of endocytosis will reduce the intracellular [Si] when culture with media containing Si above 2 mM
4. If Si is excreted from cells and if so, by what mechanism.
   - Hypothesis: Si is secreted by cells via exocytosis

3.3 Materials and methods

3.3.1 Preparation of media containing silicates and SBGs

Si-conditioned medium was prepared by adding either sodium silicate hydrate or 45S5 bioactive glasses to McCoy's Glutamax 5A culture supplemented with 10% FBS and 1% penicillin/streptomycin antibiotic. Concentrated stock solutions were prepared, and ion concentrations determined by ICP-OES followed by dilution in media to the desired Si concentration. All Si conditioned mediums were then sterilised by filtration with a 0.2 μm filter and stored at 4°C. To prepare mediums containing different Si species, silicate compounds sodium di and tri-silicates powders were obtained from Silmaco, (Belgium) and stock solutions made as described in 2.3.

3.3.2 Osteoblast cultures

Cell-Si interactions were evaluated using osteoblast-like cells (SaOS-2)[172]. Cells were cultured in McCoy's 5A Glutamax mediums supplemented as stated in section 5.2.1. The following cultures and incubations took place at 37°C (5% CO_2, 20% O_2). All experiments including SaOS-2 cells (passage 1-5) were seeded at 10'000 cells/cm^2. To assess differences in Si uptake between cell types (primary vs cancerous), primary osteoblasts were isolated from rat calvaria and kindly donated by Dr Azadeh Rezaei, according to protocols described in Orriss et al[218]. Briefly, The neonatal rats were euthanized, sterilised with 70% ethanol and transferred to a biosafety cabinet. The head was separated and an incision made along the skull to remove the skin before dividing the head in half. Following removal of the brain tissue, the jaw and excess cartilage tissues, the calvariae were washed with PBS. PBS was then replaced with 1 mL (per calvarial bone) of 0.25% trypsin/EDTA solution and calvariae then incubated at 37°C in a 5% CO_2 for 10 minutes. Trypsin was then discarded and calvariae washed with α-MEM media containing 10% FBS, 2 mM L-glutamine and 1% antibiotic/antimitotic (100

U/mL penicillin, 100 μg/mL streptomycin and 0.25 μg/mL amphotericin). The bones were then washed with α-MEM, and incubated with 800 μL of 0.2% collagenase solution, per calvarial bone for 30 minutes at 37°C. The collagenase was discarded and replaced with a fresh solution and incubated for a further 60 minutes at 37°C. Following collection of the final collagenase digestion, isolated osteoblasts were centrifuged at 5 minutes at 1500 rpm at room temperature. The resulting cell pellet was then resuspended in 1 mL (per calvarial bone) of α-MEM, filtered with a 100 μm cell strainer to remove any remaining bone tissue fragments and plated into a 75 cm^2 tissue culture flask, with 20 mL of α-MEM added. The plate was subsequently incubated at 37°C for 3 days until the cells reach confluency. Cells were then seeded into T75 flasks for Si uptake experiments.

3.3.3 Osteoblast viability with [Si] and Si species

To evaluate cell viability and potential toxicity with Si-conditioned mediums, SaOS-2 cells were seeded in 24 well plates and allowed to attach in normal culture medium for 24 hours. Cellular viability in culture with increasing Si concentrations (0, 0.5, 1, 1.5, 2.5 and 3 mM) was determined by metabolic activity, proliferation, and cell death assays over 1, 3 and 7 days. As quantification of intracellular [Si] was performed in continuous culture (without changing media), cell viability was similarly performed without a media change. To investigate the effect of glucose availability during culture, cell viability with [Si] was also performed with a medium change every two days. The same experimental set up (no medium change) was used evaluate cell viability with different Si species (ortho, di and tri-silicates and 45S5 bioactive glasses at 2 mM Si).

3.3.3.1 Metabolic activity

The metabolic activity of cells was assessed using Prestoblue fluorescent dyes (Invitrogen, Merck). Prestoblue solutions were prepared at a 1:10 dilution with

mediums containing no Si and warmed to 37°C prior to addition to cells. At each time point, cell supernatants in wells were removed, replaced with Prestoblue dye and incubated in a CO_2 incubator for 1 hour. 100µl of cell supernatants containing Prestoblue dye were then transferred to a black well 96 well plate and fluorescence of each well measured at 560:660 nm (excitation: emission) in a Fluoroscan spectrometer plate reader (Thermofisher, UK). Fluorescence was assumed to be directly proportional to metabolic activity of cultured cells.

3.3.3.2 Proliferation

Quantification of DNA from these cells was then used to determine cell numbers. Briefly, cell lysis was caused by immersing cells in 250ul of distilled water, followed by 6 freeze and thaw cycles following metabolic activity assays. DNA concentrations were then quantified using Hoechst dyes according to DNA quantification kits (Merck). Sample fluorescence was measured using the same equipment used for metabolic assays but at 360:440nm (excitation: emission) wavelengths. This data was then converted to DNA concentration using standard curve produced by a serial dilution of DNA stock solutions included with the kit.

3.3.3.3 Cell death

Release and quantification of adenosine kinases (AKs) from cells was used determine the percentage of cell death. At each time point, cell supernatants were removed from culture and Triton X-100 added at 1% of the total volume in order to lyse detached cells. Toxilight kits (Lonza) were then used to quantify AKs present in the supernatants according to manufacturer's instructions. Briefly, supernatants were added to AK detection reagents in a ratio of 1:5 and incubated at room temperature for 5 minutes. Luminescence in each sample was then measured using a Tecan infinite M200 Pro. This data was then compared to AK release from total cell lysis to produce cell death percentages.

3.3.4 Uptake of different Si species

To investigate how intracellular [Si] changes with uptake of different Si species, cells were cultured with sodium silicate, sodium-di and trisilicates and 45S5 bioactive glasses. Stock solutions of each Si species and BGs were made by adding silicate and BG powders to culture medium at 2 mg/ml and 200 mg/ml respectively before diluting to 2 mM Si. Prior to culture each Si species was incubator 37°C in a CO_2 incubator for 24 hours to equilibrate pH. Cells were then cultured with each Si species and bioactive glasses for 24 hours before quantifying intracellular [Si] and normalising to cell numbers by [DNA] quantification. Due to the relatively low intracellular [Si] per cell, a high number of cells were necessary to quantify this using ICP-OES. Due to the number of cells necessary and the time and high costs involved in primary cell isolation, SaOS-2 were used in Si uptake and secretion experiments.

3.3.5 Quantification of Si uptake over time

To determine whether a maximum intracellular quantity of Si in osteoblasts exists (and the time this takes to occur), cells were cultured in media containing the highest Si concentration that did not cause negative cell viability. SaOS-2 cells were therefore seeded at 10,000 cells/cm^2 in T75 flasks with mediums containing SS and BGs at 2 mM Si for 24, 48, 96 and 192 hours. Cells were also seeded at the same density (in parallel) in 24 well plates in order to track proliferation. At each time point, silicate mediums were removed, cells detached, centrifuged at 400g and lysed by resuspension in 70% 1M nitric acid. Further lysis was achieved by freezing cells at -20°C and then heating them to 80°C. Samples were then diluted in distilled water and [Si] quantified using an ICP-OES instrument (Thermoscientific, UK). A standard curve was created by diluting standard solutions containing known Si concentration prior to reading cell samples. Optical spectra of cell samples was then converted to [Si] using standard curves.

Intracellular [Si] was then normalised to cell numbers by quantification of DNA in well plates according to protocols used in section 5.3.2.3.

3.3.6 Mechanisms of Si uptake

To verify if the uptake and secretion of Si species in osteoblasts proceeds via the exchange of ions across the membrane or via endocytosis (or both), SaOS-2 cells were cultured with molecular inhibitors of known ion and particulate transport pathways before quantifying both intra and extracellular [Si]. Specific cell surface ion co-transport proteins were chosen based upon previous literature suggesting involvement in Si uptake. Exchange of sodium-bicarbonate[219] and sodium-phosphate[220] ions and water via Aquaporin-3[221] were chosen for this purpose.

Inhibitor	Target	Concentration (μM)
S0859	Na^+/HCO_3^-	30
PF-0686902	Na^+/P^+	0.1
DFP-00173	H_2O (Aquaporin 3)	0.1

Names and concentrations of each inhibitor can be found in Table 4. To verify efficacy of co-transport inhibition Intracellular concentrations of non-Si ions [Na] and [P] were determined by ICP-OES.

Table 4 – **Concentrations of chemical inhibitors used to block possible ion and water channels associated with uptake of Si.**

Inhibition of clathrin-mediated endocytosis in cells was performed by the addition of Dynasore hydrate (Merck, UK)[222–224] to culture medium containing Si. Macia et al observed 80 μM Dynasore to optimally inhibit GTPase activity and thus function of dynamin 1 and 2 (necessary for endocytic vesicle formation) over a 30-minute period[225]. To reduce potential toxicity of endocytic inhibition during

Si uptake experiments, culture was reduced to from 24 to 8-hours before quantification of [Si]. The concentration of Dynasore hydrate (20, 40 and 80 μM) in medium that did not cause an increase in cell toxicity (compared to a control) over an 8-hour period was chosen in endocytosis-Si inhibitions studies. To verify the extent of endocytic inhibition over the same time period, cells were loaded with 50-100 nm gold nanoparticles followed by quantification of intracellular [Au] with and without Dynasore. To investigate the influence of [Si] (and potentially different species) on endocytic uptake, intracellular [Si] was quantified following 8-hour culture with 2- and 3-mM Si, with and without Dynasore inhibitor.

3.3.7 Quantification of Si secretion

To verify whether Si is secreted, cells were cultured in Si conditioned mediums for 4 days (intracellular Si saturation point) before replacing mediums with those containing no Si for 1-3 days. At each time point (following medium replacement), intra and extracellular [Si] were quantified and normalised to cell numbers. Non-Si containing mediums (containing secreted Si) were stored at -20°C to investigate mechanisms of Si secretion.

To investigate whether Si was secreted by cells via exocytosis, exosomes were isolated from cell supernatants during secretion experiments into non-Si culture mediums. Isolation of exosomes from culture medium (containing no Si) was performed using a total exosome isolation kit (Thermofisher, UK) according to manufactures instructions. Briefly, supernatants were centrifuged at 400g to remove cell debris before adding exosomal isolation buffer (1:10) for 24 hours at 4°C to reduce the solubility of exosomes. Solutions were then centrifuged at 10,000g for 1 hour and pelleted exosomes resuspended in PBS. To purify samples containing exosomes, magnetic human CD63+ Dynabeads (Thermofisher, UK) were used according to manufactures instructions. Briefly, Dynabeads were washed with PBS containing 0.1% bovine serum albumin (BSA) and pelleted

using a neodymium magnet. The beads were then added to exosome samples and incubated at 4°C on an orbital shaker at 150 rpm for 24 hours. Nitric acid (1M) was then used to lyse exosomes and Si quantified by ICP-OES. Exosome isolation was validated visually (TEM) and quantitatively (nanoparticle tracking analysis). Prior to electron imaging, samples were fixed in a solution containing 2.5% glutaraldehyde and 4% paraformaldehyde and 0.1M sodium cacodylate in water, negatively stained in water containing 1% osmium tetroxide and dehydrated in a 30-100% ethanol dilution series. Exosomes were then embedded in epoxy resin (MERCK) in series 1:1, 1:2 and 100% ethanol to resin and cured at 60°C for 24 hours. Resin blocks were then sectioned to 60 nm and post stained in 1% Uranyl acetate-zero (UA-zero). Images were then taken at 100 KeV on a Phillips 300 TEM.

3.3.8 Statistics

A Robust Regression and Outlier Removal Test (ROUT) was used to determine if data contained anomalous or outlier values with an outlier sensitivity parameter ('Q') of 1% (Q=0.01). Significant outliers were then removed from overall data if $P<0.05$. All conditions were then assessed for normality (Gaussian distribution) using a Shapiro-Wilk test. Table 3 describes the statistical test used to determine significance between conditions dependent on; the study design, whether data was normally or non-normally distributed and their respective multiple comparisons (if applicable). Differences between conditions were then determined to be statistically significant if $P<0.05$. Asterisks (*) are used to indicate significance between conditions where *=$P<0.05$, **=$P\leq0.01$, ***=$P\leq0.001$, ****=$P\leq0.0001$ etc.

3.4 Results

3.4.1 Osteoblast viability with [Si] and Si species

To determine the maximum, non-toxic [Si] cell metabolic activity, cell proliferation and cell death were quantified in two experimental designs, continuous culture (no media changes over time), and staggered culture (media changed every two days). No significant differences in metabolic activity were observed with any [Si] concentration (0-3 mM Si) at any time point without a medium change (Figure 3.1a). A significant decrease was, however, observed in cell numbers and proliferation at [Si] above 2 mM (P≤0.05 – Figure 3.1b and c).

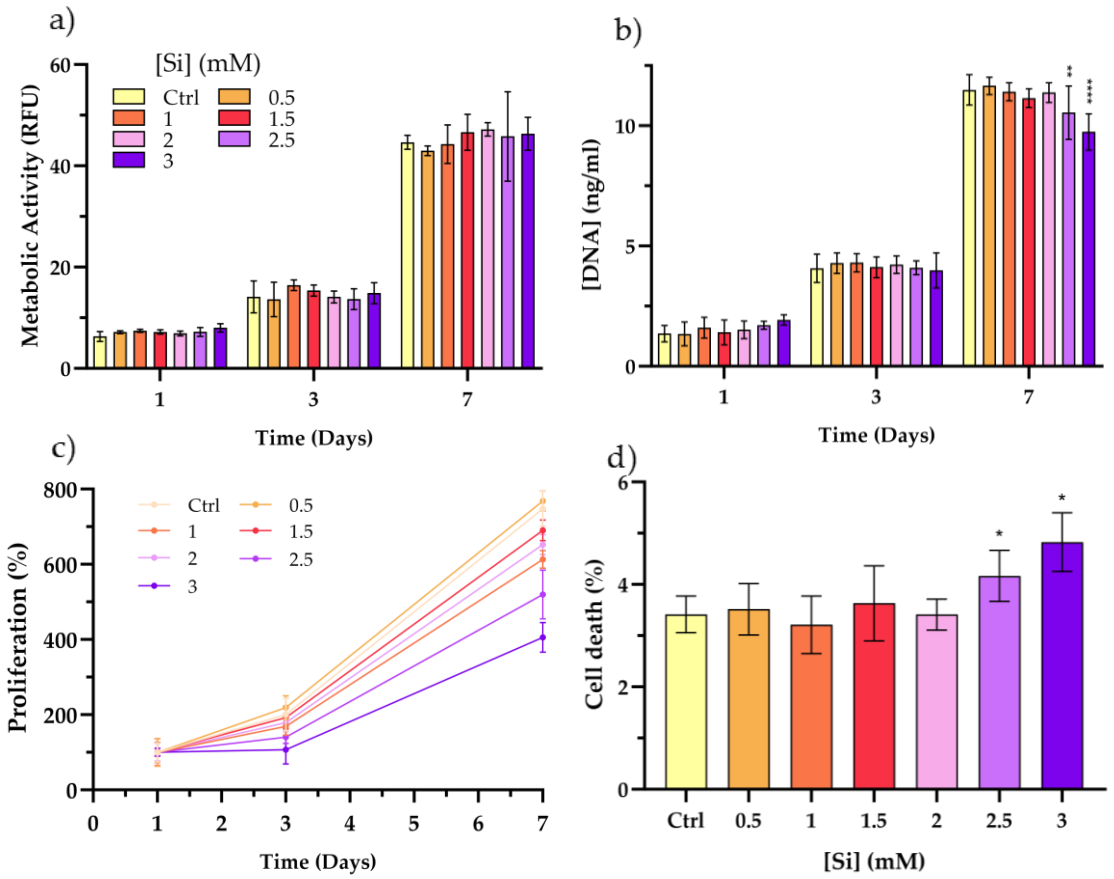

Figure 3.1 - **SaOS-2 metabolic activity, proliferation and death in media containing increasing [Si] (with no media changes).**

*Whilst [Si] above 2 mM was found to cause no differences in metabolic activity (a), significantly decreases were found in cell numbers (b) and proliferation (c) at day 7. A significant increase in cell death % was also observed at day 7 (d). Results are presented as the mean ± SD. **=P≤0.01, ****=P≤0.0001 compared to a control (no Si). Is this correct – only 3 well used?*

Percentage cell death followed a similar trend to cell numbers, producing a significant increase (P≤0.05) at [Si] greater than 2 mM Si (Figure 3.1d). When compared with viability when culture media was changed every two days, more visibly negative trends were observed with increasing [Si]. A significant decrease in metabolic activity, cell numbers and percent proliferation (Figure 3.2a, b, and c respectively) was found at 0.5 mM Si and above (P≤0.05). An increase in cell death percentage was also observed at the same [Si] (P≤0.05 – Figure 3.2d).

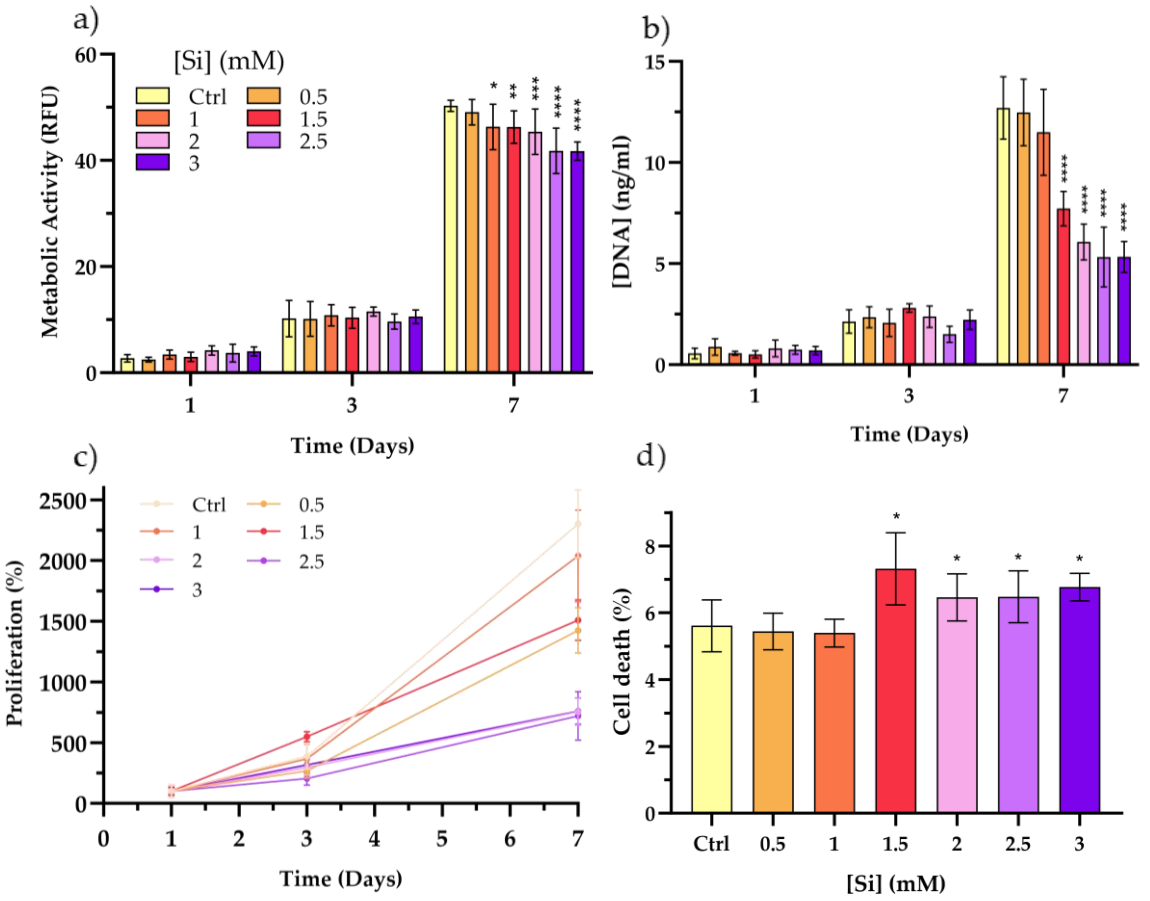

Figure 3.2 - **SaOS-2 metabolic activity, proliferation and death in media containing increasing [Si] (with media changes every 2 days).**

*[Si] above 1 mM was found to cause a decrease in metabolic activity (a), cell numbers (b) and proliferation (c) at day 7. An increase in cell death % at day 7 was observed at all time points above 1 mM Si (d). Results are presented as the mean ± SD. *=P<0.05, **=P≤0.01, ***=P≤0.001 ****=P≤0.0001 compared to a control (no Si). N=3*

Cells cultured in trisilicates and 45S5 dissolution products were found to increase metabolic activity at day 3 (P≤0.05) but not at days 1 and 7 compared to a non-Si control (Figure 3.2a). No significant differences were observed in the metabolic activity of cells cultured in meta or disilicates at any time point. No significant differences in cell number were observed at any time point (Figure 3.3b), although only 45S5 cultures were found to significantly decrease proliferation percentage (P≤0.05 – Figure 3.3c). Only trisilicates were observed to significantly increase percentage cell death (P≤0.01 – Figure 3.3d), whilst no significant differences were found in any other species and bioactive glasses compared to the control.

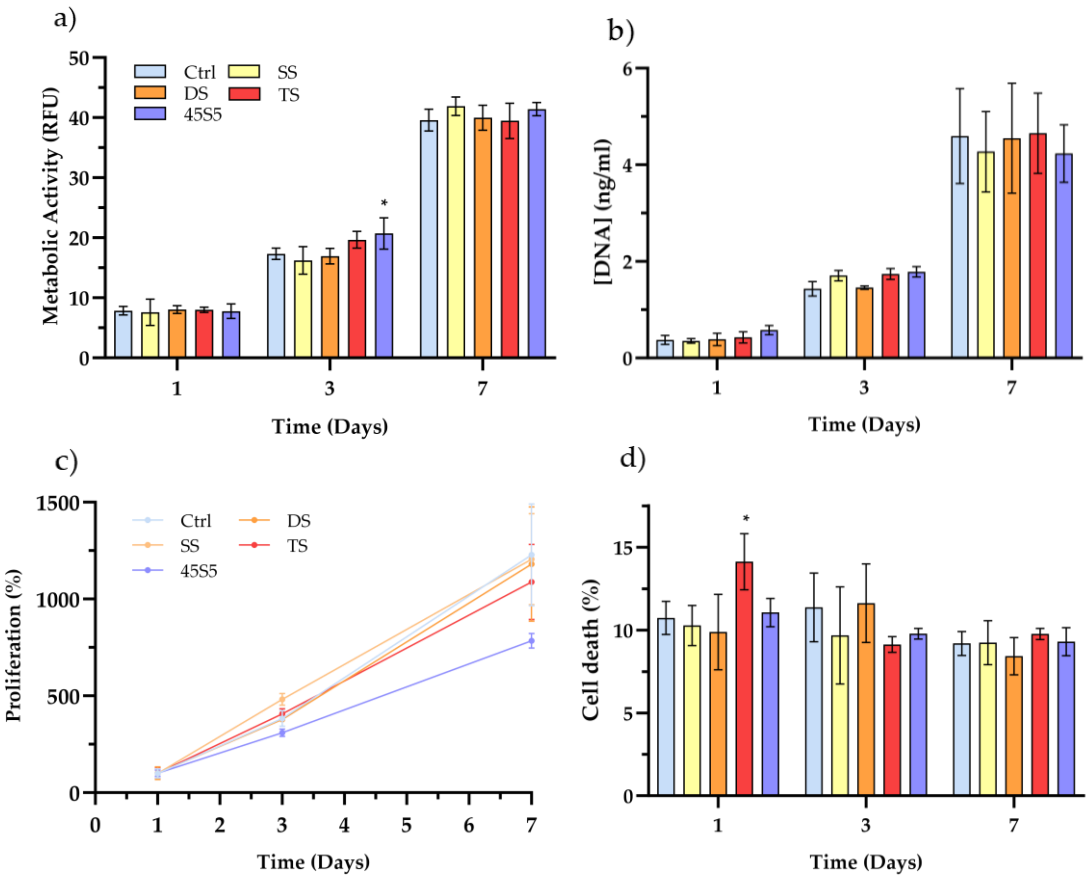

Figure 3.3 - **SaOS-2 metabolic activity, number and cell death in media containing different Si species and 45S5 bioactive glasses (BG) at 2 mM Si.**

*No significant differences were observed in either metabolic activity (a) or cell numbers (b) at any time point. BGs were found to decrease proliferation % (c) at day 3 and 7. Trisilicate caused an increase in cell death % (d) at day 1. Sodium silicate=SS, sodium disilicate=DS, sodium trisilicate=TS. Results are presented as the mean ± SD. *=P<0.05, **=P≤0.01, ***=P≤0.001 and ****=P≤0.0001 compared to a control (no Si).*

3.4.2 Uptake of different Si species

To determine whether Si species (or increasing Si chain length) influences uptake and thus intracellular concentration, cells were cultured for 1 day with Si from SS and sodium di and trisilicates. Intracellular [Si] was then compared to those of cells cultured in mediums containing Si from 45S5 bioactive glasses. Compared to orthosilicates (Mn = 377.8 μM Si), [Si] in cells was observed to decrease in di

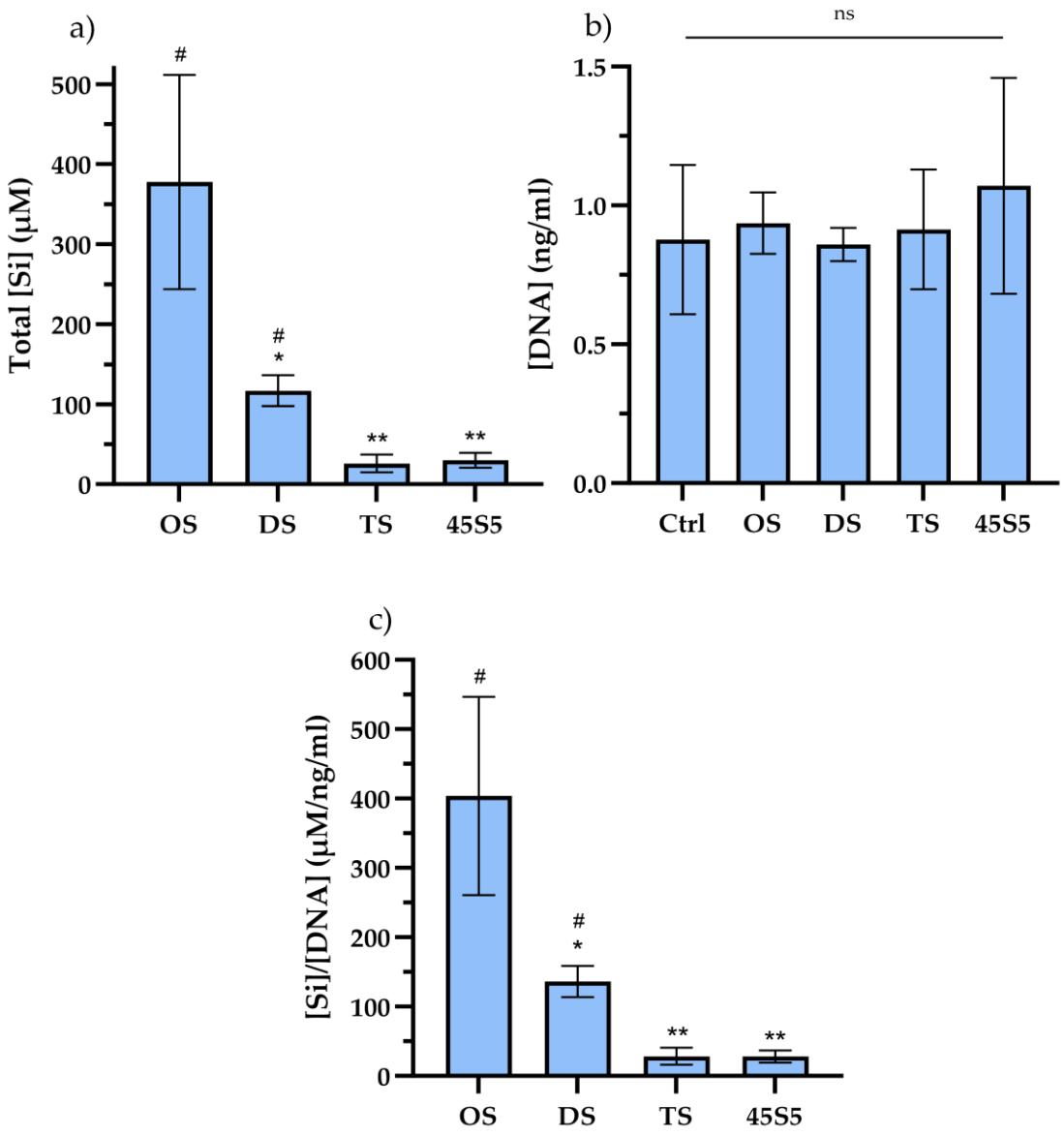

Figure 3.4 - **Intracellular [Si] following culture with different Si species and 45S5 bioactive glasses.**

*When compared to orthosilicates (OS), a significant decrease in total intracellular [Si] was found in a disilicates (DS), trisilicates (TS) and 45S5 BGs (a). When normalized against cell numbers (b), the same result was observed in [Si] per unit DNA (c). Results are presented as the mean ± SD. *=P≤0.05, **=P≤0.01 compared to SS and #=P<0.05 when compared to BGs. N=3.*

(Mn = 116.9 μM Si) and trisilicates (Mn = 25.9 μM Si) in total intracellular [Si] (Figure a). Both ortho- and disilicate conditioned mediums were determined to produce intracellular [Si] in cells significantly higher ($P \leq 0.01$) than those with trisilicate mediums (Figure 3.4c). When cultured with 45S5 bioactive glasses, however, intracellular [Si] was observed to be significantly lower ($P \leq 0.01$) than ortho and disilicates cultures but insignificantly different to trisilicates ($P > 0.05$) suggesting a possible similarity in Si species present in the two mediums.

3.4.3 Uptake Si in osteoblasts over time

To determine the maximum [Si] that could be taken up by a population of cells, Si-conditioned medium was added to cultures and [Si] quantified over time until an intracellular concentration plateau occurred. Total intracellular [Si] was observed to increase from 1 to 8 days from 26.6 to 1274.2 μM Si (Figure 3.5a). When intracellular [Si] was then normalised to cell numbers, the rate of [Si] was found to decrease with increasing time from 40.9 – 224.3 μM/ng/ml Si (Figure 3.5c). No significant differences were observed between Si concentrations at day 4 and 8 and therefore, a maximum uptake was assumed to occur at this concentration per unit DNA after 4 days. Intracellular [Si] when cultured with BG conditioned medium increased up to day 8 from 13.3 to 53.9 μM Si (Figure 3.6a). When normalised to cell numbers, however, a decrease in intracellular [Si] per unit DNA was observed from 6.1 to 4.4 μM/μg/ml Si (Figure 3.6c). No significant differences in intracellular [Si] per unit DNA were found between day 4 and 8. No differences were observed in total intracellular [Si] between SaOS-2 cells and primary rat osteoblasts (ROBs) over 4 days (Figure 5.7a). Less SaOS-2 cells were observed compared to ROBs ($P < 0.001$) (Figure 5.7b), resulting in a greater normalised intracellular [Si] ($P < 0.05$) (Figure 5.7c).

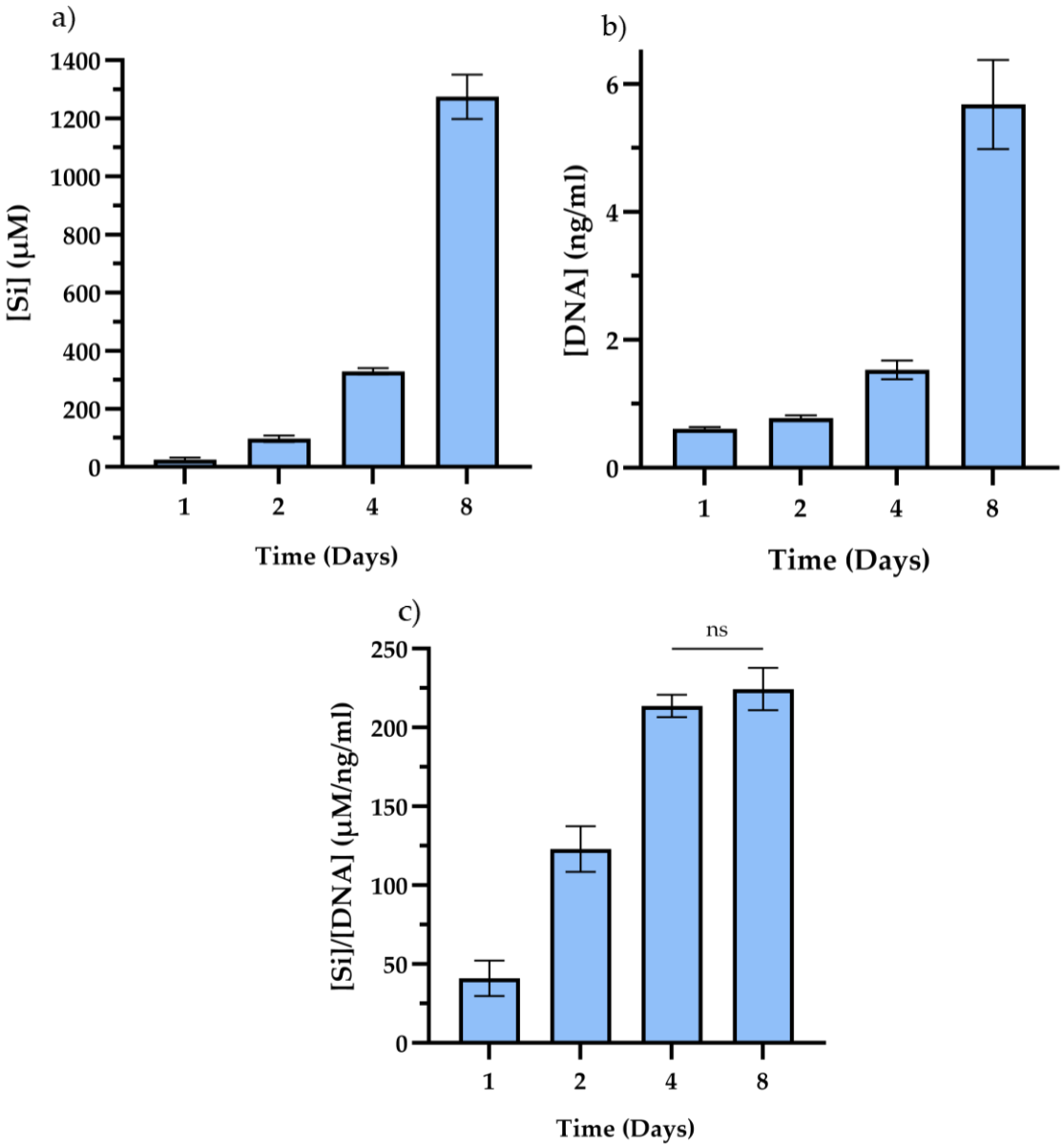

Figure 3.5 - **Intracellular [Si] over time following culture with media containing sodium silicate (SS).**

Total intracellular [Si] (a) was found to increase exponentially over 1-8 days. When normalised against cell numbers (b), intracellular [Si] per unit DNA was found to increase up to a maximum at 4 days (c). Results are presented as the mean ± SD. N=3

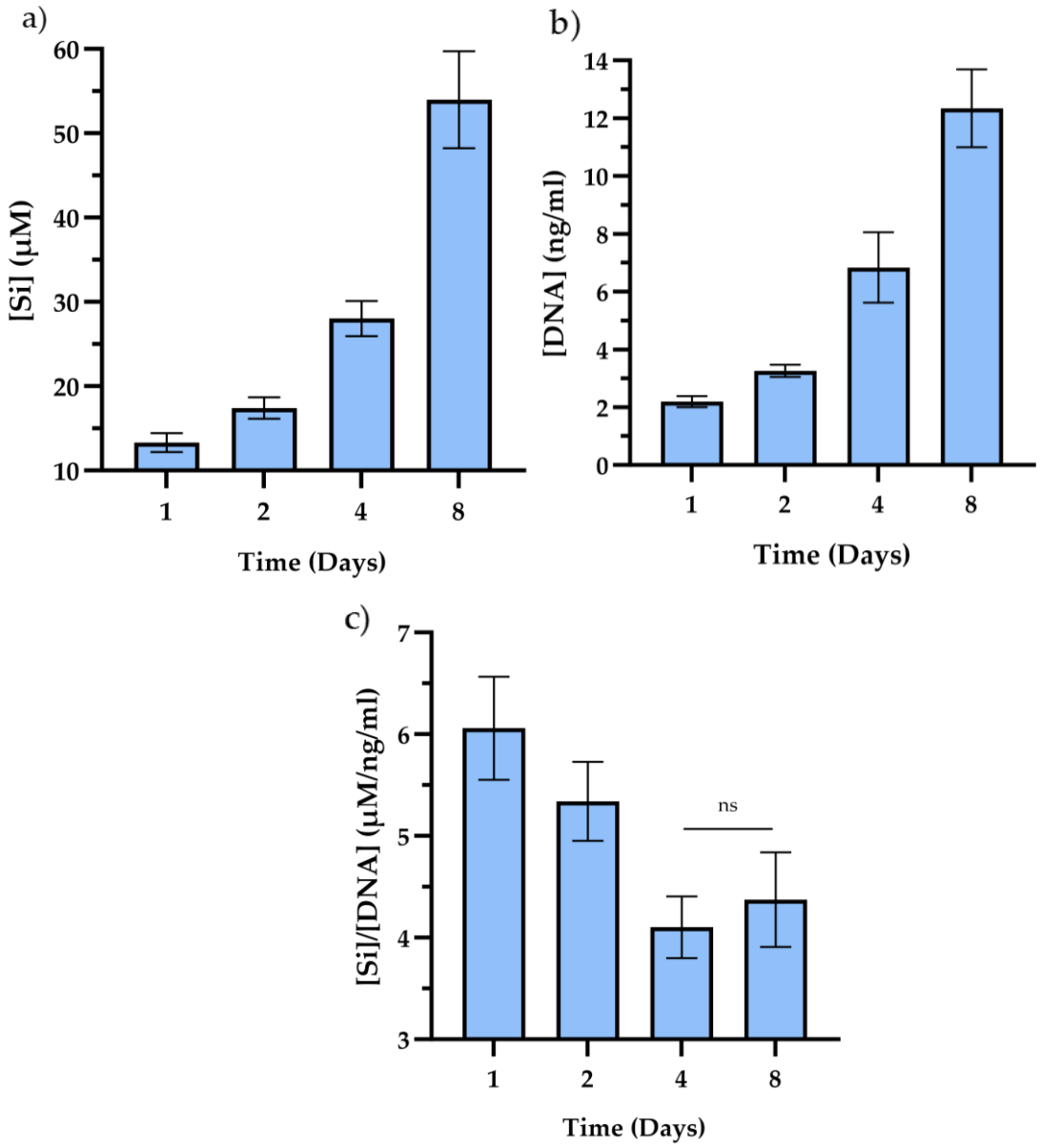

Figure 3.6 - **Intracellular [Si] over time following culture with media containing 45S5 bioactive glasses.**

Total intracellular [Si] (a) was found to increase over 1-8 days. When normalised against cell numbers (b), intracellular [Si] per unit DNA was found to decrease up to 4 days (c). Results are presented as the mean ± SD. N=3

3.4.4 Cell viability with Dynasore hydrate and Au nanoparticles

To assess whether the inhibition of endocytosis in cells via the addition of Dynasore hydrate, caused toxicity, cell viability was evaluated over an 8-hour period. Viability of cells cultured with Au nanoparticles (used to confirm endocytosis inhibition) was also assessed. No significant differences in metabolic activity were observed at 20 or 40 μM Dynasore up to 8 hours compared to the control (Figure 3.7a). At 80 μM a significant decrease in metabolic activity was

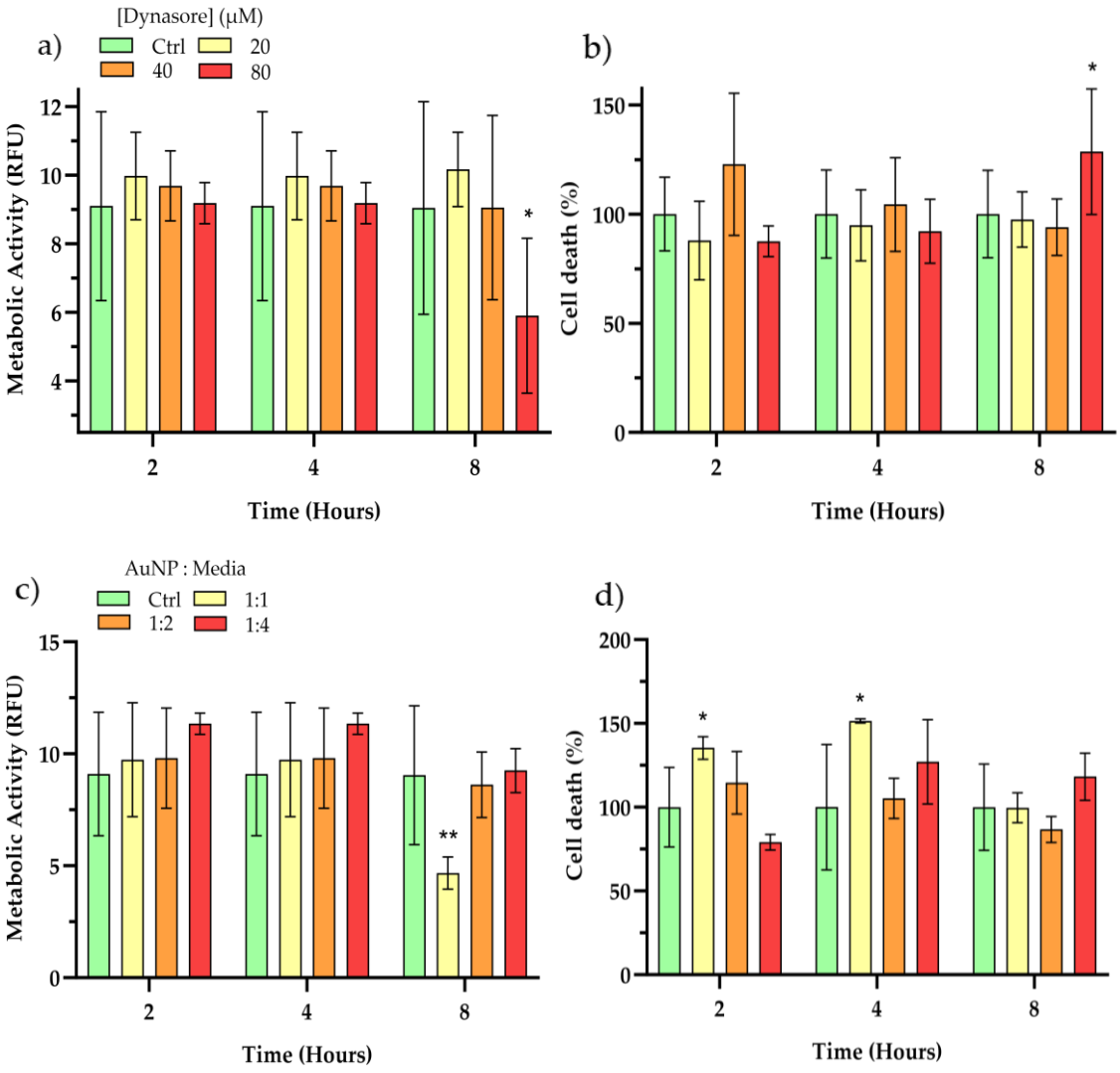

Figure 3.7 – **Metabolic activity and cell death at different concentrations of Dynasore hydrate and ratios of gold nanoparticle (AuNPs) to media.**

*No significant difference in metabolic activity (a) or cell death (b) was found below Dynasore concentrations of 80μM after 8 hours. Au NPs did not demonstrate a concentration dependent effect on metabolic activity apart (c) or cell death (d) Results are presented as the mean ± SD. *=P<0.05, **=P≤0.01 compared to a control (no Dynasore hydrate or AuNPs).*

found at 8 hours (P≤0.05), but not at 2 or 4 hours. No significant differences were observed in cell death at 20, 40 or 80 μM Dynasore up to 4 hours (Figure 3.7b). At 8 hours, however, a significant increase in cell death percentages was observed compared to the control (P≤0.05). A decrease in metabolic activity was found in the metabolic activity of cells cultured with a ratio of 1:1 gold nanoparticles to media at 8 hours but not at 2 and 4 hours (Figure 3.7c). An increase in cell death, however, was observed at 2 and 4 hours with a 1:1 ratio (Figure 3.7d)

3.4.5 Verification of endocytosis inhibition

Uptake of gold nanoparticles were used to verify whether endocytosis had been inhibited in osteoblast cells. A significant decrease (P≤0.01) compared to a control with Dynasore inhibitor (10.6 μM Au) was observed in total [Au] when cultured with 40 μM Dynasore (4.5 μM Au - Figure 3.8a). No significant differences were observed in cell numbers between cell cultured with and without Dynasore and Au particles (Figure 3.8b). A significant decrease (P≤0.01) was, therefore, observed in normalised intracellular [Au] (17.8 vs 7.7 μM/μg/ml – Figure 3.8c).

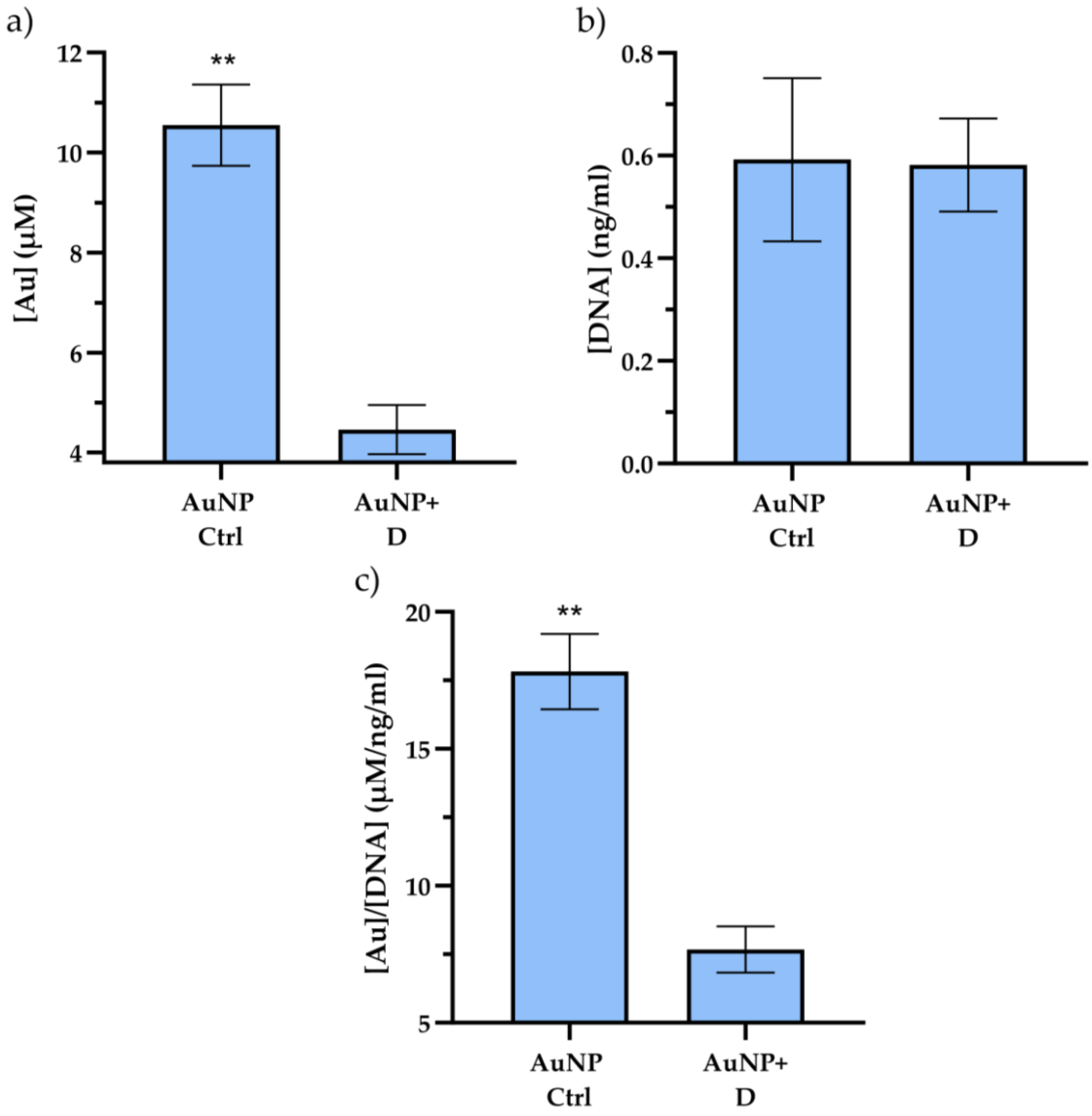

Figure 3.8 - **Intracellular [Au] following culture with media containing Dynasore hydrate after 8 hours.**

*Total intracellular [Au] (a) decreased significantly when cultured with Dynasore hydrate. When normalised against cell numbers (b), intracellular [Au] per unit DNA was also observed to be significantly lower than in controls (c). Results are presented as the mean ± SD. **=P≤0.01 compared to controls (no Dynasore hydrate). N=3.*

3.4.6 Si uptake via endocytosis and ion co-transport

To verify whether endocytosis is involved in the uptake of Si ions or particles, this uptake mechanism was inhibited with Dynasore hydrate during culture with Si-conditioned mediums. A decrease in the mean total intracellular [Si] (Figure 3.9a), [DNA] (Figure 3.9b) and intracellular [Si] normalised to cell numbers (Figure 3.9c) was observed following culture with both 2 and 3 mM and Dynasore hydrate. No significant differences were observed, however, in normalised or non-normalised intracellular [Si]. The influence of Si species on uptake

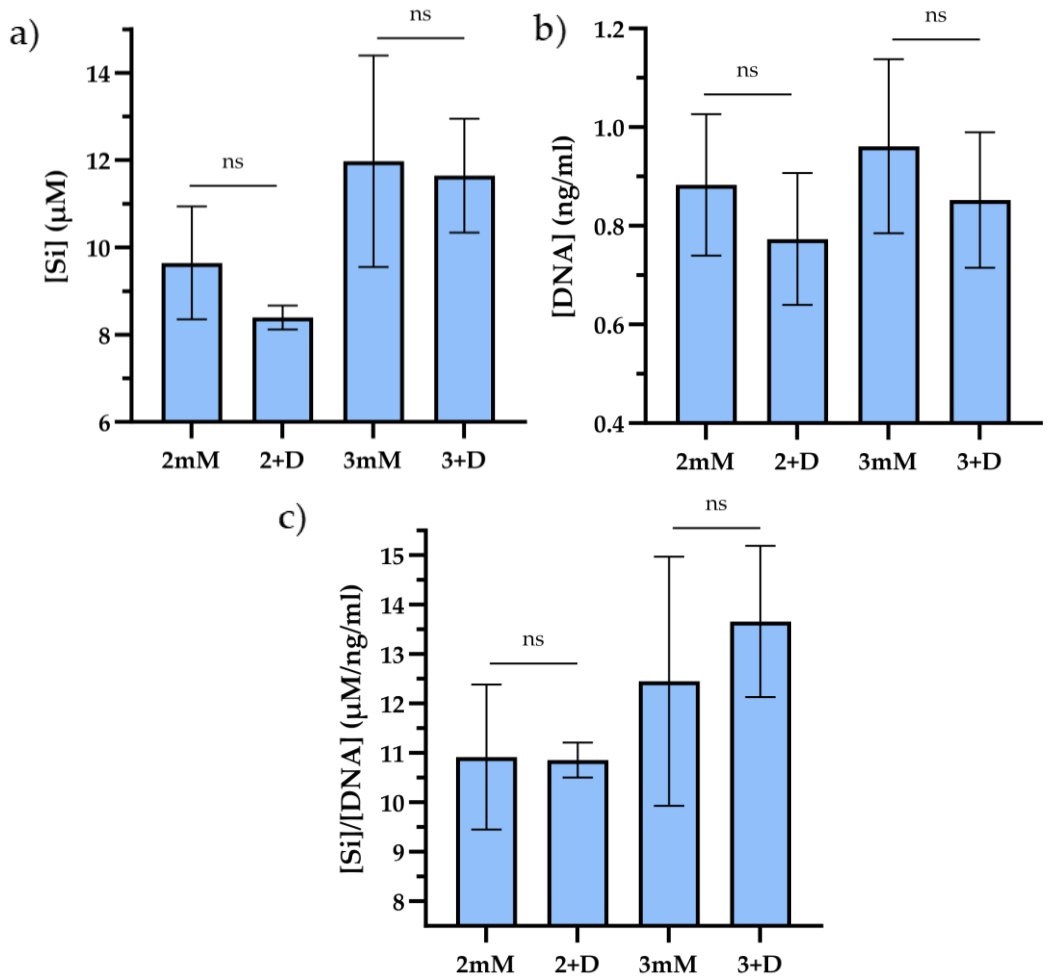

Figure 3.9 - **Comparison of intracellular [Si] following culture with media containing 2- or 3 mM Si and Dynasore hydrate after 8 hours.**

Total intracellular [Si] (a) was found to decrease when cultured with 2 mM Si and Dynasore hydrate (D). When normalised to cell numbers (b), no significant differences were observed in [Si] per unit DNA (c) in either concentration with D. Results are presented as the mean ± SD. N=3.

mechanisms was also quantified following culture with 45S5 BG dissolution products and trisilicate conditioned mediums for 8-hours. A decrease in mean total (Figure a) and normalised intracellular [Si] (Figure 3.9c) was observed in both trisilicates and 45S5. No significant differences were observed, however, in either condition.

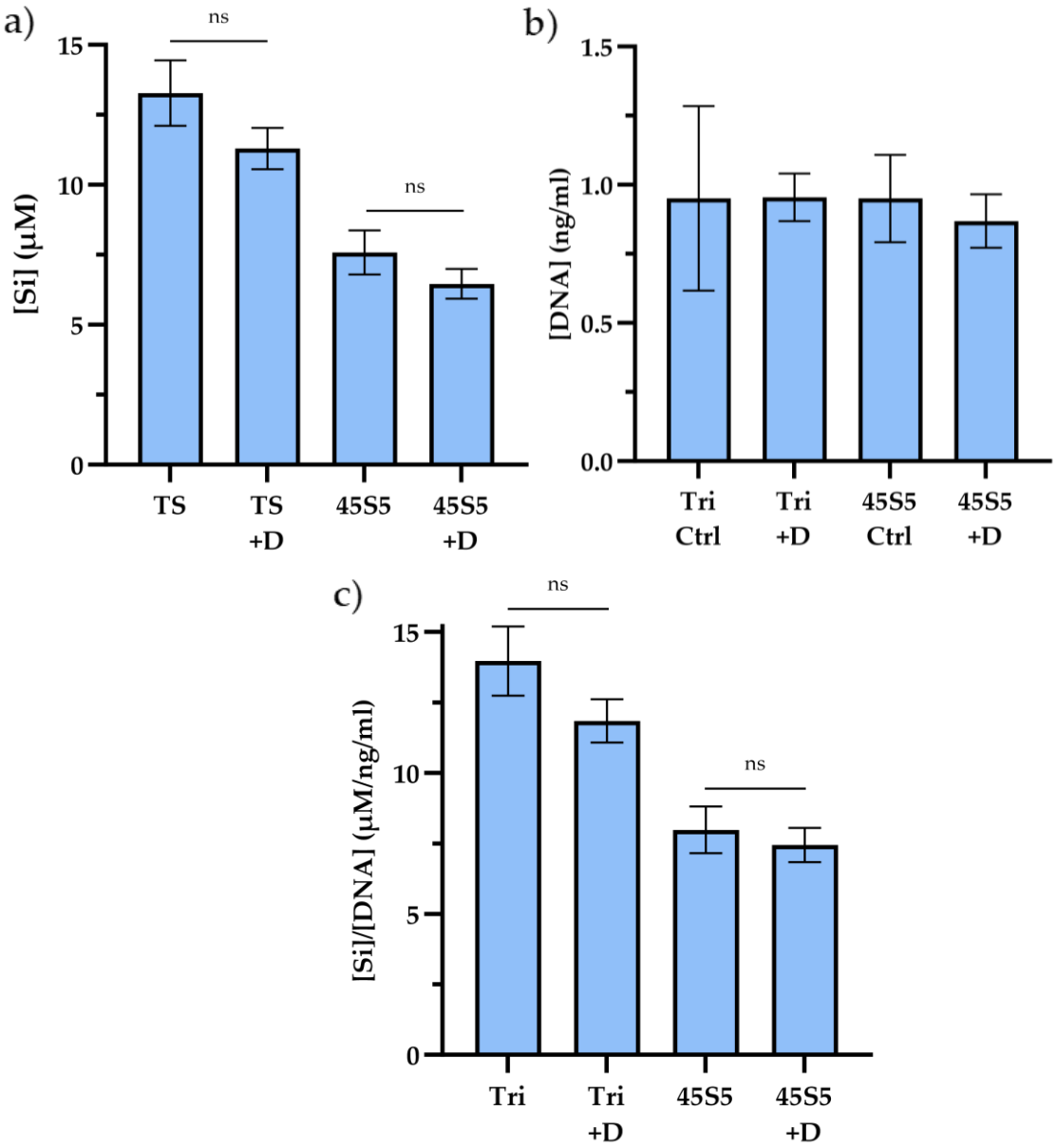

Figure 3.10 - **Comparison of intracellular [Si] following culture with sodium trisilicate and 45S5 bioactive glasses and Dynasore hydrate after 8 hours.**

No significant differences were observed in total intracellular [Si] (a), cell numbers (b) or intracellular [Si] normalised to cell numbers (c) when culture with sodium trisilicate (TS) and 45S5 BG with Dynasore hydrate (D). Results are presented as the mean ± SD. N=3

Cells cultured for 4 days with chemical inhibitors of specific membrane bound ion co-transporter proteins (Na/HCO_3, Na/P and aquaporins) were found to produce no significant differences in total or normalised intracellular [Si] (Figure 5.3a). No significant differences were observed in cell numbers with any inhibitor after 4 days (Figure 5.3b). Quantification of [P] (Figure 5.3c) and [Na] (Figure 5.3d) did not show any significant differences with any inhibitor suggesting that inhibition of that channel did not occur or intracellular changes in ion uptake were too small to be detected, compared to existing sodium and phosphorus in cells.

3.4.7 Si secretion

When Si media was replaced with Si free media, a decrease in the amount of intracellular [Si] occurred ($P \leq 0.01$), whilst extracellular [Si] increased between day 1 and 2 ($P \leq 0.05$ - Figure 3.11), suggesting secretion of Si from cells. Non-significant increases were observed in total and normalised [Si] in supernatants was observed between day 2 and 3. The decrease in intracellular [Si] was greater, and time dependent when normalised to cell number (Figure 3.11c). An increase in cell number (Figure 3.11b) may also mean distribution of intracellular Si among daughter cells during cell division, rather than excretion. To identify whether exocytosis is involved in Si secretion from cells, [Si] from exosomes (isolated from supernatants after the media change to non-Si media in Figure 3.11) was quantified. No significant differences were observed in exosome [Si] over 1-3 days when isolated from non-Si supernatants (Figure 3.12a). To verify the extent of exosome isolation, TEM images of exosomes isolated from Si secretion supernatants (Figure 3.12b) were taken. Particles (exosomes) in sizes ranging between 100-200 nm were observed in TEM images. Purified exosomes were also observed on the surface of Dynabeads, viewed in both deposited (Figure 3.12c) and cross-sectional images (Figure 3.12d). The concentration of protein BSA was quantified with and without exosomes and Dynabeads to confirm exosome binding. Dynabeads incubated with isolated exosomes were

observed to have a significantly higher [BSA] (0.45 vs 0.02 mg/ml) then those without (P≤0.01 - Figure 3.12c).

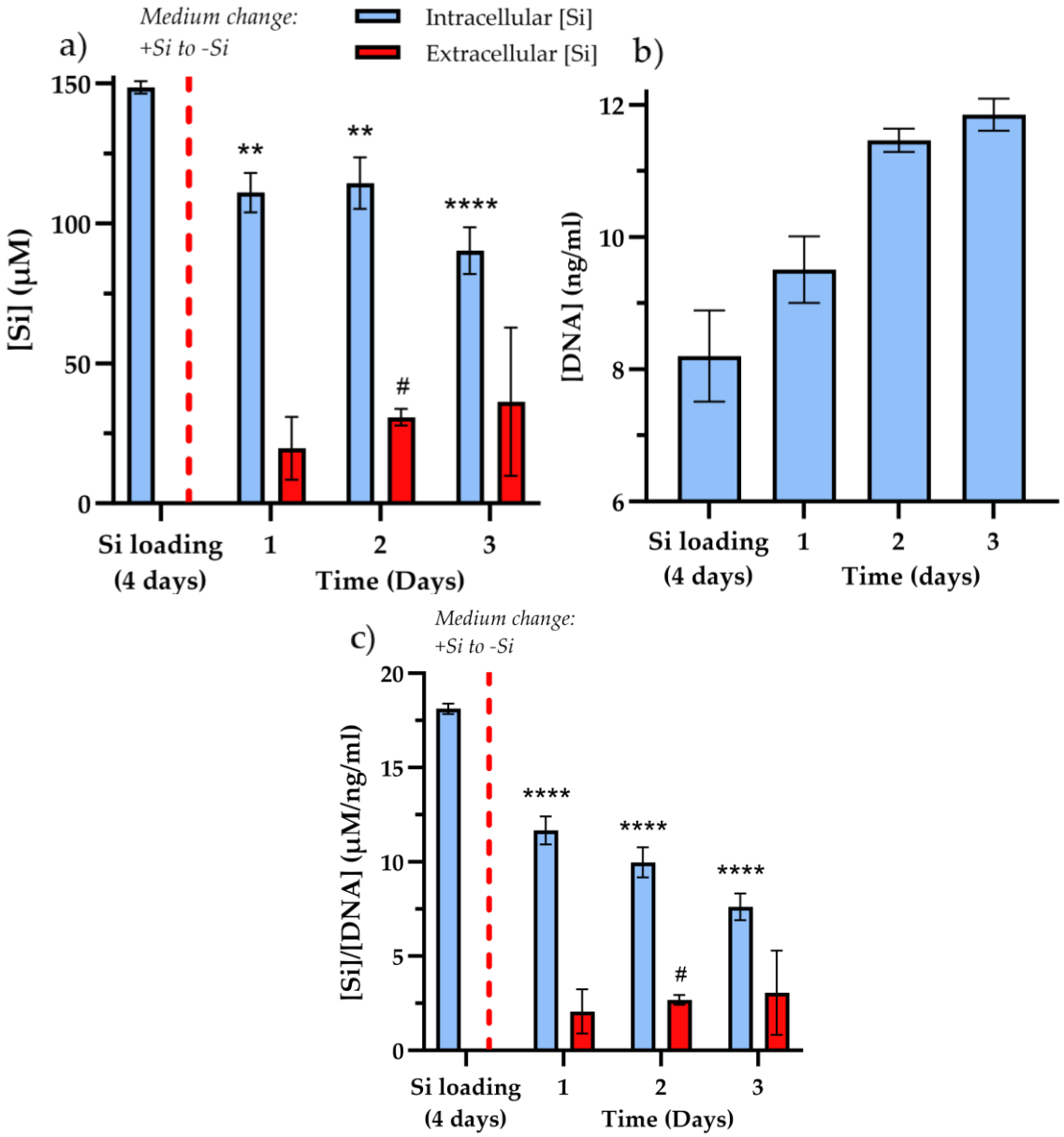

Figure 3.11 - **Quantification of intra- and extracellular [Si] following a media change from those containing Si to those containing no Si.**

*A significant decrease in total (a) and normalised (c) intracellular [Si] was observed, over 3 days when Si-containing media was replaced with media with no Si. Extracellular [Si] was found to significantly increase between day 1 and 2 . Results are presented as the mean ± SD. **=P≤0.01, ****=P≤0.0001 compared to intracellular [Si] before media change. #=P≤0.05 compared to extracellular [Si] 1 day after media change. N=3.*

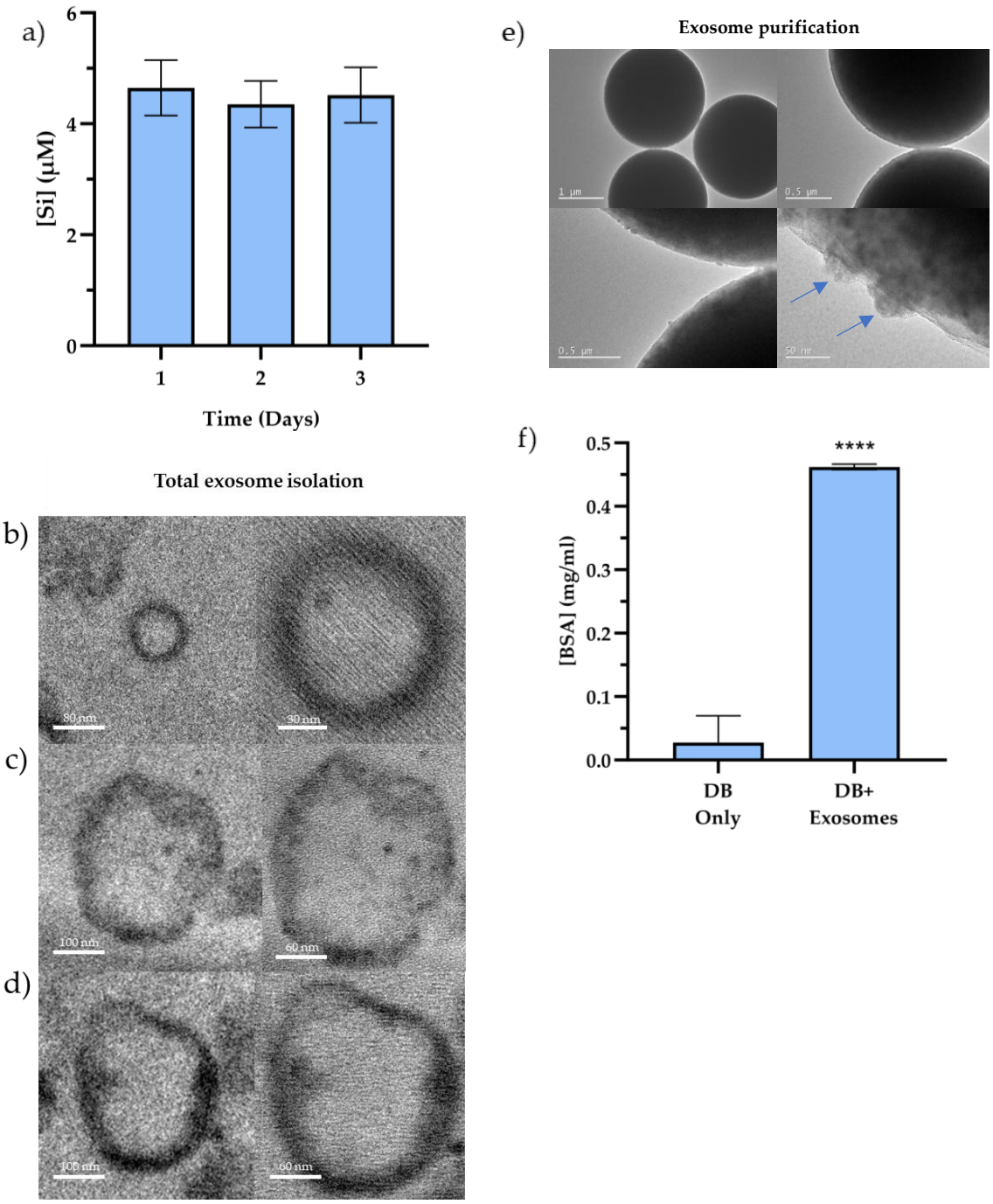

Figure 3.12 - **Quantification of [Si] in exosomes released by cells in non-Si media during Si secretion studies.**

*[Si] was detected in isolated exosomes (a). Examples of total exosome isolation by precipitation is presented in (b-d) and final purification by magnetic CD63+ Dynabeads (DBs) in (e). Quantification of total protein concentration of exosomes purified by DBs compared to DBs alone is shown in (f). Results are presented as the mean ± SD. ****=P≤0.0001 compared to DBs alone. N=3*

3.5 Discussion

Principle conclusions

1. The negative effect of Si on cells is accumulative, producing decreased cell viability (metabolic activity/proliferation) only at day 7
2. Si is taken up actively and can reach a maximum [Si] inside cells
3. BG dissolution products produce lower intracellular [Si] than when cultured with media containing Si alone
4. Si is secreted from cells over time

Understanding how (and how much) Si is internalised by cells and if it is excreted would help better design Si releasing materials and help support the argument that Si is the biologically active ion. The factors affecting the relationship between Si release from BGs and specific intracellular [Si] and uptake (and possibly secretion) rates remain poorly understood. This study has, for the first time, presented evidence of the maximum [Si] that can be uptaken by osteoblast-like cells over time. [Si] observed in cell supernatants following culture in non-Si conditioned media controls has also provided evidence to suggest that Si is secreted from cells. Compared to SS, cells cultured in BG-conditioned media produced significantly lower intracellular [Si], suggesting differences in Si species or the interaction of other ions may influence their overall uptake concentration and mechanisms.

3.5.1 How do Si species affect osteoblast viability?

Figure 1.4a showed that [Si] (non-dissolution products) above ~0.5 mM more often produced negative outcomes in previous studies when all cell responses were combined. Results in Figure 3.2 were consistent with this, demonstrating that Si above 0.5 mM produce a decrease in cell numbers and an increase in cell death. Schroder *et al.*, however, showed that the same cell line could produce an increase in metabolic activity with SS, although lower [Si] (3-100 μM)[57]. Even with different experimental parameters (e.g., cell type, species and Si source) in previous studies, the median [Si] for metabolic activity was observed to be ~10 ppm (~350 μM – Figure 1.4b). This suggests that whilst experimental parameters

are important in determining cellular responses to Si, [Si] is possibly a better indicator (or predictor) of cellular outcomes. Whilst [Si] has been reported to cause desirable cell behaviour as high as 3 mM[60], it is possible that [Si] data in these particular studies is inaccurate due to the lack direct quantification before addition to cells (e.g., by ICP-OES).

[5760]There remains, however, conflicting evidence on the mechanisms of therapeutic and toxic effects of Si, with studies reporting that [Si] up to 2 mM could protect cells against intracellular ROS damage[152, 153]. Although ionic Si may protect from ROS produced extracellularly (e.g., H_2O_2 added during culture[152]), it likely doesn't offer protection against increases in intracellular ROS caused by high concentrations of nanoparticles[149–151]. ROS has also been shown to alter the mitochondrial function of cells[226], which may explain differences between metabolic activity and [DNA] in both Figure 3.1 and 2, despite them both being in-direct measures of cell numbers.

Observed toxicity in SaOS-2 cells may therefore be explained by silica particles (identified by NTA) present in the range of 10 to 300 nm in SS and BG conditioned water and media at 2 mM Si (Figure 2.6a). Particles of this size have been shown to cause toxicity in osteoblasts[208, 216]. It remains unclear, however, why changing the media instead of a continuous culture (Figure 3.1) produces e.g., a greater decrease in cell numbers. One explanation is that internalised nanoparticles can remain inside cells and are likely replaced by medium changes once degraded by cells as shown in previous studies[227]. If Si particles only make up a fraction of available Si in media, then these may be exhausted in a continuous culture (no media changes). Repeated high concentrations of nanoparticles through media changes may exceed intracellular antioxidant levels producing more negative cellular responses. Another explanation is that media changes cause a repeated pH shift (Si media is highly alkaline), producing negative cellular responses compared to a continuous culture.

Although orthosilicates have been shown to polymerise at 2 mM[199], only trisilicates were found to cause a small (but significant) increase in cell death (Figure 3.3d). Non-significant differences in metabolic activity and proliferation were observed with ortho and disilicate species and BG dissolution products at all time points. A lack of differences here may again be due to these species not being produced by these sources and if they do, these species are likely to be unstable at 2 mM Si.

BSA (Figure 2.4f) and amide groups (Figure 2.5c/d) identified in isolated Si-conditioned media precipitates suggest that either protein precipitation (e.g., by excess sodium) or bonding to silica particles may occur. Both scenarios may result in less serum proteins being available to cells, causing a decrease in cell proliferation and functionality[228]. Although high concentrations of sodium from SS are likely responsible for this protein precipitation[207], large variance in [Si] reported to cause cell toxicity in previous studies may be explained by differences in the specific Si source and cell types.

For example, Duivenvoorden *et al*., showed that dimethyl-silanediol (DMSD) at 1 mM caused an increase in SaOS-2 cell numbers, silicon tetrachloride ($SiCl_4$) at the same concentration and above produced only decreases[229]. The same study reported that immortalised foetal osteoblasts (hFOB-1.19) produced only nonsignificant differences with either source, suggesting different culture media may alter particle formation (or Si species) or that different cell types are better able to resist oxidative damage. Tetraethyl-orthosilicate (TEOS), a precursor of sol-gel derived BGs (commonly used to model the effect of Si from BGs[60, 127]), can hydrolyse in water, producing ethanol in solution which may contribute to cell toxicity at low concentrations[230].

3.5.2 How does speciation affect intracellular [Si] in osteoblasts?

'Orthosilicates' (Si from SS) had higher intracellular [Si] per unit DNA when compared to di and trisilicates and 45S5 BG dissolution products (Figure 3.4c). An increase in atomic mass and charge acquired by Si species as they begin to polymerise may make it more difficult to be taken up by cells. Whilst membrane receptors have been suggested for orthosilicate[221, 231], it is unclear whether any exist for di or trisilicates. Before polymerisation occurs, each orthosilicate ion can contribute 1 Si atom which is significantly fewer than that found in particles (up to 500 Si atoms[232]). If particle uptake dictates overall intracellular [Si] (given that ICP-OES cannot distinguish between them), however, then the size of the particle produced by each starting species (ortho, di and trisilicates) would likely be the greatest influence of this. Smaller diameter particles have shown to be efficiently taken up by cells compared to larger ones[233]. Orthosilicates are more likely to produce smaller particles than di and trisilicates thus produce higher intracellular [Si].

Another possible explanation is that di and trisilicate salts do not actually produce the corresponding species when dissolved (producing only orthosilicate as the pH is below 9), and therefore the amount of sodium dictates precipitation and particle formation in media (as discussed in section 2.5.2). Although, [Na] was observed to be the highest in SS (~19.0 mM) followed by di (~8.2 mM) and then trisilicates (~5.9 mM), [Na] in BGs was significantly greater than SS (~50.2 mM) (Table 5b), suggesting that although it may contribute toward particle formation, the presence of high levels of Ca (and the possible formation of calcium silicate complexes) may prevent Si polymerisation.

Comparable intracellular [Si] were observed, between cells cultured with trisilicates and BGs, suggesting possible similarities in their released Si species. However, only ortho (no trisilicates) were identified in NMR spectra of BGs at 2

mM Si. This therefore implies that the uptake of Si from bioactive glasses may be influenced by the release of other ions (sodium, calcium, and phosphorus ions) from the BGs. As previously discussed, (section 2.5.2), the formation of insoluble Si-Ca or Si-HAs complexes may reduce the availability of Si to cells, therefore decreasing the intracellular [Si]. This effect has been observed *in vivo* with studies reporting that low calcium diets increased silicon digestion in rats[234]. It has been suggested therefore that either calcium may form insoluble complexes with Si (calcium silicates) or that they compete for the same uptake pathway[235, 236].

[231]It remains unclear, therefore, if greater intracellular Si produces increased desirable outcomes in cell behaviour (bone formation, protein expression etc.). If the intracellular concentration of ionic Si reaches a saturation point, then remaining observed [Si] is likely due to the uptake of Si particles. As Si particles have been largely associated with either negative or no differences in cell behaviour[149], then novel BGs dissolution products should be tailored to produce orthosilicate species and not longer chained species or particles. If calcium plays a role in preventing Si polymerisation, then BGs with greater weight % calcium may be favourable.

Intracellular [Si] was found to increase incrementally with time when culture with Si from SS (Figure 3.5a), suggesting that Si uptake is (at least in part) an active process instead of passive. Although, when normalised to cell numbers, the rate of uptake was observed to decrease up to 8 days (Figure 3.5c). As no significant differences in [Si] per cell were found between day 4 and 8, a maximum Si uptake was presumed to have occurred. This suggests that although the rate of uptake from SS initially exceeds the rate of proliferation (day 1-2), cells nearly equal the rate of Si uptake by day 8. It is unclear however, if uptake of Si stops at this time point or whether uptake is limited once the cells reach confluency (~day 5-6). Normalised to cell numbers, intracellular [Si] was found to be higher in SaOS-2 cells compared to ROBs over 4 days (Figure 5.7c) suggesting that cell type and species may influence Si uptake. Cancer cells have

been shown to uptake more nanoparticles then their corresponding primary cell types[237], possibly due to having higher metabolic activity and an over expression of specific surface receptors necessary for endocytosis.

In comparison to cells cultured with 45S5 BG dissolution products (Figure 3.6), total and normalised intracellular [Si] was significantly lower after 8 days. Whilst an increase in total intracellular [Si] was observed, the rate of uptake was lower than the rate of proliferation resulting in decreasing intracellular [Si] over time when normalised to cell numbers. Compared to a control (no Si), cells cultured in 45S5 dissolution products were also found to proliferate slower after 7 days (Figure 3.3c). Lower uptake of Si in BGs may therefore explain why [Si] required to produce all cell responses in BGs in previous studies (Figure 1.7) is higher compared to silicates alone (Figure 1.4).

3.5.3 Si uptake and secretion mechanisms in osteoblasts

If Si is taken up into cells in the form of particles, then endocytosis should be the primary mechanism for their movement across the membrane. Although precipitates were found in SS and BG in water and media (Figure 2.6), no significant differences were observed in intracellular [Si] (2 and 3 mM) following a 8-hour culture with endocytosis inhibitors (Figure 3.9c). Although it's possible that uptake of some Si particles may have been prevented, differences may have been too small to observe using ICP-OES. Culture with inhibitors and gold nanoparticles showed, however, that only a 50% reduction in intracellular [Au] suggesting that endocytosis may not have been fully inhibited. The length of time cells can survive whilst endocytosis is inhibited may also contribute to the lack of differences. Cells were observed to only remain viable with 40 μM Dynasore up to 8 hours (Figure 3.7a/b), a time period possibly too short for sufficient endocytic uptake of Si to occur and thus show differences. Uptake of Si was, however, observed up to 24 hours (Figure 3.2a), suggesting that either particles of Si can form intracellularly (following uptake via ion channels) or that Si

particles are uptaken via an endocytic pathway that is not inhibited by Dynasore. Whilst Dynasore inhibits all clatharin-mediated forms of endocytosis (pinocytosis and receptor-mediated endocytosis), phagocytosis and caveolae-mediated endocytosis are not inhibited. Ha *et al*, showed a significant decrease in the uptake of silica nanoparticles into MC3T3-E1 (osteoblast precursor) cells via use of molecular inhibitors (methyl-beta-cyclodextrin) of caveolae-mediated endocytosis[175]. NTA (Figure 5.1) showed, however, a wide range of nanoparticles in media (~50-300 nm), which may suggest that multiple endocytic pathways may be involved silica particle uptake. For example, BMSCs have been shown to uptake silica nanoparticles of approximately 100 nm via a clatharin-mediated, micropinocytosis pathway[238, 239] (also implying that the uptake of silica particles is cell type specific). Whilst decreases were found in the mean total and normalised, intracellular [Si] following culture with Dynasore, trisilicates and 45S5 dissolution products neither were observed to significantly reduce Si uptake (Figure 3.10a-c). Differences here may be due to trisilicates more easily forming particles compared to orthosilicates and BGs (releasing orthosilicates only at 2 mM Si).

A lack of differences observed in endocytosis inhibition may also suggest that the majority of Si is being taken up in the form of ions. Inhibition of three uptake mechanisms for Si suggested in previous literature (aquaporin 3, Na/HCO_3 and Na/P co-transporters) were attempted but did not show any significant differences compared to a control (Figure 5.3a). Verification of the extent of inhibition of ion exchange also showed no significant differences in either [Na] or [P] suggesting that little or no inhibition had occurred in these channels (Figure 5.3c/d). The total concentration of sodium and phosphorus in lysed cells (prepared for ICP quantification) are likely to be substantially higher than the free ions in the cytoplasm and will therefore likely mask differences in the ion exchange. In addition, it's unclear how long the effect (if any) of the chemical inhibitors would last for, given the 4-day incubation with Si.

Similarly, no significant differences were observed in [Si] when using aquaporin 3 inhibitors. Verification of whether aquaporins were inhibited is difficult as the extent of differences in water influx/efflux may not be great enough to change ions concentrations inside cells. A quantification of cell shrinkage/swelling may provide better evidence of whether aquaporins had been inhibitor. RNA silencing of membrane bound co-transporter expression (as described in previous studies[221]) would also provide better evidence of reduced ion exchange.

A detectable [Si] was identified in cell supernatants following a media change from those containing Si to those that didn't (Figure 3.11). This was mirrored by a significant decrease in intracellular [Si] after culture for 1 and 3 days in non-Si media, implying that observed Si in supernatants was likely secreted from cells. Extracellular [Si] was also found to be 3 times greater than background Si from McCoy's 5A control media (Table 6a), providing further evidence of cell secretion. Although an increase in total extracellular [Si] was found between day 1 and 2, when normalised to cell numbers no significant differences were observed. Similarly, no differences in cell numbers between day 2 and 3 was reflected in non-significant increases in extracellular [Si]. These results may suggest that some Si secretion occurs during the process of mitosis or cell death. It's unclear, however, if some internalised Si is retained during cell division.

It remains unclear, however, if Si observed in supernatants were in the form of ions or particles (or both). If exocytosis is used by cells to move Si particles out of cells, then exosomes should contain quantifiable [Si]. Although Si was detected in isolated exosomes from non-Si media (Figure 3.12), its concentration was approximately the same as that of media alone. This may imply that not enough exosomes could be isolated and [Si] in each may be too low to be detected accurately (or both). Therefore observed [Si] is likely due to contamination from media during the isolation process.

3.6 Conclusion

In agreement with the systematic review, a [Si] dependent inhibited proliferation and toxicity was observed above 56 ppm/ 2 mM. Si uptake was time dependent and increased up to 4 days, suggesting an active uptake mechanism. Si species sources (di, tri and 45S5 BGs), did not, however, affect metabolic activity, proliferation or toxicity. SS (orthosilicates) had higher osteoblast uptake compared to species containing higher Q numbers and those released from BGs, indicating Si species are important in uptake mechanisms and rate. Whilst differences in uptake between BGs and SS may be due to speciation, the presences of Na, Ca and P may also reduce Si bioavailability through complex formation or uptake pathway competition. Si was found to be present in cell supernatants and decreased intracellularly following replacement with media containing no-Si, which may imply that Si is secreted from cells.

It remains unclear, however, if desirable cell responses are directly related to intracellular concentrations. If so, then particle formation is likely the reason for this occurrence due to their larger contribution of Si particles then ions alone. High variation in the reported effects of Si is then perhaps due to the differences in the proportion of Si species compared to particles in each study investigating BG dissolution products. The respective ion release, media type, Si species and cell type's ability to deal with this will likely dictate the cellular response. Studies focusing on dissolution products of novel BGs should therefore aim to characterise the proportion of Si species to particles released into culture media.

Chapter 4. Intracellular localisation of Si

4.1 Introduction

Whilst Si has been reported to increase osteoblast differentiation[127] and bone formation[240], the uptake mechanism and intracellular location remains unknown. Identification of Si localisation could provide evidence for an intracellular role and possibly their uptake mechanisms. For example, high concentrations of Si in specific organelles, such as the mitochondria, may suggest roles in metabolic processes, whilst localisation in endosomes may imply an endocytic-mediated uptake mechanism. Whilst Si particles have been located within individual human cells[227, 241, 242], the intracellular localisation of Si ions has not yet been shown. Although its distribution has been shown in plants[243], diatoms[244] and bacteria[245] these are likely to be polymerised Si that forms their respective cell walls and exoskeletons.

A variety of techniques (e.g., electron microscopy, XRF, NanoSIMS or fluorescence) have been used in previous studies to determine differences in elemental localisation, to varying degrees of success. Whilst surface analysis techniques, such as XPS and SIMS have been shown to be effective at quantifying elements in a sample, these cannot simultaneously produce accurate cell ultrastructure images, allowing mapping/localisation of elements to individual organelles. STEM-EDX has, however, shown elemental mapping within mammalian cell structures, reporting localisation of P[223–225], S[246, 247], Ca[248–250] and N[250]. Despite this, no studies have yet successfully localised therapeutic trace elements used in BG dissolution products with cells *in vitro* (e.g., Si, Co, Sr etc) due to their low intracellular concentration being at the limits of detection by EDX.

4.1.1 Electron microscopy (EM)-based techniques for elemental mapping in cells

The most common technique for both imaging cell ultrastructure and identification of elemental distribution is the combination of electron microscopy (EM) and energy dispersed x-ray spectroscopy (EDX). Scanning-Transmission electron microscopy (STEM) coupled with EDX (STEM-EDX) has previously been the most common method of looking at the distribution of elements (mentioned in section 4.1) within cells. Samples for this technique are produced by fixing and staining cells with heavy metal atoms (commonly osmium tetroxide, OsO_4) followed by resin embedding cells into hard blocks as pellets or on coverslips. The resulting resin blocks are then cut into nanometre thick sections using an ultramicrotome. An image of intracellular morphology and organelles is then taken and EDX detectors used to identify elements in the image by collecting unique wavelength X-ray radiation emitted from the sample. Bozycki *et al*., showed that this technique could be used to determine the extent of intracellular mineralisation in bone cells[249], with phosphorus and calcium localised in vesicles of SaOS-2 cells exposed to bone mineralising agents (ascorbic acid and β-glycerophosphate), compared to controls. Localisation in vesicles could also provide evidence for mineral uptake and secretion mechanisms (endo- or exocytosis) involved with bone formation. The same authors used this technique to assess the extent of mineralisation potential between different osteoblast-like cell lines (SaOS-2 and hFOB 1.19) under different experimental conditions, e.g., increasing flavonoid concentrations[251]. TEM-EDX has also been used to map elements in larger tissues, such as the Islets of Langerhans, where high concentrations of sulphur were localised in vesicles suggesting the possible movement of proteins[250].

Whilst this technique provides nanometre resolution images, EDX detectors struggle to identify trace elements, due to low concentrations, the extremely thin

nature of TEM samples and low electron density of some elements (e.g., Si). Sample processing (e.g., fixation, staining or resin embedding cells) may also contaminate or produce unwanted elemental artifacts in EDX spectra. This task is made even more difficult for detecting Si by the fact that carbon formvar coatings (commonly used to increase conductivity of TEM grids) are frequently manufactured on silicon wafers, thereby potentially contaminating any sample placed on the grid.

Electron Energy Loss Spectroscopy (EELS) may also be used in combination with TEM to quantify and visualise elements. This technique measures the energy loss of electrons passing through a sample, with the decrease in energy associated with the unique elements present. Whilst this technique offers greater overall sensitivity compared to EDX, EELS is very sensitive to contamination which may become more likely with increasing sample thickness. Another disadvantage is that EELS can only scan relatively small areas (not whole cells) in realistic time scales making the search for Si deposits more time consuming. Scanning electron microscopy (SEM) may provide more spatial and therefore elemental information, given this method is used to image whole cells (instead of sections). Despite this, techniques such field ion beam (FIB) SEM used to mill into cells and view intracellular morphology, still suffer from low sensitivity of EDX detectors and provide less organelle clarity then TEM samples.

4.1.2 Other surface quantification techniques to map elements in cells

X-ray Fluorescence (XRF) is another commonly used technique to map elements inside of cells. This technique produces a detectable (and quantifiable) fluorescent photon from atoms in a sample when hit with x-ray radiation. Cammisuli *et al*., combined light microscopy images of cells and XRF to map out their respective elemental distribution [252]. Their study showed that iron could

aggregate outside or within cells inside vesicles (or possibly mitochondria) following treatment with iron-sulphate ($FeSO_4$). Although vesicular localisation is suggested in this study, only nuclear compartments are discernible in light micrographs of cells. Several other studies that have attempted to map elements in cells using XRF, however, did not use a comparative imaging technique (light or electron microscopy) to localise element signals to specific organelles[253–255]. This may be explained by XRF requiring sample sections to be least 1 μm thick (80-100 nm in TEM samples) to get a reliable elemental signal and light microscopy only allowing accurate visualisation of nuclear compartments. Although elements such as phosphorus have been mapped in cells using XRF, no study has used this technique in the context of bone or the localisation of Si.

To enhance the accuracy of elemental mapping to individual organelle, samples can first be imaged using TEM and then elements identified using other quantitative techniques, such a Mass Spectroscopy (MS). Although sample preparation for use between two different techniques requires longer times, higher costs and greater expertise, MS techniques provide a significantly higher element sensitivity compared to XRF or EDX. Lovrić *et al*., used Nano-Secondary Ion Mass Spectroscopy (NanoSIMS), to map the distribution of iron inside of alveolar macrophages, following imaging via TEM. High concentrations of iron were found to be localised in mitochondria, vesicles, and lipid droplets, implying its role in intracellular metabolic processes. Other authors have shown that using ^{13}C isotopic labels, dopamine could be located within the endosomes of neural crest-like (PC12) cells, suggesting its intracellular transport during neurotransmission events[256, 257].

4.1.3 Si mapping in cells using fluorescence probes

Previous studies have shown that PDMPO - found commercially as LysoSensor ™ DND-160) could be used to visualise and trace areas of low intracellular pH[258]. When Shimizu *et al*., used LysoSensor to identify regions of acidic pH in diatoms,

however, fluorescence was found to be localised to their cell walls (an area composed largely of polymerised silicon)[259]. This study and others[260] suggested that there is likely to be either a Si-PDMPO chemical bonding/affinity or an acidic shift in pH caused by Si. To demonstrate LysoSensor's efficacy as a Si probe/tracer other studies have shown that Si could be traced within the cell body of demosponges[261] and plant cells[244] over time. To date, no studies have used LysoSensor (or PDMPO alone) to trace Si in human (or any other mammalian) cells. To trace silica nanoparticles using fluorescence microscopy, previous studies have modified their particles with fluorescent molecules (e.g., TRITC) in order to localise them inside of cells[175, 262, 263]. If successful, LysoSensor could be a useful tool to localise polymerised or particulate Si without the need for chemical conjugation (a factor that may influence the way that cells interact or uptake particles). It is unclear, however, if LysoSensor would still produce detectable fluoresce if Si was ionic (as is presumed to be the case in human cells) and not a polymer.

A recent study by Merdy *et al.*, showed, however, that by adding other ions or molecules (e.g., aluminium, or humic acid) to non-buffered mediums containing Si, fluorescence of PDMPO could be significantly increased or quenched[264], implying that PDMPO may not be Si specific. The majority of cells, however, are cultured in pH buffered media and therefore this may not completely inhibit the ability to localise Si within cells *in vitro* (even in the presence of other ions).

Although if the presence of other ions does affect PDMPO-Si fluorescence then it's possible the increase in other ions (E.g., Ca, P, Na) in BGs would affect the fluorescence of PDMPO when localising Si. The reduction in the availability of free Si ions via the formation of Si complexes (e.g., calcium-silicates) would also likely reduce fluorescence due to a decrease in the number of Si-PDMPO interactions.

The following experiments will utilise a combination of techniques to localise Si within osteoblast and osteoclast cells and thus provide evidence for its intracellular role and uptake mechanisms.

4.2 Chapter aims and hypothesis

Over 20 studies have demonstrated Si has been shown to alter both intracellular protein and gene expression (section 1.6.1). Despite this, little is known as to the localisation of Si within the cell or the intracellular mechanism that causes these gene and protein changes. This chapter investigates if it is possible to image Si location within osteoblasts and if [Si] affect Si localisation within osteoblasts and osteoclasts following culture with SS and BGs dissolution products.

This chapter investigated:

1. Where Si localised within osteoblast and osteoclast cells and the differences between Si alone and Si in BG dissolution products
   - Hypothesis: Si will be evenly distributed throughout the cells, although more particles can be observed in cells cultured with Si alone then with BG dissolution products

4.3 Materials and methods

4.3.1 Osteoclast cell culture

The RAW 264.7 cell-line has been reported to be a heterogeneous cell population, containing cells with various degrees of RANKL-sensitivity, with some unresponsive and others capable of responding to RANKL to form multinucleated TRAP+ osteoclast-like cells capable of bone resorption. A RAW264.7 TRAP+ responsive colony selection approach as described by Cuetara *et al*[265] was used and performed by Dr Amy Li (UCL). Briefly, RAW264.7 cells (ECACC) were expanded in high glucose DMEM with Glutamax™

supplement (supplemented with 10% (v/v) FBS and 50 U/ml penicillin and 50 μg/ml streptomycin and RAW osteoclast subclones were selected by limited seeding dilution and colony selection with an optimised TRAP-5b assay and staining comparison. The TRAP+ OC precursor sub-clones were then selected and cultured in DMEM Glutamax medium, supplemented with 10% FBS and 100 U/ml penicillin, 100 μg/ml streptomycin and 3 ng/ml RANKL (R&D Systems, UK). For maximum osteoclast formation, 20 ng/ml RANKL was used.

4.3.2 Elemental mapping in bone cells by STEM-EDX

Cells were cultured in 0-2 mM Si-conditioned mediums (sodium silicate and 45S5 bioactive glasses) and controls (no Si) for 4 days. A maximum of 2 mM Si was used for these experiments as it produced no cytotoxic effects after 7 days (Figure 3.1).Media was then removed, and cells fixed with 4% paraformaldehyde and 2.5% glutaraldehyde solution in 0.1 M sodium cacodylate for 24 hours. Fixed samples were stained with a 1% osmium tetroxide solution in water for 1 hour followed by solutions of 1.5% potassium ferrocyanide and 1% tannic acid in 0.1M sodium cacodylate for 1 hour each. Samples were then dehydrated in a 30-100% ethanol series (10 minutes each) with de-ionised water before embedding in epoxy resins (TAAB, UK) mixed 50:50, 75:25 and 100% with ethanol for a minimum of 3 hour each. Embedded cells were then scrapped off and centrifuged into pellets at 400g for 30 minutes. Resins were hardened at 60°C for 2 days. Sections with a thickness of 60-70 nm were then cut using a ultramicrotome (Leica) and placed on carbon formvar coated grids. Images were taken using a Zeiss Gemini STEM at 30 KeV whilst elemental mapping of Si and other elements was performed in-situ using EDX.

4.3.3 Si localisation by fluorescence microscopy

Cells were seeded in 3.5 cm^2 polymer fluorodishes (Ibidi, Germany) and allowed to attach for 24 hours. Culture mediums were then replaced with 45S5 bioactive

glass and 1- and 2-mM Si-containing mediums for 1 and 4 days. To identify where Si species were located inside cells, mitochondrial and lysosomes were stained with MitoRed and lysosomal staining kit respectively (both Abcam, UK). At each time point, media was removed, and cells incubated with each stain at a 1:20 ratio with culture medium for 30 minutes at 37°C. Cells were then washed with PBS and 3 μM LysoSensor™ DND-160 (Invitrogen, UK) in culture medium added for 5 minutes at 37°C. Live cells images were then taken with a Leica DM6 CFS fluorescence microscope. Excitation and emission of 552 and 600 nm were used to view mitochondrial and whilst 538 and 650 nm used for lysosomal stains. For LysoSensor™ DND-160 (containing PDMPO), 405 and 550 nm wavelengths were used.

4.4 Results

4.4.1 Intracellular Si localisation by fluorescence microscopy

4.4.1.1 Osteoblasts

The number of fluorescent cells and their respective fluorescence intensity increased with increasing [Si] (Figure. 4.1). The control (no additional Si) had minimal fluorescence. When cultured with 45S5 BGs dissolution products, fluorescence was found to increase over time, producing intensity similar to 1 mM similar at day 4 (Figure 4.1d). The fluorescence at day 4 in cells cultured with BGs was, however, significantly less than 2 mM Si from SS containing media. When viewed using 40x objective lenses at day 1, bright field images of cells cultured with SS (Figure 4.2a) suggested the formation of large vesicles close to the nucleus. To confirm what vesicle type this was, cells were stained with lysosome specific dyes (Figure 4.2b). This stain positively overlapped with vesicles observed in brightfield images. The same regions were also observed to fluoresce when stained with LysoSensor

(Figure 4.2c), suggesting Si may be present in lysosomes. Cells cultured in BG-conditioned mediums, however, contained smaller and less frequently observed vesicles (Figure 4.2d) compared to Si from SS. Although lysosomal and LysoSensor dyes were observed to occupy similar regions within the cell (Figure 4.2e/f), these were located closer to the outer membrane with BGs compared to Si from SS which occurred closer to the nucleus. Between days 1 and 4, the Si distribution inside cells with SS media did not significantly change (Figure 4.3a-c). The distribution of Si inside cells when cultured with BGs at day 4, however, was observed to be closer to the nucleus when compared to the same condition.

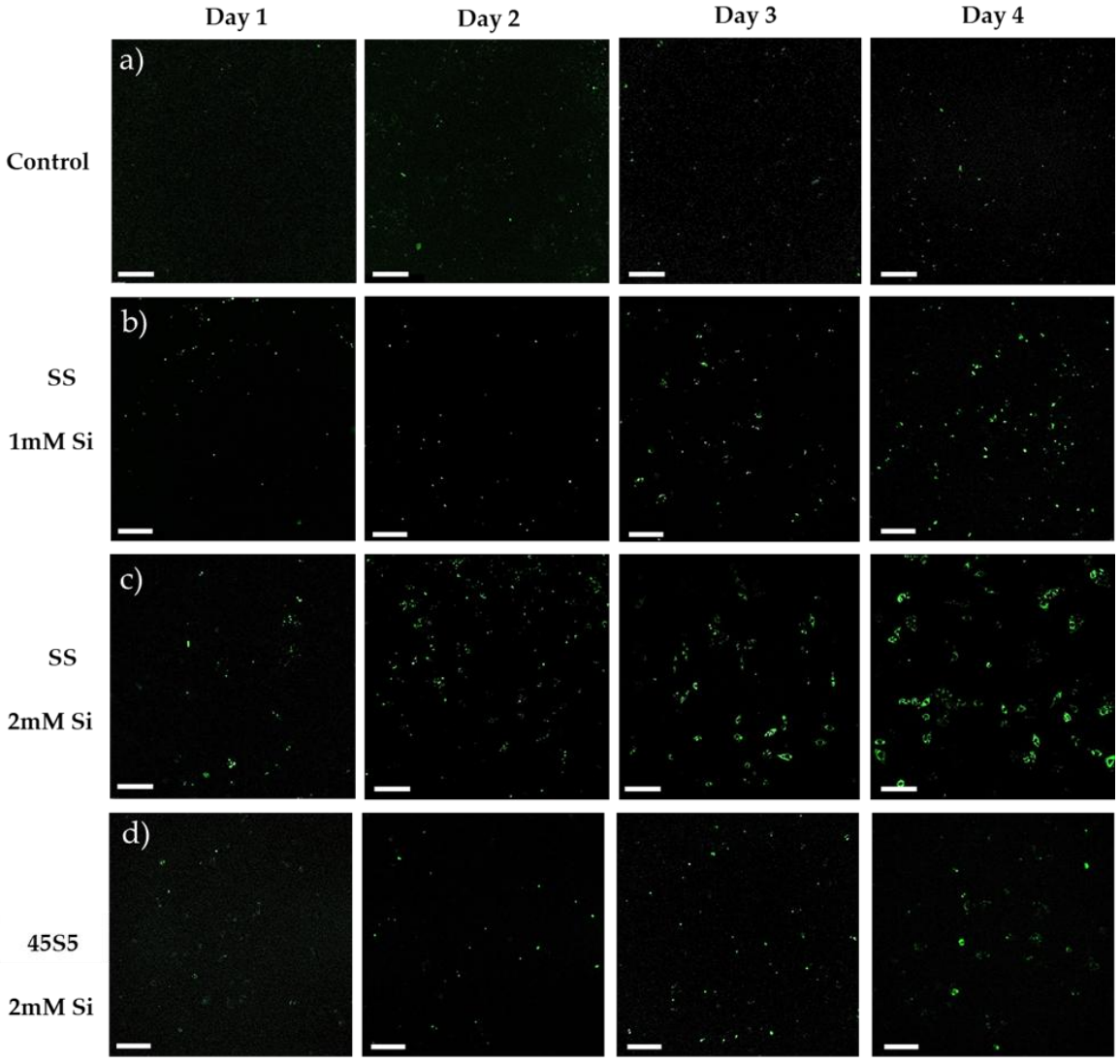

Figure 4.1 - **Si localisation in osteoblasts cultured in SS media at 1 and 2 mM Si.**

An increase in intracellular fluorescence was observed over 4 days with 1 mM a) and 2 mM b) Si conditioned media. A greater number of cells with higher levels of fluorescence intensity were observed with 2 mM Si compared 1 mM Si at day 4, whilst only low levels were found in the control. Scale bar = 10μm.

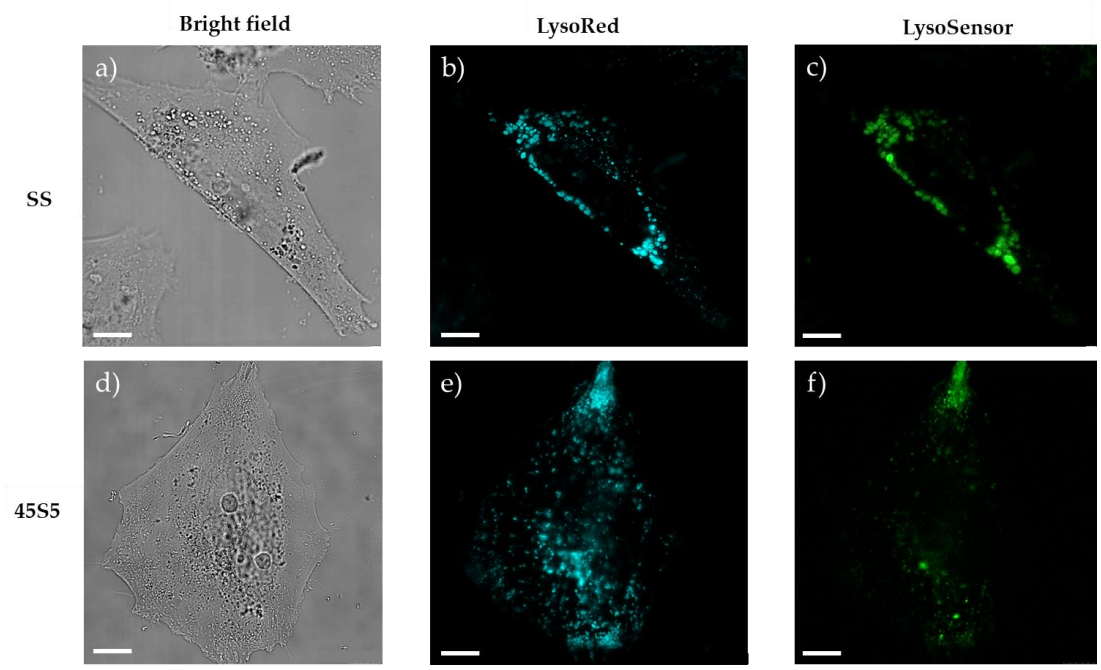

Figure 4.2 - **Si localisation in individual osteoblasts cultured for 1 day in SS and 45S5 BG conditioned media at 2 mM Si.**

Intracellular vesicles could be observed in brightfield images (a/d) whilst lysosomes (b/e) were found to overlap with 'Si' (c/f). Localisation of Si was found to occur closer to the nucleus and with higher fluorescence intensity when cultured with SS compared 45S5 dissolution products. Obj = 40x, Scale bar = 0.5µm

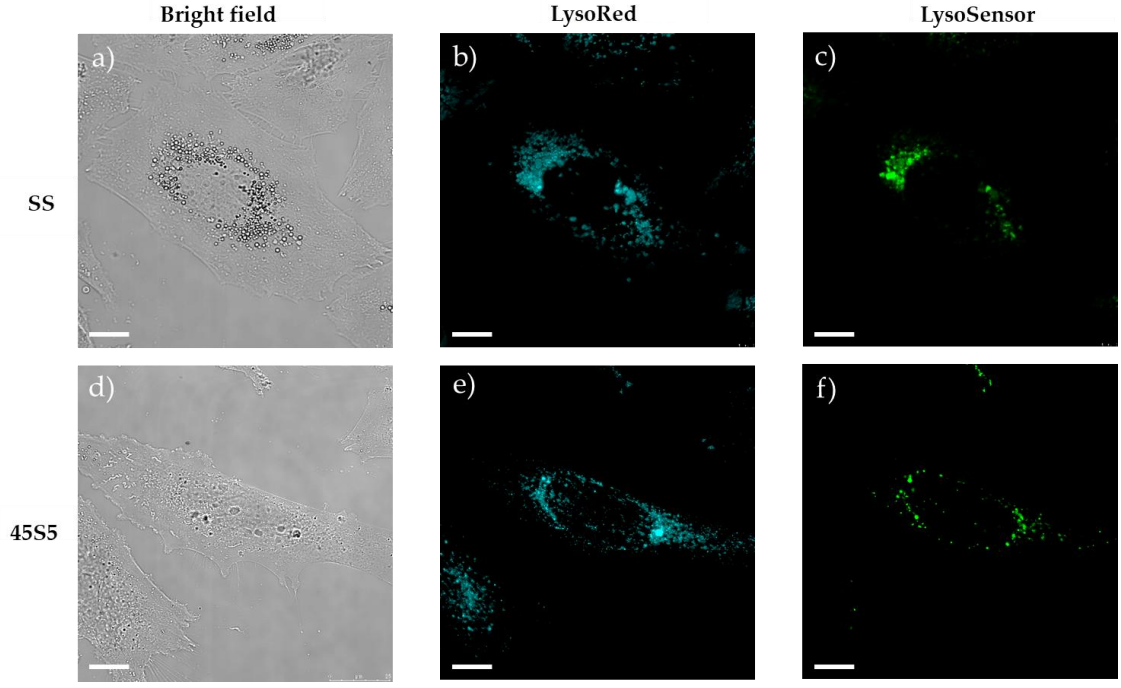

Figure 4.3 - **Si localisation in individual osteoblasts cultured for 4 days in SS and 45S5 BG conditioned media at 2 mM Si.**

Intracellular vesicles could be observed in brightfield images (a/d) whilst lysosomes (b/e) were found to overlap with 'Si' (c/f). Localisation of Si was found to occur close to the nucleus when cultured both with SS and 45S5 dissolution products. Obj = 40x Scale bar = 0.5µm

at day 1 (Figure 4.3d-f). As observed in Si uptake over time (Figure 4.1), fluorescence intensity was found to be higher in cells cultured with SS media at days 1 and 4 compared those in BG media.

4.4.1.2 Osteoclasts

Si was found to inhibit osteoclastogenesis (Figure 4.4a). Whilst the number and intensity of cells fluorescing (osteoclasts and macrophages stained with LysoSensor) was greater with SS media compared to BG media and controls (Figure 4.4d,f), some fluorescence in (healthy) osteoclasts was also observed in the control (Figure 4.4b). When viewed at higher magnification (40x objectives), no vesicles were visible in bright field images of osteoclasts (Figure 4.5a/d), in contrast to osteoblast-like cells (likely due to the comparatively larger 3D volume of osteoclasts). The same intracellular regions were occupied by LysoSensor and lysosomal stains following culture with both SS (Figure 4.5e/f) media, suggesting Si may present in lysosomes within osteoclasts. LysoSensor fluorescence intensity between SS and BG media was approximately similar within cells. As observed in osteoblasts, Si was found to be closer to the nucleus when cultured with SS media compared to BG media.

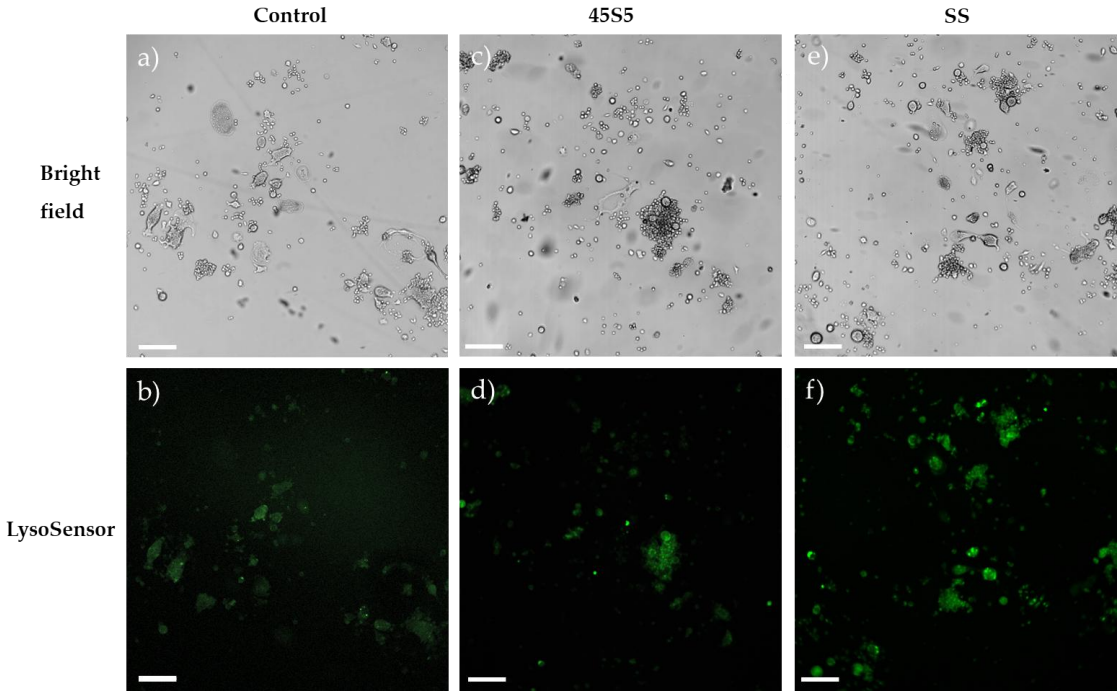

Figure 4.4 – **Si localisation in osteoclasts and undifferentiated macrophage (RAW 264.7) cultured for 1 day in SS and 45S5 BG conditioned media at 2 mM Si.**

Brightfield images showed that compared to a control (a), SS (c) and BG (e) conditions reduced the number of differentiated osteoclasts. A lower number of cells with higher fluorescence intensity were observed in cells cultured with BG (d) compared to SS (f) and the control (b). Obj = 10x, Scale bar = 20 μm

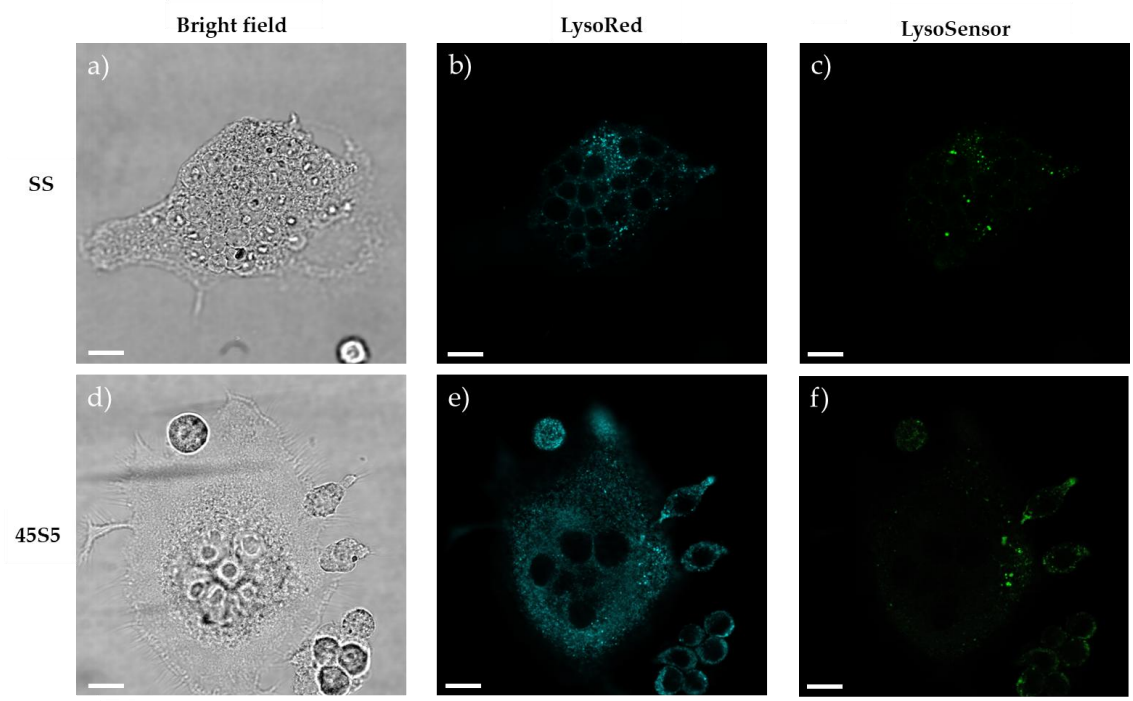

Figure 4.5 - **Si localisation in individual osteoclasts and macrophages cultured for 1 day in SS and 45S5 BG conditioned media at 2 mM Si.**

Si from both SS and 45S5 were found to be localised within lysosomes located close to nuclei. Scale bar = 5 μm

4.4.2 Intracellular Si localisation by electron microscopy

EM revealed morphological differences between the control and cells cultured in media containing Si. In cells cultured with SS conditioned-media, large, heavily stained vesicles were identified (Figure 4.6a/b)with high concentrations of Si and O, suggesting that Si may be contained within intracellular vesicles (Figure 4.6c/d). EDX mapping also demonstrated low level localisation of nitrogen was also found in these aggregates, suggesting the presence of protein aggregates or protein-Si complexes (Figure 4.6e). No localisation of Na was observed in these regions (Figure 4.6f). Scans of other organelles such as mitochondria Golgi apparatus or rough endoplasmic reticulum (Figure 5.4a,c,e), did not show any elemental localisation (Figure 5.4b,d,f)). Background Si was, however, identified in resin sections containing no cells (Figure 5.5b). Although this was significantly lower in intensity than Si found in cells (Figure 5.5a).

In contrast to SS, no localisation of Si was observed in vesicles was observed with BG dissolution products (Figure 4.7c). Although phosphorus was found to be localised within these vesicles, no localisation was observed with either calcium or sodium (Figure 4.7d-f). High concentrations of nitrogen were found, however, inside identified vesicles, again suggesting the presence of protein aggregates or possibly protein-hydroxyapatite complexes. Compared to cell cultured with Si (BG or SS), vesicles of similar size or frequency were not identified in cells cultured in control media (no Si).

Although less frequent than in osteoblasts, large heavily stained vesicles were also observed in osteoclasts when cultured with Si (Figure 4.8a/b). Si and O were found to be localised within these vesicles (Figure 4.8c/d). In contrast, no localisation of these elements was observed in nearby mitochondria or any other visible organelles within the cell. Low level intensity of sulphur (S) was also observed in these areas, suggesting the presence of protein aggregates or Si-protein complexes. No localisation of sodium was found inside the vesicles. When cultured with BG media, the same vesicles were also found but were smaller and less frequently observed than cells cultured with SS media (Figure 4.9a). Si, O and S were all found to be localised within these vesicles (Figure 4.9c/d/e). No localisation was observed with Ca and P. (Figure 4.9f/g).

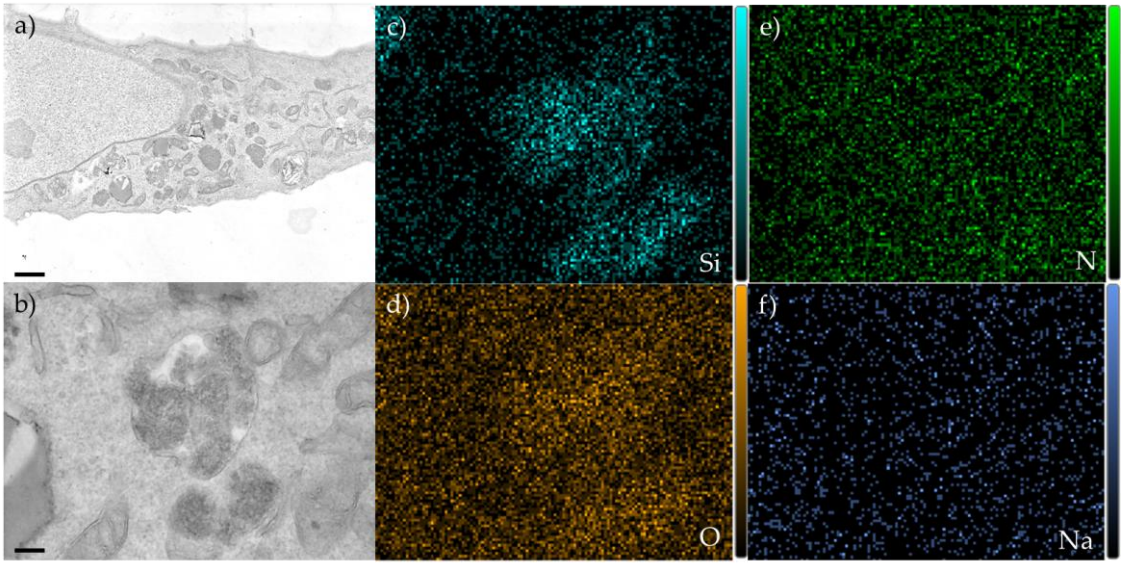

Figure 4.6 – **Si localisation in individual osteoblasts cultured in SS conditioned media for 4 days using STEM-EDX**

Large vesicles were observed in brightfield images (a/b). At high magnification, Si (c), O (d) and N (e) were all localised within vesicles whilst no localisation was found with Na (f). Scale bar (a) = 1 μm and scale bar (b) = 200 nm

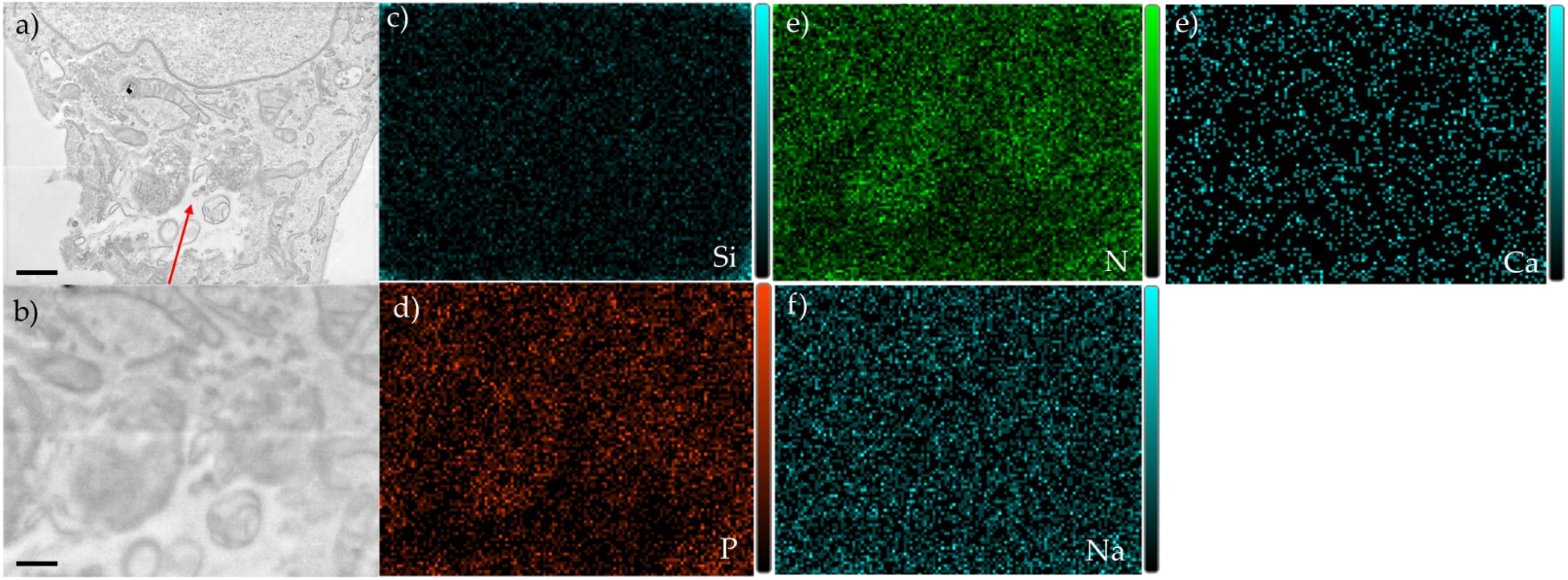

Figure 4.7 – **Si localisation in individual osteoblasts cultured in BG conditioned media for 4 days using STEM-EDX**

Large vesicles were observed in brightfield images (a). At higher magnification (b), no localisation of Si (c) was found within vesicles. P (d) and N (e), were, however, found within vesicles. No localisation was found with Ca (e) and Na (f). Scale bar (a) = 1 µm and scale bar (b) = 200 nm.

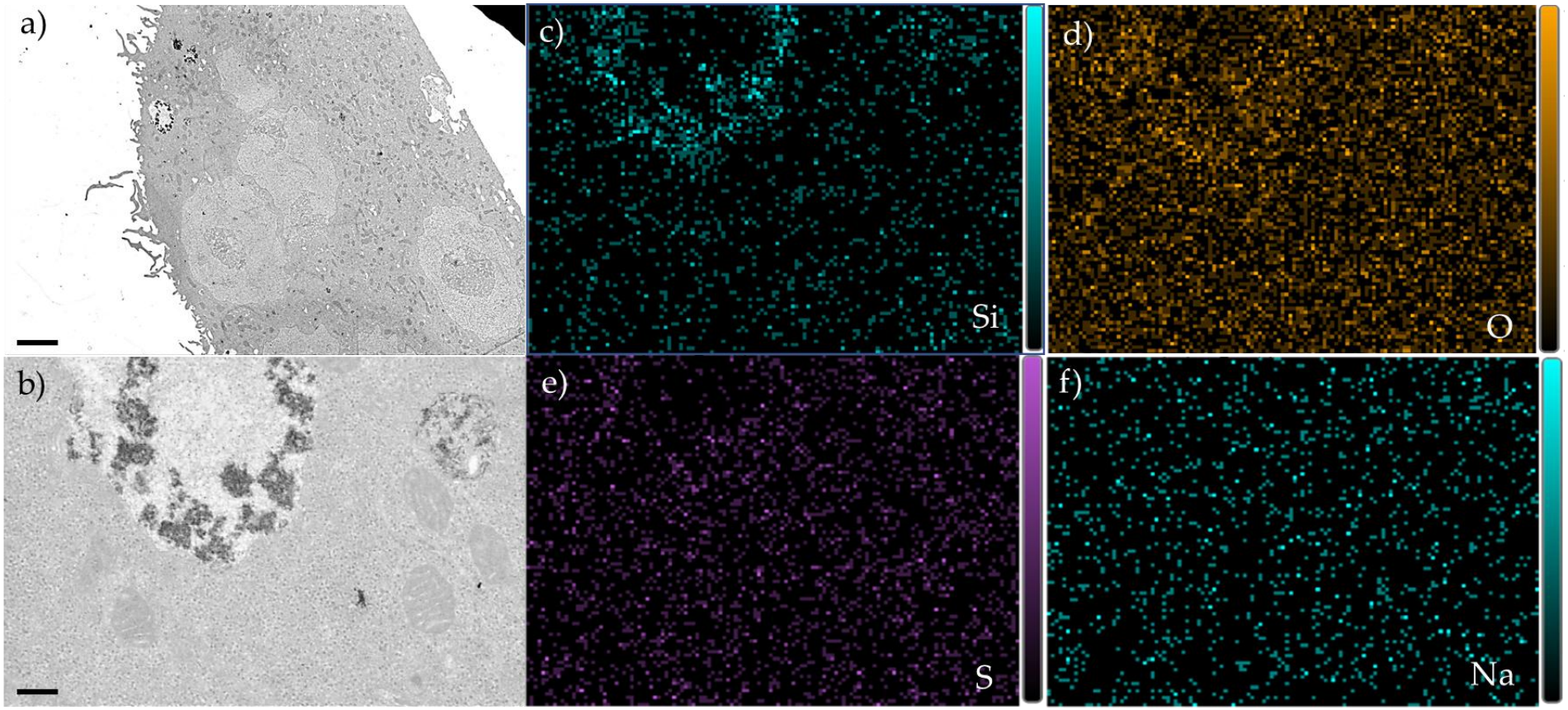

Figure 4.8 - **Si localisation in individual osteoclasts cultured in SS conditioned media for 1 day using STEM-EDX.**

Large vesicles were observed in osteoclast cells in brightfield (a). At higher magnification (b), Si (c), O (d) and S (e) were all found to be localised within these vesicles. No localisation of Na (f) was observed. Scale bar (a) = 2 μm and (b) = 1 μm.

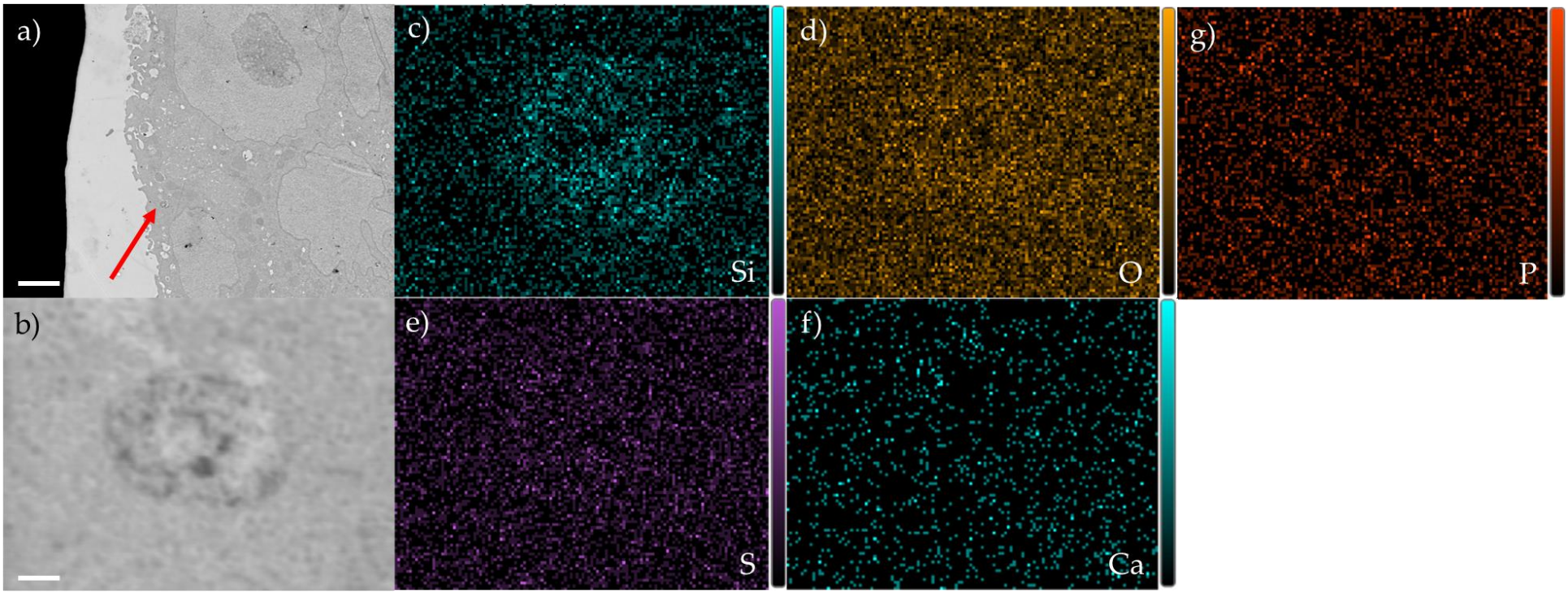

Figure 4.9 - **Si localisation in individual osteoclasts cultured in BG conditioned media for 1 day using STEM-EDX**

Vesicles were observed in osteoclast cells in brightfield (a). At higher magnification (b), a higher concentration of Si (c) was found within large vesicles. The same areas were found to contain O (d) and S (e), whilst no localisation of Na (f) and P (g) was observed. Scale bar (a) = 2 μm and scale bar (b) = 0.5 μm.

4.5 Discussion

Principle conclusions

1. Si particles can be found within lysosomes inside osteoblast and osteoclast-like cells confirmed by both fluorescence and electron microscopy, suggesting a endocytic uptake mechanism
2. BG dissolution products produce less visible particles localised in lysosomes within both cell types compared to Si alone

Despite a number of studies suggesting that Si is an important trace element in the formation of bone by cells *in vitro* and *in vivo*, to date no study has produce evidence to suggest its localisation within cells and thus its intracellular role and uptake mechanisms. This study has for the first time provided evidence of where Si is localised inside bone cells following culture with SS and BGs. Fluorescence and electron microscopy were both able to localise Si to lysosomes. This suggested that both SS and BG dissolution products produce Si particles in fully supplemented media, with Si ions and particles likely producing different cellular interactions and uptake mechanisms. STEM-EDX also indicated that proteins were present in these particles suggesting that protein aggregation may occur on Si particles or vice versa increasing overall particle size. Both methods indicated that SS media produced larger particles in cells containing more Si than that of cells cultured in BG dissolution products.

4.5.1 Where is Si located within osteoblasts?

The number of cells fluorescing, and their respective fluorescence intensity increased over time following culture in media containing Si (Figure 4.1b/c/d). The number of cells fluorescing also increased when [Si] was increased from 1-2 mM at all time points, demonstrating a concentration dependent relationship between PDMPO fluorescence intensity and [Si]. Although some fluoresce was observed in cells culture in media without Si, these cells were often dead or floating. The pH of dead or dying cells has been shown to be highly acidic[266], and would therefore produce a detectable fluorescence as LysoSensor is primarily

used a visual identifier of low intracellular pH[267]. It is therefore possible that some fluorescence may be produced by morphologically/visually healthy cells (cultured in Si media) that may be in the process of apoptosis. As 2 mM Si from SS was observed to cause no significantly negative toxic cell responses up to day 3 in proliferation or metabolic activity (Figure 1.5b/c), it can be assumed that the majority of fluorescence in cells was produced by a pH shift or an interaction between polymeric Si and PDMPO (as described in previous studies)[260, 268, 269]. Although Si has been shown previously to polymerise at 2 mM[178], fluorescence from the interaction with PDMPO, whilst at 1 mM, may infer that polymerisation occurs at a lower [Si] than previous thought. With the assumption that polymeric Si occurs only after 2 mM, then this result may indicate that fluorescence is also caused by monomeric (di or trimeric) species of Si.

Compared to Si from 45S5 BGs, fluorescence was observed to be significantly higher at all time points in cells cultured with SS (Figure 4.1d). This result agrees with Figure 2.2c, which showed that intracellular [Si] per unit DNA was significantly higher in cells cultured with SS compared to BG. As previously discussed (section 3.5.2), reduced uptake with BGs may be due to differences in Si species or increased calcium in BG media which either share an uptake pathway with Si (and thus compete for uptake) or it forms less soluble complexes with Si (calcium silicates)[78]. Although calcium may reduce overall Si uptake, it remains unclear how Si interactions with PDMPO are affected by the presence of other ions released from BGs. Merdy *et al.*, reported that aluminium could significantly reduce overall fluorescence with LysoSensor in solutions containing Si[264]. It is hence unclear whether a reduction in the fluorescence in cells cultured in BG media compared to SS is due to a decrease in Si uptake or that other ions inhibit Si-PDMPO interactions. If therefore introducing/increasing the concentration of other ions (e.g., calcium) reduces/prevents Si-PDMPO interactions and thus fluorescence in cells, the use of LysoSensor as a tool to trace Si in novel BG (multi-element) dissolution products may produce inaccurate or

misleading Si localisation. Large vesicles were observed in both SS and BG media, compared to control (Figure 4.2a/d). LysoSensor and lysosome markers were both found to produce fluorescence in regions containing these vesicles, suggesting that Si particles were likely contained within lysosomes (Figure 4.2b-f). This provides evidence to suggest that both SS and BG media produced particles in media (in addition to ions), which are likely uptaken via endocytosis. This agrees with Ha *et al.*, who found that 50 nm silica particles were located within lysosomes which increased differentiation and ECM mineralisation when cultured with osteoblast pre-cursor (MT-3T3-E1) cells[175]. Compared to cells cultured in BG media, LysoSensor fluorescence produced by SS media often occupied larger areas intracellularly and more closely mirrored fluorescence from lysosomes, again implying that SS produce more Si particles in media that are uptaken by cells. Although fluorescence indicates that lysosomes may contain Si particles, it does not provide any more information about their total composition (e.g., protein corona/Si-complexes).

Identified lysosomes at day 1 also often occurred closer to the nucleus in cells cultured in SS, compared to BG media, where lysosome/LysoSensor fluorescence was commonly observed closer to the outer cell membrane. At day 4, however, both SS and BGs conditioned media produced cells with fluorescence from both lysosome and LysoSensor stains that were close to the nucleus (Figure 4.3a-f). As SS was observed to produce more particles in media over one day compared to BG conditioned media (as evidenced in Figure 2.3b), this may explain differences in their respective vesicle localisation over time. Naruphontjirakul *et al.*, showed a very similar localisation of BG nanoparticles (90 mol% Si) in human BMSCs close to their respective nuclei[270]. Localisation near the nucleus may suggest lysosomal interaction with or transport to mitochondria or endoplasmic reticulum (protein synthesis). Si alone and from BG dissolution products have been shown to increase protein production[271–273]. Infrequent, low intensity LysoSensor fluorescence was also found outside of regions that were not also

fluorescing as a result of lysosomal stains. It is unclear whether this fluorescence is due to smaller Si particles or just localised acidic areas of the cell.

Similar to bright field images in fluorescence images, bright field in STEM also observed large, heavily stained vesicles in osteoblasts following culture with media containing SS (Figure 4.6a/b). Within these vesicles, high concentrations of silicon and oxygen were found (Figure 4.6c/d), which supports evidence (LysoSensor fluorescence -Figure 4.2) that 2 mM Si from SS media produced particulates that were likely uptaken by endocytosis. A number of studies have shown visually (using TEM) that silica nanoparticles localised inside vesicles[241, 274, 275], although only Ha *et al*., has shown this using osteoblast cells[276]. No studies to date, however, have shown this using SS or BGs dissolution products (that were not synthesised intentionally as nanoparticles) or characterised their composition or protein corona using STEM-EDX.

No localisation of sodium was observed implying that Si may be uptaken alone, its concentration is too low to be detected or that sodium is displaced by another element (e.g., calcium). The only other element to be localised in vesicles, however, was nitrogen, suggesting that proteins may form part of these particles. This agrees with Figure 2.4f, which demonstrated that isolated precipitates from media contained increasing [BSA] with increasing [Si]. Scans of other organelles such as mitochondria, Golgi apparatus or rough/smooth endoplasmic reticulum (Figure 5.3), did not show any localisation of Si or any other element. To date, no study has shown Si to be localised in any specific organelles, despite previous studies showing that Si increases proliferation and the expression of specific protein markers of differentiation and mineralisation. For example, Zhou *et al*., showed that Si increased expression of NF-κB, a protein known to influence mitochondrial activity[277, 278]. This suggests that either EDX is too insensitive to detect Si and other elements at low concentrations (a known limitation of EDX detectors[279]) or Si has an upstream effect on the intracellular pathways that affect organelle function, and therefore Si may not interact with them directly. In

addition, detection of trace level Si localisation may be further hindered by background Si detected in resins (Figure 5.4a)).

Despite vesicles being observed in STEM bright field images (Figure 4.6a) and in LysoSensor fluorescence (Figure 4.1f), sensitivity of EDX is likely to be the reason that Si was not detected in vesicles found within cells cultured in BG media (Figure 4.7c). Although localisation of P was observed in vesicles, no localisation was found with Ca, suggesting that P may have been uptaken alone and not in the form of hydroxyapatite. Despite its release from BGs, Na was also not localised intracellularly. Similar to cells cultured in SS, N was localised to the observed vesicles, suggesting that serum proteins from culture media may have formed complexes (or coronas) with uptaken calcium/phosphorus/Si particles.

4.5.2 Where is Si located within osteoclasts?

Bright field images of osteoclasts showed a lower number of differentiated cells in control compared to cells cultured in SS or BG media (Figure 4.4a,c,e). This agrees with previous studies showing that Si inhibits osteoclast differentiation and function[57, 276, 280, 281]. Similar to osteoblasts, more osteoclasts (and undifferentiated macrophages) fluoresced and with greater intensity when cultured in SS media compared to BG and the control (Figure 4.4b,d,f). SS in DMEM, like McCoy's media, was observed to form larger particles compared to BGs, when cultured over 8 days (Figure 2.5c), which may explain the differences in fluorescence between the conditions. The pH of osteoclasts has also been shown to be slightly acidic (~pH 6-7)[282] which may explain some visible fluorescence in healthy osteoclasts cultured in media containing no Si (Figure 4.4b). It is therefore unclear which fluorescent areas of these cells are caused by particulate Si and which are due to localised acidity. At higher magnification, both fluorescence from cells cultured SS and BG were found to overlap with lysosome stains suggesting that (like osteoblasts) Si at 2 mM produced particles uptaken by endocytosis (Figure 4.5b,c,e,f). Although less LysoSensor

fluorescence is observed in osteoclasts compared to osteoblasts per cell, some fluorescence may be on other focal planes due to their significant increase in size. This may also explain why vesicles are not clearly visible in bright field images (Figure 4.5a,d).

Vesicles containing large particles localised with Si and O were also observed in osteoclasts following culture with SS media (Figure 4.6a-e). Whilst a number of previous studies have looked at the negative effect of Si on osteoclast differentiation and function, none have provided direct evidence that this effect originates intra- or extracellularly. This result shows that Si at 2 mM is uptaken (in part as particles) and is transported to other parts of the cell in vesicles. Despite studies evaluating the effect of Si alone, released from BGs or nanoparticles on osteoclasts (reporting reduced osteoclastogenesis)[283–285], no studies have determined/visualised their intracellular location. Although the number of vesicles appeared to be less frequent throughout the cytoplasm compared to osteoblasts, other vesicles may be present on other nanometre sections due to the significant increase in volume. Due to this increase in size however, little to no observations were made of organelles such as Golgi apparatus and rough endoplasmic reticulum. EDX scans of these organelles would provide evidence for the role of Si (or other elements) in protein synthesis and thus osteoclast function. Despite mitochondria being frequently observed throughout the cell, no localisation of Si was identified. Similar to culture in osteoblasts, no sodium was localised in these vesicles (Figure 4.8e). Sulphur was, however, localised within vesicles suggesting that proteins make up part of uptaken particles (Figure 4.8f).

Like osteoblasts, observed intracellular vesicles following culture in BG media were also smaller in size (similar to those found in bright field/fluorescence images) compared to those identified in cells cultured in SS media. In contrast to osteoblasts, however, intracellular vesicles in cells cultured in BG media were observed to contain Si. The ability to localise Si in osteoclasts compared with

osteoblasts may be due to differences in the total [Si] uptaken in each cell type (future work). How this is then influenced by the concentration of other common ions released from BGs (Ca, P, Na, etc.) is still poorly understood. Further differences in Si uptake may be produced by disparities in particle formation based on which media (McCoy's vs DMEM) was used and their respective composition (pH, concentration of amino acids, etc.).

4.6 Conclusion

This study has for the first-time localised Si within osteoblast-like cells cultured in Si containing media. Si particles were observed within intracellular lysosomes in both osteoblast and osteoclast cells, suggesting that endocytosis may be involved in Si uptake. Osteoclasts also had more intense Si EDX and (on imaging) particles inside endosomes, suggesting cell-cell variation in uptake and/or internal processing In agreement with ICP Si uptake experiments (Chapter 3), SS conditioned media had clearer EDX particle imaging and increased fluorescent intensity imaging, suggesting higher uptake of SS compared to SiBG dissolution products. .

An increase in the number fluorescent cells cultured in SS and BG media over 8 days suggested that LysoSensor could be an effective method to track the uptake of Si in live cell cultures over time. Due to low sensitivity (and specificity to polymerised Si in the case of Lysosensor), however, STEM-EDX and fluorescence techniques could only locate Si particles and not ions

Chapter 5. General discussion

SiBG dissolution products have been shown to bone regeneration and mineralisation *in vivo* but *in vitro* there is considerable variance in the reported outcome with SiBG [Si] and reporting measures (assay, cell, and species types) used to assess cell behaviour has made identification of the most beneficial rates of Si release from BGs difficult. The individual and combinatorial effects of other commonly added therapeutic trace ions (Li, Sr, Co etc.) with Si on cells is yet another confounding factor that adds complexity to answering this question.

This thesis addresses whether Si release rates from BGs could be informed by trends in the effect of [Si] on cell responses in previous *in vitro* studies (systematic review) and (experimentally) the relationship between [Si] and the formation of different Si species. The interaction (uptake and secretion) of these different Si species with bone cells was then assessed based on intracellular [Si] and localisation, along with their respective uptake mechanisms following exposure to culture mediums containing Si.

The relationship between [Si] and the quantities of different silicate species (ortho, di, tri and polysilicates) was assessed in both SS (Si alone) and BGs. With the assumption that polymerisation of Si occurs at above 2 - 3 mM (demonstrated by previous studies[65]), this concentration was used to assess how cell uptake Si over time and what effect different species has on uptake mechanisms and its intracellular localisation. Chapter 5 attempts to combine what we have learnt experimentally and by systematic review to inform the synthesis of future novel BGs such that Si release can maximise beneficial cell behaviour.

5.1 Is [Si] important in bone regeneration?

Previous studies have made it clear that the presence of Si was critical for normal bone remodelling in humans and animals. *In vivo*, deficiency of dietary Si was responsible for the malformation of skull bone in both chicks[61, 92] and rats[91]. Some later studies found no differences in bone formation in animal models[286, 287], although many of these experiments were limited by early, insensitive instruments used to quantify Si in diets. Whilst an increase in Si was shown to influence BMD in men[109] and pre-menopausal women[105] over 10 years, short term studies of dietary silicon supplementary was observed to have little to no effect in healthy subjects[108]. The effect of Si in the short term was found to be greater, however, when given to volunteers suffering from bone related diseases. Studies showed that the BMD of patients suffering from osteoporosis increased when given silicon supplements[108, 288]. These results suggests that whilst Si is necessary for normal bone remodelling, its supplementation (either through diet or Si-releasing biomaterials e.g., SBGs) may be better suited toward the repair of diseased bone compared to damaged bone resulting from injury in healthy subjects. The reasons behind why Si is effective in repairing diseased bone and not healthy bone remains unclear, although may imply that diseased cells are impaired in their ability to interact with Si.

5.2 The importance of concentration and Si species in determining cell behaviour

Previous studies have reported correlations between [Si] and the quantity of different species. R. Iler demonstrated Si polymerisation to be concentration dependent, occurring at approximately 2 – 3 mM when pH is below 9[65]. *In vitro*, the outcome of cell behaviour has been shown to be significantly different depending on the Si species and the degree of polymerisation. Silica nanoparticles (<100 nm) have been reported to cause cellular toxicity via the

intracellular production of ROS and DNA damage[150]. It is probable that ionic (orthosilicates) Si, therefore, is the cause for the beneficial effects on cell behaviour *in vitro* such as increase proliferation, protein expression and ECM mineralisation[60, 127–129]. Novel Si releasing BGs should therefore aim to release Si at concentrations that don't encourage the formation of silica nanoparticles. It is unclear, however, what effect other ions released from BGs and components of cell culture media (e.g., serum proteins and buffers) have on the [Si] at which different Si species and polymerisation occur. This thesis attempted to explain variance in reported cell responses to SBGs *in vitro* (Figure 1.7) by improving our understanding of the factors (e.g., [Si] and other ions) that affect Si speciation. This would help provide a basis with which to tailor the release of Si from novel BGs.

Identification of silicate species released from ^{29}Si-BGs showed that above 2 mM Si (in water) disilicates begin to form (Figure 2.2) suggesting that despite the presence of other ions, the formation of Si species may follow trends identified in Si alone. When dissolved in media containing serum, however, precipitation occurred at 1 mM Si and above in both Si alone and BG dissolution products. Si alone was found to produce larger, and a higher concentration of precipitates compared to BGs (Figure), suggesting that other ions (Ca, P and Na) released by BGs may increase the Si polymerisation concentration. This may explain why negative responses to BGs (Figure 1.7) more frequently occur at a significantly higher [Si] (M_d ~50 ppm) than compared with studies focusing on Si alone (M_d ~12 ppm – Figure 1.4). Precipitates were observed to contain both Si and serum proteins, which may suggest protein facilitating aggregation or/and that particles have a protein corona (Figure f). The size distribution of these particles was found to vary based on which media was used which may, in part, explain the high standard deviation observed in the [Si] that cause different cell responses to SBGs and Si alone.

A better understanding of how environmental factors (pH, temperature etc.) affect Si species is important in explaining/predicting cell viability along with intracellular [Si] and localisation. When the media was changed every two days, [Si] above 1 mM was found to decrease metabolic activity and increase percentage cell death. This suggests that either Si particles form at concentrations below 2 mM or that monosilicates can still be toxic to cells (possibly due to localised shifts in pH). Compared to Si from SS (or 'orthosilicates'), intracellular [Si] was observed to decrease with Si from disilicates and then further from trisilicates. It is unclear, however, what proportion of this intracellular [Si] is in the ionic form and which is particulate, given that particles likely contribute more to this overall concentration. When cultured with SS, however, large particles were observed inside cells suggesting that both ions and particles were uptaken.

5.3 The need for methodological standardisation

An additional aim of systematic reviews (chapter 1) was to investigate whether lack of observed trends in reported cell responses to [Si] *in vitro* could be, in part, explained by deviation in methodological approaches to measuring cell behaviour. Whilst some cell behaviours such protein quantification had consistently used assays such as ELISAs (Figure 1.11e), behaviours e.g., toxicity were measured by several different methods (e.g., metabolic activity, DNA, membrane integrity and live/dead imaging). Standardisation of these methodologies would improve our ability to compare experimental outcomes and therefore better measure success between studies. A minimum reporting standard for new in vitro studies of cell responses to BGs was therefore proposed in Table 3 in addition to protocols recommended by ISO standards 10993-5.

The most commonly observed assay type (>52%) in systematic reviews was metabolic activity (Figure 1.11c). This is unsurprising given its recommendation by ISO standards 10993-5 to measure cell toxicity in response to soluble products of medical devices. Metabolic assays (e.g., MTT or Prestoblue) have, however,

been shown to be pH sensitive[289], a factor that could be strongly influenced by ions like Si[290]. Future studies should therefore standardise the use assays such as total DNA quantification, an assay that is unlikely to be affected by ions released from BGs.

Table 3 outlines that ion concentrations should be quantified in BG dissolution products, which may provide better explanations for specific cell outcomes (e.g., increased proliferation or cell death). Approximately 40% of studies retrieved in initial data base search were excluded for a lack of ion quantification in their dissolution products. Quantification of [Si], in particular, in dissolution products may provide evidence for the presence of different Si species or degree polymerisation. This would subsequently help predict cell responses and whether dilution of dissolution products in media is necessary to prevent potentially undesirable cell outcomes. This is particularly important in the case of selecting cell species for *in vitro* testing, since the [Si] that caused negative, and no change responses was significantly different in human vs non-human cells (Figure 1.8a/b). Although few significant differences were found in different cell type response to [Si] (Figure 1.9a-c), mixed cell type populations derived from patient or animal tissues may produce unreliable outcomes, given each cells ability to tolerate higher Si concentrations.

Further standardisation is needed when assessing cell responses to Si alone. Whilst most studies used sodium silicate as their silicate source, some studies opted for other sources such as calcium silicate (Figure 1.4c). Ions like calcium are likely to increase ECM mineralisation, thereby potentially producing false positives in the effect of Si on bone formation. Therefore, new studies focusing on the effect of Si should use a source material that does not significantly affect the cell behaviour of interest.

High variance in the [Si] that is reported to produce beneficial cell behaviour (likely due to the number of different cell types and methodological approaches),

with increasing [Si] being associated with increasingly negative outcomes (Figure 1.7a). No significant differences were observed between [Si] that caused positive outcomes and those that caused no change responses compared to a control. This suggests that whilst the beneficial impacts of Si are likely to be cell, species, and application specific (e.g., bone repair vs wound healing), negative outcomes may be less influenced by these factors. A similar trend was observed in cell responses to Si in BG dissolution products, although at significantly higher concentrations (Figure 1.7a).

This provides evidence that undesirable cellular outcomes from BG dissolution products may (in part) be caused by the polymerisation of Si, and that monosilicates (~30 - 50 ppm) were associated with desirable outcomes. Although no significant differences were observed in ALP activity and mineralised ECM, median [Si] that caused negative responses was higher (M_d = ~45 and 50 respectively) than those causing no change and positive responses (Figure 1.12a/b). The low number of data points may have also contributed to the lack of significant differences observed here.

5.4 Impact on the field of bioactive glasses

Si has been shown to be important in bone remodelling in humans and animals. Without Si, poor or irregular bone formation has been observed. Its exact intra and extracellular role in altering cell behaviour remains unclear. There exists, however, high variance in the [Si] alone and released from BGs that causes desirable and undesirable response *in vitro*. This thesis investigates whether a better understanding of the [Si] at which different Si species occur could help explain this variance and provide guidance for the releasing Si from novel BGs.

Systematic meta-analysis identified relationships between [Si] and different cell responses. When all measures of assessing cell behaviour were combined, [Si] causing negative responses (M_d = 52 ppm / 1.9 mM) was significantly higher than

that causing no change (M_d = 28 ppm / 1 mM) and positive responses (M_d = 32 ppm / 1.1 mM). This demonstrates that there may be biological 'sweet spot' in the range of 30 to 50 ppm in which desirable outcomes are more likely. Above and below this, outcomes are therefore more likely to be undesirable or have little to no significant differences on cell behaviour respectively. This may suggest that Si released from BGs should be tailored to fall within the 'optimal' concentration range or be personalised toward the specific cell type or application. Despite studies reporting that Si could increase ALP activity and ECM mineralisation, no observable trends were observed with increasing [Si], likely due to high variance in reporting measures (e.g., assays, cell, and species types).

A similar trend was observed in Si alone, although at significantly lower concentrations (negative M_d ≅12 ppm), suggesting that the release of other ions (e.g., Ca, P, Na etc.) may influence the formation of different Si species and therefore its overall effect on cell responses. This thesis investigated what influence the release other ions have on the formation of different Si species.

Experimentally, this thesis showed that when dissolved in water above 2 mM Si, ^{29}Si-45S5 BG dissolution products produced a mixture or ortho and disilicates, suggesting that polymerisation may occur close to this concentration. If it is assumed that orthosilicate species are responsible for beneficial outcomes (as describe in previous studies), then BGs should aim to tailor the release of Si to below this concentration. Successful integration of Si isotopes into melt-derived 45S5 BGs, suggested that future studies could also identify Si and other element (e.g., phosphate) species or polymerisation in novel BGs. This could provide useful insight into how the release of different trace elements (e.g., Sr, Li, Co etc.) affect the speciation of Si and thus better explain cellular outcomes.

When dissolved in cell culture media containing serum proteins, however, large precipitates were observed in both Si alone and in BG dissolution products. Si alone was found to produce significantly more frequent and larger particles,

again, implicating the role of other ions (e.g., high levels of Ca) in inhibiting Si polymerisation. Despite not observing clear trends in the effect of Ca on cell responses (Figure 1.15a) *in vitro*, an increase in the mol % of Ca in BGs may reduce the frequency of Si nanoparticles forming and thus potentially reduce the probability of undesirable cell behaviour.

Successful quantification of intracellular [Si] demonstrated that trace elements concentration could be tracked inside cells over time. Future studies could therefore use this method to quantify the concentration of other trace therapeutic ions overtime inside cells. Intracellular maximum concentrations could then be determined and released ion concentrations tailored to specific cell uptake or disease type (e.g., osteoporosis). Although, ICP-OES (used to quantify [Si]) could not distinguish between ions and particles in cell lysates, these differences could be identified visually by TEM-EDX. Despite this, EDX is not sensitive enough to detect ions and only particulate could be localised. Localisation within intracellular lysosomes suggested that at this concentration endocytosis was in part responsible for Si uptake (in addition to active transport).

5.5 Future work

Due to the high cost of Si isotopes, small quantities were only sufficient for integration into BGs and therefore Si species were not determined with Si alone (non-dissolution products). Future work would therefore examine the relationship between [Si] from SS (Si alone) and different Si species. The effect of other ions released from BGs on Si speciation and polymerisation, however, still remains unclear. In this study, BG dissolution products were filtered and diluted to specific Si concentrations to observe the relationship between [Si] and different [Si] species in the presence of other ions. It was clear, however, that the other ions (e.g., Ca and P) influence Si polymerisation given their lack of particle formation in media. Additional experiments would hence investigate how calcium, phosphorus, and sodium concentrations affect the formation of Si species. By

increasing the concentration of other release ions by changing compositional mol percentages in BGs and performing ^{29}Si-NMR, their effect on Si species could be determined. Integration of ^{29}Si isotopes with other commercially available sol-gel BG compositions (namely S54P3 and 58S) may provide useful insight to explain differences in cell responses to their dissolution products *in vitro* and *in vivo*.

A maximum intracellular [Si] was quantified in osteoblast-like cells over an 8-day period following culture with SS and 45S5 BGs. It remains unclear, however, if internalised Si is transferred to daughter cells when mitosis occurs. Proliferation rate and ultimate confluency in culture with Si may therefore alter its intracellular [Si] per cell. Future experiments would hence quantify [Si] inside of cells over a 1-day period, before a significant number of cells have time to divide. Despite visual observation that particulates were uptaken by cells, inhibition of endocytosis did not observe any significant differences in intracellular [Si]. This suggests that Si may be uptaken by another endocytosis related uptake pathway. A future study could examine other methods of complete endocytosis inhibition, e.g., silencing RNAs to reduce expression of endocytosis associated protein.

Although TEM-EDX was able to visualise Si particles inside of cells, little to no Si could be identified outside of lysosomes, suggesting EDX is too insensitive to detect ionic Si. As a more sensitive detection method does not exist that combines with TEM, future elemental localisation could be achieved with surface characterisation techniques, e.g., NanoSIMS. If ionic localisation is achieved, detection within specific organelles may be possible, improving our understanding of the specific intracellular roles.

5.6 Conclusion

This thesis has gained experimentally and by systematic reviews, a better understanding of how [Si] released from BGs affects cell behaviour and why.

When all measures of cell behaviour were combined, [Si] above ~50 ppm caused a 3 times increase in the number of negative outcomes. At concentrations approximately 30 ppm, Si was found to produce positive outcomes, where below this ~25 ppm, no significant differences were observed. This suggested that a Si concentration 'sweet spot' in its release from BGs in vitro. The same trend was observed with Si alone although at significantly lower [Si] implicating the role of Ca, P and Na in modifying Si species and polymerisation concentrations. No relationships were found between [Si] and ECM mineralisation along with ALP activity, likely due to variance in cell types, species and methodological approaches used *in vitro*.

Experimentally, Liquid state ^{29}Si NMR revealed that above 2 mM Si, dissolution products from 45S5 BGs produced disilicates, where below this, only orthosilicates existed. This implied that Si polymerisation may occur at this concentration and its species influenced heavily by its environment (e.g., other ions) than the initial glass silicate network structure of its source. In media, however, larger, and more frequent particles (containing a protein corona) were found in Si alone, further implicating the importance of ions such as Ca in determining Si polymerisation concentrations.

Increasing [Si] was observed to cause greater levels of cell toxicity when media was changed every two days, suggesting that osteoblast-like cells may be able to initially tolerate a low nanoparticle concentration. Differences in particle formation here were likely the cause of significantly greater intracellular [Si] when cultured with Si alone, than with Si released from BGs. Investigation of the uptake dynamics of Si osteoblast-like cells, showed that whilst the intracellular Si concentration reached a maximum, low levels of Si were found in supernatants, suggesting a simultaneous secretion from cells. Particles of Si were successfully visualised inside cells using TEM and their elemental composition assessed using EDX. Consistent with size quantification following precipitation in media, Si alone produced larger and more frequent intracellular particles

compared to Si from BG dissolution products. EDX analysis suggested the presence of proteins either combining with Si (protein corona) or are uptaken at the same time.

A better understanding of the factors that affect Si speciation and polymerisation are important in predicting cell outcomes. This knowledge is useful in tailoring the release rate of Si and different ions from novel BGs to better control Si species and gain more precise control over cellular behaviour.

i. Appendix

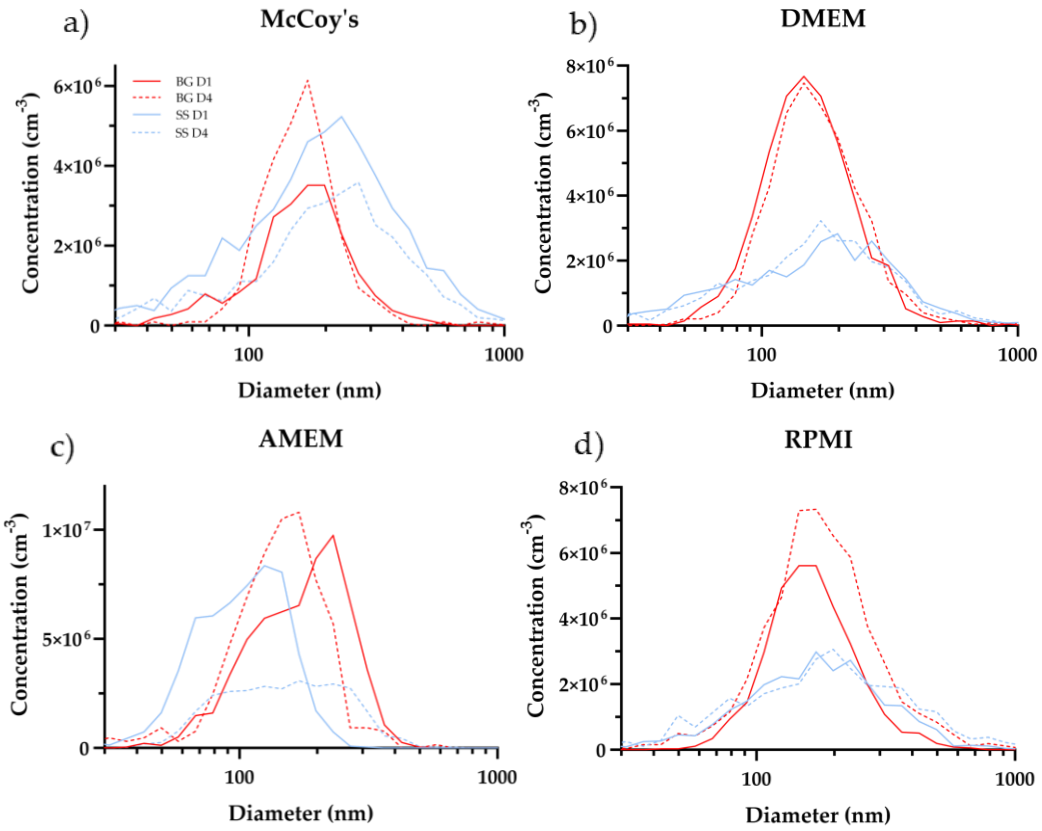

Figure 5.1 - **Particle size distribution in different media types (McCoy's, DMEM, MEM-α, RPMI) conditioned with SS and BG dissolution products determined by NTA.**

SS (blue line) conditioning was found to produce larger particles in all media types over 1 and 4 days and water compared to BG dissolution products (red line) after 4 days.

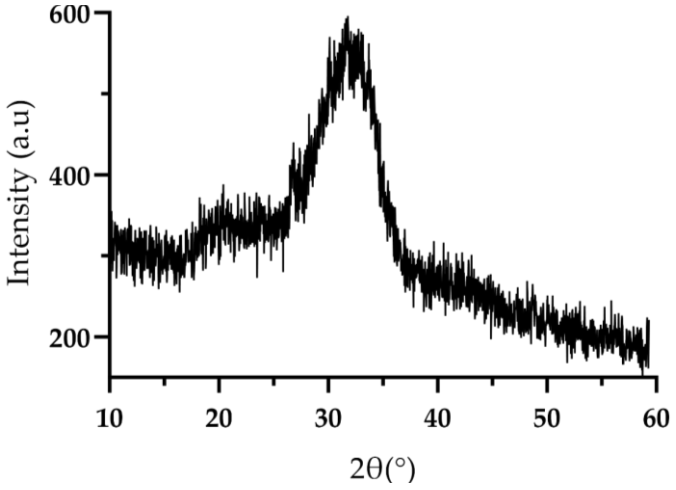

Figure 5.2 - **X-ray crystallography of 45S5 BGs containing ^{29}Si determined by XRD.**

No crystalline peaks were observed with ^{29}Si BGs suggesting glasses were near fully amorphous.

Table 5 - **Element concentrations in different cell culture media (a) along with SS and BG conditioned McCoy's 5A media (b) and water (c) at 2 mM Si.**

a)

Media	Ca (mM)	Na (mM)	P (mM)	Si (μM)
McCoy's 5A	1.1 ± 0.014	147.0 ± 3.06	1.1 ± 0.002	5.7 ± 0.19
MEM-α	1.7 ± 0.007	153.7 ± 0.33	1.1 ± 0.003	3.1 ± 0.11
DMEM	1.8 ± 0.009	165.5 ± 0.62	1.0 ± 0.005	3.7 ± 0.25
RPMI	0.6 ± 0.001	147.7 ± 0.56	4.0 ± 0.021	4.7 ± 0.19

b)

Si source	Ca (μM)	Na (mM)	P (μM)	Si (mM)
Sodium silicate	83.7 ± 0.20	19.0 ± 0.55	257.5 ± 0.26	2.0 ± 0.05
Sodium disilicate	32.5 ± 0.30	8.2 ± 0.13	89.3 ± 1.30	2.0 ± 0.06
Sodium trisilicate	5.7 ± 0.01	5.9 ± 0.02	56.9 ± 3.3	2.0 ± 0.08
45S5 BG	385.2 ± 0.03	50.2 ± 0.47	199.2 ± 0.82	2.0 ± 0.05

c)

Si source	Ca (μM)	Na (mM)	P (μM)	Si (mM)
Sodium silicate	N.D	1.91 ± 0.05	N.D	2.0 ± 0.05
Sodium disilicate	N.D	1.87 ± 0.04	N.D	2.0 ± 0.04
Sodium trisilicate	N.D	1.30 ± 0.03	N.D	2.0 ± 0.03
45S5 BG	307.7 ± 8.55	2.75 ± 0.13	2.87 ± 0.05	2.0 ± 0.08

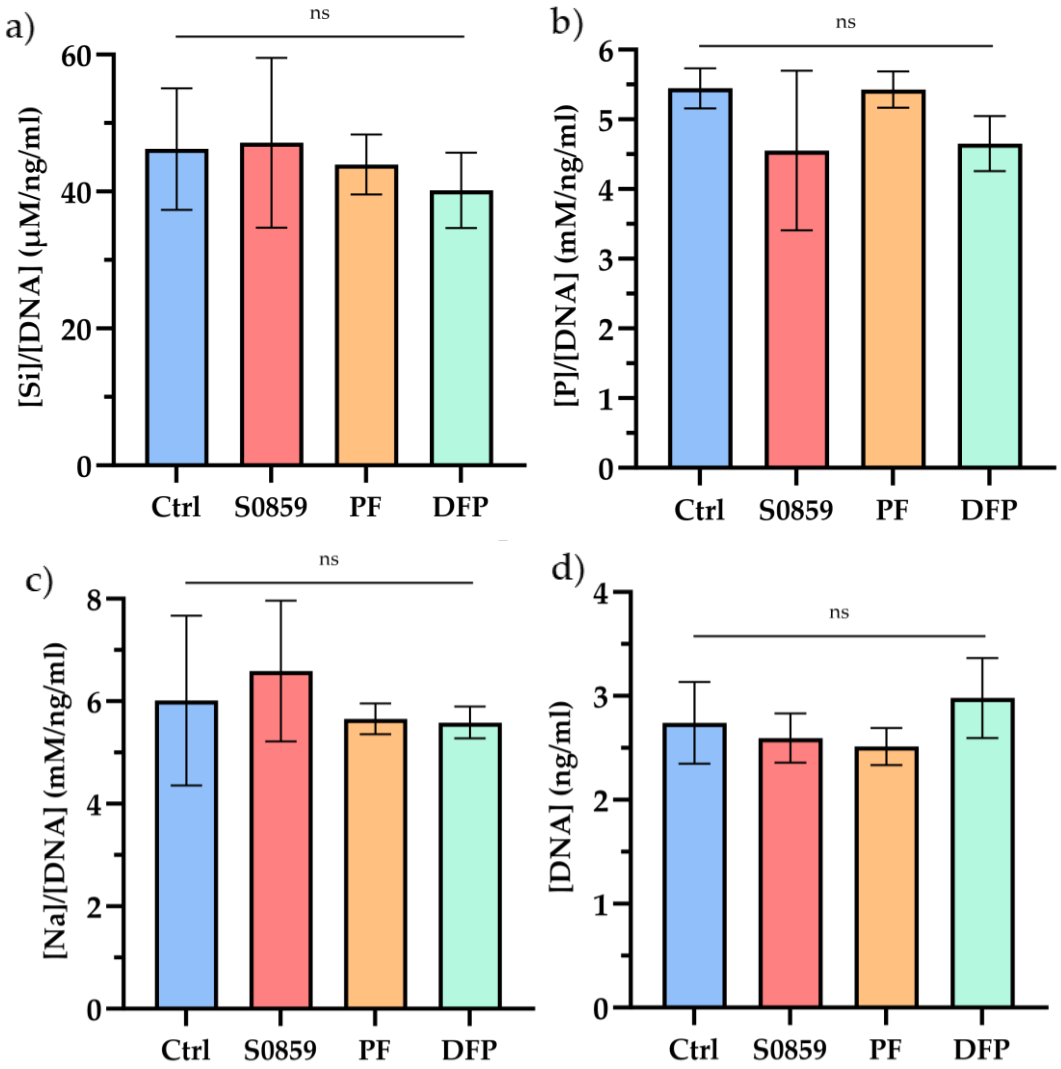

Figure 5.3 – **Inhibition and verification of Si uptake via protein co-transporter ion and water channel inhibitors.**

Quantification of intracellular [Si] (a), [P] (b), [Na] (c) and [DNA] (d) following culture for 24 hours with chemical inhibitors S0859, PF-0686902 ('PF') and DFP-00173 ('DFP'). No significant differences in the intracellular [Si], [P] or [Na] were observed with any ion or water channel inhibitor. Results are presented as the mean ± SD.

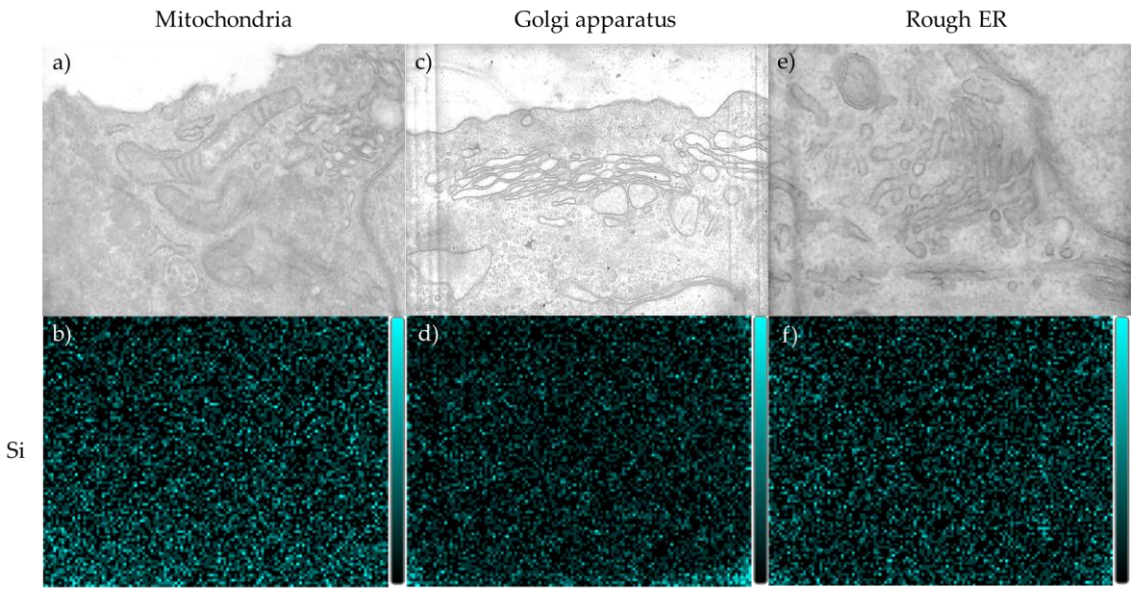

Figure 5.4 - **EDX mapping of Si within mitochondria, Golgi apparatus and rough endoplasmic reticulum.**

No Si localisation was observed in mitochondria (a/b), Golgi apparatus (c/d) and rough ER (e/f). Scale bar = 200 nm.

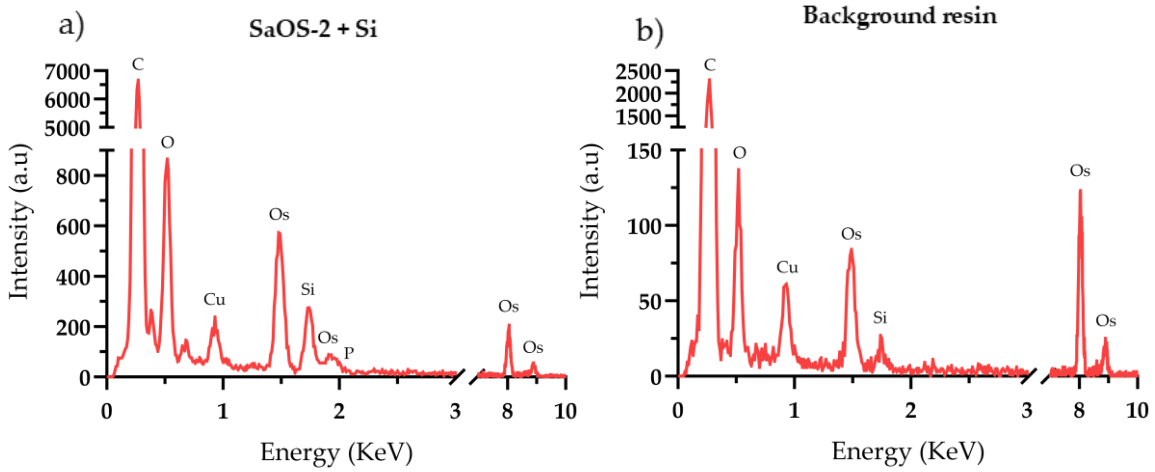

Figure 5.5 - **EDX spectra comparing levels of Si in intracellular vesicles compared to epoxy resin alone.**

Intracellular vesicles were found to contain higher levels of Si (a) then that compared to background Si observed in epoxy resin alone (b).

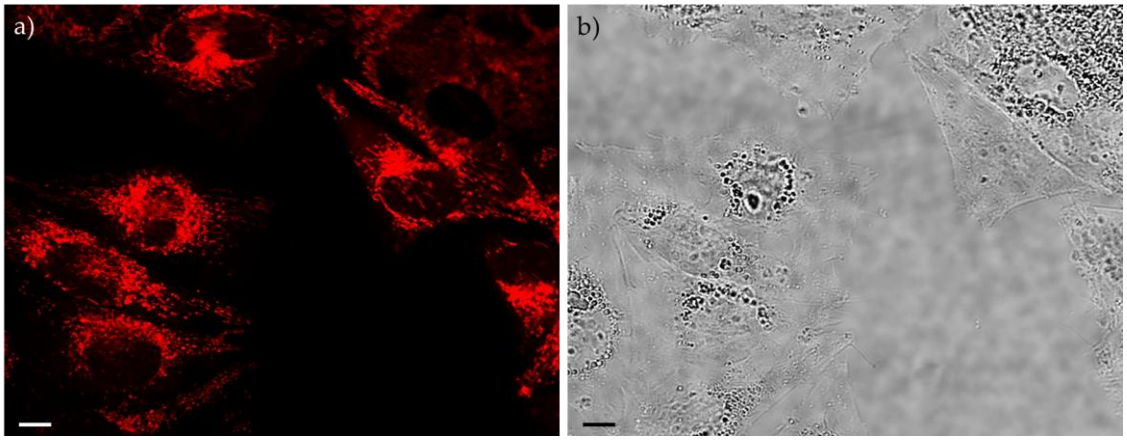

Figure 5.6 – **Mitochondrial fluorescence observed within osteoblast cells.**

Mitochondria are shown in red (a). Brightfield (b) Scale bar = 3 μm.

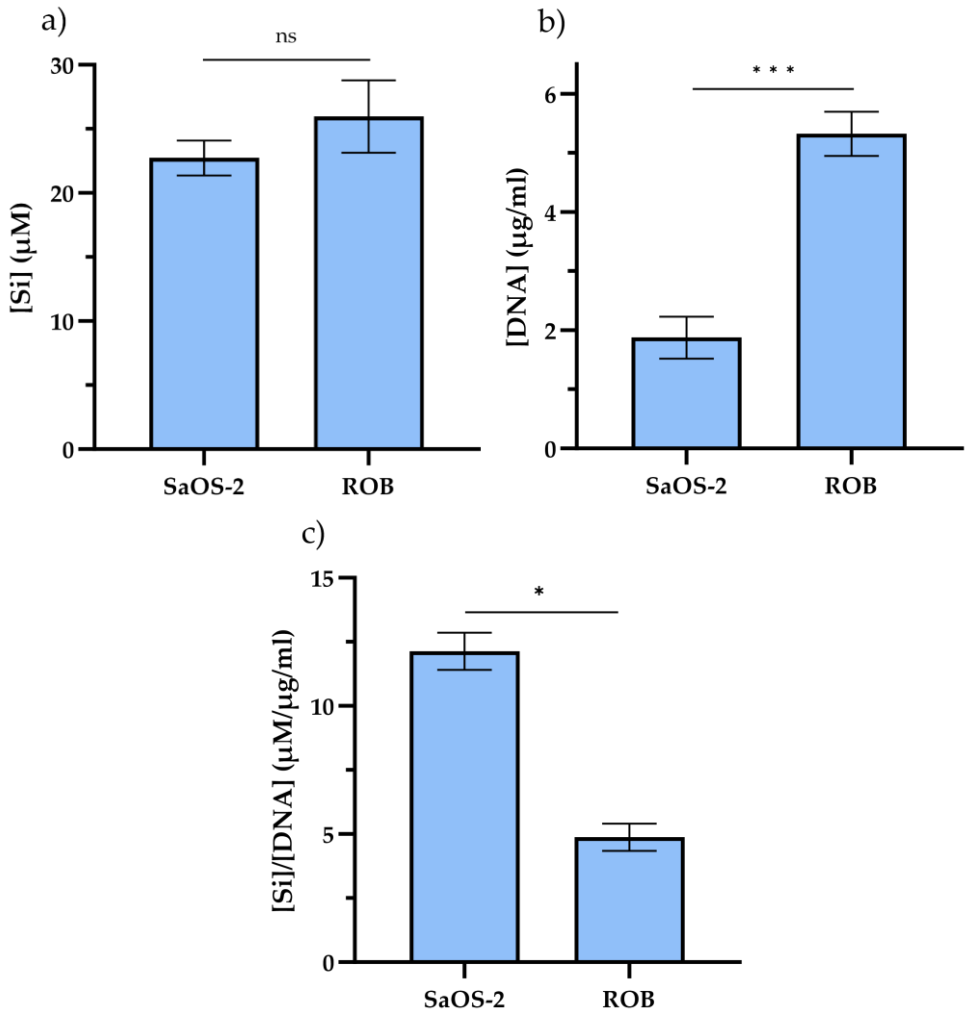

Figure 5.7 – **Intracellular [Si] in SaOS-2 compared to primary rat osteoblasts over 4 days.**

No differences were observed in total intracellular [Si] between SaOS-2 and primary rat osteoblasts (ROB) (a). A decrease in cell number was observed in SaOS-2 cells (P<0.05) (b) and therefore a decrease in [Si]/unit DNA

[Si] mM	[Si] ppm
1	28
2	56
3	84

Table 7 – Table showing the conversion of molar and ppm units for Si.

ii. Bibliography

1. P. V. Giannoudis, H. Dinopoulos, E. Tsiridis, Bone substitutes: An update. *Injury*. **36**, S20–S27 (2005).

2. L. Gutermann, S. Roy, T. Bégué, Synthetic bone subtitutes: What specificities? . *Journal de Pharmacie Clinique*. **32**, 79–87 (2013).

3. T. Kucera, K. Urban, S. Ragkou, Healing of cavitary bone defects. *European Journal of Orthopaedic Surgery and Traumatology*. **22**, 123–128 (2012).

4. E. D. Arrington, W. J. Smith, H. G. Chambers, *et al.*, Complications of iliac crest bone graft harvesting. *Clin Orthop Relat Res*, 300–309 (1996).

5. C. A. Dodd, C. M. Fergusson, L. Freedman, *et al.*, Allograft versus autograft bone in scoliosis surgery. *J Bone Joint Surg Br*. **70**, 431–434 (1988).

6. J. Van Der Stok, E. M. M. Van Lieshout, Y. El-Massoudi, *et al.*, Bone substitutes in the Netherlands - A systematic literature review. *Acta Biomater*. **7**, 739–750 (2011).

7. J. R. Jones, Review of bioactive glass: From Hench to hybrids. *Acta Biomater*. **9** (2013), pp. 4457–4486.

8. V. Brun, C. Guillaume, S. Mechiche Alami, *et al.*, Chitosan/hydroxyapatite hybrid scaffold for bone tissue engineering. *Biomed Mater Eng*. **24**, 63–73 (2014).

9. S. Ge, N. Zhao, L. Wang, *et al.*, Bone repair by periodontal ligament stem cell-seeded nanohydroxyapatite-chitosan scaffold. *Int J Nanomedicine*. **7**, 5405–5414 (2012).

10. S. M. Oliveira, R. A. Ringshia, R. Z. Legeros, *et al.*, An improved collagen scaffold for skeletal regeneration (2010), doi:10.1002/jbm.a.32694.

11. F. Xing, Z. Chi, R. Yang, *et al.*, Chitin-hydroxyapatite-collagen composite scaffolds for bone regeneration. *Int J Biol Macromol*. **184**, 170–180 (2021).

12. T. Fuji, T. Anada, Y. Honda, *et al.*, Octacalcium phosphate-precipitated alginate scaffold for bone regeneration. *Tissue Eng Part A*. **15**, 3525–3535 (2009).

13. J. F. A. Valente, T. A. M. Valente, P. Alves, *et al.*, Alginate based scaffolds for bone tissue engineering (2012), doi:10.1016/j.msec.2012.08.001.

14. S. Castañeda-Rodríguez, M. González-Torres, R. M. Ribas-Aparicio, *et al.*, Recent advances in modified poly (lactic acid) as tissue engineering materials. *J Biol Eng*. **17** (2023), doi:10.1186/S13036-023-00338-8.

15. W. Linhart, D. Briem, M. Amling, *et al.*, Mechanical failure of porous hydroxyapatite ceramics 7.5 years after implantation in the proximal tibial. *Unfallchirurg*. **107**, 154–157 (2004).

16. S.-H. Kwon, Y.-K. Jun, S.-H. Hong, *et al.*, Synthesis and dissolution behavior of b-TCP and HA/b-TCP composite powders (1200) (available at www.elsevier.com/locate/jeurceramsoc).

17. D. Bellucci, A. Sola, V. Cannillo, Hydroxyapatite and tricalcium phosphate composites with bioactive glass as second phase: State of the art and current applications. *J Biomed Mater Res A*. **104** (2016), pp. 1030–1056.

18. L. L. Hench, R. J. Splinter, W. C. Allen, *et al.*, Bonding mechanisms at the interface of ceramic prosthetic materials. *J Biomed Mater Res*. **5**, 117–141 (1971).

19. A. El-Ghannam, P. Ducheyne, I. M. Shapiro, Effect of serum proteins on osteoblast adhesion to surface-modified bioactive glass and hydroxyapatite. *Journal of Orthopaedic Research*. **17**, 340–345 (1999).

20. J. E. Won, M. A. Mateos-Timoneda, O. Castano, *et al.*, Fibronectin immobilization on to robotic-dispensed nanobioactive glass/polycaprolactone scaffolds for bone tissue engineering. *Biotechnol Lett*. **37**, 935–942 (2015).

21. S. Lin, W. Van Den Bergh, S. Baker, *et al.*, Protein interactions with nanoporous sol-gel derived bioactive glasses. *Acta Biomater*. **7**, 3606–3615 (2011).

22. Å. Rosengren, S. Oscarsson, M. Mazzocchi, *et al.*, Protein adsorption onto two bioactive glass-ceramics. *Biomaterials*. **24**, 147–155 (2003).

23. K. Magyari, E. Vanea, L. Baia, *et al.*, Attachment and conformational changes of collagen on bioactive glass surface. *Biomed Mater Eng*. **27**, 63–74 (2016).

24. W. Y. Gong, Y. M. Dong, X. F. Chen, *et al.*, Nano-sized 58S bioactive glass enhances proliferation and osteogenic genes expression of osteoblast-like cells. *Chin J Dent Res*. **15**, 145–152 (2012).

25. R. Detsch, P. Stoor, A. Grünewald, *et al.*, Increase in VEGF secretion from human fibroblast cells by bioactive glass S53P4 to stimulate angiogenesis in bone. *J Biomed Mater Res A*. **102**, 4055–4061 (2014).

26. V. G. Varanasi, J. B. Owyoung, E. Saiz, *et al.*, The ionic products of bioactive glass particle dissolution enhance periodontal ligament fibroblast osteocalcin expression and enhance early mineralized tissue development. *J Biomed Mater Res A*. **98 A**, 177–184 (2011).

27. E. Gentleman, Y. C. Fredholm, G. Jell, *et al.*, The effects of strontium-substituted bioactive glasses on osteoblasts and osteoclasts in vitro. *Biomaterials*. **31**, 3949–3956 (2010).

28. J. G. da Silva, R. Babb, C. Salzlechner, *et al.*, Optimisation of lithium-substituted bioactive glasses to tailor cell response for hard tissue repair. *J Mater Sci*. **52**, 8832–8844 (2017).

29. A. C. Marques, R. M. Almeida, A. Thiema, *et al.*, Sol-gel-derived glass scaffold with high pore interconnectivity and enhanced bioactivity. *J Mater Res*. **24**, 3495–3502 (2009).

30. L. Courthéoux, J. Lao, J.-M. Nedelec, *et al.*, Controlled bioactivity zinc-doped sol-gel-derived binary bioactive glasses. *Journal of Physical Chemistry C*. **112**, 13663–13667 (2008).

31. H. Lu, T. Zhang, X. P. Wang, *et al.*, Electrospun submicron bioactive glass fibers for bone tissue scaffold. *J Mater Sci Mater Med*. **20**, 793–798 (2009).

32. E. Norris, C. Ramos-Rivera, G. Poologasundarampillai, *et al.*, Electrospinning 3D bioactive glasses for wound healing. *Biomedical Materials (Bristol)*. **15** (2020), doi:10.1088/1748-605X/ab591d.

33. J. R. Jones, D. S. Brauer, L. Hupa, *et al.*, Bioglass and Bioactive Glasses and Their Impact on Healthcare. *Int J Appl Glass Sci*. **7**, 423–434 (2016).

34. T. B. Lovelace, J. T. Mellonig, R. M. Meffert, *et al.*, Clinical evaluation of bioactive glass in the treatment of periodontal osseous defects in humans. *J Periodontol*. **69**, 1027–1035 (1998).

35. S. J. Froum, M. A. Weinberg, D. Tarnow, Comparison of Bioactive Glass Synthetic Bone Graft Particles and Open Debridement in the

Treatment of Human Periodontal Defects. A Clinical Study. *J Periodontol*. **69**, 698–709 (1998).

36. J. Wilson, S. 6 Low, Bioactive Ceramics for Periodontal Treatment: Comparative Studies in the Patus Monkey, doi:10.1002/jab.770030208.

37. E. J. G. Schepers, P. Ducheyne, Bioactive glass particles of narrow size range for the treatment of oral bone defects: A 1-24 month experiment with several materials and particle sizes and size ranges. *J Oral Rehabil*. **24**, 171–181 (1997).

38. D. G. Gillam, J. Y. Tang, N. J. Mordan, *et al.*, The effects of a novel Bioglass® dentifrice on dentine sensitivity: A scanning electron microscopy investigation. *J Oral Rehabil*. **29**, 305–313 (2002).

39. B. Ilharreborde, E. Morel, F. Fitoussi, *et al.*, Bioactive glass as a bone substitute for spinal fusion in adolescent idiopathic scoliosis: A comparative study with iliac crest autograft. *Journal of Pediatric Orthopaedics*. **28**, 347–351 (2008).

40. L. Drago, D. Romanò, E. De Vecchi, *et al.*, Bioactive glass bag-S53P4 for the adjunctive treatment of chronic osteomyelitis of the long bones: An in vitro and prospective clinical study. *BMC Infect Dis*. **13** (2013), doi:10.1186/1471-2334-13-584.

41. P. David, F. Johannes, C.-H. Débora, *et al.*, BAG-S53P4 as an additive to bone allografts: A laboratory study using an uniaxial compression test. *Journal of Orthopaedic Research*. **33**, 1875–1879 (2015).

42. D. Bernardeschi, N. Pyatigorskaya, F. Y. Russo, *et al.*, Anatomical, functional and quality-of-life results for mastoid and epitympanic obliteration with bioactive glass s53p4: a prospective clinical study. *Clinical Otolaryngology*. **42**, 387–396 (2017).

43. H. Oonishi, L. L. Hench, J. Wilson, *et al.*, Comparative bone growth behavior in granules of bioceramic materials of various sizes. *J Biomed Mater Res*. **44** (1999), pp. 31–43.

44. E. J. G. Schepers, P. Ducheyne, Bioactive glass particles of narrow size range for the treatment of oral bone defects: A 1-24 month experiment with several materials and particle sizes and size ranges. *J Oral Rehabil*. **24**, 171–181 (1997).

45. Z. Wang, B. Lu, L. Chen, *et al.*, Evaluation of an osteostimulative putty in the sheep spine. *J Mater Sci Mater Med*. **22**, 185–191 (2011).

46. M. Zaidi, O. A. Adebanjo, B. S. Moonga, *et al.*, Emerging insights into the role of calcium ions in osteoclast regulation. *Journal of Bone and Mineral Research*. **14** (1999), pp. 669–674.

47. S. Nakamura, T. Matsumoto, J. I. Sasaki, *et al.*, Effect of calcium ion concentrations on osteogenic differentiation and hematopoietic stem cell niche-related protein expression in osteoblasts. *Tissue Eng Part A*. **16**, 2467–2473 (2010).

48. X. Wu, N. Itoh, T. Taniguchi, *et al.*, Requirement of calcium and phosphate ions in expression of sodium-dependent vitamin C transporter 2 and osteopontin in MC3T3-E1 osteoblastic cells. *Biochim Biophys Acta Mol Cell Res*. **1641**, 65–70 (2003).

49. S. Ali Akbari Ghavimi, B. N. Allen, J. L. Stromsdorfer, *et al.*, Calcium and phosphate ions as simple signaling molecules with versatile osteoinductivity. *Biomedical Materials (Bristol)*. **13** (2018), doi:10.1088/1748-605X/aac7a5.

50. M. Julien, S. Khoshniat, A. Lacreusette, *et al.*, Phosphate-dependent regulation of MGP in osteoblasts: Role of ERK1/2 and Fra-1. *Journal of Bone and Mineral Research*. **24**, 1856–1868 (2009).

51. W. Tiyasatkulkovit, S. Aksornthong, P. Adulyaritthikul, *et al.*, Excessive salt consumption causes systemic calcium mishandling and worsens microarchitecture and strength of long bones in rats. *Sci Rep*. **11** (2021), doi:10.1038/s41598-021-81413-2.

52. B. Teucher, J. R. Dainty, C. A. Spinks, *et al.*, Sodium and bone health: impact of moderately high and low salt intakes on calcium metabolism in postmenopausal women. *Journal of Bone and Mineral Research*. **23**, 1477–1485 (2008).

53. I. D. Xynos, A. J. Edgar, L. D. K. K. Buttery, *et al.*, Gene-expression profiling of human osteoblasts following treatment with the ionic products of Bioglass® 45S5 dissolution. *J Biomed Mater Res*. **55**, 151–157 (2001).

54. E. S. Thian, J. Huang, S. M. Best, *et al.*, Novel silicon-doped hydroxyapatite (Si-HA) for biomedical coatings: An in vitro study using acellular simulated body fluid. *J Biomed Mater Res B Appl Biomater*. **76**, 326–333 (2006).

55. F. J. Martínez-Vázquez, M. V. Cabañas, J. L. Paris, *et al.*, Fabrication of novel Si-doped hydroxyapatite/gelatine scaffolds by rapid

prototyping for drug delivery and bone regeneration. *Acta Biomater*. **15**, 200–209 (2015).

56. I. D. Xynos, A. J. Edgar, L. D. K. Buttery, *et al.*, Ionic products of bioactive glass dissolution increase proliferation of human osteoblasts and induce insulin-like growth factor II mRNA expression and protein synthesis. *Biochem Biophys Res Commun*. **276**, 461–465 (2000).

57. H. C. Schröder, X. H. Wang, M. Wiens, *et al.*, Silicate modulates the cross-talk between osteoblasts (SaOS-2) and osteoclasts (RAW 264.7 cells): Inhibition of osteoclast growth and differentiation. *J Cell Biochem*. **113**, 3197–3206 (2012).

58. M. Dong, G. Jiao, H. Liu, *et al.*, Biological Silicon Stimulates Collagen Type 1 and Osteocalcin Synthesis in Human Osteoblast-Like Cells Through the BMP-2/Smad/RUNX2 Signaling Pathway. *Biol Trace Elem Res*. **173**, 306–315 (2016).

59. E.-J. Kim, S.-Y. Bu, M.-K. Sung, *et al.*, Effects of Silicon on Osteoblast Activity and Bone Mineralization of MC3T3-E1 Cells. *Biol Trace Elem Res*. **152**, 105–112 (2013).

60. M. Y. Shie, S. J. Ding, H. C. Chang, The role of silicon in osteoblast-like cell proliferation and apoptosis. *Acta Biomater*. **7**, 2604–2614 (2011).

61. E. M. Carlisle, Silicon: An essential element for the chick. *Science (1979)*. **178**, 619–621 (1972).

62. E. M. Carlisle, Silicon in Bone Formation. *Silicon and Siliceous Structures in Biological Systems*, 69–94 (1981).

63. K. R. Martin, The chemistry of silica and its potential health benefits. *J Nutr Health Aging*. **11**, 94–7 (2007).

64. G. B. Alexander, Reaction of Low Molecular Weight Silicic Acids with Molybdic Acid The Reaction of Low Molecular Weight Silicic Acids with Molybdic Acid Introduction Dienert and Wandenbulcke1 23and Harmon* have (1953) (available at https://pubs.acs.org/sharingguidelines).

65. R. K. Iler, *The chemistry of silica : solubility, polymerization, colloid and surface properties, and biochemistry* (Wiley, 1979).

66. M. Dietzel, Interaction of polysilicic and monosilicic acid with mineral surfaces, 207–235 (2002).

67. M. Kley, A. Kempter, V. Boyko, *et al.*, Mechanistic studies of silica polymerization from supersaturated aqueous solutions by means of time-resolved light scattering. *Langmuir*. **30**, 12664–12674 (2014).

68. P. N. Gunawidjaja, R. Mathew, A. Y. H. Lo, *et al.*, Local structures of mesoporous bioactive glasses and their surface alterations in vitro: inferences from solid-state nuclear magnetic resonance. *Trans. R. Soc. A*. **370**, 1376–1399 (2012).

69. G. Miao, X. Chen, H. Dong, *et al.*, Investigation of emulsified, acid and acid-alkali catalyzed mesoporous bioactive glass microspheres for bone regeneration and drug delivery (2013), doi:10.1016/j.msec.2013.06.022.

70. R. K. Harris, J. Jones, C. T. G. Knight, *et al.*, Silicon-29 NMR studies of aqueous silicate solutions. Part II. Isotopic enrichment2 2 See ref. 7 for Part I. *J Mol Struct*. **69**, 95–103 (1980).

71. S. Gillete-Guyonnet, S. Andrieu, F. Nourhashemi, *et al.*, Cognitive impairment and composition of drinking water in women: Findings of the EPIDOS study. *American Journal of Clinical Nutrition*. **81**, 897–902 (2005).

72. J. A. T. Pennington, Silicon in foods and diets. *Food Addit Contam*. **8**, 97–118 (1991).

73. J. F. Popplewell, S. J. King, J. P. Day, *et al.*, "Kinetics of uptake and elimination of silicic acid by a human subject: A novel application of 32Si and accelerator mass spectrometry" in *Journal of Inorganic Biochemistry* (1998), vol. 69, pp. 177–180.

74. R. Jugdaohsingh, D. M. Reffitt, C. Oldham, *et al.*, Oligomeric but not monomeric silica prevents aluminum absorption in humans. *American Journal of Clinical Nutrition*. **71**, 944–949 (2000).

75. D. M. Reffitt, R. Jugdaohsingh, R. P. H. Thompson, *et al.*, Silicic acid: its gastrointestinal uptake and urinary excretion in man and effects on aluminium excretion. *J Inorg Biochem*. **76**, 141–147 (1999).

76. Jugdaohsingh, Dietary Silicon intake and absorption. *Am J Clin Nutr*, 887–893 (2002).

77. J. L. Kelsay, K. M. Behall, E. S. Prather, Effect of fiber from fruits and vegetables on metabolic responses of human subjects. II. Calcium, magnesium, iron, and silicon balances. *American Journal of Clinical Nutrition*. **32**, 1876–1880 (1979).

78. F. H. Nielsen, Nutritional requirements for boron, silicon, vanadium, nickel, and arsenic: current knowledge and speculation. *The FASEB Journal*. **5**, 2661–2667 (1991).

79. *Dietary Reference Intakes for Vitamin A, Vitamin K, Arsenic, Boron, Chromium, Copper, Iodine, Iron, Manganese, Molybdenum, Nickel, Silicon, Vanadium, and Zinc* (National Academies Press, Washington, D.C., 2001; http://www.nap.edu/catalog/10026).

80. S. Sripanyakorn, R. Jugdaohsingh, R. P. H. Thompson, *et al.*, Dietary silicon and bone health. *Nutr Bull*. **30** (2005), pp. 222–230.

81. K. Schwarz, A Bound Form of Silicon in Glycosaminoglycans and Polyuronides. *Proceedings of the National Academy of Sciences*. **70**, 1608–1612 (1973).

82. E. M. Carlisle, Silicon: A requirement in bone formation independent of vitamin D1. *Calcif Tissue Int*. **33**, 27–34 (1981).

83. M. R. Calomme, D. A. Vanden Berghe, Supplementation of calves with stabilized orthosilicic acid: Effect on the Si, Ca, Mg, and P concentrations in serum and the collagen concentration in skin and cartilage. *Biol Trace Elem Res*. **56**, 153–165 (1997).

84. C. D. Seaborn, F. H. Nielsen, Silicon deprivation decreases collagen formation in wounds and bone, and ornithine transaminase enzyme activity in liver. *Biol Trace Elem Res*. **89**, 251–261 (2002).

85. L. Advincula de Araújo, A. Flavia, "Use of silicon for skin and hair care: an approach of chemical forms available and efficacy" (2016), , doi:10.1590/abd1806-4841.20163986.

86. R. R. Wickett, E. Kossmann, A. Barel, *et al.*, Effect of oral intake of choline-stabilized orthosilicic acid on hair tensile strength and morphology in women with fine hair. *Arch Dermatol Res*. **299**, 499–505 (2007).

87. G.-G. S., A. S., S. Gillette-Guyonnet, *et al.*, The potential influence of silica present in drinking water on Alzheimer's disease and associated disorders. *J Nutr Health Aging*. **11**, 119–124 (2007).

88. M. Bellés, D. J. Sánchez, M. Gómez, *et al.*, Silicon reduces aluminum accumulation in rats: relevance to the aluminum hypothesis of Alzheimer disease. *Alzheimer Dis Assoc Disord*. **12**, 83–7 (1998).

89. R. Jugdaohsingh, Silicon and bone health. *J Nutr Health Aging*. **11**, 99–110 (2007).

90. C. T. Price, K. J. Koval, J. R. Langford, Silicon: A review of its potential role in the prevention and treatment of postmenopausal osteoporosis. *Int. J. Endocrinol.* **2013**, 1–6 (2013).

91. K. Schwarz, D. B. Milne, Growth-promoting effects of silicon in rats. *Nature*. **239**, 333–334 (1972).

92. E. M. Carlisle, A silicon requirement for normal skull formation in chicks. *Journal of Nutrition*. **110**, 352–359 (1980).

93. M. A. Elliot, H. M. Edwards, Effect of dietary silicon on growth and skeletal development in chickens. *Journal of Nutrition*. **121**, 201–207 (1991).

94. C. D. Seaborn, F. H. Nielsen, Dietary silicon affects acid and alkaline phosphatase and 45Calcium uptake in bone of rats. *Journal of Trace Elements in Experimental Medicine*. **7**, 11–18 (1994).

95. R. Jugdaohsingh, "Silicon and bone health" in *Journal of Nutrition, Health and Aging* (2007; https://www-proquest-com.libproxy.ucl.ac.uk/docview/222290193?accountid=14511), vol. 11, pp. 99–110.

96. M. Ji, Q. Yu, Primary osteoporosis in postmenopausal women. *Chronic Dis Transl Med*. **1**, 9–13 (2015).

97. M. Hott, C. de Pollak, D. Modrowski, *et al.*, Short-term effects of organic silicon on trabecular bone in mature ovariectomized rats. *Calcif Tissue Int*. **53**, 174–179 (1993).

98. H. Rico, C. Roca-Botran, E. R. Hernández, *et al.*, The effect of supplemental copper on osteopenia induced by ovariectomy in rats. *Menopause*. **7**, 413–416 (2000).

99. M. Calomme, P. Geusens, N. Demeester, *et al.*, Partial prevention of long-term femoral bone loss in aged ovariectomized rats supplemented with choline-stabilized orthosilicic acid. *Calcif Tissue Int*. **78**, 227–232 (2006).

100. M. H. Kim, M. K. Choi, Effect of Silicon Supplementation in Diets with Different Calcium Levels on Balance of Calcium, Silicon and Magnesium, and Bone Status in Growing Female Rats. *Biol Trace Elem Res*. **199**, 258–266 (2021).

101. M. H. Kim, Y. J. Bae, M. K. Choi, *et al.*, Silicon supplementation improves the bone mineral density of calcium-deficient ovariectomized rats by reducing bone resorption. *Biol Trace Elem Res*. **128**, 239–247 (2009).

102. F. H. Nielsen, R. Poellot, Dietary silicon affects bone turnover differently in ovariectomized and sham-operated growing rats. *Journal of Trace Elements in Experimental Medicine*. **17**, 137–149 (2004).

103. R. Jugdaohsingh, L. D. Pedro, A. Watson, *et al.*, Silicon and boron differ in their localization and loading in bone. *Bone Rep*. **1**, 9–15 (2015).

104. R. Jugdaohsingh, K. L. Tucker, N. Qiao, *et al.*, Dietary Silicon Intake Is Positively Associated with Bone Mineral Density in Men and Premenopausal Women of the Framingham Offspring Cohort. *Journal of Bone and Mineral Research*. **19**, 297–307 (2004).

105. H. M. Macdonald, A. C. Hardcastle, R. Jugdaohsingh, *et al.*, Dietary silicon interacts with oestrogen to influence bone health: Evidence from the Aberdeen Prospective Osteoporosis Screening Study. *Original Full Length Article* (2011), doi:10.1016/j.bone.2011.11.020.

106. A. Schiano, F. Eisinger, P. Detolle, *et al.*, SILICIUM, TISSU OSSEUX ET IMMUNITE. *Rev Rhum Mal Osteoartic*. **46**, 483–486 (1979).

107. J. Eisinger, D. Clairet, Effects of silicon, fluoride, etidronate and magnesium on bone mineral density: a retrospective study. *Magnesium research : official organ of the International Society for the Development of Research on Magnesium*. **6**, 247–249 (1993).

108. T. D. Spector, M. R. Calomme, S. Anderson, *et al.*, Effect on Bone Turnover and BMD of Low Dose Oral Silicon as an adjunct to Calcium / Vitamin D3 in a Randomized , Placebo-Controlled Trial. *Journal of Bone and Mineral Research*. **20**, 2012 (2012).

109. M. K. Choi, M. H. Kim, Dietary Silicon Intake of Korean Young Adult Males and Its Relation to their Bone Status. *Biol Trace Elem Res*. **176**, 89–104 (2017).

110. P. Stoor, S. Apajalahti, R. Kontio, Regeneration of Cystic Bone Cavities and Bone Defects with Bioactive Glass S53P4 in the Upper and Lower Jaws. *Journal of Craniofacial Surgery*. **28**, 1197–1205 (2017).

111. A. M. Gatti, L. A. Simonetti, E. Monari, *et al.*, Bone augmentation with bioactive glass in three cases of dental implant placement. *J Biomater Appl*. **20**, 325–339 (2006).

112. R. Subbaiah, B. Thomas, Efficacy of a bioactive alloplast, in the treatment of human periodontal osseous defects-a clinical study. *Med Oral Patol Oral Cir Bucal*. **16** (2011), doi:10.4317/medoral.16.e239.

113. V. S. Yadav, S. C. Narula, R. K. Sharma, *et al.*, Clinical evaluation of guided tissue regeneration combined with autogenous bone or autogenous bone mixed with bioactive glass in intrabony defects. *J Oral Sci*. **53**, 481–488 (2011).

114. H. Ding, C. J. Zhao, X. Cui, *et al.*, A novel injectable borate bioactive glass cement as an antibiotic delivery vehicle for treating osteomyelitis. *PLoS One*. **9**, e85472 (2014).

115. N. A. P. Van Gestel, J. Geurts, D. J. W. Hulsen, *et al.*, Clinical Applications of S53P4 Bioactive Glass in Bone Healing and Osteomyelitic Treatment: A Literature Review. *Biomed Res Int*. **2015** (2015), , doi:10.1155/2015/684826.

116. B. Ilharreborde, E. Morel, F. Fitoussi, *et al.*, Bioactive glass as a bone substitute for spinal fusion in adolescent idiopathic scoliosis: A comparative study with iliac crest autograft. *Journal of Pediatric Orthopaedics*. **28**, 347–351 (2008).

117. L. E. Westerlund, M. Borden, Clinical experience with the use of a spherical bioactive glass putty for cervical and lumbar interbody fusion. *Journal of Spine Surgery*. **6**, 49–61 (2020).

118. C. Barrey, T. Broussolle, Clinical and radiographic evaluation of bioactive glass in posterior cervical and lumbar spinal fusion. *European Journal of Orthopaedic Surgery and Traumatology*. **29**, 1623–1629 (2019).

119. N. C. Lindfors, I. Koski, J. T. Heikkilä, *et al.*, A prospective randomized 14-year follow-up study of bioactive glass and autogenous bone as bone graft substitutes in benign bone tumors. *J Biomed Mater Res B Appl Biomater*. **94**, 157–164 (2010).

120. J. Frantzén, J. Rantakokko, H. T. Aro, *et al.*, Instrumented spondylodesis in degenerative spondylolisthesis with bioactive glass and autologous bone: a prospective 11-year follow-up. *J Spinal Disord Tech*. **24**, 455–461 (2011).

121. J. Rantakokko, J. P. Frantzén, J. Heinänen, *et al.*, Posterolateral spondylodesis using bioactive glass S53P4 and autogenous bone in instrumented unstable lumbar spine burst fractures. *Scandinavian Journal of Surgery*. **101**, 66–71 (2012).

122. D. L. Wheeler, E. J. Eschbach, R. G. Hoellrich, *et al.*, Assessment of resorbable bioactive material for grafting of critical-size cancellous defects. *Journal of Orthopaedic Research*. **18**, 140–148 (2000).

123. S. Fujibayashi, M. Neo, H. M. Kim, *et al.*, A comparative study between in vivo bone ingrowth and in vitro apatite formation on Na2O-CaO-SiO2 glasses. *Biomaterials*. **24**, 1349–1356 (2003).

124. R. N. Granito, A. C. Rennõ, C. Ravagnani, *et al.*, In vivo biological performance of a novel highly bioactive glass-ceramic (Biosilicate®): A biomechanical and histomorphometric study in rat tibial defects. *J Biomed Mater Res B Appl Biomater*. **97 B**, 139–147 (2011).

125. R. N. Granito, A. C. Rennó, C. Ravagnani, *et al.*, In vivo biological performance of a novel highly bioactive glass-ceramic (Biosilicate®): A biomechanical and histomorphometric study in rat tibial defects. *J Biomed Mater Res B Appl Biomater*. **97B**, 139–147 (2011).

126. J. Turner, A. Nandakumar, N. Anilbhai, *et al.*, The effect of Si species released from bioactive glasses on cell behaviour: A quantitative review. *Acta Biomater*. **170**, 39–52 (2023).

127. S. Zou, D. Ireland, R. A. Brooks, *et al.*, The effects of silicate ions on human osteoblast adhesion, proliferation, and differentiation. *J Biomed Mater Res B Appl Biomater*. **90 B**, 123–130 (2009).

128. A. Obata, T. Ogasawara, T. Kasuga, "Combinatorial effects of inorganic ions on adhesion and proliferation of osteoblast-like cells" in *Journal of Biomedical Materials Research - Part A* (2019), vol. 107, pp. 1042–1051.

129. P. Han, C. Wu, Y. Xiao, The effect of silicate ions on proliferation, osteogenic differentiation and cell signalling pathways (WNT and SHH) of bone marrow stromal cells. *Biomater Sci*. **1**, 379–392 (2013).

130. X. Zhou, F. M. Moussa, S. Mankoci, *et al.*, Orthosilicic acid, Si(OH)4, stimulates osteoblast differentiation in vitro by upregulating miR-146a to antagonize NF-κB activation. *Acta Biomater*. **39**, 192–202 (2016).

131. P. Uribe, A. Johansson, R. Jugdaohsingh, *et al.*, Soluble silica stimulates osteogenic differentiation and gap junction communication in human dental follicle cells. *Sci Rep*. **10** (2020), doi:10.1038/s41598-020-66939-1.

132. V. G. Varanasi, K. K. Leong, L. M. Dominia, *et al.*, Si and Ca individually and combinatorially target enhanced MC3T3-E1 subclone 4 early osteogenic marker expression. *Journal of Oral Implantology*. **38**, 325–336 (2012).

133. D. V. Novack, L. Yin, A. Hagen-Stapleton, *et al.*, The IκB function of NF-κB2 p100 controls stimulated osteoclastogenesis. *Journal of Experimental Medicine*. **198**, 771–781 (2003).

134. J. Chang, Z. Wang, E. Tang, *et al.*, Inhibition of osteoblastic bone formation by nuclear factor-B. *Nat Med*. **15**, 682–689 (2009).

135. W. Dang, X. Wang, J. Li, *et al.*, 3D printing of Mo-containing scaffolds with activated anabolic responses and bi-lineage bioactivities. *Theranostics*. **8**, 4372–4392 (2018).

136. M. S. Kang, N.-H. Lee, R. K. Singh, *et al.*, Nanocements produced from mesoporous bioactive glass nanoparticles. *Biomaterials*. **162**, 183–199 (2018).

137. R. C. Bielby, I. S. Christodoulou, R. S. Pryce, *et al.*, Time- and concentration-dependent effects of dissolution products of 58S sol-gel bioactive glass on proliferation and differentiation of murine and human osteoblasts. *Tissue Eng*. **10**, 1018–1026 (2004).

138. A. Moghanian, S. Firoozi, M. Tahriri, *et al.*, A comparative study on the in vitro formation of hydroxyapatite, cytotoxicity and antibacterial activity of 58S bioactive glass substituted by Li and Sr. *Materials Science and Engineering C*. **91**, 349–360 (2018).

139. V. G. Varanasi, E. Saiz, P. M. Loomer, *et al.*, Enhanced osteocalcin expression by osteoblast-like cells (MC3T3-E1) exposed to bioactive coating glass (SiO2-CaO-P2O5-MgO-K2O-Na2O system) ions. *Acta Biomater*. **5**, 3536–3547 (2009).

140. J. Liu, S. C. F. Rawlinson, R. G. Hill, *et al.*, Fluoride incorporation in high phosphate containing bioactive glasses and in vitro osteogenic, angiogenic and antibacterial effects. *Dental Materials*. **32**, e221–e237 (2016).

141. O. Tsigkou, J. R. Jones, J. M. Polak, *et al.*, Differentiation of fetal osteoblasts and formation of mineralized bone nodules by 45S5 Bioglass® conditioned medium in the absence of osteogenic supplements. *Biomaterials*. **30**, 3542–3550 (2009).

142. I. Christodoulou, L. D. K. Buttery, P. Saravanapavan, *et al.*, Dose- and time-dependent effect of bioactive gel-glass ionic-dissolution products on human fetal osteoblast-specific gene expression. *J Biomed Mater Res B Appl Biomater*. **74**, 529–537 (2005).

143. R. L. Du, J. Chang, S. Y. Ni, *et al.*, Characterization and in vitro bioactivity of zinc-containing bioactive glass and glass-ceramics. *J Biomater Appl*. **20**, 341–360 (2006).

144. A. Obata, N. Iwanaga, A. Terada, *et al.*, Osteoblast-like cell responses to silicate ions released from 45S5-type bioactive glass and siloxane-doped vaterite. *J Mater Sci*. **52**, 8942–8956 (2017).

145. A. Obata, N. Iwanaga, A. Terada, *et al.*, Osteoblast-like cell responses to silicate ions released from 45S5-type bioactive glass and siloxane-doped vaterite. *J Mater Sci*. **52**, 8942–8956 (2017).

146. E. Jablonská, D. Horkavcová, D. Rohanová, *et al.*, A review of: In vitro cell culture testing methods for bioactive glasses and other biomaterials for hard tissue regeneration. *J Mater Chem B*. **8** (2020), pp. 10941–10953.

147. N. Noskovicova, B. Hinz, P. Pakshir, cells Implant Fibrosis and the Underappreciated Role of Myofibroblasts in the Foreign Body Reaction Laboratory of Tissue Repair and Regeneration (2021), doi:10.3390/cells10071794.

148. S. Ruijtenberg, S. van den Heuvel, Coordinating cell proliferation and differentiation: Antagonism between cell cycle regulators and cell type-specific gene expression. *Cell Cycle*. **15**, 196–212 (2016).

149. F. Zhou, F. Liao, L. Chen, *et al.*, The size-dependent genotoxicity and oxidative stress of silica nanoparticles on endothelial cells. *Environmental Science and Pollution Research*. **26**, 1911–1920 (2019).

150. S. E. Lehman, A. S. Morris, P. S. Mueller, *et al.*, Silica nanoparticle-generated ROS as a predictor of cellular toxicity: Mechanistic insights and safety by design. *Environ Sci Nano*. **3**, 56–66 (2016).

151. C. Gong, G. Tao, L. Yang, *et al.*, The role of reactive oxygen species in silicon dioxide nanoparticle-induced cytotoxicity and DNA damage in HaCaT cells. *Mol Biol Rep*. **39**, 4915–4925 (2012).

152. K. Awad, N. Ahuja, M. Fiedler, *et al.*, Ionic silicon protects oxidative damage and promotes skeletal muscle cell regeneration. *Int J Mol Sci*. **22**, 1–25 (2021).

153. F. Monte, T. Cebe, D. Ripperger, *et al.*, Ionic silicon improves endothelial cells' survival under toxic oxidative stress by overexpressing angiogenic markers and antioxidant enzymes. *J Tissue Eng Regen Med*. **12**, 2203–2220 (2018).

154. H. K. Choi, G. J. Kim, H. S. Yoo, *et al.*, Vitamin C activates osteoblastogenesis and inhibits osteoclastogenesis via Wnt/β-catenin/ATF4 signaling pathways. *Nutrients*. **11** (2019), doi:10.3390/nu11030506.

155. T. He, T. E. Peterson, E. L. Holmuhamedov, *et al.*, Human endothelial progenitor cells tolerate oxidative stress due to intrinsically high expression of manganese superoxide dismutase. *Arterioscler Thromb Vasc Biol*. **24**, 2021–2027 (2004).

156. A. M. C. Barradas, H. A. M. Fernandes, N. Groen, *et al.*, A calcium-induced signaling cascade leading to osteogenic differentiation of human bone marrow-derived mesenchymal stromal cells. *Biomaterials*. **33**, 3205–3215 (2012).

157. S. An, J. Ling, Y. Gao, *et al.*, Effects of varied ionic calcium and phosphate on the proliferation, osteogenic differentiation and mineralization of human periodontal ligament cells in vitro. *J Periodontal Res*. **47**, 374–382 (2012).

158. M. N. Lee, H. S. Hwang, S. H. Oh, *et al.*, Elevated extracellular calcium ions promote proliferation and migration of mesenchymal stem cells via increasing osteopontin expression. *Exp Mol Med*. **50** (2018), doi:10.1038/s12276-018-0170-6.

159. H. Lin, Y. Zhou, Q. Lei, *et al.*, Effect of inorganic phosphate on migration and osteogenic differentiation of bone marrow mesenchymal stem cells. *BMC Dev Biol*. **21** (2021), doi:10.1186/s12861-020-00229-x.

160. A. Rossi, P. Pizzo, R. Filadi, Calcium, mitochondria and cell metabolism: A functional triangle in bioenergetics. *Biochim Biophys Acta Mol Cell Res*. **1866** (2019), pp. 1068–1078.

161. P. R. Angelova, A. Y. Baev, A. V. Berezhnov, *et al.*, Role of inorganic polyphosphate in mammalian cells: From signal transduction and mitochondrial metabolism to cell death. *Biochem Soc Trans*. **44**, 40–45 (2016).

162. M. Dietzel, Dissolution of silicates and the stability of polysilicic acid. *Geochim Cosmochim Acta*. **64**, 3275–3281 (2000).

163. L. L. Sepulveda, P., Jones, J.R., Hench, In vitro dissolution of melt derived 45 S5 and sol–gel derived 58 S bioactive glasses. *Biomed. Mater. Res.* **61**, 301–311 (2002).

164. K. Kim, D. Dean, A. G. Mikos, *et al.*, Effect of initial cell seeding density on early osteogenic signal expression of rat bone marrow stromal cells cultured on cross-linked poly(propylene fumarate) disks. *Biomacromolecules*. **10**, 1810–1817 (2009).

165. H. Zhou, M. D. Weir, H. H. K. Xu, Effect of cell seeding density on proliferation and osteodifferentiation of umbilical cord stem cells on calcium phosphate cement-fiber scaffold. *Tissue Eng Part A*. **17**, 2603–2613 (2011).

166. J. Galvao, B. Davis, M. Tilley, *et al.*, Unexpected low-dose toxicity of the universal solvent DMSO. *The FASEB Journal*. **28**, 1317–1330 (2014).

167. B. Luzak, P. Siarkiewicz, M. Boncler, An evaluation of a new high-sensitivity PrestoBlue assay for measuring cell viability and drug cytotoxicity using EA.hy926 endothelial cells. *Toxicology in Vitro*. **83**, 105407 (2022).

168. M. Ghasemi, T. Turnbull, S. Sebastian, *et al.*, Molecular Sciences The MTT Assay: Utility, Limitations, Pitfalls, and Interpretation in Bulk and Single-Cell Analysis (2021), doi:10.3390/ijms222312827.

169. A. Van Tonder, A. M. Joubert, A. D. Cromarty, Limitations of the 3-(4,5-dimethylthiazol-2-yl)-2,5-diphenyl-2H-tetrazolium bromide (MTT) assay when compared to three commonly used cell enumeration assays. *BMC Res Notes*. **8**, 1–10 (2015).

170. I. Kosti, N. Jain, D. Aran, *et al.*, Cross-tissue Analysis of Gene and Protein Expression in Normal and Cancer Tissues. *Sci Rep*. **6** (2016), doi:10.1038/srep24799.

171. E. M. Czekanska, M. J. Stoddart, J. R. Ralphs, *et al.*, A phenotypic comparison of osteoblast cell lines versus human primary osteoblasts for biomaterials testing. *J Biomed Mater Res A*. **102**, 2636–2643 (2014).

172. C. PAUTKE, M. SCHIEKER, T. TISCHER, *et al.*, Characterization of Osteosarcoma Cell Lines MG-63, Saos-2 and U-2 OS in Comparison to Human Osteoblasts. *Anticancer Res*. **24** (2004).

173. V. Kartsogiannis, K. W. Ng, Cell lines and primary cell cultures in the study of bone cell biology. *Mol Cell Endocrinol*. **228** (2004), pp. 79–102.

174. H. Jansson, D. Bernin, K. Ramser, Silicate species of water glass and insights for alkali-activated green cement. *AIP Adv*. **5**, 067167 (2015).

175. S.-W. Ha, M. N. Weitzmann, G. R. † Beck, Bioactive Silica Nanoparticles Promote Osteoblast Differentiation through Stimulation of Autophagy and Direct Association with LC3 and p62. *ACSNano*. **8**, 5898–5910 (2014).

176. M. Tanakaa, K. Takahashib, Silicate species in high pH solution molybdate, whose silica concentration is determined by colorimetry. *Anal Chim Acta*. **429**, 117–123 (2001).

177. L. Lunevich, P. Sanciolo, A. Smallridge, *et al.*, Silica scale formation and effect of sodium and aluminium ions -29Si NMR study. *Environ Sci (Camb)*. **2**, 174–185 (2016).

178. S. Sjöberg, L.-O. Öhman, N. Ingri, *et al.*, Equilibrium and Structural Studies of Silicon(IV) and Aluminium(III) in Aqueous Solution. 11. Polysilicate Formation in Alkaline Aqueous Solution. A Combined Potentiometric and 29Si NMR Study. *Acta Chem Scand*. **39a**, 93–107 (1985).

179. M. Izumiya, M. Haniu, K. Ueda, *et al.*, Evaluation of mc3t3-e1 cell osteogenesis in different cell culture media. *Int J Mol Sci*. **22**, 7752 (2021).

180. T. Grossner, U. Haberkorn, J. Hofmann, *et al.*, Effects of Different Basal Cell Culture Media upon the Osteogenic Response of hMSCs Evaluated by 99m Tc-HDP Labeling (2022), doi:10.3390/ijms23116288.

181. L. Linati, G. Lusvardi, G. Malavasi, *et al.*, Medium-range order in phospho-silicate bioactive glasses: Insights from MAS-NMR spectra, chemical durability experiments and molecular dynamics simulations (2007), doi:10.1016/j.jnoncrysol.2007.06.076.

182. S. Lin, C. Ionescu, K. J. Pike, *et al.*, Nanostructure evolution and calcium distribution in sol–gel derived bioactive glass. *J Mater Chem*. **19**, 1276–1282 (2009).

183. R. K. Harris, R. H. Newman, 29Si N.M.R. studies of aqueous silicate solutions. *Journal of the Chemical Society, Faraday Transactions 2: Molecular and Chemical Physics*. **73**, 1204–1215 (1977).

184. R. K. Harris, C. T. G. Knight, Silicon-29 NMR studies of aqueous silicate solutions. Part IV1 1 Parts II and III are references [12] and [13] respectively.. Tetraalkylammonium hydroxide solutions. *J Mol Struct*. **78**, 273–278 (1982).

185. M. Jokinen, H. Rahiala, J. B. Rosenholm, *et al.*, Relation between aggregation and heterogeneity of obtained structure in sol-gel derived CaO-P2O5-SiO2. *J Solgel Sci Technol*. **12**, 159–167 (1998).

186. Y. You, W. Ma, F. Wang, *et al.*, Ortho-silicic acid enhances osteogenesis of osteoblasts through the upregulation of miR-130b which directly targets PTEN. *Life Sci*. **264**, 118680 (2021).

187. G. R. Beck, S. W. Ha, C. E. Camalier, *et al.*, Bioactive silica-based nanoparticles stimulate bone-forming osteoblasts, suppress bone-resorbing osteoclasts, and enhance bone mineral density in vivo. *Nanomedicine*. **8**, 793–803 (2012).

188. M. N. Weitzmann, S. W. Ha, T. Vikulina, *et al.*, Bioactive silica nanoparticles reverse age-associated bone loss in mice. *Nanomedicine*. **11**, 959–967 (2015).

189. S. W. Ha, M. Viggeswarapu, M. M. Habib, *et al.*, Bioactive effects of silica nanoparticles on bone cells are size, surface, and composition dependent. *Acta Biomater*. **82**, 184–196 (2018).

190. S. W. Ha, M. Neale Weitzmann, G. R. Beck, Bioactive silica nanoparticles promote osteoblast differentiation through stimulation of autophagy and direct association with LC3 and p62. *ACS Nano*. **8**, 5898–5910 (2014).

191. T. H. Qazi, S. Hafeez, J. Schmidt, *et al.*, Comparison of the effects of 45S5 and 1393 bioactive glass microparticles on hMSC behavior. *J Biomed Mater Res A*. **105**, 2772–2782 (2017).

192. C. A. Fyfe, H. Gies, Y. Feng, High-resolution solid-state NMR of silicates and zeolites. *J Am Chem Soc*. **111**, 7702–7707 (1987).

193. S. D. Kinrade, T. W. Swaddle, Silicon-29 NMR Studies of Aqueous Silicate Solutions. 1. Chemical Shifts and Equilibria. *Inorg Chem*. **27**, 4253–4259 (1988).

194. A. Prescha, K. Zabłocka-Slowińska, H. Grajeta, Dietary Silicon and Its Impact on Plasma Silicon Levels in the Polish Population. *Nutrients*. **11** (2019), doi:10.3390/NU11050980.

195. E. Bissé, T. Epting, A. Beil, *et al.*, Reference values for serum silicon in adults. *Anal Biochem*. **337**, 130–135 (2005).

196. A. Pedone, T. Charpentier, G. Malavasi, *et al.*, New insights into the atomic structure of 45S5 bioglass by means of solid-state NMR spectroscopy and accurate first-principles simulations. *Chemistry of Materials*. **22**, 5644–5652 (2010).

197. S. Yamada, Y. Ota, A. Obata, *et al.*, Osteoblast-like cell responses to ion products released from magnesium-and silicate-containing calcium carbonates. *Biomed Mater Eng*. **28**, 47–56 (2017).

198. T. . I.-I. Meinhold, H. P. Rothbaum, R. H. Newman, "Polymerization of Supersaturated Silica Solutions Monitored by Silicon-29 Nuclear Magnetic Resonance" (1985).

199. P. D. Taylor, R. Jugdaohsingh, J. J. Powell, "Soluble Silica with High Affinity for Aluminum under Physiological and Natural Conditions" (1997), (available at https://pubs.acs.org/sharingguidelines).

200. C. T. A. Chen, W. L. Marshall, Amorphous silica solubilities IV. Behavior in pure water and aqueous sodium chloride, sodium sulfate, magnesium chloride, and magnesium sulfate solutions up to 350°C. *GeCoA*. **46**, 279–287 (1982).

201. S. Sripanyakorn, R. Jugdaohsingh, W. Dissayabutr, *et al.*, The comparative absorption of silicon from different foods and food supplements. *Br J Nutr*. **102**, 825 (2009).

202. R. Jugdaohsingh, D. M. Reffitt, C. Oldham, *et al.*, Oligomeric but not monomeric silica prevents aluminum absorption in humans. *Am J Clin Nutr*. **71**, 944–949 (2000).

203. A. Hoppe, N. S. Güldal, A. R. Boccaccini, A review of the biological response to ionic dissolution products from bioactive glasses and glass-ceramics. *Biomaterials*. **32** (2011), pp. 2757–2774.

204. L. L. Hench, Genetic design of bioactive glass. *J Eur Ceram Soc*. **29**, 1257–1265 (2009).

205. D. Fologea, B. Ledden, D. S. McNabb, *et al.*, Electrical characterization of protein molecules by a solid-state nanopore. *Appl Phys Lett*. **91** (2007), doi:10.1063/1.2767206.

206. L. Medda, M. Monduzzi, A. Salis, The molecular motion of bovine serum albumin under physiological conditions is ion specific. *Chemical Communications*. **51**, 6663–6666 (2015).

207. P. P. Madeira, I. L. D. Rocha, M. E. Rosa, *et al.*, On the aggregation of bovine serum albumin. *J Mol Liq*. **349** (2022), doi:10.1016/j.molliq.2021.118183.

208. S. W. Ha, M. Viggeswarapu, M. M. Habib, *et al.*, Bioactive effects of silica nanoparticles on bone cells are size, surface, and composition dependent. *Acta Biomater*. **82**, 184–196 (2018).

209. M. Kastelic, Y. V. Kalyuzhnyi, B. Hribar-Lee, *et al.*, Protein aggregation in salt solutions. *Proc Natl Acad Sci U S A*. **112**, 6766–6770 (2015).

210. Z. L. Kang, X. hua Zhang, X. Li, *et al.*, The effects of sodium chloride on proteins aggregation, conformation and gel properties of pork myofibrillar protein Running Head: Relationship aggregation, conformation and gel properties. *J Food Sci Technol*. **58**, 2258 (2021).

211. D. Sahu, G. M. Kannan, M. Tailang, *et al.*, Cytotoxicity of Nanoparticles: A Comparison between Particle Size and Cell Type (2016), doi:10.1155/2016/4023852.

212. I. A. Silver, M. Erecinska, Interactions of Osteoblastic and other Cells with Bioactive Glasses and Silica In Vitro and In Vivo. *Materwiss Werksttech*. **34**, 1069–1075 (2003).

213. Identification of a mammalian silicon transporter Enhanced Reader (2017) (available at moz-extension://be84739c-ce3c-4e5a-8b86-

abd7fe53b4a5/enhanced-reader.html?openApp&pdf=https%3A%2F%2Fjournals.physiology.org%2Fdoi%2Fpdf%2F10.1152%2Fajpcell.00219.2015).

214. H.-C. Schr, S. Perovi, M. Rothenberger, *et al.*, "Silica transport in the demosponge Suberites domuncula: fluorescence emission analysis using the PDMPO probe and cloning of a potential transporter" (2004), (available at http://spongebase.genoserv.de/).

215. Aquaporins Mediate Silicon Transport in Humans Enhanced Reader.

216. X. Xu, K. Zhang, L. Zhao, *et al.*, Characteristics of three sizes of silica nanoparticles in the osteoblastic cell line, MC3T3-E1. *RSC Adv*. **4**, 46481–46487 (2014).

217. I. I. Slowing, J. L. Vivero-Escoto, Y. Zhao, *et al.*, Drug Delivery: Exocytosis of Mesoporous Silica Nanoparticles from Mammalian Cells: From Asymmetric Cell-to-Cell Transfer to Protein Harvesting (Small 11/2011). *Small*. **7**, 1498–1498 (2011).

218. I. R. Orriss, M. O. R. Hajjawi, C. Huesa, *et al.*, Optimisation of the differing conditions required for bone formation in vitro by primary osteoblasts from mice and rats. *Int J Mol Med*. **34**, 1201–1208 (2014).

219. F. F. T. Ch'en, F. C. Villafuerte, P. Swietach, *et al.*, S0859, an N-cyanosulphonamide inhibitor of sodium-bicarbonate cotransport in the heart. *Br J Pharmacol*. **153**, 972–982 (2008).

220. A. M. Azzarolo, G. Ritchie, G. Quamme, Inhibition of sodium-phosphate cotransport in renal brush-border membranes with the stilbenedisulfonate, H2-DIDS. *Biochimica et Biophysica Acta (BBA) - Biomembranes*. **1069**, 70–76 (1991).

221. A. P. Garneau, G. A. Carpentier, A. A. Marcoux, *et al.*, Aquaporins mediate silicon transport in humans. *PLoS One*. **10** (2015), doi:10.1371/journal.pone.0136149.

222. G. Preta, J. G. Cronin, I. M. Sheldon, Dynasore - Not just a dynamin inhibitor. *Cell Communication and Signaling*. **13**, 1–7 (2015).

223. T. Kirchhausen, E. Macia, H. E. Pelish, USE OF DYNASORE, THE SMALL MOLECULE INHIBITOR OF DYNAMIN, IN THE REGULATION OF ENDOCYTOSIS (2008), doi:10.1016/S0076-6879(07)38006-3.

224. Y. Wu, W. Tang, P. Wang, *et al.*, Cytotoxicity and Cellular Uptake of Amorphous Silica Nanoparticles in Human Cancer Cells. *Particle and Particle Systems Characterization*. **32**, 779–787 (2015).

225. E. Macia, M. Ehrlich, R. Massol, *et al.*, Dynasore, a Cell-Permeable Inhibitor of Dynamin. *Dev Cell*. **10**, 839–850 (2006).

226. A. J. Robinson, S. Davies, R. L. Darley, *et al.*, Reactive Oxygen Species Rewires Metabolic Activity in Acute Myeloid Leukemia. *Front Oncol*. **11** (2021), doi:10.3389/FONC.2021.632623/FULL.

227. J. Wang, Y. Yu, K. Lu, *et al.*, Silica nanoparticles induce autophagy dysfunction via lysosomal impairment and inhibition of autophagosome degradation in hepatocytes. *Int J Nanomedicine*. **12**, 809 (2017).

228. S. Ansari, K. Ito, S. Hofmann, Alkaline Phosphatase Activity of Serum Affects Osteogenic Differentiation Cultures. *ACS Omega*. **7**, 12724–12733 (2022).

229. W. C. M. Duivenvoorden, A. Middleton, S. D. Kinrade, Divergent effects of orthosilicic acid and dimethylsilanediol on cell survival and adhesion in human osteoblast-like cells. *Journal of Trace Elements in Medicine and Biology*. **22**, 215–223 (2008).

230. A. A. Kapasi, G. Patel, A. Goenka, *et al.*, "Ethanol promotes T cell apoptosis through the mitochondrial pathway."

231. M. Hildebrand, B. E. Volcani, W. Gassmann, *et al.*, A gene family of silicon transporters. *Nature*. **385** (1997), pp. 688–689.

232. N. Alyabyeva, A. Ouvrard, A. M. Zakaria, *et al.*, Probing Nanoparticle Geometry down to Subnanometer Size: The Benefits of Vibrational Spectroscopy. *Journal of Physical Chemistry Letters*. **10**, 624–629 (2019).

233. K. Yin Win, S. S. Feng, Effects of particle size and surface coating on cellular uptake of polymeric nanoparticles for oral delivery of anticancer drugs. *Biomaterials*. **26**, 2713–2722 (2005).

234. M.-H. Kim, M.-K. Choi, Effect of Silicon Supplementation in Diets with Different Calcium Levels on Bone Mineral Metabolism and Bone Status in Growing Female Rats. *Curr Dev Nutr*. **4**, 1817–1817 (2020).

235. Nutritional requirements for boron, silicon, vanadium, nickel, and arsenic: current knowledge and speculation - PubMed, (available at https://pubmed.ncbi.nlm.nih.gov/1916090/).

236. R. Jugdaohsingh, SILICON AND BONE HEALTH. *J Nutr Health Aging*. **11**, 99 (2007).

237. E. C. Costa, V. M. Gaspar, J. G. Marques, *et al.*, Evaluation of nanoparticle uptake in co-culture cancer models. *PLoS One*. **8** (2013), doi:10.1371/JOURNAL.PONE.0070072.

238. D.-M. Huang, Y. Hung, B.-S. Ko, *et al.*, Highly efficient cellular labeling of mesoporous nanoparticles in human mesenchymal stem cells: implication for stem cell tracking. *The FASEB Journal*. **17** (2005), doi:10.1096/fj.05-4288fje.

239. H. Ren, S. Chen, Y. Jin, *et al.*, A traceable and bone-targeted nanoassembly based on defect-related luminescent mesoporous silica for enhanced osteogenic differentiation †. *J. Mater. Chem. B*. **5**, 1585 (2017).

240. H. Zhou, G. Jiao, M. Dong, *et al.*, Orthosilicic Acid Accelerates Bone Formation in Human Osteoblast-Like Cells Through the PI3K–Akt–mTOR Pathway. *Biol Trace Elem Res*. **190**, 327–335 (2019).

241. M. V. D. Z. Park, H. W. Verharen, E. Zwart, *et al.*, Genotoxicity evaluation of amorphous silica nanoparticles of different sizes using the micronucleus and the plasmid lacZ gene mutation assay. *Nanotoxicology*. **5**, 168–181 (2011).

242. K. Solarska-ściuk, K. Adach, M. Fijałkowski, *et al.*, Identifying the Molecular Mechanisms and Types of Cell Death Induced by bio- and pyr-Silica Nanoparticles in Endothelial Cells. *International Journal of Molecular Sciences 2022, Vol. 23, Page 5103*. **23**, 5103 (2022).

243. W. Roos, Ion mapping in plant cells - Methods and applications in signal transduction research. *Planta*. **210**, 347–370 (2000).

244. C. Law, C. Exley, New insight into silica deposition in horsetail (Equisetum arvense). *BMC Plant Biol*. **11** (2011), doi:10.1186/1471-2229-11-112.

245. J. Li, P. Liu, N. Menguy, *et al.*, Intracellular silicification by early-branching magnetotactic bacteria. *Sci Adv*. **8**, 6045 (2022).

246. A. F. Coskun, G. Han, S. Ganesh, *et al.*, Nanoscopic subcellular imaging enabled by ion beam tomography. *Nature Communications 2021 12:1*. **12**, 1–19 (2021).

247. A. A. Legin, A. Schintlmeister, M. A. Jakupec, *et al.*, NanoSIMS combined with fluorescence microscopy as a tool for subcellular imaging of isotopically labeled platinum-based anticancer drugs. *Chem Sci*. **5**, 3135–3143 (2014).

248. V. Tardillo Suárez, B. Gallet, M. Chevallet, *et al.*, Correlative transmission electron microscopy and high-resolution hard X-ray fluorescence microscopy of cell sections to measure trace element concentrations at the organelle level. *J Struct Biol*. **213**, 107766 (2021).

249. L. Bozycki, M. Komiazyk, S. Mebarek, *et al.*, Analysis of minerals produced by hFOB 1.19 and Saos-2 cells using transmission electron microscopy with energy dispersive X-ray microanalysis. *Journal of Visualized Experiments*. **2018** (2018), doi:10.3791/57423.

250. M. Scotuzzi, J. Kuipers, D. I. Wensveen, *et al.*, Multi-color electron microscopy by element-guided identification of cells, organelles and molecules. *Scientific Reports 2017 7:1*. **7**, 1–8 (2017).

251. J. Mroczek, S. Pikula, S. Suski, *et al.*, Apigenin Modulates AnxA6- and TNAP-Mediated Osteoblast Mineralization. *Int J Mol Sci*. **23**, 13179 (2022).

252. F. Cammisuli, S. Giordani, A. Gianoncelli, *et al.*, Iron-related toxicity of single-walled carbon nanotubes and crocidolite fibres in human mesothelial cells investigated by Synchrotron XRF microscopy. *Sci Rep*. **8** (2018), doi:10.1038/S41598-017-19076-1.

253. C. Sanchez-Cano, I. Romero-Canelón, Y. Yang, *et al.*, Synchrotron X-Ray Fluorescence Nanoprobe Reveals Target Sites for Organo-Osmium Complex in Human Ovarian Cancer Cells. *Chemistry – A European Journal*. **23**, 2512–2516 (2017).

254. S. Corezzi, L. Urbanelli, P. Cloetens, *et al.*, Synchrotron-based X-ray fluorescence imaging of human cells labeled with CdSe quantum dots. *Anal Biochem*. **388**, 33–39 (2009).

255. P. J. Endres, K. W. MacRenaris, S. Vogt, *et al.*, Quantitative imaging of cell-permeable magnetic resonance contrast agents using X-ray fluorescence. *Mol Imaging*. **5**, 485–497 (2006).

256. S. Rabasco, T. D. K. Nguyen, C. Gu, *et al.*, Localization and Absolute Quantification of Dopamine in Discrete Intravesicular Compartments Using NanoSIMS Imaging. *Int J Mol Sci*. **23** (2021), doi:10.3390/IJMS23010160.

257. J. Lovrić, J. Dunevall, A. Larsson, *et al.*, Nano Secondary Ion Mass Spectrometry Imaging of Dopamine Distribution Across Nanometer Vesicles. *ACS Nano*. **11**, 3446–3455 (2017).

258. Z. Diwu, C. S. Chen, C. Zhang, *et al.*, A novel acidotropic pH indicator and its potential application in labeling acidic organelles of live cells. *Chem Biol*. **6**, 411–418 (1999).

259. K. Shimizu, Y. Del Amo, M. A. Brzezinski, *et al.*, A novel fluorescent silica tracer for biological silicification studies. *Chem Biol*. **8**, 1051–1060 (2001).

260. M. Parambath, Q. S. Hanley, F. J. Martin-Martinez, *et al.*, The nature of the silicaphilic fluorescence of PDMPO. *Physical Chemistry Chemical Physics*. **18**, 5938–5948 (2016).

261. H.-C. Schröder, S. Perović-Ottstadt, M. Rothenberger, *et al.*, Silica transport in the demosponge Suberites domuncula: fluorescence emission analysis using the PDMPO probe and cloning of a potential transporter. *Biochem J*. **381**, 665–73 (2004).

262. S. J. Soenen, B. Manshian, S. H. Doak, *et al.*, Fluorescent non-porous silica nanoparticles for long-term cell monitoring: Cytotoxicity and particle functionality. *Acta Biomater*, 9183–9193 (2013).

263. Z. Chu, Y. Huang, Q. Tao, *et al.*, Cellular uptake, evolution, and excretion of silica nanoparticles in human cells †. *Nanoscale*. **3** (2011), doi:10.1039/c1nr10499c.

264. P. Merdy, C. Neytard, J. D. Meunier, *et al.*, PDMPO: A specific silicon or silica, pH sensitive fluorescent probe? *RSC Adv*. **10**, 31003–31011 (2020).

265. B. L. U. Cuetara, T. N. Crotti, A. J. O'donoghue, *et al.*, "CLONING AND CHARACTERIZATION OF OSTEOCLAST PRECURSORS FROM THE RAW264.7 CELL LINE."

266. Y. Su, H. Ren, M. Tang, *et al.*, Role and dynamics of vacuolar pH during cell-in-cell mediated death. *Cell Death & Disease 2021 12:1*. **12**, 1–12 (2021).

267. Z. Diwu, C.-S. Chen, C. Zhang, *et al.*, A novel aciclotropic pH indicator and its potential application in labeling acidic organelles of live cells (available at http://biomednet.com/elecref/1074552100600411).

268. K. Shimizu, Y. Del Amo, M. A. Brzezinski, *et al.*, A novel fluorescent silica tracer for biological silicification studies. *Chem Biol*. **8**, 1051–1060 (2001).

269. H. C. Schröder, S. Perovíc-Ottstadt, M. Rothenberger, *et al.*, Silica transport in the demosponge Suberites domuncula: Fluorescence emission analysis using the PDMPO probe and cloning of a potential transporter. *Biochemical Journal*. **381**, 665–673 (2004).

270. P. Naruphontjirakul, O. Tsigkou, S. Li, *et al.*, Human mesenchymal stem cells differentiate into an osteogenic lineage in presence of strontium containing bioactive glass nanoparticles. *Acta Biomater*. **90**, 373–392 (2019).

271. M.-Y. Shie, S.-J. Ding, H.-C. Chang, The role of silicon in osteoblast-like cell proliferation and apoptosis (2011), doi:10.1016/j.actbio.2011.02.023.

272. X. Zhou, F. M. Moussa, S. Mankoci, *et al.*, Orthosilicic acid, Si(OH)4, stimulates osteoblast differentiation in vitro by upregulating miR-146a to antagonize NF-κB activation. *Acta Biomater*. **39**, 192–202 (2016).

273. M. Ojansivu, A. Mishra, S. Vanhatupa, *et al.*, The effect of S53P4-based borosilicate glasses and glass dissolution products on the osteogenic commitment of human adipose stem cells. *PLoS One*. **13**, e0202740 (2018).

274. J. Sun, Y. Liu, M. Ge, *et al.*, A Distinct Endocytic Mechanism of Functionalized-Silica Nanoparticles in Breast Cancer Stem Cells. *Scientific Reports 2017 7:1*. **7**, 1–13 (2017).

275. J.-H. Park, H. Jeong, J. Hong, *et al.*, The Effect of Silica Nanoparticles on Human Corneal Epithelial Cells OPEN. *Nature Publishing Group* (2016), doi:10.1038/srep37762.

276. G. R. Beck, S.-W. Ha, C. E. Camalier, *et al.*, Bioactive silica-based nanoparticles stimulate bone-forming osteoblasts, suppress bone-resorbing osteoclasts, and enhance bone mineral density in vivo. *Nanomedicine*. **8**, 793–803 (2012).

277. P. Cogswell, D. Kashatus, … J. K.-J. of B., *et al.*, NF-κB and IκBα are found in the mitochondria: evidence for regulation of mitochondrial gene expression by NF-κB. *ASBMB* (available at https://www.jbc.org/article/S0021-9258(19)30884-1/abstract).

278. V. Bottero, V. Busuttil, A. Loubat, *et al.*, Activation of nuclear factor κB through the IKK complex by the topoisomerase poisons SN38 and doxorubicin: a brake to apoptosis in HeLa human carcinoma cells. *AACR* (available at https://aacrjournals.org/cancerres/article-abstract/61/21/7785/508039).

279. M. S. I. Khan, S. W. Oh, Y. J. Kim, Power of Scanning Electron Microscopy and Energy Dispersive X-Ray Analysis in Rapid Microbial Detection and Identification at the Single Cell Level. *Scientific Reports 2020 10:1*. **10**, 1–10 (2020).

280. Ž. Mladenović, A. Johansson, B. Willman, *et al.*, Soluble silica inhibits osteoclast formation and bone resorption in vitro. *Acta Biomater*. **10**, 406–418 (2014).

281. W. Ma, & Fu'an Wang, Y. You, *et al.*, Ortho-silicic Acid Inhibits RANKL-Induced Osteoclastogenesis and Reverses Ovariectomy-Induced Bone Loss In Vivo (2011), doi:10.1007/s12011-020-02286-6/Published.

282. T. Nordstrom, O. D. Rotstein, R. Romanek, *et al.*, Regulation of Cytoplasmic pH in Osteoclasts CONTRIBUTION OF PROTON PUMPS AND A PROTON-SELECTIVE CONDUCTANCE*. *Journal of Biological Chemistry*. **270**, 2203–2212 (1995).

283. G. R. Beck, S.-W. Ha, C. E. Camalier, *et al.*, Bioactive silica-based nanoparticles stimulate bone-forming osteoblasts, suppress bone-resorbing osteoclasts, and enhance bone mineral density in vivo. *Nanomedicine*. **8**, 793–803 (2012).

284. X. Liu, Y. Sun, J. Shen, *et al.*, Strontium doped mesoporous silica nanoparticles accelerate osteogenesis and angiogenesis in distraction osteogenesis by activation of Wnt pathway (2021), doi:10.1016/j.nano.2021.102496.

285. H. Nabeshi, T. Yoshikawa, T. Akase, *et al.*, Effect of amorphous silica nanoparticles on in vitro RANKL-induced osteoclast differentiation in murine macrophages (2011), doi:10.1186/1556-276X-6-464.

286. C. D. Seaborn, F. H. Nielsen, Effects of Germanium and Silicon on Bone Mineralization Seaborn and Nielsen. *Biol Trace Elem Res*. **1**, 51 (1994).

287. M. A. Elliot, H. M. Edwards, Some effects of dietary aluminum and silicon on broiler chickens. *Poult Sci*. **70**, 1390–1402 (1991).

288. A. Schiano, F. Eisinger, P. Detolle, *et al.*, Silicon, bone tissue and immunity. *Rev Rhum Mal Osteoartic*. **46**, 483–486 (1979).

289. A. M. Galow, J. Gimsa, WST-assay data reveal a pH dependence of the mitochondrial succinate reductase in osteoblast-like cells. *Data Brief*. **12**, 442–446 (2017).

290. J. Nordström, E. Nilsson, P. Jarvol, *et al.*, Concentration-and pH-dependence of highly alkaline sodium silicate solutions (2011), doi:10.1016/j.jcis.2010.12.085.

291. A. Pielesz, J. Fabia, W. Biniaś, *et al.*, Graphene Oxide and Stabilized Ortho-Silicic Acid as Modifiers of Amnion and Burn Affected Skin: A Comparative Study . *Nanotechnol Sci Appl*. **14**, 49–67 (2021).

292. A. Lassus, Colloidal Silicic Acid for Oral and Topical Treatment of Aged Skin, Fragile Hair and Brittle Nails in Females. *Journal of International Medical Research*. **21**, 209–215 (1993).

293. A. Lassus, Colloidal Silicic Acid for the Treatment of Psoriatic Skin Lesions, Arthropathy and Onychopathy. A Pilot Study. *Journal of International Medical Research*. **25**, 206–209 (1997).

294. C. Exley, O. Korchazhkina, D. Job, *et al.*, Non-invasive therapy to reduce the body burden of aluminium in Alzheimer's disease. *J Alzheimers Dis*. **10**, 17–24 (2006).

295. E. Foglio, B. Buffoli, C. Exley, *et al.*, Regular consumption of a silicic acid-rich water prevents aluminium-induced alterations of nitrergic neurons in mouse brain: histochemical and immunohistochemical studies. *Histol Histopathol*. **27**, 1055–1066 (2012).

296. J. A. Edwardson, P. B. Moore, I. N. Ferrier, *et al.*, Effect of silicon on gastrointestinal absorption of aluminium. *The Lancet*. **342**, 211–212 (1993).

297. D. M. Reffitt, R. Jugdaohsingh, R. P. H. Thompson, *et al.*, Silicic acid: its gastrointestinal uptake and urinary excretion in man and effects on aluminium excretion. *J Inorg Biochem*. **76**, 141–147 (1999).